From Resection to Resolution: Biochemical Investigation of Early and Late Steps of Homologous Recombination

DISSERTATION

ZUR

ERLANGUNG DER NATUWISSENSCHAFTLICHEN DOKTORWÜRDE

(DR. SC .NAT.)

VORGELEGT DER

MATHEMATISCH- NATUWISSENSCHAFTLICHEN FAKULTÄT

DER

UNIVERSITÄT ZÜRICH

VON

Roopesh Anand

AUS INDIEN

PROMOTIONSKOMITEE:

PROF. DR. PETR CEJKA (VORSITZ UND LEITUNG DER DISSERTATION)
PROF. DR. JOSEF JIRICNY
PROF. DR. PRIMO SCHÄR

ZÜRICH, 2016

TO MY FATHER

TABLE OF CONTENTS

ZUSAMMENFASSUNG

Homologe rekombination (HR) und Non-homologous end joining (NHEJ) sind zwei Reparaturmechanismen, welche Zellen verwenden um DNS-Doppelstrangbrüche (DSB) zu reparieren. Der entscheidende Schritt dabei ist die Resektion der 5' DNS Enden, die mechanistisch den DNS-Reparatur Signalweg bestimmt, indem sie HR fördert und NHEJ hemmt. Aufgrund zahlreiche Studien ist bekannt, dass der MRE11-RAD50-NBS1 (MRN) Komplex und das CtIP Protein an der Einleitung der Resektion beteiligt sind. Allerdings hat die einzige Nuklease in dem Komplex, MRE11, entgegengestzte Polarität (3' zu 5') zu der Richtung der Resektion (5' zu 3'). Um dieses Rätsel zu lösen wurde ein so-genanntes bidirektionales Resektionsmodel vorgeschlagen. MRE11 soll dabei mithilfe seiner endonukleolytischer Aktivität Einschnitt(e) in der Nähe des DSB schaffen, die als Einstieg für seine 3' zu 5' Exonuklease dienen, sodass diese zum DSB hin arbeiten kann. Obwohl dieses Modell das Polaritätsparadox löst, fehlte das mechanistische Verständnis einer solchen endonukleolytischen Aktivität. Ich zeige nun, dass CtIP die Endonuklease-Aktivität von MRN an doppelsträngiger DNS (dsDNS) stimuliert. Dabei ist die Phosphorylierung von CtIP an T847 absolut notwendig für diesen Effekt. Ebenfalls ist das Blockieren der DNS Enden, vor allem am 5' Ende, erforderlich für MRN-pCtIP Aktivität. Übereinstimmend mit dem vorgeschlagenen Modell ist die Position des ersten Einschnittes von MRN-CtIP ~20 Nukleotide von dem 5' DNS Ende entfernt. Die endonukleolytische Aktivität ist spezifisch für das MRE11 Protein, da die nukleolytisch-inaktive (H129L D130V) Variante von MRE11 keine Einschnitte vollbringen kann. Weiterhin zeigen RAD50 Mutanten, die entweder kein ATP mehr binden (RAD50K42A), oder hydrolisieren (RAD50K42R) können, ebenfalls keine endonukleolytische Aktivität. Somit sind auch RAD50 und seine ATPase Aktivität notwendig für die Einschnitte von MRN. Interessanterweise, auch das Enfernen von NBS1 aus dem MRN Komplex führt zum Verlust der Endonuklease-Aktivität, im Unterschied zur Hefe. Somit zeigt meine Arbeit, dass NBS1 und RAD50 unabdingbare Komponenten des MRN Komplexes sind, um die

Endonuklease-Aktivität von MRE11 im Menschen zu stimulieren. Es ist bekannt, dass CtIP tetramerisiert, indem es ein Dimer von Dimeren über seinen N-Terminus bildet. Diese Oligomerisation von CtIP ist wichtig für seine in vivo Funktionen in HR. Ich habe die pCtIP L27E Mutante, die keine Tetramere, jedoch aber Dimere bilden kann, analysiert. Ich fand heraus, dass die Oligomerisation von CtIP notwendig für seine Funktion ist, da die Mutante nur sehr schlecht die Endonuklease-Aktivität von MRN stimulieren konnte. Ausserdem, wenn man die 160 N-terminalen Aminosäuren von CtIP, die für Dimerisation und Tetramerisation verantwortlich sind, entfernt (1-160Δ pCtIP), kann das Protein ebenfalls die Endonuklease von MRN nur sehr schlecht stimulieren. Im Unterschied zur Hefe, kann CtIP die endonukleolytische Aktivität von MRN am ssDNS zirkularen Plasmid fördern. Zudem sind Mg^{2+}, Mn^{2+} und ATP wichtig für optimale MRN-pCtIP Aktivität.

In meinem zweiten Projekt habe ich mich mit der homologe Rekombination in der Meisose befasst. Meiotische HR führt zur Bildung von sogenannten „double Holliday junctions“ (dHJ) während der Reparatur von programmierten DSB. Durch einen bisher unbekannten Mechanismus werden die dHJ zu „crossover“ (CO) weiterverarbeitet, welche zu erhöhter genetischer Diversität führt. Es ist sehr wahrscheinlich, dass in meiotische Zellen der MLH1-MLH3 (MutLγ) Komplex, eine mutmassliche Endonuklease, für das Prozessieren von dHJs zu CO Produkten verantwortlich ist. Zusätzliche wurde gezeigt, dass MSH4-MSH5 (MutSγ) eine Funktion im MutLγ-abhängigen Mechanismus hat. Während sehr viele genetische Daten diese Mechanismen zum Schneiden von dHJs durch MutLγ und zusätzlichen Proteine belegen, konnte der mechanistische Hintergrund dazu noch nicht aufgezeigt werden. Zusammen mit Nicolas Weyland habe ich begonnen, MLH1-MLH3 zusammen mit MSH4-MSH5 auf biochemischer Ebene zu charakterisieren. Wir haben gezeigt, dass MutLγ vorzugsweise dHJs und ähnliche Strukturen bindet. Weitere Experimente zeigten, dass vorallem der Kern von dHJs gebunden werden.

Ich konnte zeigen, dass hMutLγ, in Reaktionen welche Mn^{2+} beinhalten, unspezifisch einen Strang von doppelsträngige DNS schneidet. Diese Aktivität

konnte nicht mit der Nuklease-inaktiven hMutLγ (MLH1-MLH3D1223N) Mutante gesehen werden, was darauf hindeutet, dass die Aktivität tatsächlich durch hMutLγ katalysiert wurde. Die Aktivität wurde durch die Präsenz von ATP in der Reaktion weiter verstärkt.

Mit Hilfe von aufgereinigtem hMutSγ konnte ich bestätigen, dass der Komplex bevorzugterweise an HJ bindet als an doppelsträngige DNS und dass der Komplex, nachdem er ATP gebunden hat, an den HJ-Armen entlang gleitet.
Wir zeigten auch, dass hMutLγ direkt mit MutSγ interagiert *in vitro*. Des Weitere konnten wir zeigen, dass hMutLγ zusammen mit MutSγ an HJ bindet. Dieser Effekt scheint spezifisch für HJ zu sein, da mit doppelsträngiger DNS keine solche Beobachtungen gemacht wurden. Zusammengefasst deutet das darauf hin, dass h MutSγ den hMutLγ-DNS Komplex stabilisiert.

SUMMARY

Cells utilize two major pathways to repair DNA double strand breaks (DSB) including homologous recombination (HR) and non-homologous end joining (NHEJ). DNA end resection of the 5'-terminated DNA at DSBs is the key event, which mechanistically determines the repair pathway choice by promoting HR while inhibiting NHEJ. Numerous studies have established the role of the MRE11-RAD50-NBS1 (MRN) complex and CtIP in the initiation of resection. However, the nucleolytic polarity of the only nuclease in the complex, MRE11, is the opposite (3' to 5') to the direction of resection (5' to 3'). To solve this enigma, a so-called bidirectional resection model has been proposed. MRE11 was anticipated to make incision(s) close to the DSB by its endonucleolytic activity, which creates an entry site for its 3' to 5' exonuclease that proceeds back towards the DSB. Although this model solves the polarity paradox, the mechanistic understanding of such nicking activity by MRE11 was undefined. Here I show that CtIP stimulates the endonuclease activity of MRN on double stranded DNA (dsDNA). Phosphorylation of CtIP (pCtIP) at T847 is absolutely required for this stimulatory effect. The blocking of DNA ends, especially at the 5' end, is required to observe this MRN-pCtIP activity. In agreement with the proposed model, the position of the first incision by MRN-pCtIP complex maps to [symbol about] 20 nucleotides away from the 5' DNA end. The nicking activity is intrinsic to MRE11, as nuclease-dead (H129L D130V) variant of MRE11 does not show any clipping activity. Additionally, RAD50 mutants deficient in ATP binding (RAD50K42A) or ATP hydrolysis (RAD50K42R), fail to show any clipping activity, indicating the essential role of RAD50 and its ATPase activity. Interestingly, the removal of NBS1 from MRN complex results in the loss of the clipping activity. Therefore, unlike in yeast, my work establishes NBS1 as the indispensable component of the MRN complex together with RAD50 to stimulate MRE11-catalyzed clipping activity in humans. CtIP tetramerizes by making a dimer of dimers through its amino-terminus and such oligomerization is important for its *in vivo* functions in HR. The analysis of pCtIP L27E mutant, in which tetramerization is abolished while dimerization is preserved, revealed a reduced capacity to promote MRN, suggesting that proper oligomeric structure

of CtIP is likely essential for its optimal activity. Furthermore, the deletion of 160 amino acids from the amino-terminus of CtIP (1-160Δ pCtIP), which disrupts the CtIP dimerization and consequently its tetramerization as well, reduces the pCtIP capacity to stimulate MRN drastically. In contrast to yeast, pCtIP also stimulates the MRN endonuclease on ssDNA circular plasmid. In terms of co-factors, Mg^{2+}, Mn^{2+} and ATP were found to be important for the optimum activity of of MRN-pCtIP.

My second project was focused on meiotic homologous recombination. Meiotic HR favours the formation of double Holliday junctions (dHJ) as intermediates of programmed DSB repair. These are, by a yet unknown mechanism, processed exclusively to preferentially to crossovers (CO to facilitate the production of genetic diversity. Meiotic cells have a dedicated and biased mechanism in place to ensure the formation of obligate COs. MLH1-MLH3 (MutLγ) has been strongly implicated in meiosis as a putative endonuclease responsible for cleaving dHJs in a biased manner to produces COs. Additionally, MSH4-MSH5 (MutSγ) has also been shown to function in the MutLγ mediated pathway. Despite the availability of extensive genetic data, the mechanistic understanding of the biased cleavage of dHJs by MutLγ and its partners remains elusive. Here, in collaboration with Nicolas Weyland, I set out to study and characterize the biochemical behaviour of human MLH1-MLH3 in conjunction with human MSH4-MSH5. Previously, we showed that hMutLγ prefers binding to HJs and similar structures. Further analysis indicated that it presumably binds to the core of a HJ. Here I could show that hMutLγ nicks super-coiled dsDNA non-specifically in the presence of Mn^{2+}. No such activity with nuclease-dead hMutLγ (MLH1-MLH3D1223N) was observed, proving that the observed activity is intrinsic to hMutLγ. The presence of ATP further simulates the nicking activity of hMutLγ. Using purified hMutSγ, I could confirm that it prefers binding to HJs over dsDNA and slides upon HJ arms upon ATP binding. We could also show that hMutLγ directly interacts with hMutSγ *in vitro*. Furthermore, DNA binding analysis of hMutLγ and hMutSγ revealed that hMutLγ binds cooperatively to HJ with hMutSγ. No such observation with dsDNA emphasizes the specific nature of the observed effect

with HJ. The data also indicates that hMutSγ further stabilizes the hMutLγ-DNA complex.

1. Introduction

Cell theory, originally formulated in 1838 by Theodor Schwann and Matthias Jacob Schlieden, states that all life forms arise from pre-existing life (Sharp, 1921). At the most basic level, the process of cell division ensures this continuation of life on earth. In unicellular organisms cell division is important for their further proliferation whereas in multicellular organisms, it is required for both propagation of their species as well as for normal development of an individual organism.

Each cell division accompanies duplication of its entire structure and constituents, which include DNA as well. DNA is one of the most important constituents of the cell as it contains overall instruction for creating an individual organism (Alberts et al., 2015). The process of duplication of DNA known as DNA replication must be carefully regulated to accurately copy the genetic information from mother cell to daughter cell. A single error in replication may lead to unfavourable mutation, which may in turn predispose an individual to various diseases including cancer. Therefore high fidelity in copying DNA during replication is of utmost importance to the cells. The cells must avoid any damage and irreversible loss of DNA sequence, as once lost or altered cells have no means to recover the original information.

Other than the errors caused during replication infidelity, both endogenous as well as exogenous sources can physically damage DNA. While exogenous sources include UV radiation, X-rays, mutagenic chemicals etc., endogenous damage can occur by metabolites such as reactive oxygen species (ROS), reactive nitrogen species (NOS), lipid peroxidation products etc., which are produced during various cellular processes (Cadet and Wagner, 2013) . Similarly obstacles encountered during normal process of DNA replication may lead to strand discontinuities. Depending on the kind of damage different DNA lesions may arise, which may be toxic to the cells. Fortunately, with millions of years of evolution cells have developed an array of different pathways to repair such

lesions. These DNA repair pathways are highly conserved from prokaryotes to humans.

In summary, when cells face any DNA damage their fate is decided by their ability to repair that damage. Depending on the DNA lesion, cells recognize the problem and activate appropriate repair pathway(s) to repair the damage. Once damage is repaired cells can continue to perform their normal function. On the other hand, if cells fail to repair the lesions, cells can initiate the process of programmed cell death such as apoptosis and consequently be removed from the cell pool. However, in rare instances when repair is not entirely accurate or is defective it can lead to alteration of DNA sequence of important genes, which are required for cell maintenance and proliferation. These alterations can either inactivate the tumour suppressor genes or activate the oncogenes, which in turn can result in uncontrolled cellular proliferation. This uncontrolled growth may eventually give rise to cancer.

1.1. Nature and sources of DNA lesions

The integrity of DNA structure and its sequence is important for its normal function. DNA itself is a highly stable molecule, though spontaneous damage occurs frequently due to biochemical nature of DNA (Figure 1). For instance, N-glycosidic bond between pentose sugar and bases is labile in nature and hence can spontaneously break even under normal conditions. Each single cell looses approximately 2000-10,000 purines per day due to spontaneous breakage (Lindahl, 1993; Lindahl and Nyberg, 1972). Similarly, 100-500 cytosine bases are converted into uracil bases per cell every day by the process of deamination (Barnes and Lindahl, 2004). Additionally, reactive metabolites like ROS, methyl donor *S-adenosylmethionine* produced during normal cellular metabolism have the potential to react with DNA to alter its structure (Rydberg and Lindahl, 1982). It has been estimated that oxidative DNA damage alone in humans produces 10,000 DNA lesions per cell per day (Fraga et al., 1990). The exogenous sources such as ultraviolet (UV) radiation from sunlight can form in between two adjacent pyrimidines (Grossman et al., 1988). On the other hand, mutagenic chemicals present in the environment including acetaldehyde can produce DNA "adducts" whereas substances like cisplatin can crosslink DNA strand in between the same (intra) or opposite (inter) strands (Wozniak and Blasiak, 2002). All such DNA lesions if not repaired in time can present an obstacle during replication or transcription influencing the normal division and survival of the cells. Apart from DNA base modifications, adducts and crosslinking, DNA strands can break directly upon impact from high-energy radiations like ionizing radiations (IR) (Liu et al., 2000; Lomax et al., 2013; Santivasi and Xia, 2014). Other than IR, certain chemicals like camptothecin (CPT) and etoposide can indirectly produce DNA breaks by inhibiting topoisomerases activity (Liu et al., 2000; Walles et al., 1996). As mentioned earlier, breaks can occur either in one or both DNA strands known as SSB and DSB, respectively. In certain conditions, if SSB persists for a long time, it can be converted into a DSB. For instance, the replication of parental strand containing a SSB results in one ended DSB when the replication fork reaches the affected region (Mehta and Haber, 2014). Similarly, when two SSBs occur nearby to each other on opposite strands of

duplex DNA, these SSBs can turn into a DSB. The process of replication itself can introduce mutations by incorporation of mispaired nucleotide in the newly synthesized strand by DNA polymerase (Pray, 2008). Likewise, insertion and deletion of short DNA sequences, often within repeats, can also take place during replication.

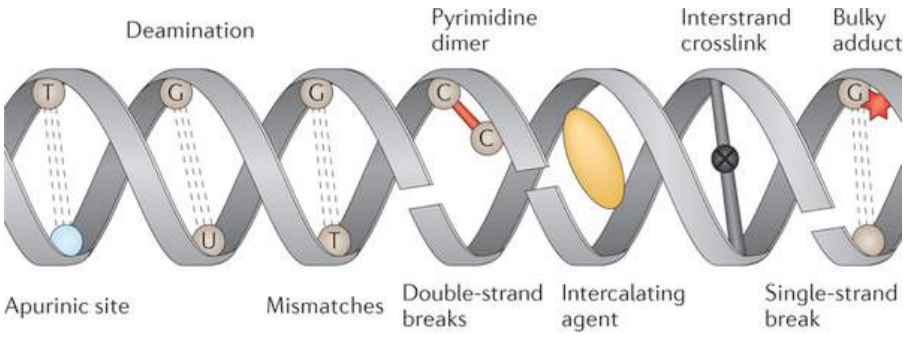

Figure 1. An overview of various types of DNA lesions. (Adapted from Helleday et al, 2014 *Nature Reviews Genetics*)

Any damage resulting in the alteration of either structure or sequence has the potential to be lethal for the cell. As many of these lesions are endogenous and can arise spontaneously or due to reactive metabolites, it is not possible for the cells to completely avoid DNA damage. To deal with such high levels of routine DNA damage, cells have developed various DNA repair pathways. Although most repair pathways repair damage efficiently, in some instances the process of repair may itself modify DNA. The main lesions relevant to my doctoral work include single and double strand DNA breaks.

1.1.1 Single strand break (SSB)

The integrity and continuity of DNA strands is important for normal cellular survival and proliferation. DNA strands can break under various conditions leaving 3' and 5' termini, which can accompany the loss of nucleotides (Caldecott, 2008). SSBs can be produced directly upon disintegration of oxidized sugar or indirectly during repair of modified DNA lesions by other sources. They can also occur due to abortive activity of topoisomerases (Wang, 2002). The unwinding of DNA, which occurs during replication and transcription, exerts

topological constrain on the DNA helix, which must be released for continued propagation of replication/transcription machinery. DNA topoisomerases continuously cleave and readily reseal one or both strands of helix to relax the strain. This action of topoisomerases produces transient nicked DNA-protein complex, which is rapidly resealed by enzymes in the subsequent reaction step. However, when this transient complex encounters RNA or DNA polymerase or is inhibited by drugs, it can be converted into a SSB. If not repaired in due time, SSBs can block replication and may result in the formation of DSBs. They can also affect transcription, as RNA polymerase cannot pass through them. Generally, cells can efficiently repair these breaks but high levels of SSBs can induce prolonged checkpoint activation, resulting in exhaustion of the repair machinery and apoptosis (Wang, 2002).

1.1.2 Double strand break (DSB)

Among all DNA lesions, DSB is one of the most lethal DNA lesions. The failure to repair even single DSB can have deleterious effect on the cell (Rich et al., 2000). DSBs are more dangerous to genomic integrity than SSB or any other DNA lesion affecting single strand because lost information/sequence in the damaged strand can be restored by taking information from the intact complementary strand, which is not possible when both DNA strands are damaged. As described above, DSBs can arise through the failure to repair SSBs on time before DNA replication. Certain chemicals such as camptothecin or etoposide can trap the transient topoisomerase-DNA complex and lead to single or double strand DNA breaks, respectively (Liu et al., 2000; Walles et al., 1996). Other exogenous sources such as IR can directly induce DSBs by breaking the phosphodiester bond of DNA or indirectly by producing SSBs through radiolysis of water. At high doses of IR, the formation of nicks in complementary strand within one helical turn also gives rise to DSBs. Any impediment or pausing of replication fork by collision either with the transcription machinery or unusual DNA structures can also cause DSBs. Despite their lethality, cells themselves, in certain conditions, deliberately introduce DSBs and exploit their repair mechanism to their advantage. In meiotic cells, programmed DSBs are introduced by topoisomerase-like Spo11 (SPOrulation 11)(Keeney et al., 1997). These DSBs facilitate the genetic exchange

between homologous chromosome and their proper separation during transitions to anaphase I in meiosis (see more detail in section 1.5) (Borde and de Massy, 2013). Similarly, DSBs are introduced during VJD and class-switch recombination (Bassing et al., 2002; Stavnezer et al., 2008). The consequences of failure to repair DSBs can be multiple and may include genomic instability, cell death and neoplastic transformation in multicellular organisms (Mladenov et al., 2016). DSBs can be generally repaired by either non-homologous end joining (NHEJ) or homologues recombination (HR) pathways.

1.2 DNA repair pathways

1.2.1 Base excision repair (BER)

BER is responsible for correcting modified bases, which induce a minimal structural distortion in DNA helix structure. These modifications primarily involve deamination, oxidation and methylation. BER pathway can generally be divided into five sequential steps: lesion recognition and removal of damaged base, incision of abasic site, processing of terminated end, gap filling by DNA polymerase and final ligation of strand (Krokan and Bjoras, 2013). BER begins with recognition and removal of damaged base by a specific DNA glycosylase enzyme. Different types of damaged bases are recognized and processed by distinct DNA glycosylases. In mammals, 11 glycosylases have been discovered to date (Jacobs and Schar, 2012; Svilar et al., 2011). Upon recognition, the glycosylase flips the damaged base out and cleaves the N-glycosidic bond between the base and sugar creating an abasic site (Huffman et al., 2005). Such sites are recognized by AP endonucleases, which create nicks required for further processing (Mol et al., 2000). Certain glycosylases function as bi-functional enzymes posses also the nuclease activity and do not require the AP endonuclease (Jacobs and Schar, 2012). Nicking of abasic sites by AP endonuclease or bi-functional glycosylase can produce non-conventional 5' or 3' termini, which can be refractory to DNA synthesis or nick ligation. Therefore, such termini must be processed. Cells posses specialised proteins, which carry out this function. For instances, polymerase Pol β in humans additionally posses dRP lyase which functions to remove 5'-dRP moiety, making nicked termini suitable for ligation (Beard et al., 2006; Loeb and Monnat, 2008). PNKP is another primary enzyme that removes blocking 3'-PO_4 group and prepares the nicked ends for ligation (Bernstein et al., 2005). In a subsequent step, DNA polymerase β must fill the remaining gap. Finally, the remaining nick is sealed by a DNA ligase, which completes the BER.

1.2.2 Nucleotide excision repair (NER)

NER removes bulky DNA lesions, which result in a significant DNA helix

distortion. The prominent lesions repaired by NER include UV-induced cyclo pyrimidine dimers (CPDs), 6-4 photoproducts (6-4 PPs), adducts formed by chemical mutagens such as benzo[a]pyrene or cisplatin, ROS-generated cyclopurines and various other bulky lesions (Scharer, 2013). As with all DNA lesions, their detection is of paramount importance for their repair. In NER, the bulkiness and thermodynamic destabilization induced by DNA lesions are key factors for their recognition. NER pathway can be sub-categorized into global genome-NER (GG-NER) and transcription-coupled NER (TC-NER) depending on occurrence of damage and its mode of detection. In GG-NER, various DNA bulky lesions, which can be chemically different in structures, are detected directly by XPC-RAD23B complex. This remarkable ability of XPC-RAD23B stems from its binding capacity to ssDNA produced due to distortion or destabilization of DNA (Gunz et al., 1996; Huang et al., 1992; Liu et al., 2011; Sugasawa et al., 1998). In CPD detection, which mildly destabilizes DNA (Reardon and Sancar, 2003; Sugasawa et al., 2001) and hence is only poorly detected by XPC itself, the recognition is aided by UV-DDB complex (Scharer and Campbell, 2009; Sugasawa et al., 2005). After lesion recognition, another protein complex TFIIH (transcription initiation factor IIH) that is composed of 10 protein subunits is recruited to damage site (Araujo et al., 2001; Compe and Egly, 2012; Evans et al., 1997; Riedl et al., 2003; Volker et al., 2001; Yokoi et al., 2000). Two protein subunits of TFIIH, XPB and XPD possess a helicase activity (Coin et al., 2007). Structural studies of XPB and XPD homologs in various organisms indicate that while XPB is required for TFIIH anchoring by DNA melting upon ATP binding, XPD subsequently translocate 5' to 3' to detect and verify the lesion (Scharer, 2013). XPD translocation is stalled by the presence of the DNA lesion hence verifying its presence. Once verification by XPD is complete, the assembly of the pre-incision complex, which includes XPA, RPA and XPG takes place. XPA is considered the central coordinator of the NER reaction as it interacts with TFIIH, RPA, XPC-RAD23B, DDB2, ERCC1-XPF and PCNA proteins (Bunick et al., 2006; Gilljam et al., 2012; Li et al., 1994; Nocentini et al., 1997; Park et al., 1995; Wakasugi et al., 2009; You et al., 2003). It specifically binds to kink DNA and not directly to the DNA lesion, hence making sure everything is ready and in place for dual incision in next step (Camenisch et al., 2006; Missura et al., 2001). The

structure specific nuclease XPG that is recruited through TFHII has both structural and catalytic roles. The second endonuclease, ERCC1-XPF is recruited to DNA lesion by its interaction with XPA. RPA plays an important role in coordinating excision and synthesis events by binding to non-damaged ssDNA and hence helping to position both nucleases correctly on the damaged strand (Camenisch et al., 2006). Once both nucleases are in place, the initial 5' incision is made by ERCC1-XPF, which is capable of initiating repair synthesis. XPG makes second incision 3' to lesion and this results in the excision and release of 22-30 nucleotides containing the lesion and the TFIIH complex with it (Fagbemi et al., 2011). The gap produced by the oligonucleotide release is filled by DNA pol δ and pol ε with PCNA, RFC, and RPA (Araujo et al., 2000; Ogi and Lehmann, 2006; Shivji et al., 1995). Some studies have also implicated translesion polymerase pol κ to be involved in DNA synthesis (Moser et al., 2007; Ogi and Lehmann, 2006). The final step of sealing the nick is carried out by DNA ligase I (Moser et al., 2007).

Transcription-coupled NER (TC-NER) specifically repairs DNA lesions, which inhibit transcription by blocking the transcript elongation by RNA polymerase II (Vermeulen and Fousteri, 2013). Damage detection is therefore indirect in TC-NER and hence does not require XPC-RAD23B. During transcription, UVSSA, USP7 and Cockayne syndrome protein CSB transiently interact with RNA pol II (Fei and Chen, 2012; Yang, 2008). The stalling of RNA pol II by the DNA lesion stabilizes the interaction between CSB and CSA factors. The CSB-CSA complex has been proposed to push RNA pol II backwards exposing the lesion and making it accessible for TFIIH to bind. From this step onwards, the TC-NER pathway follows the same mechanism as described for GG-NER. As TC-NER is always associated with transcription, the efficiency of NER is higher in actively transcribed regions in comparison to transcriptionally silent regions (Vermeulen and Fousteri, 2013; Yang, 2008).

1.2.3 Post-replicative mismatch repair (MMR)

DNA replication is an extremely accurate process for copying DNA due to strict DNA base-complementarity, high fidelity and proof reading exonuclease activity

of the replicative polymerases. Despite such measures, errors such as non-canonical mismatched base pairing and insertion-deletion loops still occur during replication at the rate of about 1:1,000,000 (Arana and Kunkel, 2010). Microsatellite instability (MSI), which is caused by alteration in number of microsatellite repeats by IDLs, is one of the characteristics of defective MMR in humans (Boland and Goel, 2010). Essentially, MMR pathway involves 3 steps: recognition of the mispair or IDL, removal of the wrongly incorporated nucleotide and resynthesis of DNA. Repair of mispaired nucleotides and IDLs in higher eukaryotes begins with recognition by heterodimers MSH2-MSH6 (MutSα) and MSH2-MSH3 (MutSβ) respectively (Jiricny, 2013). While MutSα can recognize single mismatches as well as 1-2 unpaired nucleotides, MutSβ recognizes IDLs of 2-10 nucleotides in length. Both subunits of the MutS complexes contain Walker ATP binding motif in their C-terminal regions (Jiricny, 2006). Although their mode of substrate recognition is slightly different, upon recognition, the repair involves the same set of proteins and follows same pathway.

Here, I only describe the repair of mismatches or 1-2nt long IDLs. Initially, MutSα encircles DNA and slides loosely on DNA unless it encounters a mismatch. Upon recognition of the mismatch, MutSα bends DNA, which brings its conformational change resulting in ADP-ATP exchange and inhibition of ATP hydrolysis. The ATP binding releases MutSα from the mismatch and it subsequently moves away from the mismatch freely as a sliding clamp (Jiricny, 2006). In subsequent and not very well understood step, the MLH1-PMS2 (MutLα) heterodimer is recruited and forms a ternary complex with MutSα and duplex DNA. MutLα forms a heterodimer through its C-terminal domain and similarly to MutSα, it is proposed to encircle DNA by further dimerization of its amino-terminal nucleotide binding domains (Guarne, 2012). The mismatch containing strand must be degraded to remove the mispaired nucleotide. However, as both strands in duplex contain undamaged nucleotides at the mismatch site, it is challenging for the cells to determine "correct" nascent DNA strand to degrade. To overcome this problem, cells use the discontinuities within the newly synthesized strands as markers for strand degradation. The strand excision is carried out by

exonuclease EXO1 that has a 5' to 3' polarity (Tran et al., 2004a). While 5' to 3' degradation of the error containing lagging DNA strand by EXO1 is straightforward due to its discontinuous synthesis by Okazaki fragments, situation becomes more complex when error occurs in the leading strand (Claverys and Lacks, 1986). As replication occurs in the 5' to 3' direction, only free 3' end is available for EXO1 in the leading strand for degradation. Due to its opposite polarity, EXO1 is unable to degrade the error containing leading strand directly. To overcome this paradox, MutLα comes into the action with its cryptic endonuclease activity. The activation of MutLα latent endonuclease activity minimally requires a mismatch, MutSα, RFC, PCNA and ATP. Once MutLα is enzymatically active, it endonucleolytically nicks the strand past the mismatch and hence creates the entry point for EXO1 to degrade the strand in 5' to 3' direction resulting in the removal of the mismatch (Dzantiev et al., 2004; Kadyrov et al., 2006). Strand excision is followed by the resynthesis of the degraded strand by DNA polymerase delta (δ) and replication resumes normally (Wu et al., 2003).

1.2.4 Double strand break repair (DSBR)

The DSBs present serious threat for the cell survival and genomic stability. The failure to repair even a single DSB can lead to cell death (Rich et al., 2000). Moreover, incorrect DSB repair may also lead to genomic instability by chromosomal aberration (Jeggo and Lobrich, 2015). Decades of research have resulted in the development of various experimental tools, which can distinguish the use of particular pathway for repair of natural and artificially induced DSBs. By taking advantage of such tools in combination with other techniques, it has been well established that cells can repair DSBs either by non-homologous end joining (NHEJ) or homologous recombination (HR) (Figure 2). Various factors such as the source (exo- vs. endogenous) and nature of DSBs (Double sided end (DSE) vs single sided end (SSE), DNA end structure (ligatable vs. non-ligatable, presence of non-canonical chemistry), cell cycle stage (G1 vs. S & G2), repair end goal (accurate or mutagenic) influence the DSB repair pathway choice (Ceccaldi et al., 2016). To deal with such different requirements, both NHEJ and HR processes use several related yet distinct sub-pathways of their own.

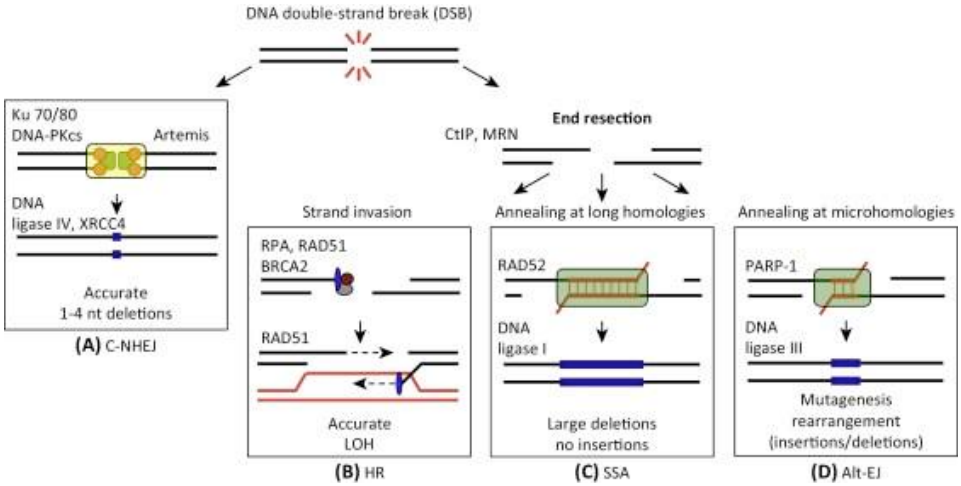

Figure 2. Double strand break repair pathways choice. The occurrence of DNA end resection determines the repair pathway choice. When extensive end resection is suppressed in G1 phase, C-NHEJ is favoured. In S and G2 phase, resection is promoted by various HR factors and therefore HR, SSA and Alt-EJ can repair DSBs. Alt-EJ can also occur in G1 phase as well due to limited resection (adapted from Ceccaldi et al, 2016 *Trends in Cell Biology*).

Generally, NHEJ is efficient but error-prone, whereas HR is relatively slower but more accurate. In NHEJ, DSBs are repaired by a direct ligation of broken ends, which is followed by sealing of the gap by a DNA ligase (Davis and Chen, 2013). The propensity of error occurrence during repair by NHEJ primarily depends on the nature of the lesion. For example, DSBs produced by a nuclease with intact complementary overhangs, i.e. "clean" breaks, can be re-ligated with perfect accuracy without any error (Feldmann et al., 2000; Kabotyanski et al., 1998; Smith et al., 2001; Smith et al., 2003). However, naturally occurring accidental DSBs produced by various DNA damaging agents are almost never "clean". DSBs produced by sources such as IR leave ends unsuitable for direct re-ligation, known as "dirty ends" and hence require additional processing of ends preceding ligation (Chiruvella et al., 2013). As with other repair pathways, NHEJ utilizes multiple proteins to accomplish the repair, which may also involve DNA polymerases and nucleases. Depending upon the structure of the broken ends, DNA overhangs can either be cleaved by a nuclease or receding strand can be extended by a polymerase. The end processing is not coordinated between the two ends, which can result in processing of one end by polymerase and other by nuclease (Lieber, 2008). The blunt ends created after these polymerase/nuclease activities are ligated DNA ligase IV. This processing of ends may thus be

accompanied by the insertion (less likely) or deletion (more likely) of small DNA fragments. As most DSBs produced are not "clean" and repaired imprecisely, NHEJ is generally considered error prone DNA repair pathway.

Conversely, HR is considered accurate as it uses a homologous template for repair (Jasin and Rothstein, 2013). This process of copying the DNA sequence from the homologous sequence guarantees accuracy in most cases. However, similarly to NHEJ, repair outcomes of HR in terms of accuracy may differ. Essentially, repair of DSBs by HR initiates with limited strand resection of both 5' ends. It leaves 3' overhangs, one of which finds and invades the complementary sequence on the donor duplex upon homology search (Renkawitz et al., 2014). The donor duplex can either be a sister chromatid, homologous chromosome or repeated regions on the same or a different chromosome. The choice of the donor duplex is critical for the overall accuracy of HR. While repair by a sister chromatid is extremely accurate due to the identical DNA sequence, copying DNA from the homologous chromosomes, which mostly have different sequences, or from heterologous regions results in a "less accurate" outcome. This may result in the loss of heterozygosity (LOH) (Moynahan and Jasin, 2010), which can lead to the loss of a single functional allele of an important gene by copying the DNA sequence from the non-functional allele and making an individual prone to various diseases including cancer. The strand invasion is followed by extension of 3' invaded strand by replicative polymerases Pol δ and Pol ε (Li et al., 2009; Maloisel et al., 2008). Mutations can arise during this step due to inefficient MMR or when repair is carried out by error-prone translesion polymerases (Hicks et al., 2010; Pomerantz et al., 2013; Sebesta et al., 2013).

The DSB repair pathway choice is primarily determined by the phase of the cell cycle (Ceccaldi et al., 2016). While NHEJ is functional throughout the cell cycle, HR is only functional in S and G2 phase (Chiruvella et al., 2013; Karanam et al., 2012). The differential use of the repair pathways during various cell cycle phases maximizes the efficiency and accuracy of repair. Primarily in G1 phase, DSBs are repaired by NHEJ as HR is restricted due to obvious lack of sister chromatids. Once cell enters in S-phase, HR machinery can be activated. NHEJ remains active in S and G2 phase and still repairs the majority of DSBs, a

significant number of DSBs are now repaired by HR (Hinz et al., 2005; Mao et al., 2008; Rothkamm et al., 2003; Takata et al., 1998). As both repair pathways are simultaneously active in S and G2 phase, they both compete for the same substrate. How is it determined, which pathway is employed for the DSB repair? Mechanistically, DNA end resection is the key event that determined the choice of the repair pathway (Symington and Gautier, 2011). Once HR specific- proteins resect DNA extensively, it becomes unsuitable for NHEJ. Therefore, DNA end resection represents a committing step for HR.

1.2.4.1 Non-homologous end joining (NHEJ)

NHEJ primarily involves the ligation of the broken ends at DSB sites. As described earlier, the repair by NHEJ may be erroneous in nature. This feature of NHEJ can be attributed to its lack of any inherent mechanisms to restore the lost sequence and to guide the ligation of correct DNA molecules. In principle, NHEJ can join any two ends irrespective of their origin, which can result in chromosomal translocation (Frit et al., 2014; Ghezraoui et al., 2014; Lieber et al., 2010). These limitations inherent to NHEJ make it more error-prone than HR. However, NHEJ is a guardian of genome stability as null phenotype of core NHEJ proteins like Ku show gross abnormality in efficient DNA repair and *Ku70*$^{-/-}$ human cells are not viable (Bogue et al., 1998; Chistiakov et al., 2009; Fattah et al., 2008; Gu et al., 1997; Jung and Alt, 2004; Kragelund et al., 2016; Li et al., 2007; Nussenzweig et al., 1996). In fact, the rapid and efficient execution of repair by NHEJ makes it a preferred choice in DSB repair. Thus sequence alteration by NHEJ is therefore a small price to pay for maintaining overall genomic stability.

As described earlier, DNA end joining by NHEJ can occur by several related yet distinct NHEJ mechanisms (Chiruvella et al., 2013). Majority of DSBs are repaired by canonical or classical form of NHEJ (C-NHEJ), which specifically requires the DNA-PK holoenzyme. Alternative-NHEJ or as more aptly described as Alt-EJ is another form of NHEJ which occurs independently of DNA-PK and repairs a subset of DSBs. Alt-EJ, though not well understood, is believed to encompasses distinct mechanisms for DSB repair. Microhomology mediated end joining

(MMEJ) is a form of Alt-EJ which utilizes microhomology (short homologous DNA sequence) present at the DSBs (Sinha et al., 2016). Although the outcome of DSB repair by both C-NHEJ and alt-EJ can be similar, their distinct requirements of proteins and the use of microhomology set them apart. While DNA end joining by C-NHEJ can either be accurate or imprecise, most forms of alt-NHEJ, especially MMEJ, are almost always mutagenic due to deletion of several nucleotides to find microhomology (Sfeir and Symington, 2015).

1.2.4.2 Mechanism of DSBR by NHEJ

C-NHEJ repair mechanism can be divided into sequential steps, which are DNA end recognition and assembly of C-NHEJ proteins, bridging of DNA ends, DNA end processing (if required) and DNA ligation (Figure 3). The initiation of C-NHEJ begins with extremely rapid recruitment of C-NHEJ specific DNA-end binding heterodimer Ku, which is composed of subunits Ku70 and Ku80. Ku binding to DNA ends prevents their non-specific processing by nucleases, helps in bridging the two ends together and functions as a scaffold to promote the stabilization of NHEJ protein complex on the DSB (Davis and Chen, 2013). Ku, directly or indirectly, recruits core C-NHEJ proteins, which include DNA dependent protein kinase catalytic subunit (DNA-PKcs) (Uematsu et al., 2007), X-ray cross complementing protein 4 (XRCC4) (Mari et al., 2006; Nick McElhinny et al., 2000), DNA Ligase IV (Costantini et al., 2007) and XRCC4-like factor (XLF) (Yano et al., 2008) and Aprataxin-and-PNK-like factor (APLF) (Grundy et al., 2013). Ku directly recruits DNA-PKcs (Gottlieb and Jackson, 1993). Together with Ku and DNA, DNA-PKcs form the DNA-PK holoenzyme, which phosphorylates various C-NHEJ proteins. Structurally, DNA-PKcs also tethers DNA ends together by the formation of a synaptic complex (Cary et al., 1997; Weterings and van Gent, 2004). DNA ligase IV is a specific C-NHEJ ligase required for the final step of DNA ligation. DNA-ligase IV forms a complex with its non-enzymatic partner XRCC4, which stabilizes and stimulates Ligase IV and also serve as a second scaffold to other C-NHEJ proteins (Grawunder et al., 1997). XLF interacts with the XRCC4-Lig IV complex and stimulates Ligase IV (Ahnesorg et al., 2006; Lu et al., 2007). XRCC4-XLF complex is proposed to multimerize to form a long super-helical structure, which may further stabilize and bridge DNA ends (Andres and Junop,

2011; Hammel et al., 2010; Wu et al., 2011). Ligase IV has the unique capacity of ligating incompatible DNA ends, ligating one strand independently of another, and ligating DNA ends across gaps (Gu et al., 2007; Ma et al., 2004). It makes Ligase IV an ideal ligating enzyme to deal with a wide variety of DSB structures repaired by C-NHEJ. DSBs produced by various sources can lead to a variety of complex DNA ends that may require prior processing before ligation. For example, DSB ends can present non-ligatable 5′ hydroxyls or 3′ phosphates ends. Similarly, DSB formation can leave 3' or 5' overhangs at the ends, which must be excised for ligation. Several end-processing enzymes with different activities have been discovered, which are important for C-NHEJ. Artemis is a nuclease, which has been shown to possess both ssDNA 5' to 3' exonuclease as well as 5' endonuclease activity on 5' overhangs, which creates blunt ended duplexes (Ma et al., 2002; Povirk et al., 2007). WRN, with its 3' to 5' exonuclease activity, is another nuclease implicated in C-NHEJ (Kusumoto et al., 2008). PNKP is another special enzyme with both kinase and phosphatase activity, which is functional in C-NHEJ. It can add phosphate to the 5'-OH group and remove 3' phosphate at DNA ends by its kinase and phosphatase domain, respectively (Bernstein et al., 2005). Apratxin with its nucleotide hydrolase and transferase activity catalyzes the removal of adenylate groups from 5' termini (Gong et al., 2011; Tumbale et al., 2011). Additionally, when necessary, gap filling at DSB ends can be carried out by template-dependent polymerase μ or by template-independent pol λ (Nick McElhinny et al., 2005; Ramadan et al., 2004).

Alt-NHEJ is another form of NHEJ, which has been shown to have residual activity in every studied system when C-NHEJ is inactivated (Frit et al., 2014). Alt-NHEJ is a less defined pathway than C-NHEJ. The extensive use of microhomology by Alt-NHEJ is its characteristics feature (MMEJ) but microhomology independent repair by Alt-NHEJ has been observed (Boboila et al., 2012; Lieber, 2010). It has been thus suggested that Alt-NHEJ encompasses distinct sub-pathways and Alt-EJ is more appropriate term to use instead. Furthermore, the presence of terminal microhomology at DSB site improves efficiency of repair by C-NHEJ (Lieber, 2010). Therefore it is not the repair outcome, but the lack of a requirement for the core C-NHEJ proteins including

Ku, DNA-PKcs and Ligase IV by Alt-EJ, which distinguishes it from C-NHEJ. In fact, Ku suppresses Alt-EJ, which establishes a competition between these pathways (Audebert et al., 2004; Wang et al., 2006). Recent evidence suggests Alt-EJ being a "back-up" mechanism for C-NHEJ and HR (Iliakis et al., 2015). It has been postulated that Alt-EJ with its several sub-pathways can take over a partially processed DNA intermediates when both C-NHEJ and HR were engaged but somehow failed to complete the repair. The involvement of MRE11-RAD50-NBS1 (MRN) and CtIP, the usage of microhomology (possibly produced by a limited resection) and its marked enhancement in G2 in comparison to G1 provides a further evidence for Alt-EJ being a back-up mechanism for HR (Iliakis, 2009; Rositsa Dueva, 2013). Alt-EJ is also known to play a role in V(D)J recombination and class switch recombination (Kotnis et al., 2009; Malu et al., 2012). The Alt-EJ repair mechanism, like C-NHEJ, also requires DSB recognition, synapsis, end processing and ligation . Poly(ADP)-ribose polymerase 1 (PARP-1) is a sensor of SSB and DSB, and functions in various DNA repair pathways. Its substitutes the role of DNA-PK in Alt-EJ by tethering the DNA ends and also provides the scaffold activity. DNA Ligase 3 is the main ligase for joining the ends in absence of Ligase IV activity in Alt-EJ (Frit et al., 2014). Microhomology usage, when required, needs limited resection of DNA, which is followed by action of Pol θ, a low fidelity polymerase, to synthesize the resected strand. Multiple studies have indicated the role of MRN with CtIP, which have been postulated to be responsible for the limited resection required for MMEJ (Badie et al., 2015; Lee-Theilen et al., 2011; Quennet et al., 2011; Rass et al., 2009a).

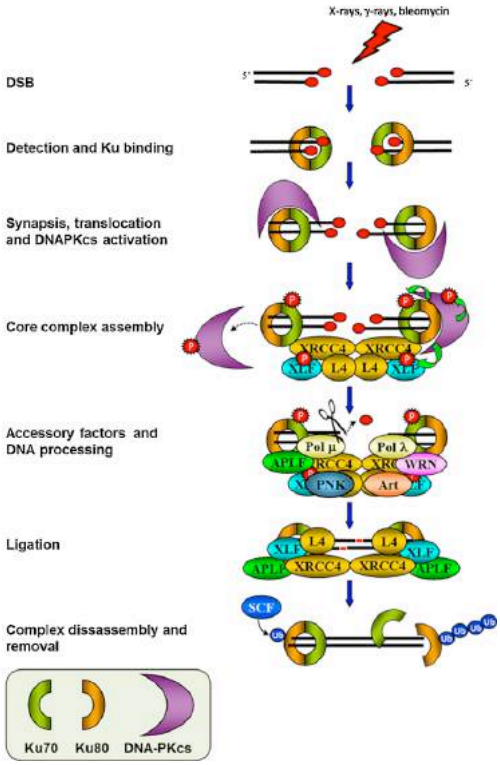

Figure 3. Mechanism of classical non-homologues end joining (C-NHEJ). In the initial steps of C-NHEJ, Ku heterodimer is recruited to DSBs and slides over the ends forming the tight interaction with DNA-PKcs. DNA -PKcs is activated by DNA end-bound Ku, which results in the further loading of XRCC4, Lig4 and XLF. The "core" NHEJ complex is stabilized by the autophosphorylation of DNA-PKcs, which leads to its dissociation from the complex. Other processing factors including nucleases and polymerase are recruited to the core complex via interaction with Ku to modify the DSB termini for ligation. Finally, DNA ligase 4 ligates the processed compatible ends, which is facilitated by XLF and APFL (adapted from Grundy at al, 2014 *DNA Repair*).

1.2.4.3 Homologous recombination (HR)

HR is a template-dependent repair pathway. The lack of a sister-chromatid in the G1 phase restricts HR to S and G2 phases. In principle, if evoked during the G1 phase, HR can use homologous chromosomes as a template for repair, which can lead to loss of heterozygosity (Orthwein et al., 2015). Therefore, HR must be suppressed during G1 to prevent any such occurrence. The suppression and implementation of HR in the G1 and S/G2 phases, respectively, is regulated at multiple levels by various proteins(Heyer et al., 2010; Mathiasen and Lisby, 2014). DSB resection is essential for the initiation of HR (Mimitou and Symington, 2009; Paques and Haber, 1999). This is positively regulated by a cyclin dependent kinase (CDK) activity. While resection is inhibited in the G1

phase, upon the entrance into the S phase CDK activates the resection machinery (Symington, 2016). In case of compromised HR, the degree of resection may determine the usage of alternative pathways for DSB repair. Depending on the length of resection, DSBs can either be repaired by MMEJ (5-25 nt) or by single strand annealing (SSA, more than ~ 25 nt) (Ceccaldi et al., 2016; Sharma et al., 2015).

Why is a complex mechanism such as HR used when more efficient NHEJ is available at cell's disposal throughout the cell cycle? It is generally believed that one reason has to with the nature of the DSBs. During replication, the forks encounter relatively high level of SSBs in comparison to DSBs (20:1) (Roots et al., 1985; Tounekti et al., 2001). When replication fork collides with a SSB, this becomes converted to a DSB due to free end of newly synthesized strand (Mehta and Haber, 2014). These single-ended DSBs are unsuitable for repair by NHEJ due to the absence of other end. HR therefore is a more suitable pathway to repair such one-ended DSBs. The frequency of DSBs, without significant exogenous factors, is sufficiently high enough that deficiency of single HR-specific protein is embryonically lethal(Hakem et al., 1998; Hakem et al., 1996; Lim and Hasty, 1996; Suzuki et al., 1997; Tsuzuki et al., 1996). Hypomorphic mutations render cells more sensitive to DSBs inducing agents and predispose affected individuals to cancer (O'Driscoll, 2012; Prakash et al., 2015).

1.2.4.4 Mechanism of DSBR by HR

Mre11-Rad50-Xrs2/NBS1, is a multifunctional protein that acts as DSB sensor, co-activator of DSB induced checkpoint signalling and an effector (Lamarche et al., 2010). It is recruited quickly to the break site upon DSB induction (Nelms et al., 1998). Its disruption leads to defective ATM checkpoint signalling and defective HR (Carson et al., 2003; Girard et al., 2002; Stewart et al., 1999; Uziel et al., 2003). MRX/N localization at DSBs is followed by the recruitment of various important proteins, which play different roles at both early and later stages of HR. Among such proteins, CtIP, which interacts directly with MRN also accumulate at DSBs (Chen et al., 2008a; Sartori et al., 2007; Wang et al., 2013a; You et al., 2009). The processing of DSBs initiates with DNA end resection in a 5'

to 3' direction (Figure 4). This resection leaves 3' ssDNA overhangs at both ends of the DSB. Mechanistically, resection occurs in successive phases of short and long-range excision, which are mediated by MRX/N with Sae2/CtIP and Exo1/EXO1 or BLM/Sgs1 (slow growth suppressor 1)-DNA2 or WRN respectively (Symington, 2016). The 3' ssDNA produced due to the resection is coated by Replication protein-A (RPA) to prevent non-specific degradation from nucleases (Chen et al., 2013; Lisby et al., 2004; Wang and Haber, 2004). Subsequently, RPA is displaced from ssDNA by RAD51 with the help of several mediators to form ssDNA-RAD51 nucleoprotein filament known as "pre-synaptic" complex (San Filippo et al., 2008). In the next step, known as synapsis, ssDNA-RAD51 complex searches for a homologous sequence and mediates strand invasion by displacing the strand on the donor duplex forming the displacement loop (D-loop)(Krejci et al., 2012). Strand invasion, mediated by Rad51, is a defining feature of HR. DNA pairing in between invaded strand and the donor duplex with complementary sequence occurs by canonical Watson-Crick base pairing. Once DNA pairing is stabilized, the invaded strand is extended by DNA synthesis with a DNA polymerase. The extension restores any missing DNA sequence by copying the sequence of donor duplex. The extended D-loop can be processed by distinct mechanisms, which may yield different repair outcomes in terms of exchange of DNA sequence between afflicted chromosome and the donor duplex (Ceccaldi et al., 2016). In first mechanism of synthesis dependent strand annealing (SDSA), the extended 3' strand is displaced and anneals back to its original complementary strand. Any gap or flaps created are processed by a polymerase or a flap-endonuclease. DNA ligase eventually ligates the single nucleotide gap, hence completing the repair. SDSA exclusively produces non-crossover products, which means non-reciprocal exchange of information between donor and the repaired duplex. Non-crossover can result in gene conversion, which may eventually result in LOH (Chen et al., 2007; Thiagalingam et al., 2001). Alternatively, the extended strand in a D-loop can be captured by the original strand without being dissociated from complementary donor strand. The second end capture results in the formation of a key recombination intermediate termed a double Holliday junction (dHJ) (Bzymek et al., 2010; Heyer, 2004). This can be processed by two distinct mechanisms;

dissolution and resolution. While dissolution produces non-crossovers only, resolution can result in both non-crossover and crossover products. The crossovers represent a final repair product with physical exchange of DNA segments between donor and repaired chromosomes. Dissolution is carried out by Sgs1 -Top3 (Topoisomerase 3)-Rmi1(RecQ-mediated genome instability 1)/BLM-TOPOIIIα-RMI1-RMI2 complex where Sgs1/BLM converge two Holliday junctions towards each other by branch migration together with the topoisomerase activity of Top3/ TOPOIIIα (Swuec and Costa, 2014). Convergent branch migration ultimately produces a hemicatenane structure, which is finally resolved by Topoisomerase Top3/TOPOIIIα in conjunction with Rmi1/RMI1-RMI2. In somatic cells, dissolution is the primary mechanism for the elimination of dHJ in mitotic cells. Dissolution occurs primarily in S-phase (Sarbajna and West, 2014). Resolution, on the other hand, involved dHJ processing by either of structure-selective endonucleases (SSE). In total, 3 SSE, which include Mms4-Mus81/MMS4-EME1, Slx1-Slx4/SLX1-SLX4 and Yen1/GEN1 have been identified in both yeast and mammals to complete the resolution of dHJ and other recombination intermediates (Matos and West, 2014). Depending on the cleavage of dHJ by these SSE i.e. symmetrical or asymmetrical, they can produce both non-crossover and crossover products respectively. Somatic cells utilize resolution to eliminate unprocessed recombination intermediate including dHJ that escaped from the dissolution pathway (more details in section 1.6.1). The SSE enzymes operate primarily in the G2 or even the M phases of the cell cycle.

Single strand annealing (SSA) is another distinct mutagenic pathway, functional in both yeast and humans though it has been best defined in yeast (Stark et al., 2004). SSA is distinct from HR as it lacks strand invasion step and is Rad51 independent, it shares initial DNA end resection step as well as several proteins that also participate in HR (Ivanov et al., 1996). SSA primarily occurs when DSBs are flanked by tandem repeated sequences. Briefly, similarly to HR, the resection of DSB is followed by a formation of 3' overhangs. The overhangs align and anneal to each other, which is mediated by Rad52 and Rad59 (Davis and Symington, 2001; Pannunzio et al., 2010; Symington, 2002). The resulting flaps are cleaved by Rad1-Rad10 nuclease with the help of Msh2-Msh3 and the gap is

finally sealed by DNA ligase (Spies and Fishel, 2015; Sugawara et al., 1997; Tomkinson et al., 1993). The cleavage of flaps results in the loss of DNA sequence. Therefore, SSA is always mutagenic in nature. As research on DNA end resection is a focus of my doctoral research, the topic will be further covered in the next chapter.

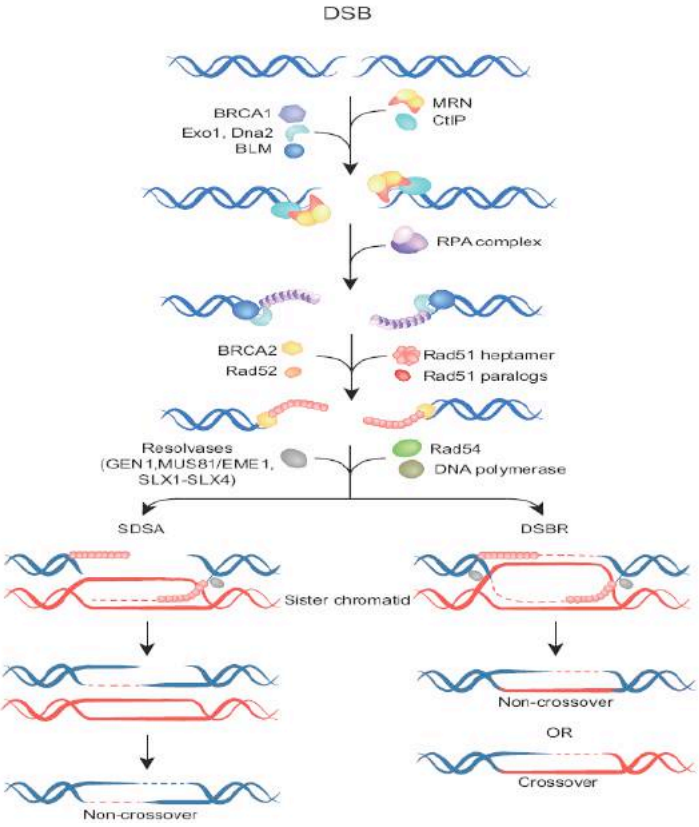

Figure 4. Mechanism of double strand break repair by HR in eukaryotes. Repair by HR initiates with the short- range resection of 5' termini in 5' to 3' direction by MRN/X and CtIP/Sae2. It is followed by the long- range resection, which is carried out by EXO1/Exo1 or BLM-DNA2/Sgs1-Dna2. RPA coats the 3' overhangs (ssDNA) to prevent the formation of secondary structures and nucleolytic degradation. RAD51/Rad51 is loaded on RPA-coated ssDNA, which is mediated by BRCA2/Rad52 and other RAD51 paralogs. RAD51-nucleofilament finds the homologues DNA sequence and invades the donor duplex by strand exchange. The invaded strand is extended by polymerase. Following this step, repair can occur by SDSA or DSBR. In SDSA, the extended strand anneals back to its original duplex, followed by further DNA synthesis of resected complementary strand and ligation. In DSBR, the extended strand is captured by the afflicted duplex without dissociating with the donor duplex giving rise to double Holliday junctions (HJ). These dHJs are further processed by either dissolution or resolution. While dissolution produces non-crossovers only, resolution can result in both crossover and noncrossovers (adapted from Dueva and Lliaka, 2013 *Translational Cancer Research*).

1.3 DNA end resection

DSB resection initiates the HR repair pathway. Resected DSBs inhibit the error-prone NHEJ and direct repair to HR for faithful restoration of the lost DNA sequence. Here I describe the end resection mechanisms in bacteria and eukaryotes.

1.3.1 Bacteria

RecBCD initiates the major recombination pathway utilized by most gram-negative bacteria including *Escherichia coli (E. coli)* (Dillingham and Kowalczykowski, 2008). RecBCD is a heterotrimeric complex, which collectively carries out the DSB end resection (Blackwood et al., 2013). In RecBCD complex, the RecB subunit functions as nuclease and also possesses a slow 3' to 5' helicase activity (Dillingham et al., 2003; Wang et al., 2000). RecC recognizes a specific 8-base pair non-palindromic Chi sequence (5' GCTGGTGG 3') and regulates RecB activities, whereas RecD possesses a fast 5' to 3' helicase activity (Dixon and Kowalczykowski, 1993). RecB and RecD motors translocate on 5' and 3' strand strands respectively, but in the same overall direction (Finkelstein et al., 2010). The simultaneous unwinding of the duplex by both helicases produces a long 5' tail and a short 3' tail due to the different speed of the respective helicases (Taylor and Smith, 2003). During such unequal unwinding period, RecB resects 3' end more efficiently than 5' end. Upon encountering the Chi sequence, RecD is inactivated which makes unwinding slow as it is now driven by RecB only (Spies et al., 2003). Furthermore, RecC interaction with Chi sequence brings confirmation change in RecB, which opens its molecular latch allowing 3' tail to exit RecB (Handa et al., 2012; Yang et al., 2012). This modulation of RecB by RecC and Chi sequence suppresses 3' end cleavage and stimulates the 5' end degradation. Simultaneously, RecB also facilitates RecA (ortholog of RPA) loading on the resulting 3' tail (Anderson and Kowalczykowski, 1997). The RecF pathway represents an additional repair mechanism, which is responsible for residual recombination in the absence of *recB* and *recC* (Persky and Lovett, 2008). In this particular mechanism, resection is carried out by 5' to 3'

exonuclease RecJ, which is further stimulated by the 3' to 5' RecQ helicase (Han et al., 2006; Handa et al., 2009).

1.3.2 Eukaryotes

In eukaryotes, DNA end resection occurs in two sequential phases of short-range and long-range resection (Symington, 2016) (Figure 5). In short-range resection, Mre11-Rad50-Xrs2/NBS1 complex initiates resection with Sae2/CtIP and excise both 5' DNA ends up to ~ 300 nucleotides (in yeast) (Garcia et al., 2011; Zakharyevich et al., 2010a). Mre11/MRE11 in MRX/N complex is the nuclease responsible for the initial limited resection (Mimitou and Symington, 2009). Mre11/MRE11 is known to possess Mn^{2+} – dependent 3' to 5' exo- and endonuclease activity on secondary structures of ssDNA and hairpins (Paull and Gellert, 1998; Usui et al., 1998). However, it has been very well established that end resection occurs in opposite direction from 5' to 3' (Sun et al., 1991; White and Haber, 1990; Zhu et al., 2008). To solve this paradox, current model suggests that Mre11/MRE11 with Sae2/CtIP incises dsDNA through its endonuclease activity in the close the vicinity of DSB. This incision by MRX/N is followed by the excision of nicked strand in 3' to 5' direction by MRE11 back towards the DSB. This model was supported by the seminal studies carried out in meiotic cells of *S. cerevisiae.* In yeast meiotic cells, the Spo11 transesterase generates DSBs intentionally so that recombination can occur between homologues chromosomes (Bergerat et al., 1997; Keeney et al., 1997). Spo11 remains covalently attached to the DSB ends. Its ultimate removal is essential for HR progression. Upon endonucleolytic cleavage of dsDNA by MRX, Spo11 bound oligonucleotide (12 to 40 nt) is released (Garcia et al., 2011; Mimitou and Symington, 2009; Neale et al., 2005). On the other hand, in nuclease deficient *mre11* mutant, Spo11 remains attached to DSB ends, which leads to HR defect (Furuse et al., 1998; Hartsuiker et al., 2009a; Moreau et al., 1999; Nairz and Klein, 1997). Similarly, *rad50Δ and sae2Δ/ctp1Δ* mutants in budding and fission yeast exhibit the identical phenotype as observed in *mre11-nd* mutant (Hartsuiker et al., 2009a; Milman et al., 2009). Xrs2 and NBS1 are equally important in MRX/N complex as *xrs2Δ* mutants are equally defective for HR while *NBS1* deletion is embryonically lethal in mice (D'Amours and Jackson,

2001; Zhu et al., 2001). MRX likely makes multiple incisions on the 5' strand. While the released oligonucleotide bound to Spo11 is up to ~ 40 nt in length, *exo1* deletion still results in the resection of ~270 nt (Dna2-Sgs1 normally do not function in meiosis) (Manfrini et al., 2010; Zakharyevich et al., 2010b). In some cases, MRX/Sae2 seem to cleave further away from the DSB (Neale et al., 2005). The state/structure of the DSB ends influences the DNA end resection by MRX/N. The formation of a covalent DNA-protein complex e.g. with Spo11 or with TopI or TopII, can block the access of Exo1 or Dna2 nuclease (Alani et al., 1990; Nairz and Klein, 1997) (Connelly et al., 2003; Hartsuiker et al., 2009b; Takeda et al., 2016). Hence as described above, the Mre11 nuclease activity becomes indispensable for elimination of such blocks and thus for DNA end resection. In contrast, endonuclease (HO or I-SceI) generated DSBs with "clean" ends can be processed by either overexpression of Exo1 or by deletion of Ku in *mre11Δ* background (Mimitou and Symington, 2010; Shim et al., 2010; Tomita et al., 2003). Furthermore, inactivation of the Mre11 nuclease with Exo1 deletion still results in a substantial resection, most likely mediated by Sgs1-Dna2 (Moreau et al., 2001; Tsubouchi and Ogawa, 2000). Moreover, *mre11-nd* cells are only partially sensitive to IR and do not exhibit as severe phenotype as observed in *mre11Δ* cells, which points at a structural role of Mre11 at a DSB (Krogh et al., 2005; Llorente and Symington, 2004; Moreau et al., 1999) (Lobachev et al., 2002). In principle, secondary structures at ends may also require the MRX nuclease activity for their elimination. Repair of DSBs at inverted Alu repeats, which are believed to form hairpin or cruciform structures upon DSB induction, requires Mre11 nuclease and Sae2.

The 3' tailed ssDNA, produced by initial resection, is coated by RPA, which prevents the formation of secondary structures in ssDNA. The resected 5' strands are further resected extensively in long-range resection by two distinct but redundant pathways. These pathways involve either Exo1/EXO1 mediated resection or Dna2/DNA2, which functions in conjunction with either Sgs1/BLM or WRN in an alternative pathway (Symington, 2016). Exo1/EXO1 is a member of XPG/Rad2 and FEN-1 family and has 5' to 3' dsDNA exonuclease and 5' flap endonuclease activity and can carry out the resection alone (Szankasi and Smith,

1992, 1995; Tran et al., 2004b). Exo1 recruitment at DSBs is facilitated by MRX (Shim et al., 2010). Additionally, MRX with Sae2 also stimulates Exo1 mediated degradation, likely by opening or 5' clipping of dsDNA by MRX, which creates a suitable substrate for Exo1 (Cannavo et al., 2013; Nicolette et al., 2010a). Additionally, multiple incisions by MRX-Sae2 may also serve as entry points for Exo1 to resect DNA. In the reconstituted system, RPA, BLM and MRN stimulate EXO1/Exo1 activity (Cannavo et al., 2013; Nimonkar et al., 2011; Nimonkar et al., 2008). In the other redundant pathway, Dna2/DNA2 functions with Sgs1/BLM or WRN to process the DNA ends. Dna2/DNA2 is an ssDNA endonuclease, which requires helicase activity of Sgs1/BLM to unwind dsDNA for 5' to 3' degradation (Gravel et al., 2008; Mimitou and Symington, 2008; Sturzenegger et al., 2014; Thangavel et al., 2015; Zhu et al., 2008). Top3 and Rmi1 have a structural function in this step with Sgs1 within the STR complex and promote resection by Dna2 (Cejka et al., 2010a; Niu et al., 2010). *In vitro*, Dna2/DNA2 can degrade ssDNA in both 3' and 5' directions (Bae et al., 2001; Cejka et al., 2010a; Niu et al., 2010). RPA restricts its nuclease activity to 5' to 3' direction only. Dna2 also possesses 3' to 5' helicase activity but it is largely dispensable for end resection (Cejka et al., 2010a; Nimonkar et al., 2011; Niu et al., 2010; Zhu et al., 2008).

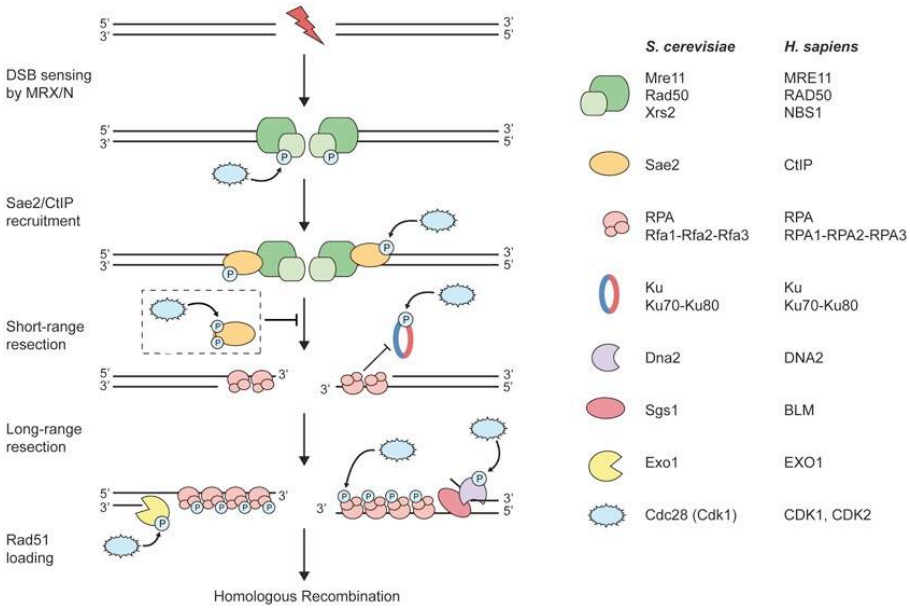

Figure 5. Mechanism of DNA end resection in *S. cerevisiae* and humans. End resection is preceded by sensing of the DSBs by MRX/N complex. Upon recruitment on DSBs, MRX/N facilitates the recruitment of multiple HR associated proteins including CtIP/Sae2. The CDK/Cdc28 phosphorylates the Sae2/CtIP in cell cycle specific manner (upon entering into the S-phase), which leads to further phosphorylation of Sae2/CtIP by ATM and ATR in response to DSBs (not shown). According to proposed bidirectional model, MRX/N with Sae2/CtIP endonucleolytically incises the strands with 5' termini in the near vicinity of DSBs. MRX/N enters through these nicks and degrades the DNA in 3' to 5' direction in short-range resection by its 3' to 5' exo nucleolytic activity. The resected ends are unsuitable substrate for Ku binding and hence NHEJ is inhibited. The 3' ssDNA generated due to resection is coated by RPA. Exo1/EXO1 or Sgs1-Dna2/DNA2-BLM further extensively degrades the DNA in 5' to 3' direction in long-range resection (adapted from Ferretti et al, 2013 *Frontiers in Genetics*).

1.3.2.1 MRN

The MRN complex is shown to function in both NHEJ and HR (Lamarche et al., 2010). In yeast, MRX is required for NHEJ; the role of human MRN in NHEJ is more restricted to Alt-EJ pathway (Boulton and Jackson, 1998; Di Virgilio and Gautier, 2005; Huang and Dynan, 2002; Rass et al., 2009b; Xie et al., 2009; Zhang and Paull, 2005). MRE11 contains phosphoesterase motifs in its amino terminal region and mutation of the conserved residues in these motifs abrogates its nuclease activity (Bressan et al., 1998; Furuse et al., 1998; Moreau et al., 1999; Trujillo and Sung, 2001; Usui et al., 1998). Although the requirement for Mre11 nuclease activity in certain cases is absolute as e.g. in the Spo11-induced DSB repair, *Mre11-nd* (H125) mutants in yeast show a mild radiosensitivity in comparison to *mre11* null mutants (Krogh et al., 2005; Llorente and Symington, 2004; Moreau et al., 1999). This indicates a structural role of Mre11 in DSB

repair besides its contribution through its enzymatic activity. In agreement, the crystal structure of Mre11 revealed a high structural conservation of the amino terminal region and its dimeric state in all 3 domains of life (Schiller et al., 2014). Disruption of Mre11 dimerization in yeast confers a *mre11Δ* phenotype (Schiller et al., 2012; Williams et al., 2008).

RAD50 is a member of the SMC (structural maintenance complex) proteins and contains Walker A and B motifs at its amino and carboxyl termini respectively (Alani et al., 1990). The ATPase activity of Rad50 is essential for MRX/N function in resection (Alani et al., 1990; Chen et al., 2005). It also contains an extended coiled-coil structure, which folds back upon itself by intermolecular association to form an anti-parallel coiled-coil (~500 Å) structure (Hopfner et al., 2002; Hopfner et al., 2000a). At the apex of the other end of coiled-coil region is Zn-hook domain. MR is the minimal unit of MRX/N found in most organisms, which exists as heterotetramer M_2R_2 (Lim et al., 2011). The globular head region of M_2R_2 is composed of two ABC-ATPase domains and two Mre11 molecules. ATP binding by the ATPase domains of RAD50 brings a conformational change and aids in dimerization of Rad50 at the nucleotide-binding domain (NBD) (Hopfner et al., 2000b). In addition, the Zn-hook can also mediate both intra- (within M_2R_2) as well as intermolecular (between two M_2R_2) interactions (de Jager et al., 2001; Hopfner et al., 2002; Hopfner et al., 2001; Moreno-Herrero et al., 2005). The intermolecular binding between two M_2R_2 by Zn-hook provides the MR complex its ability to bridge two DNA molecules by tethering them together. Expectedly, the length of the coiled-coil affects DNA tethering by MR (Deshpande et al., 2014; Hohl et al., 2011). While reduction of the coiled-coil length in MR mainly causes NHEJ defects, mutation of Zn^{2+} hook impairs its both HR and NHEJ functions(Hohl et al., 2011). Moreover, the folded ATP-binding domains of Rad50 bind to Mre11 dimer near to DNA binding domain of Mre11 (Lafrance-Vanasse et al., 2015). This architectural organization of MR puts Mre11 under the control of the Rad50 ATPase activity. In *Pyrococcus furiosus*, it was shown that ATP binding by Rad50 induces "closed" confirmation, which promotes DNA tethering whereas "open" confirmation by ATP hydrolysis is essential for nuclease activity (Deshpande et al., 2014).

Xrs1/Nbs1/NBS1 is the eukaryotic-specific and non-enzymatic subunit of the MRX/N complex, present in *S. cerevisiae, S. pombe* and mammals respectively (Stracker and Petrini, 2011). The disruptive mutation of *NBS1* gene in humans causes Nijmegen breakage syndrome (NBS) (Carney et al., 1998; McKinnon and Caldecott, 2007). Xrs2/NBS1 carries the nuclear localization signal (NLS) and facilitates the transportation of MRX/N into nucleus (Carney et al., 1998; Nakada et al., 2003; Tsukamoto et al., 2005). The phosphopeptide-binding domain, FHA (Fork-head associated) and BRCT domain (BRCA1 carboxy-terminal), are present in both yeast and mammals (Becker et al., 2006; Lloyd et al., 2009; Williams et al., 2009). Through these domains, NBS1 and in effect the MRN complex interacts with various mediator/effector proteins, which include CtIP, γ-H2AX, ATM and MDC1 (Chapman and Jackson, 2008; Kobayashi et al., 2002; Lloyd et al., 2009; Palmbos et al., 2008; Wang et al., 2013b; Williams et al., 2009). Additionally, all NBS1 orthologs have conserved Mre11 interacting motif at their carboxy terminus (Desai-Mehta et al., 2001; Schiller et al., 2012; Tauchi et al., 2001; You et al., 2005). NBS1 is phosphorylated by ATM at sites S278 and S343, which mediates the intra-S phase checkpoint activation (Buscemi et al., 2001; Lim et al., 2000). The lack of NBS1 in mice is embryonic lethal while cells from the NBS patients are highly sensitive to IR indicating the dysfunctional NHEJ (Tauchi et al., 2002b; Zhu et al., 2001). Similarly in Nbs1 deficient DT40 chicken cells, they show great reduction in sister chromatid exchange (SCE) upon mitomycin C exposure and defects in MMEJ (Tauchi et al., 2002a). However, cells from NBS patients show elevated level of chromosomal translocation at T-cell receptors (TCR) (Tauchi et al., 2002b). It is consistent with the residual role of MRN in Alt-EJ, specifically in V(D)J recombination (Zha et al., 2009).

1.3.2.2 CtIP

CtIP was initially identified as co-factor of CtBP (C-terminal binding protein), which acts as co-repressor of transcription (You and Bailis, 2010). It has been shown to physically interact with the MRN complex and especially with the FHA domain of NBS1 but its recruitment to damage sites by MRN may be indirect as CtIP accumulates after 5-15 minutes of DNA damage (Chen et al., 2008b; Lloyd et

al., 2009; Sartori et al., 2007; Williams et al., 2009; You et al., 2009; Yuan and Chen, 2009). Both amino and carboxy termini of CtIP have been shown to participate in the interaction with MRN. CtIP (and Sae2) is a highly phosphorylated protein in S phase and mutants lacking the specific phosphorylation sites exhibit DNA end resection and HR defects (Huertas et al., 2008; Huertas and Jackson, 2009; Yu and Chen, 2004). CtIP is targeted by both ATM and CDK2 (Li et al., 2000; You et al., 2009). The cell cycle specific phosphorylation of CtIP by CDK2 at sites S327 and T847 is essential for its function in resection and hence HR (Huertas and Jackson, 2009; Yu et al., 2006). The mutation of S327A impairs the CtIP recruitment at DSB whereas mutants with T847A are defective in resection. In yeast, the mutation of equivalent site of T847 in Sae2 (S267A) renders the cells HR deficient, especially when DNA ends are capped by protein block or secondary structures like hairpin (Huertas et al., 2008). BRCA1 also interacts with CtIP upon S327 phosphorylation and ubiquitinates the later (Yu et al., 2006). However, there are conflicting reports regarding the functional importance of this interaction (Nakamura et al., 2010). Recently it was shown that BRCA1 interaction with CtIP, though not essential, accelerates the MRN-CtIP mediated resection (Cruz-Garcia et al., 2014). In response to DNA damage, CtIP is also targeted by ATM and has been implicated in the facilitation of CtIP localization to the damage sites (You et al., 2009). Specifically, three sites in CtIP i.e. S664, S745 and T859 have been identified to be targeted by ATM (Kousholt et al., 2012; Wang et al., 2013b; You et al., 2009). However, these sites were dispensable for the recruitment of CtIP but combined phospho-deficient mutants of these sites showed severe HR defects (Wang et al., 2013b). In particular, mutants of T859A exhibited strongly reduced HR while combined mutations of S664A S745A had only limited HR defects. Furthermore, it was shown that cell cycle regulated phosphorylation of CtIP by CDK2 is pre-requisite for ATM activity on the identified sites (Wang et al., 2013b). The structural analysis of the N-terminal domain of CtIP showed that it exists as a homo-tetramer, which is arranged as dimer of dimer in a head to head configuration by their amino termini (Davies et al., 2015). The disruption of CtIP tetramerization by a mutation of the conserved residues implicated in the self-

interaction impairs its recruitment and consequently results in a defective HR (Davies et al., 2015; Wang et al., 2012).

1.4 Regulation of DNA end resection

DNA end resection represents the crossroad between NHEJ and HR (Symington and Gautier, 2011). DSB repair by HR upon DNA end resection must be restricted to the S/G2 phase to prevent ectopic recombination with a non-sister chromatid sequence. Therefore it is not surprising that resection is primarily regulated by CDK activity in a cell cycle-dependent manner (Shrivastav et al., 2008). NHEJ is the predominant pathway to repair DSBs throughout the cell cycle (Chiruvella et al., 2013; Karanam et al., 2012). Ku binds to the DNA ends and facilitates NHEJ and thereby suppresses HR by preventing DNA end resection. In S/G2 phase, many HR proteins are targeted by CDK (along with other kinases including ATM and ATR), which activates their HR function (Krejci et al., 2012). Hence low activity of CDK/CDK2 and Ku-bound ends in G1 inhibits DSB end resection (Aylon et al., 2004; Clerici et al., 2008; Ira et al., 2004). Ku deletion in G1 arrested yeast cells restores the Mre11-dependent initial resection, though HR is still defective due to the absence of long-range DNA end resection (Barlow et al., 2008; Clerici et al., 2008; Zierhut and Diffley, 2008). In accordance, CDK inhibition in G2/M phase arrested cells impairs resection (Aylon et al., 2004; Clerici et al., 2008; Ira et al., 2004). In S/G2 phase, the majority of DSBs are still repaired by NHEJ by a Ku-dependent pathway (Mao et al., 2008). The suppression of short-range resection by CDK inhibition can be alleviated by the deletion of *Yku80* in G1 or G2 cells. However, CDK activity becomes essential for resection when Ku is present (Clerici et al., 2008).

How does CDK actually regulate HR in upon S-phase transition? Sae2/CtIP with MRX/N is required for initial short-range resection. It is phosphorylated by CDK/CDK2 upon entering in S/G2 phases (Huertas et al., 2008; Huertas and Jackson, 2009; Manfrini et al., 2010). Additionally, Sae2/CtIP is further phosphorylated by ATM upon DSB induction, which is necessary for its role in HR (Wang et al., 2013b). In particular, phosphorylation by CDK/CDK2 at sites S267 and T847 in Sae2 and CtIP respectively is critical for DNA end resection. In

mammalian cells, while phospho-deficient mutant of CtIP at T847 site show impaired resection, phosphomimetic mutants can bypass the requirement of CDK2 activity (Huertas and Jackson, 2009). In addition, embryonic lethality of mice with homozygous mutation of CtIP$^{T847/T847A}$ emphasizes the importance of CtIP phosphorylation by CDK2 (Polato et al., 2014). Hence, according to the current model, resection is inhibited in G1 due to a low activity of CDK/CDK2 and the failure of removal of Ku from DNA ends by MRX-Sae2/MRN-CtIP complex. Conversely, cells transition to S-phase by CDK/CDK2 also results in the phosphorylation of Sae2/CtIP, which empowers MRX-Sae2/MRN-CtIP complex to remove DNA-end bound Ku and promoting resection.

Resection is the key event, which determines the pathway choice in DSB repair. However, to reach the stage where resection can occur, various proteins promote their specific pathway while negatively regulate the alternative pathway (Symington, 2014a). In particular, the tumour suppressors 53BP1 and BRCA1 have been shown to crucial for promoting NHEJ or HR in mammalian cells (Daley and Sung, 2014). In the G1 phase, 53BP1 accumulates at DSBs and prevents end resection (Bothmer et al., 2010) (Figure 6). Upon entering the S-phase, 53BP1 is replaced by BRCA1, which facilitates the resection (Bunting et al., 2010). The cell lethality associated with other severe defects in BRCA1 deficient cells can be rescued by a 53BP1 deletion (Bouwman et al., 2010; Bunting et al., 2012; Bunting et al., 2010). Similarly, embryonic lethality due to BRCA1 deficiency in mice can be rescued by elimination of 53BP1 (Bunting et al., 2010). Interestingly, elimination of 53BP1 results in the localization of BRCA1 at DBSs in G1 phase while BRCA1 depletion results in 53BPA accumulations at break sites in S-phase (Escribano-Diaz et al., 2013). It indicates that the recruitment mechanism for both proteins is intact throughout cell cycle and additional level of regulation is required to determine the repair pathway choice.

The RNF8-RNF168 (E3 ligases) mediated ubiquitination of histone H2A is required for the recruitment of both 53BP1 and BRCA1 (Daley and Sung, 2014; Mailand et al., 2007). 53BP1 is recruited to the break sites through association with multiple proteins, which also involve its interactions with the BRCT

domains of MDC1, dimethylated H4 at K20 (H4K20me2) and ubiquitinated H2A at K15 (Botuyan et al., 2006; Eliezer et al., 2009). RIF1 and PTIP are effector proteins of 53BP1, which together attenuate the resection though the exact mechanism is still not clear (Callen et al., 2013; Chapman et al., 2013; Di Virgilio et al., 2013; Escribano-Diaz et al., 2013; Zimmermann et al., 2013). The interactions between these effectors and 53BP1 are ATM-phosphorylated dependent, indicating them as specific to DNA damage response (Bothmer et al., 2011). Similar to 53BP1, BRCA1 recruitment is dependent on RNF8-RNF168 but unlike 53BP1, it also requires RNF8-RNF168 downstream RAP80 associated complex for its efficient recruitment (Kim et al., 2007; Mailand et al., 2007; Sobhian et al., 2007; Wang et al., 2007). BRCA1 is an E3 ubiquitin ligase and it is known to ubiquitinate CtIP though functional importance of this modification is not known. BRCA1 also interacts with MRN through phosphorylated CtIP (Chen et al., 2008b; Yu et al., 2006). How BRCA1 influences resection is still not well understood. Intriguingly, phosphorylation dependent CtIP resection is proficient in 53BP1 and BRCA1 deficient cells (Bunting et al., 2010). It indicates that BRCA1 may function upstream of CtIP to relieve 53BP1 suppressing effect on resection. Investigation of the interplay between 53BP1 and BRCA1 by super resolution microscopy hints that BRCA1 may spatially exclude 53BP1 from DBS sites (Chapman et al., 2012).

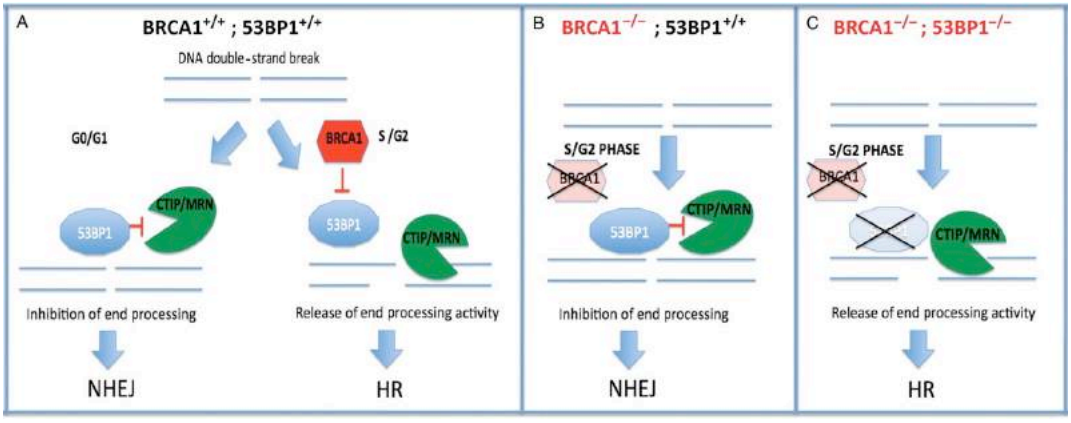

Figure 6. Regulation of DNA end resection by 53BP1 and BRCA1. In G^0/G1 phase, BRCA1 binding to DSBs is inhibited by 53BP, which in turn prevents end resection by MRN and CtIP and promotes NHEJ. In S-phase/G2 phase, BRCA1 is activated by not well-understood mechanism and inhibits the 53BP1 binding to DNA, which allows MRN and CtIP to resect the DNA ends leading to promotion of HR. Removal of BRCA1 in S-phase permits the 53BP1 binding to DSB, which suppress resection and consequently HR. When both 53BP1 and BRCA1 are lacking, resection still occurs in S/G2 phase indicating the upstream role of 53BP1 and BRCA1 before resection (adapted from Aly and Ganesan, 2011 *Journal of Molecular Cell Biology*).

1.5 Meiosis and homologous recombination

With millions of years of evolution and through the process of meiosis, cells have developed an ingenious way to exploit and employ DSB repair process to a specific purpose (Bernstein and Bernstein, 2010). In eukaryotes, diploid cells undergo two successive cell divisions to produce four haploid gametes. In short, meiosis is a specialized cell division, which exclusively occurs in the germ cells and consists of one round of replication followed by two rounds of cell division i.e. meiosis I and meiosis II (Alberts et al., 2015). The defining and distinct feature of meiosis from mitosis is the alignment and separation of replicated homologous chromosomes in meiosis I. In meiosis II, each chromosome containing a pair of attached sister chromatids is further split into single chromatids, giving rise to four haploid cells. Although the origin and the detailed mechanism of meiosis still lacks consensus among biologists, it has been firmly established that the process of meiosis creates genetic diversity in the population by exploiting recombination (Wilkins and Holliday, 2009). Other than recombination, the random distribution of parental homologous chromosomes to haploid daughter cells during segregation also contributes to genetic diversity. The proper alignment of homologous chromosomes by recombination ensures their correct segregation and hence prevents adverse situation such as non-disjunction, which can lead to aneuploidy resulting in pathological conditions including Down's syndrome(Antonarakis, 1991; Antonarakis et al., 1992) .

Meiosis I and meiosis II are divided into five sequential events according to cytologically visible structures. These sub-phases of meiosis I and meiosis II are prophase I and II, metaphase I and II, anaphase I and II and telophase I and II respectively. Prophase I is the longest phase of meiosis, which is further sub-divided into four stages, namely leptotene, zygotene, pachytene and diplotene. The process of alignment and recombination between homologous chromosomes occurs in prophase I. The brief detail of summary of actions in during the prophase I is shown in Figure 7.

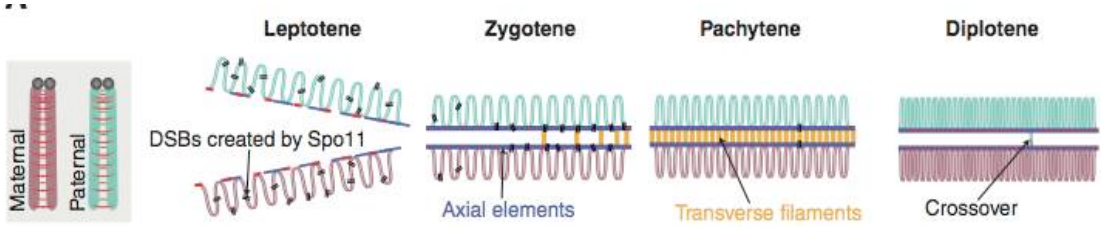

Figure 7. Different stages of prophase I in meiosis. Prophase I initiates with the leptotene stage in which chromatids become individualized and visible. DSBs occur in leptotene. In the next stage of zygotene, homologous chromosomes begin to line up with each other, which is facilitated by the synaptonemal complex (SC) . The synapsis is fully competed in pachytene and crossing over occurs during this stage forming chiasmata sites. During deplotene, SC degrades and connections between homologous chromosomes are lost except at the sites of chiasmata until they are resolved at anaphase I.

Although both somatic and germ cells utilize HR pathway to repair DSBs, there are some major mechanistic variations between the mechanisms of the processes and its final outcome (Andersen and Sekelsky, 2010). The first difference lies in the origin of DSBs. While DSBs in mitosis are accidental in nature, meiotic DSBs are produced in a programmed manner by meiosis-specific nuclease Spo11 (Murakami and Keeney, 2008). Second, while sister chromatids are overwhelmingly used as template in mitotic cells to avoid loss of heterozygosity, homologous chromosomes are the preferred choice as a template for DSBR in meiotic cells (Bzymek et al., 2010; Kadyk and Hartwell, 1992; Lao and Hunter, 2010; Schwacha and Kleckner, 1997). The third major difference is in the final outcome of the DSB repair. DSBR in the mitotic cells predominantly results in non-crossover products with only a small proportion of crossover products (Haber and Hearn, 1985; Nickoloff and Brenneman, 2004; Stark and Jasin, 2003). In contrast, meiotic cells have a specific pathway dedicated to produce exclusively crossover products (Guillon et al., 2005; Martini et al., 2006; Mehrotra and McKim, 2006). Despite that, non-crossovers are still detected in meiotic HR, which arise due to pathways operational in vegetative cells (Andersen and Sekelsky, 2010).

1.5.1 Gene conversion (GC), noncrossover (NCO), and crossover (CO)

The actual exchange of genetic information between donor and acceptor duplex in HR is primarily determined by the choice of template for repair and by the

specific processing of recombination intermediates. As explained above, both crossover and noncrossover products form during meiotic HR. It is believed that noncrossover products can arise early in meiosis due to SDSA, or later upon dissolution and symmetrical resolution of dHJs (Youds and Boulton, 2011). In contrast, crossovers can only be produced by an asymmetrical cleavage of dHJs (Heyer, 2004; Wyatt and West, 2014). Noncrossovers only involve non-reciprocal exchange of information by copying donor DNA sequence through DNA synthesis. Typically, NCO between sister-chromatids results in no DNA sequence alteration of the repaired duplex. On the other hand, the extent of dissimilarity or heterology at repair site between non-sister chromatid sequences determines the level of genetic alteration. The process of sequence modification of the newly repaired duplex due to heterology between donor and acceptor duplexes is known as gene conversion (Chen et al., 2007). Additionally, when DNA synthesis during the 3' strand extension is erroneous and MMR is defective to remove wrongly incorporated mispaired nucleotides, gene conversion can occur even in between sister chromatids. Similarly to noncrossovers, crossover events between sister chromatids do not exhibit any change of DNA sequence. In contrast, COs occurring between homologs drastically alters the identity of both resulting duplexes through the asymmetrical cleavage of dHJ, which results in the complete exchange of flanking regions at one side of the dHJ. Moreover, like with the case of NCOs, GC can accompany COs in addition to physical swapping of DNA irrespective of template used for repair.

1.5.2 Regulation of COs

Crossing over in meiosis is required to provide physical connection between homologous chromosomes for their subsequent segregation (Bascom-Slack et al., 1997). Therefore, meiotic HR ensures the formation of at a minimal number of COs known as obligate COs (Jones, 1984; Martini et al., 2006). In fact, the Spo11-induced DSBs are produced in excess to guarantee the formation of these obligate COs (Keeney, 2008). For example, only 1 out of 10 DSBs are repaired as COs in mouse spermatocytes (Borner et al., 2004; Moens et al., 2002). In both *S. cerevisiae* and *C. elegans,* only half of DSBs are finally converted to COs while rest

are repaired as either interhomolog (IH) NCOs or intersister (IS) recombinants (Chen et al., 2008c; Hillers and Villeneuve, 2003; Mancera et al., 2008). Most organisms have regulatory mechanisms known as CO homeostasis, which ensures the formation of obligate COs upon diminished DSBs (Martini et al., 2006). In *S. cerevisiae*, when DSBs levels are reduced by the usage of hypomorphic mutant of *spo11*, obligatory COs still form at the expense of decreased NCOs. Besides CO homeostasis, another regulatory mechanism known as CO interference exists in meiosis, which governs the spatial distance between the multiple COs on the same chromosome (class I COs) (Hillers, 2004; HJ, 1916). In essence, the presence of CO at particular site decreases the likelihood of the formation of another CO in the near vicinity. In budding yeast, multiple COs (~5-6) form on each chromosome, which are evenly spaced from each other (Mancera et al., 2008). Such spatial distribution of COs would not have been observed if COs occurred independently of each other. However, situation is quite complicated, as COs can be both interference dependent (Class I COs) or independent (Class II COs), which arise due to distinct pathways that will be described in Section (Allers and Lichten, 2001; Kohl and Sekelsky, 2013)

1.6 Mechanism of meiotic homologues recombination

The process of meiotic HR is best understood in *S. cerevisiae*, but the mechanism is highly conserved in many-studied organisms though some substantial differences exist. Here, I will describe the mechanism of meiotic HR as discovered in *S. cerevisiae.*

Meiotic homologous recombination begins with the introduction of DSBs by Spo11 (Keeney, 2008). Spo11 is related to archaeal topoIV topoisomerase, and functions as a homodimer (Bergerat et al., 1997). It cleaves both strands of DNA duplex by transesterification reaction and covalently attaches to both 5' ends through tyrosine-DNA linkage (Keeney et al., 1997). In yeast, the reduced level or failure in production of DSBs leads to meiotic arrest or formation of inviable gametes with aneuploidy (Szekvolgyi et al., 2015). However, the nature of Spo11-induced DSBs is not unique in the sense that DSBs produced by other exogenous factors such as IR, HO endonuclease, I-SceI endonuclease etc. can compensate for the loss of Spo11 activity (Farah et al., 2009; Kolodkin et al., 1986; Malkova et al., 2000). Similar to CO interference, the distribution of DSBs on the chromosomes is non-random and the presence of one DSB inhibits the occurrence of another DSB in the near vicinity by "DSB interference" (Szekvolgyi et al., 2015). Such interference exerts this effect on the same (i.e. *cis*) as well as homologous chromosome on a cognate allelic site (*trans*) (Fan et al., 1997; Robine et al., 2007; Rocco et al., 1992; Xu and Kleckner, 1995; Zhang et al., 2011). In addition, DSB levels are regulated by the process of DSB homeostasis, in which suppression of a "hotspot" region elicits the production of DSBs elsewhere to maintain the sufficient number of DSBs (Pecina et al., 2002; Robine et al., 2007). The DSB production by Spo11 is followed by resection, which is initiated by the MRX -Sae2 complex. As explained earlier in Section X, MRX-Sae2 complex nicks the strand endonucleolytically to remove DNA bound-Spo11 and resects the DNA back to towards the breaks. Like in the vegetative cells, the limited resection is followed by long-range resection, which is mediated by Exo1 only as Sgs1-Dna2 usually do not participate in resection in meiosis (Symington, 2014b). The presence of Spo11 at DNA ends is inhibitory to resection by Exo1, and the initial

processing by MRX-Sae2 is therefore essential. However, extensive resection in meiosis is not strictly necessary as *exo1Δ* mutant, while showing a dramatic decrease in resection, still forms recombination intermediates normally (Zakharyevich et al., 2010b).

In the subsequent step, 3' overhangs produced by resection are coated by RPA, which is followed by DNA strand invasion. The invasion of the 3' overhang into donor duplex creates structures known as single end invasions (SEIs) (Hunter and Kleckner, 2001). Unless stabilized by additional factors, these structures can be disrupted by the dissociation of invaded strand from the donor duplex. The "ZMM" proteins, including the Msh4-Msh5 (MutS homolog 4 and 5) heterodimer have been proposed to function as stabilizing factor for SEIs (Bishop and Zickler, 2004; Borner et al., 2004; Hunter and Kleckner, 2001). Other than stabilizing SEIs, Msh4-Msh5 is postulated to function the in later steps of HR as well (see section 1.7.2) (Moens et al., 2002; Snowden et al., 2004). The DNA strand exchange in meiosis is primarily carried out by meiosis-specific protein Dmc1 with the help of Rad51 (Bishop et al., 1992) (Brown and Bishop, 2015). The catalytic DNA strand exchange activity is provided by meiosis-specific protein Dmc1 while Rad51, with its dispensable enzymatic activity, is still required for Dmc1's normal function (Cloud et al., 2012). Deletion of *DMC1* in budding yeast results in the accumulation of DSBs and blockage at the strand-exchange stage while *rad51Δ* mutants show somewhat lesser impairment (Bishop et al., 1992; Schwacha and Kleckner, 1997; Shinohara et al., 1992; Shinohara et al., 1997). This differential usage of strand exchange proteins has been attributed to Dmc1's capacity to promote inter-homolog (IH) bias, which is necessary for meiotic recombination (Hong et al., 2013; Lao et al., 2013). Next, similarly to the mitotic HR, invaded strand is elongated by DNA synthesis, which results in D-loop extension. At this step, the invaded strand can anneal back to the original strand by the SDSA pathway producing NCO products only (McMahill et al., 2007; Sun et al., 1991). The balance between pro- and anti-CO factors is crucial for the successful recombination. Many recombination intermediates produced during HR can be reverted back to the preceding structure by DNA helicases, including Sgs1, Srs2 and Mph1 (Wu and Hickson, 2006). The role of Sgs1 is more complex

as though it functions as anti-CO in mitotic HR; it is designated as central regulator for the production of crossover in meiosis, however the underlying mechanism is not clear (De Muyt et al., 2012; Zakharyevich et al., 2012). Sgs1 also removes non-productive multi-chromatic structures arising due to DNA entanglements (Oh et al., 2007).

Once cells have stabilized the extended D-loop and overcame the hurdles imposed by various helicases, the second end of the broken chromosome is captured, which ultimately results in dHJ formation (Kowalczykowski, 2015). The elimination of dHJs is essential for the proper segregation of chromosomes. Like somatic cells, meiotic cells are also equipped with multiple pathways, which include dissolution, resolution and CO-biased resolution to remove dHJs (Jasin and Rothstein, 2013). The mechanistic details of these pathways are described in the subsequent sections (Figure 8).

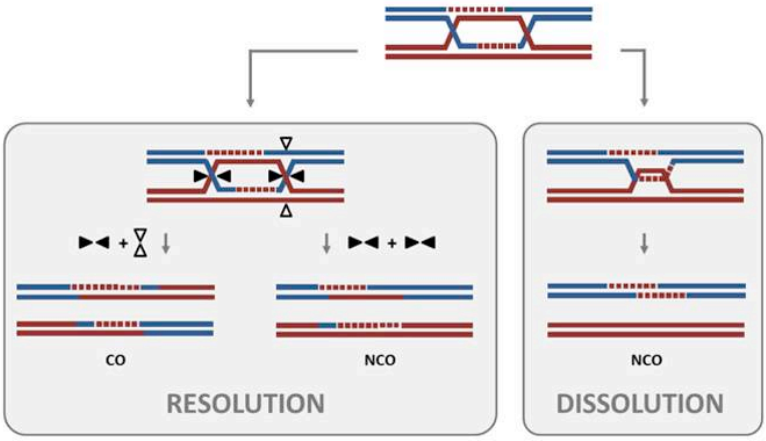

Figure 8. Removal of double Holliday junction. The specific processing of dHJ determines the nature of final product. The convergent branch migration of holliday junctions in dHJ, followed by untangling of hemicatenane structure results in dissolution, which only give rise to non-crossover products. The symmetrical cleavage of dHJ produces non-crossovers products while asymmetrical cleavage results in crossover products. Gene conversion can occur in all described situations irrespective of mode of dHJ processing (modified from Knoll et al, 2014 *Frontier in Plant Science*).

1.6.1 Dissolution

Dissolution is a primary mechanisms used in mitotic cells to remove dHJs, and results in NCOs only (Bizard and Hickson, 2014). It is carried out by the concerted efforts of Sgs1, Top3 and Rmi1 that together form a "dissolvasome"

complex (Cejka et al., 2012). Similarly, BLM-TOPIIIIα-RMI1 (BTR) complex with the additional partner protein termed RMI2 forms the dissolvasome complex in humans (Plank et al., 2006; Raynard et al., 2006). The mechanism of dissolution is mainly studied by reconstitution of the dissolution reaction *in vitro* with the use of purified recombinant proteins and oligo- and plasmid-based dHJ substrates. Mechanistically, two Holliday junctions in dHJ are converged in the centre by branch migration driven mainly by Sgs1, and supported by the topoisomerase activity of Top3. The convergence of HJs produces hemicatenane structure, which is topologically removed by Top3 (Bizard and Hickson, 2014). The third partner of STR complex, Rmi1 strongly stimulates the dissolution reaction (Cejka et al., 2010b). Specifically, analysis of Rmi1 with plasmid-based dHJ showed its role primarily in the final decatenation step rather than in a branch migration.

The exact mechanism of branch migration by Sgs1 is not fully understood. However Sgs1 unwinding and annealing activities have been suspected to function in a coordinated manner to carry out the branch migration. The ATPase activity of Sgs1/BLM is necessary for branch migration (Cejka et al., 2010b; Raynard et al., 2006; Wu and Hickson, 2003). Deletion of *SGS1* in mitotic cells results in increased HR, illegitimate recombination and gross chromosomal rearrangements (Myung et al., 2001; Myung and Kolodner, 2002; Onoda et al., 2000; Watt et al., 1996; Yamagata et al., 1998). Humans possess four more RecQ homologs in addition to BLM, the closet counterpart of Sgs1. However, no other human homolog can replace BLM functionally in dissolution (Wu et al., 2005). BLM mutations in humans cause Bloom syndrome, which predisposes affected individuals to cancer development (Ellis and German, 1996). Consistently, cells from the Bloom syndrome patients show increased sister chromatid exchange (SCE) level with other chromosome segregation defects (Chaganti et al., 1974). Removal of *TOP3* in *Schizosaccharomyces pombe, Drosophila melanogaster* and mice is lethal, while *top3Δ* mutants of *S. cerevisiae* although viable grow very slowly (Goodwin et al., 1999; Li and Wang, 1998; Maftahi et al., 1999; Plank et al., 2005). The slow growth of *top3Δ* mutants can be suppressed by the deletion of *sgs1*(Gangloff et al., 1994). Yeast mutants lacking Rmi1 phenocopy *top3Δ*

features (Chang et al., 2005). Like Top3 and Sgs1, deletion of Rmi1 is synthetically lethal with the deficiency in HJ resolvases (Mullen et al., 2005). Though dissolution occurs frequently in somatic cells to remove dHJs, most of the NCOs produced during meiosis arise by the SDSA pathway. The relative contribution of dissolution in NCOs production during meiosis is currently not known. The plurality of functions of STR/BTR proteins at multiple steps in HR makes it difficult to determine the level of NCOs by dissolution.

1.6.2 Resolution by structure selective endonuclease (SSE)

Dissolution primarily occurs in during S-phase in somatic cells. Double HJs, which escape processing by dissolution, are eliminated later in the cell cycle by the nucleolytic activity of specific SSEs known as "resolvases"(Matos and West, 2014). In particular, deletion of *SGS1* in budding yeast results in the accumulation of JMs, which are later processed by resolvases (Dayani et al., 2011; Matos et al., 2011). This indicates that resolution functions as back pathway for joint molecule processing in vegetative cells (Szakal and Branzei, 2013). These resolvases include Mus81-Mms4, Slx1-Slx4 and Yen1 in budding yeast, while in humans they are MUS81-EME1/EME2, SLX1-SLX4 and GEN1 (Blanco and Matos, 2015). Although the action and regulation of these nucleases have been best defined in vegetative cells, they follow a similar pattern of regulation in meiotic cells as well (Matos and West, 2014). However, as dissolution is less frequent (or absent) in meiosis, the requirement for SSEs in meiosis is higher than in vegetative cells. In Mus81-Mms4, both subunits contain a distinctive ERCC4 (ERCC excision repair 4) nuclease domain but disruptive mutation in the nuclease domain of Mms4 renders it non-enzymatic partner of Mus81 (Ciccia et al., 2008). Therefore Mms4 plays only a structural role, enhancing the overall nuclease activity of the complex. Mus81-Mms4 is capable of cleaving a variety of structures including 3'-flaps, D-loop and nicked-HJ, showing a lower activity on intact HJs (Boddy et al., 2001; Ciccia et al., 2003; Constantinou et al., 2002; Doe et al., 2002; Kaliraman et al., 2001). In mitotic cells, Mus81-Mms4 activity is low during S- and G2 phase (Gallo-Fernandez et al., 2012; Matos et al., 2011; Matos et al., 2013; Szakal and Branzei, 2013). At the onset of mitosis, the concerted action of Cdc28 and Cdc5 results in the

phosphorylation of Mms4 at it N-terminal region enhancing the nuclease activity of Mus81-Mms4. Similarly in meiotic cells, phosphorylation by Cdc28 and Cdc5 occurs at the onset of first meiotic division (Matos et al., 2011). MUS81-EME1 in humans has acquired slightly different approach than yeast for its activation. Similar to yeast orthologs, CDK1 phosphorylates MUS81-EME1 at the onset of mitosis, which increases its HJ processing capacity (Wyatt et al., 2013). However, this modification also leads to MUS81-EME1 association with another SSE SLX1-SLX4 forming SLX-MUS complex, which then functions as a single active nuclease complex to process JMs (Castor et al., 2013; Garner et al., 2013). It is noteworthy that in budding yeast, *slx1Δ* and *slx4Δ* mutants do not show any significant meiotic defects (Mullen et al., 2001; Zakharyevich et al., 2012). In contrast to Mus81-Mms4 activation, phosphorylation of Yen1 by CDK inhibits its activity (Blanco et al., 2014; Eissler et al., 2014; Matos et al., 2011). Specifically, the phospho-deficient mutations of CDK-sites S655 and S679 could bypass the requirement of Cdc-14 phosphatase, which targets Yen1 and allows its entry into nucleus. (Eissler et al., 2014; Kosugi et al., 2009). Additionally, the phospho-mimicking mutations of S655 and S679 impair Yen1 nuclease activity (Eissler et al., 2014). Upon entering the anaphase, Cdc14 phosphatase removes CDK-mediated phosphorylation from Yen1, which enables its import into nucleus and transforms it into a potent nuclease (Blanco et al., 2014; Eissler et al., 2014). Similarly to Yen1, human GEN1 entry into the nucleus is inhibited by CDK1 mediated phosphorylation in S-and G2 phases (Matos et al., 2011). However, the nuclease activity of GEN1 is not affected by its phosphorylation to the degree of Yen1 (Chan and West, 2014). Only in late meiosis at the second division, CDK1 mediates the break down of nuclease envelope, which allows GEN1 localization into nucleus (Guttinger et al., 2009). This temporal and sequential application of distinct JMs processing mechanisms ensures the removal of all JMs with the formation of desired products i.e. CO or NCO in both meiosis and mitosis.

All identified resolvases cleave a variety of branched structures. While Yen1/GEN1 and Slx1-Slx4/SLX1-SLX4 can cleave intact HJs, Mus81-Mms4 requires a nick in the HJ structure to cleave it, at least *in vitro* (Blanco and Matos, 2015). Additionally, Yen1/GEN1 is a canonical HJ resolvase, which cleaves HJs by

making symmetrical and opposite incisions across the junction to produce ligatable products. In contrast, other resolvases asymmetrically nicks HJs, generating products, which cannot be ligated *in vitro*. The *in vivo* analysis has showed that in spite of having different modes of cleavage, all these nucleases produce equal amount of CO and NCO products (Schwartz and Heyer, 2011). Importantly, COs produced by resolvases are interference independent (de los Santos et al., 2003; de los Santos et al., 2001; Interthal and Heyer, 2000; Oh et al., 2008). In fission yeast, Mus81-Eme1 (ortholog of Mms4) is the primary nuclease responsible for COs production and hence COs in *S. pombe* do not exhibit interference (Boddy et al., 2001). The symmetrical cleavage by resolvases indicates that the nicking of two HJs in the dHJ structure is not coordinated and hence independent of each other. Therefore this random processing by these resolvases equally generates both CO and NCO products. Such mode of cleavage is not ideal when a particular final product, i.e. CO, is desired. Therefore as CO formation is necessary in meiosis for genetic recombination and proper chromosome segregation, meiotic cells cannot rely solely on the activity of the above described nucleases, and therefore require a dedicated mechanism to ensure formation of obligate COs (see section 1.8).

1.7 Mlh1-Mlh3 (MutLγ) mediated biased resolution

The identification of the above described resolvases solved how COs form in somatic cells. However various studies carried out in budding yeast, mice and humans indicated the existence of an additional pathway responsible for the formation of majority of COs in meiosis (Zakharyevich et al., 2012). Analysis of recombination products by DNA physical assay in budding yeast provided a deeper insight into the nature and logistic of JMs processing and thereby CO formation. More than decade earlier, it was shown that the removal of Mus81-Mms4 pathway in yeast resulted only in a 20% decrease in COs (Argueso et al., 2004). By extending the scope of the investigation, another seminal study showed that deletion of all three identified resolvases similarly resulted in only ~ 20% reduction of CO numbers, which corroborated the previous findings (Zakharyevich et al., 2012). Multiple studies in different organisms revealed the existence of a pathway dependent on Mlh1-Mlh3 in meiosis responsible for CO formation (Baker et al., 1996; Hunter and Borts, 1997). Specifically, a single deletion of *MLH3* in budding yeast exhibited 70% reduction in CO levels, while a disruption of *MLH3* in mice rendered them sterile (Lipkin et al., 2002; Wang et al., 1999). Consistent with earlier findings, disruption of *mlh3* in addition to triple deletion of *mms4 slx4 yen1* resulted in a complete elimination of COs (Zakharyevich et al., 2012). Surprisingly, the COs formation by Mlh1-Mlh3 was dependent on the presence of Sgs1, which had been previously described as anti-CO factor. How does Sgs1 act as pro-crossover factor in meiosis besides being responsible for majority of NCOs in vegetative cells? Whether it cooperates with Mlh1-Mlh3 at later stage or helps earlier in preparing the appropriate substrate for Mlh1-Mlh3 processing is still a matter of on-going investigation. In addition to Sgs1, Exo1 was also shown to play an essential structural role in CO formation together with Mlh1-Mlh3, which was independent of its nucleolytic activity (Zakharyevich et al., 2010a). Mlh1-Mlh3 processes JMs to produce exclusively COs, while Mus81-Mms4 processes a subset of JMs generating COs and NCOs in an equal ratio. However, when Sgs1 is missing, NCOs are reduced and JMs level rises, which are primarily resolved by Mus81-Mms4. Additionally, while Slx1-Slx4 becomes indispensable in the *sgs1Δ mms4Δ* mutants, Yen1 can only partially

compensate the for loss of *mms4* in these mutants (Zakharyevich et al., 2012). The normal formation of JMs in the absence of *mlh1* or *mlh3* further suggests their later role in CO formation. Many studies have indicated that Mlh1-Mlh3 and Msh4-Msh5 function in the same pathway and give rise to obligate COs, which are class I-interference dependent.

1.7.1 Role of Mlh1-Mlh3 in meiosis and CO formation

MutLγ was initially suspected to play role in the MMR pathway as it belongs to the MutL family of proteins. Although several reports suggest its minimal but consistent role in MMR, its major function has been discovered in meiotic CO formation. Unlike in case of the NCOs products, COs can only arise upon nucleolytic cleavage of dHJs. Another member of the MutL family, MutLα (Mlh1-Pms1 in yeast; MLH1-PMS2 in mammals) with a nuclease domain in Pms1/PMS2, has been firmly established as cryptic endonuclease in MMR (see section 1.2.3) (Kadyrov et al., 2006). Sequence alignment of Mlh3/MLH3 with Pms1 and PMS2 subunits identified the presence of conserved nuclease motif $DQHAX_2EX_4E$ in the C-termini of the polypeptides. Remarkably, a disruption of this motif in budding yeast MLH3 phenocopies *mlh3Δ* mutant defects, indicating the functional importance of this nuclease motif (Nishant et al., 2008). Similarly, triple deletion mutant of *mms4Δ slx1Δ yen1Δ* with nuclease dead *mlh3* exhibited severe reduction in CO as was observed for the *mms4Δ slx1Δ yen1Δ mlh3Δ* quadruple mutant (Zakharyevich et al., 2012). Besides genetic evidence, biochemical characterization of yeast MutLγ revealed its nicking activity on super-coiled dsDNA in the presence of Mn^{2+} (Ranjha et al., 2014). Additionally, both yeast and human MutLγ exhibited DNA binding preference to HJ-like structures. In mice, deletion of *MLH1* leads to 10-fold reduction in COs, increased frequency of aneuploidy and apoptosis (Baker et al., 1996). Similarly, the lack of MLH3 also results in aneuploidy and apoptosis. Both $MLH1^{-/-}$ and $MLH3^{-/-}$ mice are infertile (Lipkin et al., 2002).

1.7.2 Role of Msh4-Msh5 (MutSγ) in meiosis and CO formation

Like MutLγ, Msh4 and Msh5 were initially suspected to function in MMR pathways as they structurally belong to MutS family of MMR proteins (Lynn et al., 2007). However, it was shown later that they function in meiosis as a heterodimer and have no role in MMR (Hollingsworth et al., 1995). Functionally, they have been categorized as part of the ZMM group (acronym for yeast proteins Zip1/ Zip2/ Zip3/ Zip4, Msh4/Msh5, Mer3). Mutation of any ZMM group member results in the reduction or absence of COs (Borner et al., 2004; Sym et al., 1993). The orthologs of Msh4-Msh5 have been discovered in many organisms. Intriguingly, while the loss of Msh4 or Msh5 results in a 50-70% reduction of COs in *S. cerevisiae*, the absence of MutSγ in *C. elegans* and mouse eliminates COs completely (de Vries et al., 1999; Edelmann et al., 1999; Hollingsworth et al., 1995; Kelly et al., 2000; Kneitz et al., 2000; Ross-Macdonald and Roeder, 1994; Zalevsky et al., 1999). Similarly in *Arabidopsis thaliana (A. thaliana)*, COs are reduced but not completely abolished in the absence of *atmsh4* or *atmsh5* (ortholog of MSH4 and MSH5 respectively) (Berchowitz et al., 2007). It indicates that although the majority of COs are produced by the MutSγ pathway in *S. cervisiae* and *A. thaliana*, residual COs still occur in their absence. In both organisms, further investigations of the nature of MutSγ dependent and independent COs revealed that while former showed interference, latter COs were interference independent (Kohl and Sekelsky, 2013). Consistently, all COs in *S. pombe*, which lacks MutSγ orthologs, are non-interfering whereas all COs in *C. elegans*, which absolutely depend on MutSγ, display interference (Meneely et al., 2002; Munz, 1994). These observations clearly establish the role of MutSγ in COs formation in the MutLγ-dependent pathway.

Evidences from various studies indicate the role of MutSγ in both early and late stages of recombination. Null mutant of *msh5* exhibits a marked reduction in SEI formation (Borner et al., 2004). In agreement, human MutSγ binds to pro-HJ structures, which resemble SEIs (Snowden et al., 2004). MutSγ is believed to function after strand invasion, most likely in the stabilization of SEI structures. In

additions to its early role, MutSγ has been proposed to have a late role in meiotic HR to facilitate biased CO formation mediated by MutLγ. *S. cerevisiae msh4* and *msh4 mlh1* mutants have similar reduction in the recombination rate (Hunter and Borts, 1997; Stahl et al., 2004). In mouse meiotic cells, Msh4 co-immunoprecipitates with Mlh3 and recombinant Msh4 directly interacts with *in vitro* translated Mlh3 (Santucci-Darmanin et al., 2002). Biochemical analysis of human MutSγ revealed that it binds to the core of oligo-based HJ and slides along the HJ arms upon ATP binding (Snowden et al., 2004). The sliding effect was independent of MutSγ ATP hydrolysis activity. However, whether and how MutSγ promotes CO-specific HJ resolution together with MutLγ in meiotic cells remains to be established.

2. Results

2.1 Phosphorylated CtIP functions as a co-factor of the MRE11-RAD50-NBS1 endonuclease in DNA end resection

Roopesh Anand, Lepakshi Ranjha, Elda Cannavo and Petr Cejka[1]

Manuscript accepted in *Molecular Cell*

I designed the research together with P.C. and performed all the experiments except electrophoretic mobility shift assays (EMSA). The EMSAs were carried out by L.R and yeast proteins used in this study were purified and provided by E.C. All authors analysed the data and I wrote the manuscript with P.C.

Phosphorylated CtIP functions as a co-factor of the MRE11-RAD50-NBS1 endonuclease in DNA end resection

Roopesh Anand, Lepakshi Ranjha, Elda Cannavo and Petr Cejka[1]

Institute of Molecular Cancer Research, University of Zurich, Winterthurerstrasse 190, CH-8057 Zurich, Switzerland

[1]To whom correspondence should be addressed. Tel: +41 44 635 4786;
Email: cejka@imcr.uzh.ch

SUMMARY

To repair a DNA double-strand break (DSB) by homologous recombination (HR), the 5'-terminated strand of the DSB must be resected. The human MRE11-RAD50-NBS1 (MRN) and CtIP proteins were implicated in the initiation of DNA end resection, but the underlying mechanism remained undefined. Here we show that CtIP is a co-factor of the MRE11 endonuclease activity within the MRN complex. This function is absolutely dependent on CtIP phosphorylation that includes the key cyclin-dependent kinase target motif at Thr-847. Unlike in yeast where the Xrs2/NBS1 subunit is dispensable *in vitro*, NBS1 is absolutely required in the human system. The MRE11 endonuclease in conjunction with RAD50, NBS1 and phosphorylated CtIP preferentially cleaves 5'-terminated DNA strands near DSBs. Our results define the initial step of HR that is particularly relevant for the processing of DSBs bearing protein blocks or secondary DNA structures.

INTRODUCTION

To repair a DSB, cells employ either homologous recombination (HR) or non-homologous end-joining (NHEJ) pathway. Whereas HR is template-directed and largely accurate, NHEJ occurs through a ligation of the broken DNA ends in the absence of homology and may therefore lead to mutations in the vicinity of the break site (Chiruvella et al., 2013; Kowalczykowski, 2015). HR commences by a nucleolytic processing of the DSB (Cejka, 2015). Specifically, the 5'-terminated strand of the DSB must be resected to reveal a 3'-terminated ssDNA tail, which becomes a substrate for the strand exchange protein RAD51. RAD51 then catalyzes the invasion of the nucleoprotein filament into homologous DNA, where the newly paired 3'-terminated DNA may prime DNA synthesis (Kowalczykowski, 2015). The choice whether or not to resect broken DNA is thus a critical regulatory step that affects the DSB repair pathway choice. Misregulation of the balance between two key DSB repair pathways leads to

genome instability that is typical in many cancer types (Jackson and Bartek, 2009; O'Driscoll, 2012).

The mechanism of DNA end resection has been extensively studied in recent years. Research from multiple laboratories established that DNA resection is in most cases a two-stage process (Mimitou and Symington, 2008; Zhu et al., 2008). The first step is slow and involves 5' end resection that is limited up to ~200-300 nucleotides away from the DSB. In contrast the second resection step is relatively fast and capable to resect DNA thousands of nucleotides in length. The first phase is catalyzed by the Mre11-Rad50-Xrs2 (MRX) complex and Sae2 in *Saccharomyces cerevisiae (S. cerevisiae)* and the MRE11-RAD50-NBS1 (MRN) complex and CtIP in human cells (Gravel et al., 2008; Mimitou and Symington, 2008; Zhu et al., 2008). The initial 5' DNA end resection by these proteins is especially important for the processing of DNA ends with non-canonical structures, such as protein blocks or DNA secondary structures (Mimitou and Symington, 2010). This has been revealed particularly in yeast meiotic recombination, where Sae2 and the nuclease activity of Mre11 are absolutely required for the resection of DSBs covalently bound by the Spo11 transesterase (Bergerat et al., 1997; Keeney et al., 1997; Moreau et al., 1999; Neale et al., 2005). Topoisomerase poisoning may also result in covalent TopoII-DNA or TopoI-DNA adducts at the ends of broken DNA. Here, the requirement for MRX/N and Sae2/CtIP is less pronounced, possibly due to the presence of Tdp1 and Tdp2 enzymes that can compete for the same substrate (Cortes Ledesma et al., 2009; Deng et al., 2005; Hartsuiker et al., 2009b; Liu et al., 2002; Neale et al., 2005; Pouliot et al., 1999). Moreover, poisoning of TopoI does not necessarily lead to DSBs (Ray Chaudhuri et al., 2012). Nevertheless, Mre11 nuclease and Sae2/CtIP-deficient cells are sensitive to topoisomerase inhibitors in various organisms (Deng et al., 2005; Hartsuiker et al., 2009b; Huertas and Jackson, 2009; Nakamura et al., 2010; Sartori et al., 2007). In budding yeast, the requirement for MRX in DNA end resection can sometimes be bypassed to process "clean" DNA ends, in particular in the absence of the Ku heterodimer (Bonetti et al., 2010; Clerici et al., 2008; Foster et al., 2011; Mimitou and Symington, 2010; Moreau et al., 1999). In contrast fission yeast and higher eukaryotes rely on MRN and Ctp1/CtIP for resection in most cases, and the nuclease of MRE11 is essential for

viability in mouse cells (Buis et al., 2008; Langerak et al., 2011; Sartori et al., 2007). In addition to a catalytical role, the MRN/X complex also has a structural role to promote recruitment of factors belonging to the second resection step (Cejka et al., 2010a; Nicolette et al., 2010b; Nimonkar et al., 2011; Niu et al., 2010). In yeast, this includes either the exonuclease Exo1 or the helicase-nuclease Sgs1-Dna2 pair (Mimitou and Symington, 2008; Zhu et al., 2008). In human cells, processive long-range DNA end resection may be similarly catalyzed by the nuclease of EXO1 or DNA2, the latter of which functions in conjunction with either BLM or WRN helicase (Gravel et al., 2008; Nimonkar et al., 2011; Sturzenegger et al., 2014). The long-range DNA end resection catalyzed by these enzymes is relatively well understood and has also been reconstituted *in vitro* (Cannavo et al., 2013; Cejka et al., 2010a; Nicolette et al., 2010b; Nimonkar et al., 2011; Niu et al., 2010). In contrast, the nuclease function during the initial resection step is less defined. In particular, the involvement of Mre11/MRE11 in the first resection step has been perplexing as Mre11/MRE11 is a 3'-5' exonuclease (Furuse et al., 1998; Paull and Gellert, 1998; Trujillo et al., 1998; Usui et al., 1998). This nuclease polarity would lead to 5'-terminated DNA, which is in disagreement with the DSB repair model and direct observations in multiple organisms, which demonstrate that 5'-terminated DNA is being degraded (Sun et al., 1991; White and Haber, 1990; Zhu et al., 2008). To this point a bidirectional DSB repair model has been proposed, where DNA is first incised endonucleolytically away from the DNA break, and the Mre11 exonuclease proceeds back towards the DNA end in a 3'-5' direction (Keeney et al., 1997; Neale et al., 2005; Shibata et al., 2014; Zakharyevich et al., 2010b), possibly in conjunction with EXD2 (Broderick et al., 2016). The endonucleolytic cleavage creates an entry site for the long-range resection machinery to resect DNA in a 5'-3' direction away from the DSB (Cejka et al., 2010a; Gravel et al., 2008; Mimitou and Symington, 2008; Nimonkar et al., 2011; Niu et al., 2010; Sturzenegger et al., 2014; Zhu et al., 2008). Recently, using recombinant *S. cerevisiae* proteins *in vitro*, we could demonstrate that Sae2 activates a cryptic endonuclease activity within the Mre11 subunit of the MRX complex that cleaves preferentially 5'-terminated DNA in the vicinity of protein blocks (Cannavo and Cejka, 2014). This provided a direct support for the bidirectional repair model

and provided strong evidence that DSB resection is initiated by the endonuclease activity of Mre11, which cleaves DNA in a way that initiates 5' DNA end resection. Interestingly, the *Escherichia coli (E. coli)* SbcCD can similarly cleave dsDNA past protein blocks, indicating that this might be a conserved mechanism (Connelly et al., 2003). At the same time, it has been shown that also Sae2 and CtIP possess an intrinsic endonuclease activity, and in particular the 5' flap endonuclease of CtIP has been proposed to process DNA adducts at DSBs (Lengsfeld et al., 2007; Makharashvili et al., 2014; Wang et al., 2014). Contrary to these observations, other groups purified nuclease-free Sae2/CtIP (Andres et al., 2015; Cannavo and Cejka, 2014; Niu et al., 2010). Therefore, the mechanism by which MRN and CtIP proteins process 5'-terminated DNA at DSBs, particularly in human cells, remains unresolved.

Resected DSBs are in general non-ligatable and DNA end resection thus commits the DSB repair to the HR pathway (Dupre et al., 2008; Shibata et al., 2014). Human cells employ a number of factors that regulate the balance between HR and NHEJ. In particular the 53BP1 protein through its multiple effectors including PTIP, REV7 and RIF1 functions as a general inhibitor of DNA end resection (Bunting et al., 2010; Zimmermann and de Lange, 2014). On the other hand BRCA1, possibly in complex with BARD1, may function to counteract 53BP1 (Bouwman et al., 2010; Bunting et al., 2010; Chen et al., 2008b), or even directly promote resection through a physical interaction with CtIP (Chen et al., 2008b; Yu and Chen, 2004). Vegetative cells typically use a sister chromatid as a template for DSB repair during HR. Therefore, DNA end resection is typically only activated during the S and G2 phases of the cell cycle when such homologous template is available. This is achieved by a regulatory mechanism dependent on the phosphorylation of Sae2/CtIP by the cyclin-dependent kinase (CDK). Phosphorylation of Sae2 at S267 and CtIP at T847 by CDK is essential for resection *in vivo* (Huertas et al., 2008; Huertas and Jackson, 2009). The requirement for CDK can be partially bypassed in cells expressing the phospho-mimicking Sae2 S267E or CtIP T847E variants, implicating Sae2/CtIP as exclusive CDK targets in HR (Huertas et al., 2008; Huertas and Jackson, 2009). Using purified recombinant proteins *in vitro*, we show here that CtIP functions as co-factor of MRE11 endonuclease activity within the human MRN complex. This

function of CtIP is absolutely dependent on its phosphorylation that includes the CDK site T847. Unlike in yeast where the Mre11-Rad50 complex is sufficient for resection *in vitro*, we show that NBS1 is an essential reaction component in the reconstituted human system. These results imply MRE11 as the primary nuclease in the initiation step of DSB end resection. The reconstituted reaction will be invaluable to define mechanisms that regulate this critical step in DSB repair.

RESULTS

Phosphorylated CtIP promotes the MRE11 endonuclease within the human MRE11-RAD50-NBS1 complex

Sae2 from *S. cerevisiae* promotes the endonuclease activity of Mre11 within the Mre11-Rad50-Xrs2 (MRX) complex to initiate resection of protein-blocked dsDNA ends (Cannavo and Cejka, 2014). To investigate whether human CtIP similarly promotes the endonuclease of the human MRE11-RAD50-NBS1 (MRN) complex, we initially expressed and purified MRN and CtIP from baculovirus infected *Spodoptera frugiperda 9* (*Sf9*) cells using a procedure similar to that used previously for yeast MRX and Sae2 (Cannavo and Cejka, 2014)(Figure S1A and S1B). Recombinant MRN showed a manganese-dependent 3' to 5' exonuclease activity as reported previously (Paull and Gellert, 1998) (Figure S1C and S1D). CtIP failed to stimulate either the endonuclease or the 3'-5' exonuclease of MRN (Figures 1A and S1E). The function of CtIP in homologous recombination is strongly dependent on its phosphorylation, especially by a cyclin-dependent kinase (CDK) (Huertas and Jackson, 2009). To enrich for phosphorylated variants of recombinant CtIP, we modified its preparation procedure by supplementing the *Sf9* culture and extracts with phosphatase inhibitors. This procedure yielded CtIP that exhibited an electrophoretic mobility shift (Figures S1F and 1B) that disappeared upon treatment with λ-phosphatase (Figure 1C). The phosphorylated CtIP, hereafter referred to as pCtIP, lacked a detectable intrinsic nuclease activity in our assays (Figure S1G). Strikingly however, the combination of both pCtIP and MRN resulted in an endonucleolytic cleavage of a synthetic 70 bp-long dsDNA substrate blocked on both ends with

biotin-streptavidin (Figure 1D). Treatment of pCtIP with λ-phosphatase eliminated this activity (Figure 1E), showing that CtIP phosphorylation is indeed required for the observed endonucleolytic cleavage. A failure to phosphorylate CtIP by CDK at T847 was shown to impair resection and cause cellular sensitivity to DNA-damaging drugs *in vivo* (Huertas and Jackson, 2009). Accordingly, the non-phosphorylatable CtIP T847A mutant (Figure S1H) was severely impaired in the dsDNA-clipping assay (Figure 1F), despite being phosphorylated at other residues resulting in a phosphorylation-dependent electrophoretic mobility shift (Figure S1H). The previously established control of DNA end resection by CDK can therefore be reconstituted in the minimal *in vitro* resection system as well.

To determine whether the nuclease of MRE11 is responsible for the observed endonucleolytic cleavage, we mutated the conserved nuclease motif within MRE11 to prepare the M(H129L D130V)RN complex (Figure S1G). The M(H129L D130V)RN variant behaved similarly as the wild type complex during purification, and lacked magnesium-dependent 3'-5' exonuclease activity, as expected (Figure S1K and S1L) (Arthur et al., 2004). Similarly as in *S. cerevisiae*, the nuclease-deficient variant was completely deficient in the clipping assay (Figure 1G) (Cannavo and Cejka, 2014), showing that the nuclease of MRE11 is entirely responsible for the observed endonucleolytic cleavage activity.

The endonucleolytic cleavage was dependent on concentrations of both MRN and CtIP (Figure 2A-D). Unlike the MRE11 exonuclease, the endonuclease of MRN-pCtIP required both manganese and magnesium metal cofactors for optimal activity (Figure S2A). While low manganese concentrations were sufficient, at least 5 mM magnesium was required for optimal activity (Figure S2B and S2C), in agreement with a significantly higher cellular magnesium concentration than that of manganese (Tholey et al., 1988). Increasing the salt concentration in the reaction resulted in the reduction of the pCtIP-stimulated endonuclease activity of MRN indicating its dependence on ionic interactions between MRN and pCtIP and/or with DNA (Figure S2D). Next, we tested whether phosphorylation affects the DNA binding capacity of CtIP. We observed that phosphorylation of CtIP reduced its affinity to DNA (Figure 2E). CtIP could stabilize MRN on DNA, however its capacity to do so was severely impaired in case of the hyperphosphorylated CtIP variant (Figure 2E). Our results thus

suggest that the stabilization of MRN and CtIP on DNA, as well as the proposed DNA end bridging function that was described for Ctp1 of *S. pombe* (Andres et al., 2015), might be dispensable for the dsDNA clipping reaction, at least in the reconstituted system. Finally, we tested the requirement for species-specific interactions. Yeast Sae2 did not promote the nuclease of human MRN and *vice versa*, pCtIP did not promote the nuclease of yeast MRX, both at 37°C and 30°C (Figure 2F and S2E). Species-specific interactions between the two cognate complexes are therefore likely required for the observed DNA clipping activity. In summary, we demonstrate that phosphorylated CtIP functions as a co-factor of the MRN endonuclease in a species-specific reaction that is able to process protein-blocked DNA ends.

ATP hydrolysis by RAD50 and a structural function of NBS1 are required for the CtIP-MRN endonuclease

The MRN-pCtIP clipping activity required ATP, which could not be replaced by ADP or the non-hydrolysable ATP analogue ATPγS (Figure 3A). We next mutated the conserved lysine residue within the Walker A motif of RAD50 into either arginine, resulting in the MR(K42R)N complex (Figure S3A), which is expected to be deficient in ATP hydrolysis, or into alanine, resulting in MR(K42A)N (Figure S3B) deficient in ATP binding (Paull and Gellert, 1999). Both mutations eliminated the endonuclease activity in conjunction with CtIP, proving that ATP hydrolysis by the RAD50 subunit is required for the DNA clipping activity (Figure 3B and 3C). In contrast, the RAD50 mutations had no significant effect on the manganese-dependent exonuclease of MRE11 within the MRN complex variants (Figure S3C-F). ATP hydrolysis by RAD50 is therefore either specifically required for the MRN complex to melt into dsDNA and/or mediates a conformational change that is essential to trigger the MRE11 endonuclease within the MRN-pCtIP complex (Deshpande et al., 2014; Lammens et al., 2011; Paull and Gellert, 1999).

Interestingly, yeast Xrs2 is essential for the nuclear import of the MRX complex, but is not required for most MRX functions in homologous recombination *per se*; in accord, Xrs2 is not required for the Sae2-stimulated dsDNA clipping reaction by MRX (Oh *et al.*, Symington laboratory, manuscript

under revision). Here we purified the human MRE11-RAD50 (MR) complex using the same procedure as MRN (Figure S4A). In contrast to the MR complex and Sae2 from *S. cerevisiae*, human MR complex failed to cleave dsDNA in conjunction with pCtIP (Figure 4A), while the MR was exonuclease-proficient in the absence of NBS1 (Figure 4B and S4B). These results show a differential requirement for the Xrs2/NBS1 factor in homologous recombination between lower and higher eukaryotes and are in agreement with previous observations that NBS1 is required for ATP-dependent functions of the human MRN complex (Paull and Gellert, 1999). In summary, our results demonstrate that phosphorylated CtIP functions as a co-factor of the MRE11 endonuclease within the MRN complex in a process that also requires ATP hydrolysis by RAD50 and a structural role of NBS1.

CtIP-MRN endonuclease preferentially clips 5' terminated DNA strands of protein-blocked DNA ends

In the absence of streptavidin, the free DNA ends were resected by MRN exonucleolytically in the 3'-5' direction. This can be seen in Figure 5A (lane 3), where the unblocked 3' end-labeled DNA substrate was cleaved to produce a species that is likely the terminally labeled mononucleotide migrating at the bottom of the gel. The exonuclease of MRE11 was unaffected by pCtIP (Figure 5A, lane 5), as also observed on a 5'-labeled DNA substrate (Figure S5A). This 3'-5' directionality of resection is paradoxically the opposite than that postulated by the DSB repair model and observed by various methods in diverse organisms including human cells *in vivo* (Sun et al., 1991; White and Haber, 1990; Zhou et al., 2014; Zhu et al., 2008). We next analyzed the positions of the endonucleolytic cleavage to determine whether it may explain the MRE11 nuclease polarity paradox. On 3'-end labeled substrates of 70 bp in length blocked with streptavidin on both DNA ends, the clipping reactions with MRN and pCtIP consistently produced DNA fragments of ~50 and ~30 nt in length indicative of an endonuclease activity (Figure 1D, lane 5; Figure 5A, lane 10). This corresponds to cleavage sites located ~20 and ~40 nt away from the protein blocked 5'-terminated DNA end. Kinetic analysis suggested that the site closer to the 5' end is cleaved slightly faster, however we could not determine whether a

small number of sites is initially cleaved at the 40 nt position or whether the cleavage occurs simultaneously in some cases (Figure 5B). To distinguish between these scenarios, we prepared the streptavidin-blocked dsDNA substrate with a ^{32}P-label on the 5' end. In this case, we could exclusively detect a fragment of ~20 nt in length upon the reaction with the MRN-pCtIP complex (Figure 5C). This demonstrated that the first cleavage event occurs near the 5' end and the second site is cut subsequently, which can only be detected using a 3'-labeled DNA. We speculate that MRN-pCtIP bound near the DNA end may create a secondary protein block that is subsequently recognized by another MRN-pCtIP complex to cleave at the second site, which might lead to the resection of longer stretches of DNA in a stepwise manner.

We next prepared a 5'-labeled DNA blocked on a single DNA end. Using this substrate, MRN and pCtIP also yielded a fragment of ~20 nt in length (Figure 5D), indicating that the cleavage site is determined by a protein block located at the 5' DNA end respective to the cut site. In this case however, as the substrate was free on the other end, we also observed an electrophoretic mobility shift of the substrate DNA indicative of a 3'-5' exonuclease activity in reactions containing MRN. This likely lowered the effective MRN concentration in the reactions that was available for the endonucleolytic cleavage, which may explain the lower efficiency of the DNA clipping (Figure 5D). Importantly, the position of the DNA cleavage did not change when we extended the length of DNA in the 3' direction from the cut site (Figure S5B). These experiments collectively demonstrated that the cleavage occurs preferentially on the 5' -terminated DNA strand ~20 nt away from a protein-blocked DNA end.

Phosphorylated CtIP promotes MRN cleavage near DNA secondary structures

Several lines of evidence suggest that the MRX/MRN complex may cleave near DNA secondary structures such as hairpins or cruciform structures, which may arise at inverted DNA repeats. This is best evidenced in yeast, where both Sae2 and the nuclease of Mre11 are required for recombination induced by a DNA fragment bearing inverted repeats at DSB ends *in vivo* (Lobachev et al., 2002). Consistently, recombinant yeast Mre11 and human MRE11 exhibit endonuclease

activities on ssDNA near hairpin DNA structures (Paull and Gellert, 1998; Trujillo and Sung, 2001). Surprisingly, we observed previously that Sae2 did not promote the capacity of MRX to cleave near DNA secondary structures *in vitro* (Cannavo and Cejka, 2014), and L. Symington and colleagues established that hairpin cleavage can be catalyzed by Mre11 in the absence of Sae2 in some cases *in vivo* (manuscript under review). In contrast, we observed here that pCtIP stimulated the capacity of human MRN to cleave M13 ssDNA containing a variety of DNA secondary structures ~1.5-2-fold (Figure 5E and 5F). Similarly as with protein blocked DNA substrates, this stimulatory effect was entirely dependent on phosphorylated CtIP, and pCtIP possessed no capacity to cleave these structures on its own. Similarly to the MRN-pCtIP endonuclease activity on protein-blocked dsDNA, the enhancement of MRN endonuclease by pCtIP on DNA secondary structures was completely dependent on ATP (compare Figure 5E and Figure S5C) and was most vigorous when both magnesium and manganese were present (Figure S5D). With magnesium alone, the MRN endonuclease was very weak and entirely dependent on pCtIP; with manganese alone, the MRN endonuclease was strong but completely independent of pCtIP. Taken together, we demonstrate that the dsDNA clipping by MRN and pCtIP can initiate not only the resection of protein-blocked DNA ends, but also DNA molecules bearing secondary structures.

Oligomerization of CtIP promotes its capacity to resect DNA ends in conjunction with MRN

The N-terminal domain of CtIP contains a coiled-coiled region that adopts a tetrameric structure in solution. More specifically, the tetramers consist of two coiled-coil dimers assembled in an anti-parallel dimer-of-dimers configuration (Davies et al., 2015), which is conserved in evolution (Andres et al., 2015). To investigate whether CtIP oligomerization regulates its capacity to activate the endonuclease of MRN, we prepared CtIP variants that affect the oligomer assembly. The elimination of the first 160 amino acids of CtIP, which completely abolishes CtIP oligomerization (Davies et al., 2015), dramatically increased the solubility and thus the yield of the recombinant CtIP variant (Figure S6A); the polypeptide was similarly hyperphosphorylated upon treatment of *Sf*9 cells with

phosphatase inhibitors (Figure S6B). In contrast to the full-length polypeptide, the truncated variant was however largely inactive in the clipping assay (Figure 6A and 6D). We next prepared the pCtIP L27E mutant (Figure S6C), which does not affect the coiled-coil structures required for CtIP dimerization but specifically eliminates tetramerization and largely abolishes DNA end resection *in vivo* (Davies et al., 2015). Similarly to the wild type polypeptide, the L27E variant exhibited electrophoretic mobility shift that could be eliminated upon treatment with λ-phosphatase. This indicates that the L27E mutation does not apparently interfere with the capacity of the CtIP variant to undergo phosphorylation (Figure S6D). Also, the pCtIP L27E variant was highly soluble and could be purified with high yields. Figure 6B shows that pCtIP L27E could clearly stimulate the MRN endonuclease yet quantitative comparison revealed that it was less efficient in doing so than wild type pCtIP (Figure 6B-D), which could partially explain defects in DNA end resection caused by the CtIP L27E mutation *in vivo*. It is not possible to distinguish whether the reduced capacity to promote MRN observed with the pCtIP Δ1-160 variant was due to its presumably monomeric form or other defects caused by the elimination of the N-terminal domain. However, the fact that a single L27E mutation reduced the capacity of the MRN-pCtIP complex to clip protein-blocked DNA strongly suggest that a proper oligomeric structure of CtIP is required for its optimal capacity to promote the endonuclease of MRN and therefore for its function in the initiation of DNA end resection.

DISCUSSION

Our data demonstrate that phosphorylated CtIP specifically promotes the MRE11 endonuclease activity. We show that MRN and pCtIP form a very integrated functional unit. The dsDNA clipping activity described here is dependent on the integrity of the MRE11 nuclease active site, requires ATP hydrolysis by RAD50, as well as the structural role of the NBS1 subunit. The reaction is optimal when both magnesium and manganese cofactors are present. We believe that the requirement for manganese reflects the preference of the MRE11 nuclease for this metal cofactor, whereas magnesium is essential for the ATPase of RAD50. We show that low manganese concentration is sufficient for optimal DNA

cleavage efficiency, whereas this activity increased with magnesium concentration. This corresponds well to the physiological concentrations of these two metal co-factors *in vivo*, where magnesium largely extends that of manganese (Tholey et al., 1988). Whereas the MRE11 exonuclease degrades DNA with a 3'-5' polarity, the endonuclease of MRN-pCtIP reported here targets preferentially the 5'-terminated strand in the vicinity of protein blocks. The DSB repair model posits that specifically the 5'-terminated DNA must be degraded. This leads to the formation of 3'-tailed DNA that serves as a template for the DNA strand exchange proteins RAD51 and/or DMC1 (Kowalczykowski, 2015). Upon DNA strand exchange and invasion into homologous DNA, the 3'- tailed DNA can prime DNA synthesis. This is in agreement with physical assays in several organisms including human cells that conclusively demonstrate that 5'-terminated DNA is preferentially (Sun et al., 1991; White and Haber, 1990; Zhou et al., 2014; Zhu et al., 2008), although not solely (Hartsuiker et al., 2009b), resected. Therefore, unlike the exonuclease of MRE11 that resects DNA with the 'wrong' polarity, the endonuclease reported here preferentially cleaves 5'-terminated DNA (Figure 5). This might explain the MRE11 nuclease polarity paradox, as proposed previously by the bidirectional DNA end resection model by multiple groups (Keeney et al., 1997; Neale et al., 2005; Shibata et al., 2014; Zakharyevich et al., 2010b). Our results thus provide a direct evidence for the bidirectional model in human cells.

The general reaction mechanism described here appears to be conserved in evolution from prokaryotes to eukaryotes, although it shows different levels of complexity. In *E. coli*, the SbcCD complex (a functional counterpart of MRE11-RAD50) cleaves DNA in the vicinity of protein blocks, DNA secondary structures or even free DNA ends (Connelly et al., 2003; Lim et al., 2015). DNA cleavage past protein blocks did not require ATP hydrolysis in *E. coli* (Connelly et al., 2003). In contrast ATP hydrolysis by Rad50 is essential in the yeast system, where additionally Sae2, which is absent in prokaryotes, provides a critical stimulatory function (Cannavo and Cejka, 2014). The Xrs2 subunit of the MRX complex carries a nuclear localization signal. Placing a nuclear localization signal on the C-terminus of Mre11 could generally overcome homologous-recombination defects of yeast *xrs2*Δ cells (Oh *et al.*, manuscript under revision). Symington and

colleagues demonstrated that Xrs2 *per se* is required for the checkpoint and non-homologous end-joining function of the MRX complex in yeast, but largely dispensable for DNA end resection. Consequently, the yeast MR complex was fully proficient in the dsDNA clipping reaction in conjunction with Sae2 in the absence of Xrs2 (Oh et al., manuscript under revision). We show here that the NBS1 subunit becomes an essential component of the dsDNA clipping machinery and NBS1 is thus an integral component of the human pCtIP-MRN endonuclease (Figure 4). This points at a differential requirement for the Xrs2/NBS1 subunit in evolution, which could enable additional regulatory control that might only apply to higher eukaryotes.

Our data demonstrate a clear requirement for CtIP phosphorylation in the reconstituted reaction. When we initially purified the CtIP protein according to a similar procedure as used for yeast Sae2 (Cannavo and Cejka, 2014), we did not detect any effect on the endonuclease of MRN. We had to modify the preparation procedure by treating the *Sf*9 cells with camptothecin (CPT) to induce DNA damage response phosphorylation cascade and additionally to actively inhibit protein dephosphorylation by treating the *Sf*9 cells with phosphatase inhibitors. These modifications resulted in a phosphorylation-dependent electrophoretic mobility shift of purified recombinant pCtIP. We show than only this hyperphosphorylated variant became capable to promote the MRN endonuclease (Figure 1). In contrast yeast Sae2 expressed and purified from *Sf*9 cells was capable to promote MRX even without these modifications (Cannavo and Cejka, 2014). However, dephosphorylation of the Sae2 preparation similarly impaired the dsDNA clipping reaction (Cannavo and Cejka, 2014), showing that phosphorylation of Sae2/CtIP is important in both experimental systems. Jackson and colleagues previously demonstrated that phosphorylation of CtIP at the CDK site T847 is essential for the DNA end resection activity *in vivo*; this CDK site is conserved in all CtIP/Sae2 homologues (Huertas et al., 2008; Huertas and Jackson, 2009). The non-phosphorylatable CtIP T847A variant was deficient in DNA end resection *in vivo*, pointing towards an essential regulatory control mechanism by CDK (Huertas and Jackson, 2009). This likely ensures that resection only takes place in S/G2 phases of the cell cycle, when sister chromatid is available as a homologous template for repair. The phospho-mimicking CtIP

T847E mutation represents one of the two key requirements that was necessary to activate homologous recombination in G1 cells (Orthwein et al., 2015), further underlining the critical importance of this posttranslational modification in DSB repair pathway choice. We demonstrated here that the CtIP T847A mutant non-phosphorylatable at the key CDK site was severely impaired in the dsDNA clipping in conjunction with MRN even in the minimal reconstituted system. This indicates that CtIP phosphorylation likely regulates MRN and CtIP interaction with each other or with DNA. To this point, we found that phosphorylated pCtIP showed a much lower affinity to DNA (Figure 2). Furthermore, pCtIP was much less capable to stabilize MRN bound to DNA compared to the non-phosphorylated CtIP variant. These results infer that the DNA-binding capacity of CtIP and the stabilization of MRN-DNA interaction is likely not rate-limiting for dsDNA clipping. Rather, these results suggest that CtIP phosphorylation may regulate the interaction with the MRN complex, which is supported by our observation that only the cognate MRX-Sae2 and MRN-pCtIP polypeptides promoted the dsDNA clipping reaction (Figure 2). CtIP however interacts with MRN through multiple interaction sites, and thus the critical interaction interphase between MRN and CtIP that may be regulated by CtIP phosphorylation remains to be identified (Sartori et al., 2007; Yuan and Chen, 2009).

Our data suggest that pCtIP functions as a co-factor of the MRE11 endonuclease, as the endonuclease activity in our assays was dependent on the integrity of the MRE11 endonuclease active site (Figure 1). This is intriguing, as CtIP was previously reported to possess an inherent 5' flap endonuclease activity capable to cleave branched DNA structures, which was suggested to be specifically required for the processing of protein-blocked DNA ends (Makharashvili et al., 2014; Wang et al., 2014). Our preparation of pCtIP did not possess this activity, yet it was capable to promote the endonuclease of MRE11. The reason for this difference is not clear, and may result from diverse purification procedures. The intrinsic CtIP endonuclease activity described previously is clearly distinct from the pCtIP-stimulated MRE11 nuclease reported here, as the CtIP endonuclease did not require phosphorylation of the

CtIP-T847 CDK site that is essential for resection *in vivo* and in the reconstituted system presented here.

What may be the nature of blocks that direct the MRN-pCtIP endonuclease *in vivo*? Meiotic Spo11 is a good candidate, in fact processing of meiotic DNA breaks requires both the nuclease of Mre11 as well as Sae2 in yeast, and this process is likely highly conserved in evolution (Keeney et al., 1997; Mahadevaiah et al., 2001; Neale et al., 2005; Robert et al., 2016). Likewise, the processing of stalled DNA-topoisomerase adducts requires the MRE11 nuclease and Sae2/CtIP (Paull, 2010), and may be explained by the mechanism reported here. Interestingly, the MRE11-dependent DNA end resection is capable to resect up to ~200-300 nts *in vivo*. This may be either due to a stepwise resection mechanism as suggested here (Figure 5), or a mutually non-exclusive cleavage further away from the DNA end (Garcia et al., 2011). Interestingly, in yeast meiotic cells the Mre11-dependent resection endpoints correlated with nucleosome positions, suggesting that chromatin may play a critical role in regulating resection (E. Mimitou and S. Keeney, personal communication). Clearly, the identification of the physiological protein blocks that promote the MRN-pCtIP endonuclease represents an important future challenge. We also show here that not only protein blocks, but also DNA secondary structures can direct the MRN-pCtIP endonuclease, and therefore the mechanism reported here might likely be generally applicable. Collectively, we believe that the reaction described here reconstitutes the first steps in DSB repair that requires the human MRE11 endonuclease. This assay will be essential to define the function of factors that may regulate this process, including EXD2, RECQ4, SOSS1 and MCM8-9 (Broderick et al., 2016; Lee et al., 2015; Lu et al., 2016a; Richard et al., 2011). The mechanism described here may explain the processing of DNA ends with non-canonical structures, such as those containing protein adducts that arise during anti-cancer therapy with topoisomerase inhibitors.

EXPERIMENTAL PROCEDURES

Cloning, expression and purification of recombinant proteins

The sequences of all oligonucleotides used for cloning in this study are listed in Table S1. Recombinant MRN was expressed and purified as a complex in *Sf*9 cells

by co-infection with baculoviruses prepared from individual pFastBac1 plasmids pTP17, pFB-RAD50-FLAG and pTP36 coding for MRE11-6xhis, RAD50-FLAG and NBS1. To prepare pFB-RAD50-FLAG, the FLAG-tag sequence was fused with the C-terminus of RAD50 by amplifying RAD50 from pTP11 by PCR using primers RAD50_F and RAD50_FLAG_R. The amplified PCR product was digested with BamHI and XhoI (New England Biolabs) and inserted in pFB-MBP-MLH3-his (Ranjha et al., 2014), which generated pFB-RAD50-FLAG. The pTP17, pTP11 and pTP36 vectors were a kind gift from T. Paull (University of Texas at Austin). The MRN variants were prepared by mutating the respective pFastBac1 plasmids by QuikChange site-directed mutagenesis kit following manufacturer's instructions (Agilent Technology). To prepare the MRE11 (H129L D130V) nuclease-dead variant, we used oligonucleotides hMRE11_ND_F and hMRE11_ND_R. To prepare the ATP hydrolysis and binding deficient variants of RAD50, we used primer pairs hRAD50_ATP_B_F and hRAD50_ATP_B_R to generate the RAD50 K42A mutation and primers hRAD50_ATP_H_F and hRAD50_ATP_H_R to generate the RAD50 K42R mutant. Bacmids, primary and secondary baculoviruses for all constructs were prepared using standard procedures according to manufacturer's instructions (Bac-to-Bac, Life Technologies). The transfection of *Sf*9 cells was carried out using a Trans-IT insect reagent (Mirus Bio). The sequence of all constructs amplified by PCR was verified by sequencing and is available on request.

For the large-scale expression and purification of the MRN complex, *Sf*9 cells were seeded at 0.5×10^6 per ml and co-infected 16 h later with recombinant baculoviruses expressing MRE11-6xhis, RAD50-FLAG and NBS1. The optimal ratio of the recombinant baculoviruses had been determined in previous small-scale experiments. The infected cells were incubated in suspension at 27°C for 52 h with constant agitation. The cells were then harvested (500 g, 10 min) and washed once with phosphate buffered saline (PBS). The cell pellets were snap frozen in liquid nitrogen and stored at -80°C. All subsequent purification steps were carried out at 4°C or on ice. The *Sf*9 cell pellets were resuspended in 3 volumes of lysis buffer (Tris-HCl, pH 7.5, 50 mM; β-mercaptoethanol, 2 mM; ethylenediaminetetraacetic acid (EDTA), 1 mM; Protease inhibitory cocktail, Sigma P8340, 1:400; phenylmethylsulfonyl fluoride (PMSF), 1 mM; leupeptin, 30

μg/ml; imidazole, 20 mM) for 20 min with continuous stirring. Glycerol was added to 16% (v/v) concentration. Next, 5 M NaCl was added slowly to reach a final concentration of 305 mM. The cell suspension was further incubated for 30 min with continuous stirring, centrifuged at 57'800 g for 30 min to obtain soluble extract. Pre-equilibrated nickel-nitrilotriacetic acid (Ni-NTA) agarose resin (Qiagen) was added to the cleared extract and incubated for 1 h with continuous mixing. The Ni-NTA resin was separated from the soluble extract by centrifugation at 2'000 g for 2 min and the supernatant was discarded. The Ni-NTA resin was washed extensively batch wise as well as on disposable columns (Thermo Scientific) with wash buffer (Tris-HCl, pH 7.5, 50 mM; β-mercaptoethanol, 2 mM; NaCl, 300 mM; glycerol, 10%; PMSF, 1 mM; imidazole, 20 mM), transferred and further washed on a disposable column (Thermo Scientific). The bound proteins were eluted with elution buffer (Tris-HCl, pH 7.5, 50 mM; β-mercaptoethanol, 1 mM; NaCl, 300 mM; glycerol, 10%; leupeptin, 10 μg/ml; PMSF, 1 mM; imidazole, 250 mM). The eluate was diluted 3x with dilution buffer (Tris-HCl, pH 7.5, 50 mM; NaCl, 300 mM; glycerol, 10%; leupeptin, 10 μg/ml; PMSF, 1 mM) to decrease the concentration of β-mercaptoethanol and imidazole. The diluted Ni-NTA eluate was then incubated with pre-equilibrated anti-FLAG M2 Affinity Gel (A2220, Sigma) for 1 h with continuous mixing. The FLAG resin was washed extensively on a disposable column (Thermo Scientific) with FLAG wash buffer (Tris-HCl, pH 7.5, 50 mM; NaCl, 150 mM; glycerol, 10%; PMSF, 1 mM; β-mercaptoethanol, 1 mM). Finally, recombinant MRN was eluted from the FLAG resin by FLAG wash buffer supplemented with 3xFLAG peptide (200 μg/ml, Sigma, F4799). Fractions containing protein were pooled, aliquoted, snap frozen and stored at –80°C. All MRN variants were expressed and purified using the identical procedure. To prepare the MRE11-RAD50 heterodimer, the NBS1 virus was excluded during the infection of *Sf*9 cells and the purification was carried out exactly as described above for the MRN complex.

The gene coding for CtIP was amplified by PCR from vector pEGFP-C1-CtIP (kindly provided by A. Sartori, University of Zurich) using oligonucleotides CtIP_F and CtIP_R. The amplified product was digested with NheI and XmaI restriction endonucleases (New England Biolabs) and inserted into plasmid pFB-MBP-MLH3-his to prepare the pFB-MBP-CtIP-his construct. The non-

phosphorylatable mutant of CtIP at site T847 was prepared by site-directed mutagenesis with oligonucleotides CtIP_T847A_F and CtIP_T847A_R as described above. The tetramerization deficient CtIP L27E variant was prepared with oligonucleotides CtIP_L27E_F and CtIP_L27E_R. To remove the first 160 amino acids from the N-terminus of CtIP, the CtIP gene was amplified with oligonucleotides MBP-161CtIP and CtIP_R by PCR. The amplified product was digested with NheI and XmaI and inserted into pFB-MBP-MLH3-his to prepare pFB-MBP-CtIPΔ1-160-his.

CtIP was expressed in *Sf*9 cells similarly as described above for MRN. To obtain hyperphosphorylated variant of CtIP (pCtIP), the *Sf*9 cell culture was supplemented with 25 nM okadaic acid (Calbiochem) for the last 4 h before harvesting (i.e. 48 h upon infection with recombinant baculovirus) to inhibit protein dephosphorylation. Furthermore, 1 μM camptothecin (Sigma) was added to the cell culture 1 h before collection (i.e. after 51 h after infection) to activate DNA damage checkpoint signaling. The CtIP variants including CtIP T847A, CtIP L27E and CtIP Δ1-160 were also expressed similarly as described above to obtain the hyper-phosphorylated species. Cells were pelleted, washed with PBS, frozen in liquid nitrogen and stored at -80°C. All subsequent steps were carried out at 4°C or on ice. Cell pellets were resuspended in 3 volumes of lysis buffer [Tris-HCl, pH 7.5, 50 mM; dithiothreitol, 1 mM; EDTA, 1 mM; Protease inhibitory cocktail, Sigma P8340, 1:400; PMSF, 1 mM; leupeptin, 30 μg/ml; NaCl, 300 mM; glycerol, 10% and phosphatase inhibitors including okadaic acid (Calbiochem), 25 nM; Na_3VO_4 (Sigma), 1 mM; NaF (Applichem), 20 mM; $Na_4O_7P_2$ (Applichem), 15 mM; Nonidet P-40 substitute (Sigma), 0.5% (v/v)]. The re-suspended cells were sonicated 6 times for 45 s with 70% cycle and max power (Sonopuls GM70, Bandelin) and the cell lysate was centrifuged at 74'000 g for 45 min. Pre-equilibrated amylose resin (New England Biolabs) was added to the cleared soluble extract and incubated for 1 h with continuous mixing. The resin was then collected by centrifugation at 2'000 g for 2 min and washed extensively batch wise as well as on disposable columns (Thermo Scientific) with wash buffer (Tris-HCl, pH 7.5, 50 mM; β-mercaptoethanol, 2 mM; NaCl, 300 mM; glycerol, 10%; PMSF, 1 mM; leupeptin, 10 μg/ml; Nonidet P-40 substitute (Sigma), 0.5% (v/v)). Protein was eluted with wash buffer containing 10 mM maltose (Sigma).

The eluates were further treated with PreScission protease for 90 min to cleave of the maltose binding protein affinity tag (MBP). The sample was then supplemented with 20 mM imidazole and further incubated with pre-equilibrated Ni-NTA agarose resin (Qiagen) for 1 h. The Ni-NTA resin was transferred on a disposable column and washed extensively with Ni-NTA wash buffer (Tris-HCl, pH 7.5, 50 mM; β-mercaptoethanol, 2 mM; NaCl, 150 mM; glycerol, 10%; PMSF, 1 mM; imidazole, 20 mM). CtIP was eluted with Ni-NTA wash buffer containing 300 mM imidazole. The amount of protein in the individual fractions was estimated by Bradford assay (Biorad). Pooled fractions were further dialyzed in dialysis buffer (Tris-HCl, pH 7.5, 50 mM; β-mercaptoethanol, 2 mM; NaCl, 150 mM; glycerol, 10%; PMSF, 1 mM) for 2 h to remove imidazole. Finally, the sample was aliquoted, snap frozen and stored at -80°C. To prepare non-phosphorylated CtIP, the phosphatase inhibitors were excluded from the above procedure. All CtIP variants were expressed and purified using an identical procedure with the exception of CtIP Δ1-160, which was highly soluble and did not require a detergent in the lysis buffer and subsequent sonication. Specifically, the *Sf*9 cell pellet with CtIP Δ1-160 was resuspended in 3 volumes of lysis buffer (Tris-HCl, pH 7.5, 50 mM; dithiothreitol, 1 mM; EDTA, 1 mM; Protease inhibitory cocktail, Sigma P8340, 1:400; PMSF, 1 mM; leupeptin, 30 μg/ml; NaCl, 300 mM; glycerol, 10% and phosphatase inhibitors including okadaic acid (Calbiochem), 25 nM; Na_3VO_4 (Sigma), 1 mM; NaF (Applichem), 20 mM; $Na_4O_7P_2$ (Applichem), 15 mM) for 20 min with continuous stirring. Glycerol was added to 16 % (v/v) concentration. 5 M NaCl was added slowly to reach a final concentration of 305 mM. The cell suspension was further incubated for 30 min with continuous stirring, centrifuged at 74'000 g for 45 min to obtain soluble extract. From this step onwards, the CtIP Δ1-160 variant was purified as described above for other CtIP constructs.

Where indicated, the protein was dephosphorylated with λ-phosphatase (New England Biolabs). To this point, the CtIP variant (1-1.5 μg) was incubated in a 20 μl volume with 200 U λ-phosphatase for 15 min at 30°C in PMP buffer supplemented with magnesium chloride according to manufacturer's recommendation (New England Biolabs). For 'mock' controls, λ-phosphatase

was excluded from the reactions. The samples from mock- and λ-phosphatase treated reactions were subsequently immediately used in nuclease assays.

Nuclease assays

Nuclease assays were carried out in a 15 μl volume in a reaction buffer containing Tris-acetate pH 7.5, 25 mM; manganese acetate, 1 mM; magnesium acetate, 5 mM; dithiothreitol, 1 mM; ATP, 1 mM; bovine serum albumin, (New England Biolabs), 0.25 mg/ml; phosphoenolpyruvate, 1 mM; pyruvate kinase, (Sigma), 80 U/ml and oligonucleotide-based DNA substrate, 1 nM (in molecules, endonuclease assays with 70 bp-long structures) or 0.5 nM (in molecules, exonuclease assays with 50 bp-long structures). Where indicated, reactions were supplemented with streptavidin (15 nM, Sigma) and incubated for 5 min at room temperature to block the end(s) of biotinylated substrates. Recombinant proteins were then added to the reactions on ice and the samples were incubated for 30 min at 37°C. Reactions were stopped with 0.5 μl Proteinase K (20.6 mg/mL, Roche); and 1 μL solution containing 5% SDS and 0.25 M EDTA for 30 minutes at 37°C. Finally, 16.5 μL loading buffer (95% formamide, 20 mM EDTA and bromophenol blue) was added to all the samples and the products were separated on 15% polyacrylamide denaturing urea gels (19:1 acrylamide-bisacrylamide, BioRad). The gels were fixed in a solution containing 40% methanol, 10% acetic acid and 5% glycerol for 30 min at room temperature and dried on a 3 mm CHR paper (Whatman). The dried gels were exposed to storage phosphor screens (GE Healthcare) and scanned by a Typhoon Phosphor imager (FLA 9500, GE Healthcare). Nuclease assays with circular ssDNA substrate (M13, 250 ng per reaction, New England Biolabs) were carried out similarly except for the incubation time was 1 h and the reaction products were separated on 1% agarose gels post-stained with GelRed (1:20'000, Biotium) for 45 min. The stained gels were imaged on a gel imager (Alpha Innotech).

Electrophoretic mobility shift assays

The reactions (15 μl) were carried out in the same buffer as nuclease assays without streptavidin. Proteins were added on ice and incubated for 30 min at 4°C. 5 μl loading dye (50% glycerol, bromophenol blue) was added to reactions

and products were separated by electrophoresis on 0.6% agarose at 4°C. The gels were dried on DE81 ion-exchange paper (Whatman), exposed to storage phosphor screens and analyzed as described above.

Oligonucleotide-based DNA substrates

DNA substrates were prepared with oligonucleotides purchased from Microsynth (Switzerland) that had been purified by polyacrylamide gel electrophoresis. The oligonucleotides were radioactively labeled at either the 5' end with T4 polynucleotide kinase (New England Biolabs) and [γ-^{32}P] ATP or at the 3' end with terminal deoxynucleotidyl transferase (New England Biolabs) and [α-^{32}P] cordycepin 5' triphosphate according to manufacturer's recommendations. The 5' and 3' radiolabelled oligonucleotides were annealed with a 2-fold excess of the complementary 'cold' oligonucleotides in PNK and TdT buffer respectively (New England Biolabs). To prepare the 70 bp-long dsDNA substrate with biotin at both ends the oligonucleotides PC210 and PC211 were used as described previously (Cannavo and Cejka, 2014). The oligonucleotides used to prepare the 70 bp-long dsDNA substrate with a block at only one end were PC206 (G**T**AAGTGCCGCGGTGCGGGTGCCAGGGCGTGCCCTTGGGCTCCCCGGGCGCGTACTC CACCTCATGCATC) and PC209 (GATGCATGAGGTGGAGTACGCGCCCGGGGAGCCCAAGGGCACGCCCTGGCACCCGCA CCGCGGCACT**T**AC), the bold **T** represents the site of the biotin modification. The oligonucleotides used to prepare the 100 bp-long dsDNA substrate were Bio100 (G**T**AAGTGCCGCGGTGCGGGTGCCAGGGCGTGCCCTTGGGCTCCCCGGGCGCGTACTC CACCTCATAATCTTCTGCCATGGTCGTAGCAGCCTCCTGCATC) and Bio100C (GATGCAGGAGGCTGCTACGACCATGGCAGAAGATTATGAGGTGGAGTACGCGCCCG GGGAGCCCAAGGGCACGCCCTGGCACCCGCACCGCGGCACTTAC). The 50 bp-long dsDNA substrate was prepared by annealing oligonucleotides X12-3 and X12-4C and the 50 bp-long Y-structured DNA was prepared with oligonucleotides PC1253 and PC1254 as described previously (Cejka and Kowalczykowski, 2010; Ranjha et al., 2014).

SUPPLEMENTAL INFORMATION

Supplemental information includes six figures and one table.

AUTHOR CONTRIBUTIONS:

R.A., E.C. and P.C. designed the experiments. L.R. carried out electrophoretic mobility shift assays, all other experiments were carried out by R.A. The paper was written by R.A. and P.C. and all authors commented on the manuscript.

ACKNOWLEDGEMENTS:

We thank to Lucie Mlejnkova, Maryna Levikova and Cosimo Pinto for helpful comments on the manuscript. We thank Tanya Paull (University of Texas, Austin) and Alessandro Sartori (University of Zurich) for DNA constructs. This work was supported by the Swiss National Science Foundation grant PP00P3 159323 to P.C.

REFERENCES

Andres, S.N., Appel, C.D., Westmoreland, J.W., Williams, J.S., Nguyen, Y., Robertson, P.D., Resnick, M.A., and Williams, R.S. (2015). Tetrameric Ctp1 coordinates DNA binding and DNA bridging in DNA double-strand-break repair. Nat Struct Mol Biol *22*, 158-166.

Arthur, L.M., Gustausson, K., Hopfner, K.P., Carson, C.T., Stracker, T.H., Karcher, A., Felton, D., Weitzman, M.D., Tainer, J., and Carney, J.P. (2004). Structural and functional analysis of Mre11-3. Nucleic Acids Res *32*, 1886-1893.

Bergerat, A., de Massy, B., Gadelle, D., Varoutas, P.C., Nicolas, A., and Forterre, P. (1997). An atypical topoisomerase II from Archaea with implications for meiotic recombination. Nature *386*, 414-417.

Bonetti, D., Clerici, M., Manfrini, N., Lucchini, G., and Longhese, M.P. (2010). The MRX complex plays multiple functions in resection of Yku- and Rif2-protected DNA ends. PLoS One *5*, e14142.

Bouwman, P., Aly, A., Escandell, J.M., Pieterse, M., Bartkova, J., van der Gulden, H., Hiddingh, S., Thanasoula, M., Kulkarni, A., Yang, Q.*, et al.* (2010). 53BP1 loss rescues BRCA1 deficiency and is associated with triple-negative and BRCA-mutated breast cancers. Nat Struct Mol Biol *17*, 688-695.

Broderick, R., Nieminuszczy, J., Baddock, H.T., Deshpande, R.A., Gileadi, O., Paull, T.T., McHugh, P.J., and Niedzwiedz, W. (2016). EXD2 promotes homologous recombination by facilitating DNA end resection. Nat Cell Biol *18*, 271-280.

Buis, J., Wu, Y., Deng, Y., Leddon, J., Westfield, G., Eckersdorff, M., Sekiguchi, J.M., Chang, S., and Ferguson, D.O. (2008). Mre11 nuclease activity has essential roles in DNA repair and genomic stability distinct from ATM activation. Cell *135*, 85-96.

Bunting, S.F., Callen, E., Wong, N., Chen, H.T., Polato, F., Gunn, A., Bothmer, A., Feldhahn, N., Fernandez-Capetillo, O., Cao, L.*, et al.* (2010). 53BP1 inhibits homologous recombination in Brca1-deficient cells by blocking resection of DNA breaks. Cell *141*, 243-254.

Cannavo, E., and Cejka, P. (2014). Sae2 promotes dsDNA endonuclease activity within Mre11-Rad50-Xrs2 to resect DNA breaks. Nature *514*, 122-125.

Cannavo, E., Cejka, P., and Kowalczykowski, S.C. (2013). Relationship of DNA degradation by Saccharomyces cerevisiae exonuclease 1 and its stimulation by RPA and Mre11-Rad50-Xrs2 to DNA end resection. Proc Natl Acad Sci U S A *110*, E1661-1668.

Cejka, P. (2015). DNA end resection: nucleases team up with the right partners to initiate homologous recombination. J Biol Chem.

Cejka, P., Cannavo, E., Polaczek, P., Masuda-Sasa, T., Pokharel, S., Campbell, J.L., and Kowalczykowski, S.C. (2010). DNA end resection by Dna2-Sgs1-RPA and its stimulation by Top3-Rmi1 and Mre11-Rad50-Xrs2. Nature *467*, 112-116.

Cejka, P., and Kowalczykowski, S.C. (2010). The full-length Saccharomyces cerevisiae Sgs1 protein is a vigorous DNA helicase that preferentially unwinds holliday junctions. J Biol Chem *285*, 8290-8301.

Chen, L., Nievera, C.J., Lee, A.Y., and Wu, X. (2008). Cell cycle-dependent complex formation of BRCA1.CtIP.MRN is important for DNA double-strand break repair. J Biol Chem *283*, 7713-7720.

Chiruvella, K.K., Liang, Z., and Wilson, T.E. (2013). Repair of double-strand breaks by end joining. Cold Spring Harb Perspect Biol *5*, a012757.
Clerici, M., Mantiero, D., Guerini, I., Lucchini, G., and Longhese, M.P. (2008).

The Yku70-Yku80 complex contributes to regulate double-strand break processing and checkpoint activation during the cell cycle. EMBO Rep *9*, 810-818.

Connelly, J.C., de Leau, E.S., and Leach, D.R. (2003). Nucleolytic processing of a protein-bound DNA end by the E. coli SbcCD (MR) complex. DNA Repair (Amst) *2*, 795-807.

Cortes Ledesma, F., El Khamisy, S.F., Zuma, M.C., Osborn, K., and Caldecott, K.W. (2009). A human 5'-tyrosyl DNA phosphodiesterase that repairs topoisomerase-mediated DNA damage. Nature *461*, 674-678.

Davies, O.R., Forment, J.V., Sun, M., Belotserkovskaya, R., Coates, J., Galanty, Y., Demir, M., Morton, C.R., Rzechorzek, N.J., Jackson, S.P.*, et al.* (2015). CtIP tetramer assembly is required for DNA-end resection and repair. Nat Struct Mol Biol *22*, 150-157.

Deng, C., Brown, J.A., You, D., and Brown, J.M. (2005). Multiple endonucleases function to repair covalent topoisomerase I complexes in Saccharomyces cerevisiae. Genetics *170*, 591-600.

Deshpande, R.A., Williams, G.J., Limbo, O., Williams, R.S., Kuhnlein, J., Lee, J.H., Classen, S., Guenther, G., Russell, P., Tainer, J.A.*, et al.* (2014). ATP-driven Rad50 conformations regulate DNA tethering, end resection, and ATM checkpoint signaling. Embo J *33*, 482-500.

Dupre, A., Boyer-Chatenet, L., Sattler, R.M., Modi, A.P., Lee, J.H., Nicolette, M.L., Kopelovich, L., Jasin, M., Baer, R., Paull, T.T.*, et al.* (2008). A forward chemical genetic screen reveals an inhibitor of the Mre11-Rad50-Nbs1 complex. Nat Chem Biol *4*, 119-125.

Foster, S.S., Balestrini, A., and Petrini, J.H. (2011). Functional interplay of the Mre11 nuclease and Ku in the response to replication-associated DNA damage. Mol Cell Biol *31*, 4379-4389.

Furuse, M., Nagase, Y., Tsubouchi, H., Murakami-Murofushi, K., Shibata, T., and Ohta, K. (1998). Distinct roles of two separable in vitro activities of yeast Mre11 in mitotic and meiotic recombination. Embo J *17*, 6412-6425.

Garcia, V., Phelps, S.E., Gray, S., and Neale, M.J. (2011). Bidirectional resection of DNA double-strand breaks by Mre11 and Exo1. Nature *479*, 241-244.

Gravel, S., Chapman, J.R., Magill, C., and Jackson, S.P. (2008). DNA helicases Sgs1 and BLM promote DNA double-strand break resection. Genes Dev *22*, 2767-2772.

Hartsuiker, E., Neale, M.J., and Carr, A.M. (2009). Distinct requirements for the Rad32(Mre11) nuclease and Ctp1(CtIP) in the removal of covalently bound topoisomerase I and II from DNA. Mol Cell *33*, 117-123.

Huertas, P., Cortes-Ledesma, F., Sartori, A.A., Aguilera, A., and Jackson, S.P. (2008). CDK targets Sae2 to control DNA-end resection and homologous recombination. Nature *455*, 689-692.

Huertas, P., and Jackson, S.P. (2009). Human CtIP mediates cell cycle control of DNA end resection and double strand break repair. J Biol Chem *284*, 9558-9565.

Jackson, S.P., and Bartek, J. (2009). The DNA-damage response in human biology and disease. Nature *461*, 1071-1078.

Keeney, S., Giroux, C.N., and Kleckner, N. (1997). Meiosis-specific DNA double-strand breaks are catalyzed by Spo11, a member of a widely conserved protein family. Cell *88*, 375-384.

Kowalczykowski, S.C. (2015). An Overview of the Molecular Mechanisms of Recombinational DNA Repair. Cold Spring Harb Perspect Biol *7*.

Lammens, K., Bemeleit, D.J., Mockel, C., Clausing, E., Schele, A., Hartung, S., Schiller, C.B., Lucas, M., Angermuller, C., Soding, J.*, et al.* (2011). The Mre11:Rad50 structure shows an ATP-dependent molecular clamp in DNA double-strand break repair. Cell *145*, 54-66.

Langerak, P., Mejia-Ramirez, E., Limbo, O., and Russell, P. (2011). Release of Ku and MRN from DNA ends by Mre11 nuclease activity and Ctp1 is required for homologous recombination repair of double-strand breaks. PLoS Genet *7*, e1002271.

Lee, K.Y., Im, J.S., Shibata, E., Park, J., Handa, N., Kowalczykowski, S.C., and Dutta, A. (2015). MCM8-9 complex promotes resection of double-strand break ends by MRE11-RAD50-NBS1 complex. Nat Commun *6*, 7744.

Lengsfeld, B.M., Rattray, A.J., Bhaskara, V., Ghirlando, R., and Paull, T.T. (2007). Sae2 is an endonuclease that processes hairpin DNA cooperatively with the Mre11/Rad50/Xrs2 complex. Mol Cell *28*, 638-651.

Lim, C.T., Lai, P.J., Leach, D.R., Maki, H., and Furukohri, A. (2015). A novel mode of nuclease action is revealed by the bacterial Mre11/Rad50 complex. Nucleic Acids Res *43*, 9804-9816.

Liu, C., Pouliot, J.J., and Nash, H.A. (2002). Repair of topoisomerase I covalent complexes in the absence of the tyrosyl-DNA phosphodiesterase Tdp1. Proc Natl Acad Sci U S A *99*, 14970-14975.

Lobachev, K.S., Gordenin, D.A., and Resnick, M.A. (2002). The Mre11 complex is required for repair of hairpin-capped double-strand breaks and prevention of chromosome rearrangements. Cell *108*, 183-193.

Lu, H., Shamanna4, R.A., Keijzers, G., Anand, R., Rasmussen, L.J., Cejka, P., Croteau, D.L., and Bohr, V.A. (2016). RECQL4 Promotes DNA End Resection in Repair of DNA Double-Strand Breaks. Cell Rep *In press*.

Mahadevaiah, S.K., Turner, J.M., Baudat, F., Rogakou, E.P., de Boer, P., Blanco-Rodriguez, J., Jasin, M., Keeney, S., Bonner, W.M., and Burgoyne, P.S. (2001). Recombinational DNA double-strand breaks in mice precede synapsis. Nat Genet *27*, 271-276.

Makharashvili, N., Tubbs, A.T., Yang, S.H., Wang, H., Barton, O., Zhou, Y., Deshpande, R.A., Lee, J.H., Lobrich, M., Sleckman, B.P.*, et al.* (2014). Catalytic and noncatalytic roles of the CtIP endonuclease in double-strand break end resection. Mol Cell *54*, 1022-1033.

Mimitou, E.P., and Symington, L.S. (2008). Sae2, Exo1 and Sgs1 collaborate in DNA double-strand break processing. Nature *455*, 770-774.

Mimitou, E.P., and Symington, L.S. (2010). Ku prevents Exo1 and Sgs1-dependent resection of DNA ends in the absence of a functional MRX complex or Sae2. Embo J *29*, 3358-3369.

Moreau, S., Ferguson, J.R., and Symington, L.S. (1999). The nuclease activity of Mre11 is required for meiosis but not for mating type switching, end joining, or telomere maintenance. Mol Cell Biol *19*, 556-566.

Nakamura, K., Kogame, T., Oshiumi, H., Shinohara, A., Sumitomo, Y., Agama, K., Pommier, Y., Tsutsui, K.M., Tsutsui, K., Hartsuiker, E.*, et al.* (2010). Collaborative action of Brca1 and CtIP in elimination of covalent modifications from double-strand breaks to facilitate subsequent break repair. PLoS Genet *6*, e1000828.

Neale, M.J., Pan, J., and Keeney, S. (2005). Endonucleolytic processing of covalent protein-linked DNA double-strand breaks. Nature *436*, 1053-1057.

Nicolette, M.L., Lee, K., Guo, Z., Rani, M., Chow, J.M., Lee, S.E., and Paull, T.T. (2010). Mre11-Rad50-Xrs2 and Sae2 promote 5' strand resection of DNA double-strand breaks. Nat Struct Mol Biol *17*, 1478-1485.

Nimonkar, A.V., Genschel, J., Kinoshita, E., Polaczek, P., Campbell, J.L., Wyman, C., Modrich, P., and Kowalczykowski, S.C. (2011). BLM-DNA2-RPA-MRN and EXO1-BLM-RPA-MRN constitute two DNA end resection machineries for human DNA break repair. Genes Dev *25*, 350-362.

Niu, H., Chung, W.H., Zhu, Z., Kwon, Y., Zhao, W., Chi, P., Prakash, R., Seong, C., Liu, D., Lu, L.*, et al.* (2010). Mechanism of the ATP-dependent DNA end-resection machinery from Saccharomyces cerevisiae. Nature *467*, 108-111.

O'Driscoll, M. (2012). Diseases associated with defective responses to DNA damage. Cold Spring Harb Perspect Biol *4*.

Orthwein, A., Noordermeer, S.M., Wilson, M.D., Landry, S., Enchev, R.I., Sherker, A., Munro, M., Pinder, J., Salsman, J., Dellaire, G.*, et al.* (2015). A mechanism for the suppression of homologous recombination in G1 cells. Nature *528*, 422-426.

Paull, T.T. (2010). Making the best of the loose ends: Mre11/Rad50 complexes and Sae2 promote DNA double-strand break resection. DNA Repair (Amst) *9*, 1283-1291.

Paull, T.T., and Gellert, M. (1998). The 3' to 5' exonuclease activity of Mre 11 facilitates repair of DNA double-strand breaks. Mol Cell *1*, 969-979.

Paull, T.T., and Gellert, M. (1999). Nbs1 potentiates ATP-driven DNA unwinding and endonuclease cleavage by the Mre11/Rad50 complex. Genes Dev *13*, 1276-1288.

Pouliot, J.J., Yao, K.C., Robertson, C.A., and Nash, H.A. (1999). Yeast gene for a Tyr-DNA phosphodiesterase that repairs topoisomerase I complexes. Science *286*, 552-555.

Ranjha, L., Anand, R., and Cejka, P. (2014). The Saccharomyces cerevisiae Mlh1-Mlh3 heterodimer is an endonuclease that preferentially binds to Holliday junctions. J Biol Chem *289*, 5674-5686.

Ray Chaudhuri, A., Hashimoto, Y., Herrador, R., Neelsen, K.J., Fachinetti, D., Bermejo, R., Cocito, A., Costanzo, V., and Lopes, M. (2012). Topoisomerase I poisoning results in PARP-mediated replication fork reversal. Nat Struct Mol Biol *19*, 417-423.

Richard, D.J., Savage, K., Bolderson, E., Cubeddu, L., So, S., Ghita, M., Chen, D.J., White, M.F., Richard, K., Prise, K.M.*, et al.* (2011). hSSB1 rapidly binds at the sites of DNA double-strand breaks and is required for the efficient recruitment of the MRN complex. Nucleic Acids Res *39*, 1692-1702.

Robert, T., Nore, A., Brun, C., Maffre, C., Crimi, B., Bourbon, H.M., and de Massy, B. (2016). The TopoVIB-Like protein family is required for meiotic DNA double-strand break formation. Science *351*, 943-949.

Sartori, A.A., Lukas, C., Coates, J., Mistrik, M., Fu, S., Bartek, J., Baer, R., Lukas, J., and Jackson, S.P. (2007). Human CtIP promotes DNA end resection. Nature *450*, 509-514.

Shibata, A., Moiani, D., Arvai, A.S., Perry, J., Harding, S.M., Genois, M.M., Maity, R., van Rossum-Fikkert, S., Kertokalio, A., Romoli, F.*, et al.* (2014). DNA double-strand break repair pathway choice is directed by distinct MRE11 nuclease activities. Mol Cell *53*, 7-18.

Sturzenegger, A., Burdova, K., Kanagaraj, R., Levikova, M., Pinto, C., Cejka, P., and Janscak, P. (2014). DNA2 cooperates with the WRN and BLM RecQ helicases to mediate long-range DNA end resection in human cells. J Biol Chem *289*, 27314-27326.

Sun, H., Treco, D., and Szostak, J.W. (1991). Extensive 3'-overhanging, single-stranded DNA associated with the meiosis-specific double-strand breaks at the ARG4 recombination initiation site. Cell *64*, 1155-1161.

Tholey, G., Ledig, M., Mandel, P., Sargentini, L., Frivold, A.H., Leroy, M., Grippo, A.A., and Wedler, F.C. (1988). Concentrations of physiologically important metal ions in glial cells cultured from chick cerebral cortex. Neurochem Res *13*, 45-50.

Trujillo, K.M., and Sung, P. (2001). DNA structure-specific nuclease activities in the Saccharomyces cerevisiae Rad50*Mre11 complex. J Biol Chem *276*, 35458-35464.

Trujillo, K.M., Yuan, S.S., Lee, E.Y., and Sung, P. (1998). Nuclease activities in a complex of human recombination and DNA repair factors Rad50, Mre11, and p95. J Biol Chem *273*, 21447-21450.

Usui, T., Ohta, T., Oshiumi, H., Tomizawa, J., Ogawa, H., and Ogawa, T. (1998). Complex formation and functional versatility of Mre11 of budding yeast in recombination. Cell *95*, 705-716.

Wang, H., Li, Y., Truong, L.N., Shi, L.Z., Hwang, P.Y., He, J., Do, J., Cho, M.J., Li, H., Negrete, A.*, et al.* (2014). CtIP maintains stability at common fragile sites and inverted repeats by end resection-independent endonuclease activity. Mol Cell *54*, 1012-1021.

White, C.I., and Haber, J.E. (1990). Intermediates of recombination during mating type switching in Saccharomyces cerevisiae. Embo J *9*, 663-673.

Yu, X., and Chen, J. (2004). DNA damage-induced cell cycle checkpoint control requires CtIP, a phosphorylation-dependent binding partner of BRCA1 C-terminal domains. Mol Cell Biol *24*, 9478-9486.

Yuan, J., and Chen, J. (2009). N terminus of CtIP is critical for homologous recombination-mediated double-strand break repair. J Biol Chem *284*, 31746-31752.

Zakharyevich, K., Ma, Y., Tang, S., Hwang, P.Y., Boiteux, S., and Hunter, N. (2010). Temporally and biochemically distinct activities of Exo1 during meiosis: double-strand break resection and resolution of double Holliday junctions. Mol Cell *40*, 1001-1015.

Zhou, Y., Caron, P., Legube, G., and Paull, T.T. (2014). Quantitation of DNA double-strand break resection intermediates in human cells. Nucleic Acids Res *42*, e19.

Zhu, Z., Chung, W.H., Shim, E.Y., Lee, S.E., and Ira, G. (2008). Sgs1 helicase and two nucleases Dna2 and Exo1 resect DNA double-strand break ends. Cell *134*, 981-994.

Zimmermann, M., and de Lange, T. (2014). 53BP1: pro choice in DNA repair. Trends Cell Biol *24*, 108-117.

FIGURE LEGENDS

Figure 1. Phosphorylated pCtIP stimulates the MRE11 endonuclease within the MRN complex. (A) Nuclease assay with MRN and non-phosphorylated CtIP on a 3' end-labeled 70 bp-long dsDNA blocked at both ends with streptavidin. (B) Electrophoretic mobility of CtIP prepared without phosphatase inhibitors (lane 2) and pCtIP (lane 3) prepared with phosphatase inhibitors. (C) Electrophoretic mobility of pCtIP either not-treated (lane 2) or treated (lane 3) with λ phosphatase. (D) Nuclease assay with MRN and pCtIP. (E) Nuclease assay with MRN and either mock- or λ-phosphatase treated pCtIP. (F) Nuclease assay with MRN and either wild type pCtIP or pCtIP T847A variant. (G) Nuclease assay with either wild type MRN or the nuclease-deficient M(H129L D130V)RN variant and pCtIP.

Figure 2. Species-specific interactions between cognate MRN and pCtIP, but not the DNA-binding capacity of pCtIP regulate the endonuclease activity. (A) Nuclease assay with pCtIP (60 nM) and various concentrations of MRN (B) Quantitation of experiments such as shown in panel A; n=2, error bars, SEM. (C) Nuclease assay with MRN (25 nM) and various concentrations of pCtIP. (D)

Quantitation of experiments such as shown in panel C; n=2, error bars, SEM. (E) Binding of MRN and phosphorylated CtIP or non-phosphorylated CtIP to dsDNA. (F) Nuclease assay with yeast MRX, human MRN, yeast Sae2 and human pCtIP, as indicated, carried out at 37°C. Only combination of the cognate polypeptides results in the stimulation of the endonuclease activity. Note that yeast MRX shows Sae2-independent DNA cleavage activity at 37°C.

Figure 3. ATP binding and hydrolysis by RAD50 is essential for the pCtIP-stimulated endonuclease of MRN. (A) Nuclease assay with MRN and pCtIP and its dependence on ATP and its analogues. (B) Nuclease assay with wild type MRN and the ATP hydrolysis-deficient MR(K42R)N variant and pCtIP. (C) Nuclease assay with wild type MRN and the ATP binding-deficient MR(K42A)N variant and pCtIP.

Figure 4. NBS1 is required for the endonuclease of MRN-pCtIP. Nuclease assay with MRE11-RAD50-NBS1 (MRN) or MRE11-RAD50 (MR) and pCtIP. (B) Nuclease assay with MR complex on 5' end-labeled dsDNA, either with 5 mM magnesium (left part) or 5 mM manganese (right part).

Figure 5. MRN-pCtIP preferentially cleave near 5' ends of blocked dsDNA ends. (A) Nuclease assay with MRN and pCtIP on DNA substrates not blocked (–Strep) or blocked (+Strep) with streptavidin. 3' end-labeled dsDNA was used. (B) Kinetic analysis of the nuclease activity of MRN and pCtIP on blocked dsDNA labeled at the 3' end. (C) Nuclease assay with MRN and pCtIP on blocked dsDNA labeled at the 5' end. (D) Nuclease assay with MRN and pCtIP on dsDNA blocked at only one end and labeled at the 5' end. (E) Nuclease assay with MRN and pCtIP or CtIP on circular ssDNA. (F) Quantitation of experiments such as shown in panel E; n=2, error bars, SEM.

Figure 6. Oligomerization of pCtIP regulates its capacity to stimulate the MRN endonuclease. (A) Nuclease assay with MRN and pCtIP Δ1-160 truncation mutant. (B) Nuclease assay with MRN and tetramerization-deficient pCtIP L27E. (C) Nuclease assay with MRN and wild type pCtIP, pCtIP L27E or pCtIP Δ1-160.

(D) Quantitation of the experiments such as shown in panel C; n=2, error bars, SEM.

SUPPLEMENTARY FIGURE LEGENDS

Figure S1 (related to Figure 1). (A) Samples from a representative purification of the MRN complex analyzed by polyacrylamide gel electrophoresis. The gel was stained with Coomassie brilliant blue. Ni-NTA flowthrough and eluate, flowthrough and eluate from nickel-nitrilotriacetic acid (Ni-NTA) resin; Flag flowthrough and eluate, flowthrough and eluate from anti-Flag affinity resin. (B) Samples from a representative purification of non-phosphorylated CtIP analyzed by polyacrylamide gel electrophoresis. The gel was stained with Coomassie brilliant blue. MBP, maltose-binding protein; PP, PreScission protease. (C) Nuclease assay with wild type MRN on 5' end-labeled dsDNA with either 5 mM magnesium (left part) or 5 mM manganese (right part). MRN exhibits manganese-dependent 3'-5' exonuclease activity. (D) Nuclease assay with wild type MRN on 3' end-labeled dsDNA with either magnesium (left part) or manganese (right part). MRN exhibits manganese-dependent 3'-5' exonuclease activity. (E) Nuclease assay with MRN and various concentrations of non-phosphorylated CtIP on 5' end-labeled dsDNA. (F) Samples from a representative purification of phosphorylated CtIP (treated with phosphatase inhibitors) analyzed by polyacrylamide gel electrophoresis. The gel was stained with Coomassie brilliant blue. MBP, maltose binding protein; PP, PreScission protease. (G) Nuclease assay with pCtIP on a 5' end-labeled Y-structured DNA substrate. (H) Samples from a purification of pCtIP T847A analyzed by polyacrylamide gel electrophoresis. The sample was treated with phosphatase inhibitors. This CtIP variant cannot be phosphorylated on a key CDK site (T847). (I) Polyacrylamide gel electrophoresis of purified recombinant wild type pCtIP (lane 2), and the pCtIP T847A variant either not treated (lane 3) or treated (lane 4) with λ phosphatase. The pCtIP T847A mutant is phosphorylated on other residues than T847, which results in a phosphorylation-dependent electrophoretic mobility shift. (J) Samples from a representative purification of the nuclease-deficient M(H129L D130V)RN complex analyzed by polyacrylamide gel electrophoresis. (K) Nuclease assay with wild type or nuclease-deficient M(H129L D130V)RN variant on 5'-end labeled dsDNA, either with 5 mM magnesium (left part) or 5 mM manganese (right part). (L) Nuclease assay with wild type or nuclease-

deficient M(H129L D130V)RN variant on 3' end-labeled dsDNA, either with 5 mM magnesium (left part) or 5 mM manganese (right part).

Figure S2 (related to Figure 2). (A) Nuclease assay with MRN and pCtIP in the presence of magnesium and/or manganese, as indicated. (B) Nuclease assay with MRN, pCtIP, 1 mM manganese and various concentrations of magnesium. (C) Nuclease assay with MRN, pCtIP, 5 mM magnesium and various concentrations of manganese. (D) Nuclease assay with MRN and pCtIP and its dependence on NaCl concentration. (E) Nuclease assay with yeast MRX, human MRN, yeast Sae2 and human pCtIP, as indicated, carried out at 30°C. Only combination of the cognate polypeptides results in the stimulation of the endonuclease activity.

Figure S3 (related to Figure 3). (A) Samples from a representative purification of the MR(K42R)N complex deficient in ATP hydrolysis. The gel was stained with Coomassie brilliant blue. (B) Samples from a representative purification of the MR(K42A)N complex deficient in ATP binding. The gel was stained with Coomassie brilliant blue. (C) Nuclease assay with MR(K42R)N variant on 5' end-labeled dsDNA, either with 5mM magnesium (left part) or 5 mM manganese (right part). (D) Nuclease assay with MR(K42R)N variant on 3' end-labeled dsDNA, either with 5 mM magnesium (left part) or 5 mM manganese (right part). (E) Nuclease assay with MR(K42A)N variant on 5' end-labeled dsDNA, either with 5mM magnesium (left part) or 5 mM manganese (right part). (F) Nuclease assay with MR(K42A)N variant on 3' end-labeled dsDNA, either with 5 mM magnesium (left part) or 5 mM manganese (right part).

Figure S4 (related to Figure 4). (A) Samples from a representative purification of the MR complex analyzed by polyacrylamide gel electrophoresis. The gel was stained with Coomassie brilliant blue. (B) Nuclease assay with MR complex on 3' end-labeled dsDNA, either with 5 mM magnesium (left part) or 5 mM manganese (right part).

Figure S5 (related to Figure 5). (A) Nuclease assay with MRN and various concentration of pCtIP on unblocked 5' end-labeled dsDNA. (B) Nuclease assay

with MRN and pCtIP on 100 bp-long dsDNA with a single streptavidin block and labeled at the 5' end, see cartoon for details. (C) Nuclease assay with MRN and pCtIP on circular ssDNA in the absence of ATP. (D) Nuclease assay with MRN and pCtIP on circular ssDNA in the presence of magnesium and/or manganese, as indicated.

Figure S6 (related to Figure 6). (A) Samples from a representative purification of pCtIP Δ1-160 truncation mutant analyzed by polyacrylamide gel electrophoresis. The gel was stained with Coomassie brilliant blue. (B) The pCtIP Δ1-160 was either not-treated (lane 2) or treated with λ phosphatase (lane 3). The pCtIP Δ1-160 variant shows a phosphorylation-dependent shift in electrophoretic mobility. (C) Samples from a representative purification of pCtIP L27E deficient in oligomerization analyzed by polyacrylamide gel electrophoresis. The gel was stained with Coomassie brilliant blue. (D) The pCtIP L27E was either not-treated (lane 2) or treated with λ phosphatase (lane 3). The pCtIP L27E variant shows a phosphorylation-dependent shift in electrophoretic mobility.

Anand et al. Figure 1

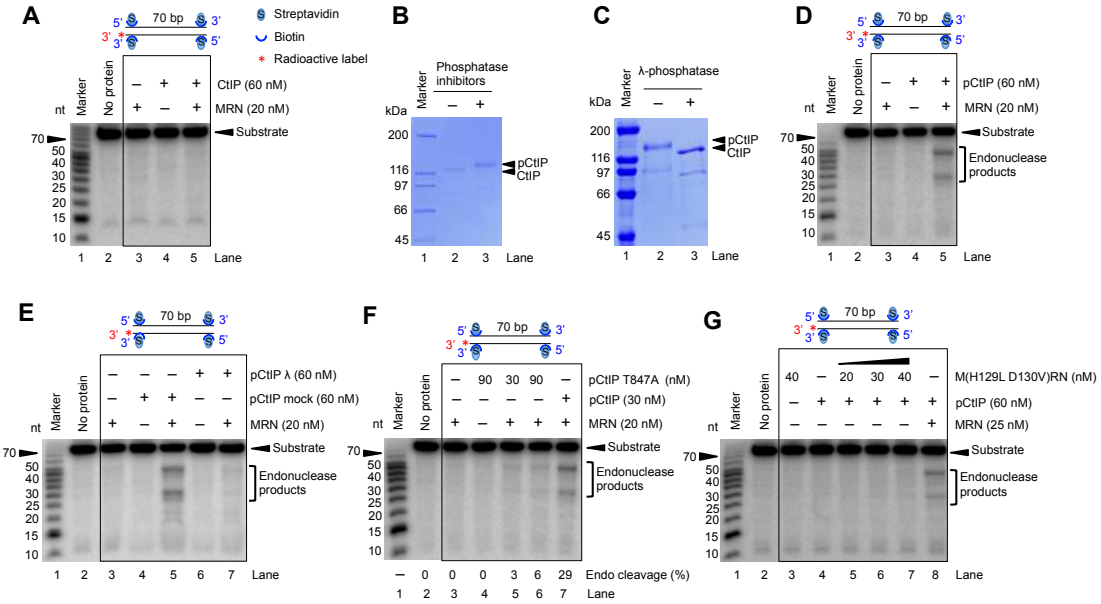

Anand et al. Figure 2

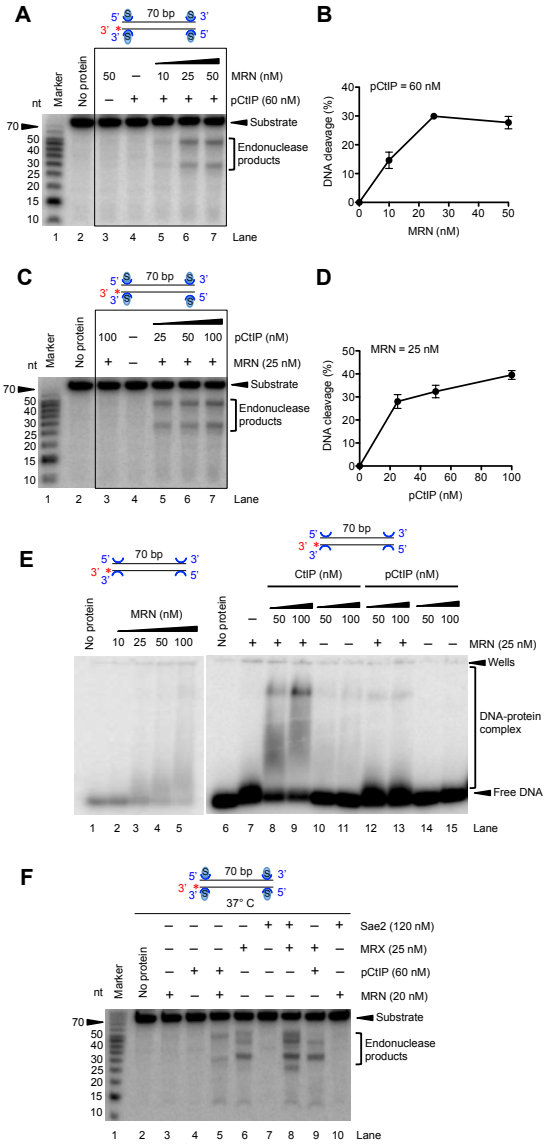

Anand et al. Figure 3

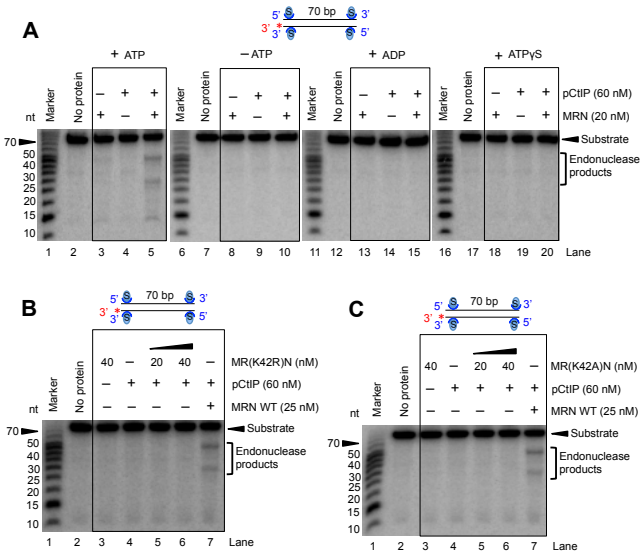

Anand et al. Figure 4

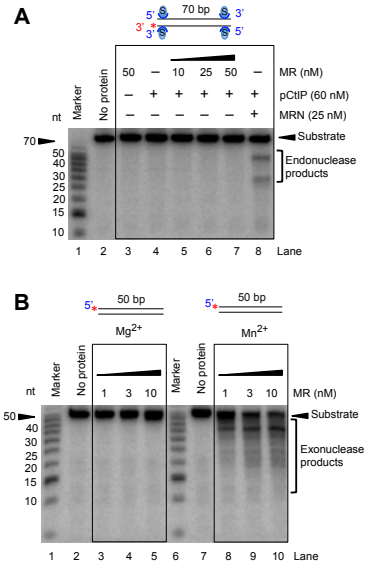

Anand et al. Figure 5

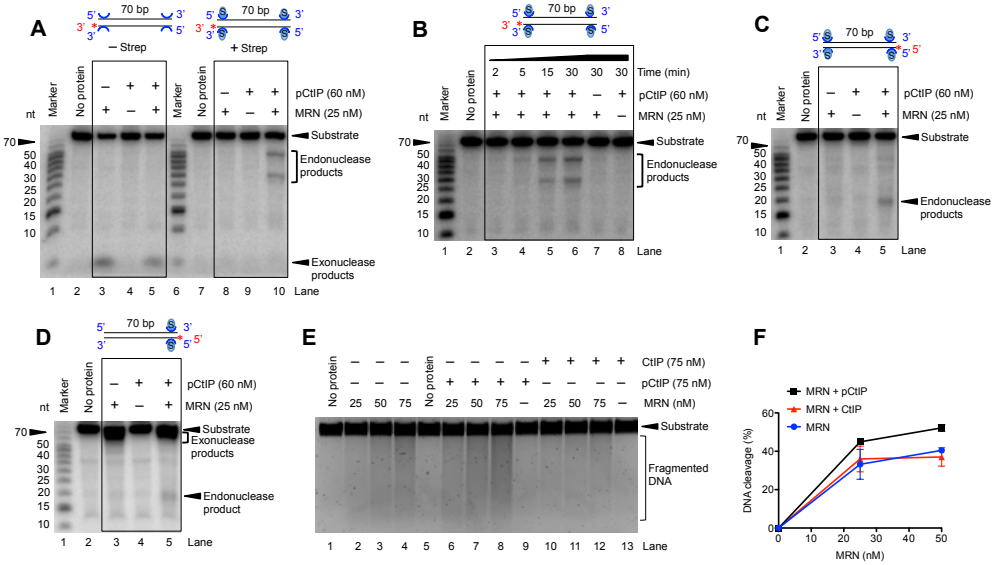

Anand et al. Figure 6

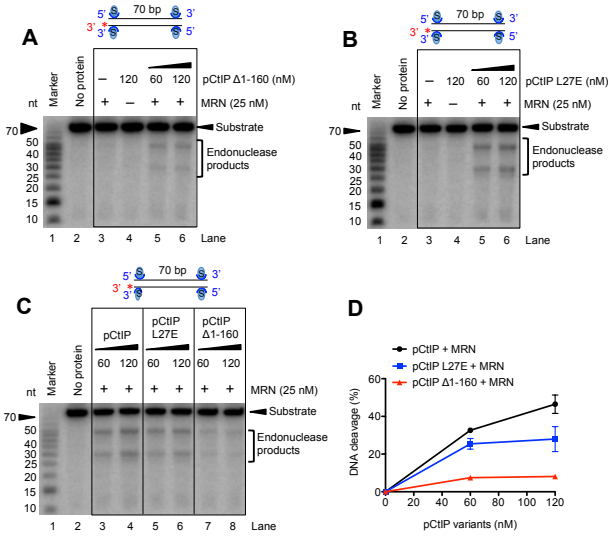

Supplementary figure 1 (related to Figure 1)

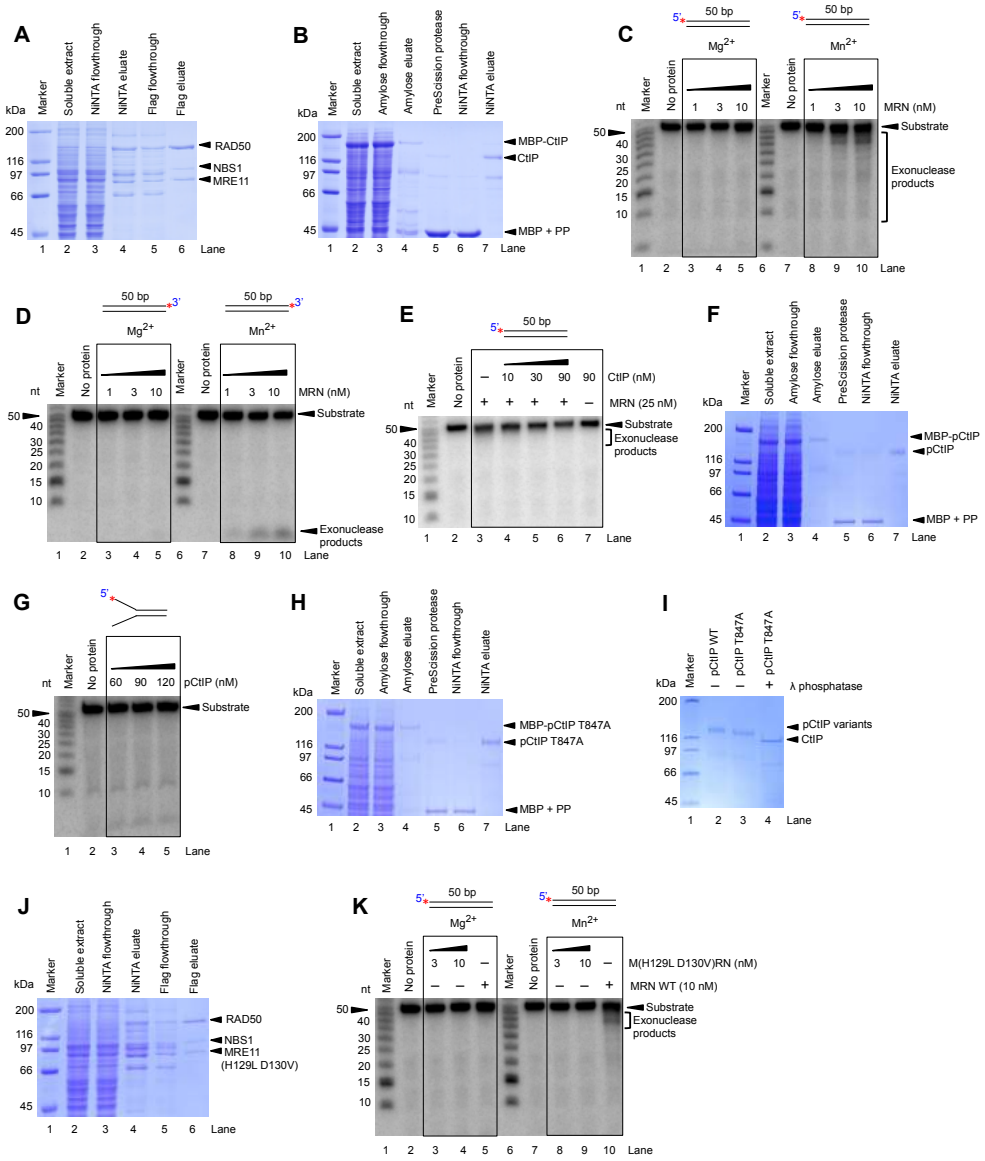

Supplementary figure 1 contd. (related to Figure 1)

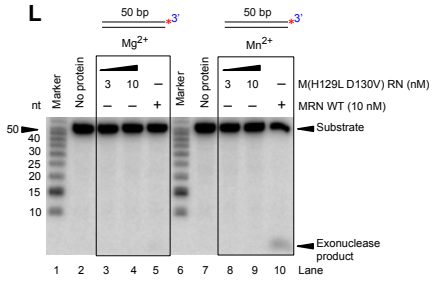

Supplementary Figure 2 (related to Figure 2)

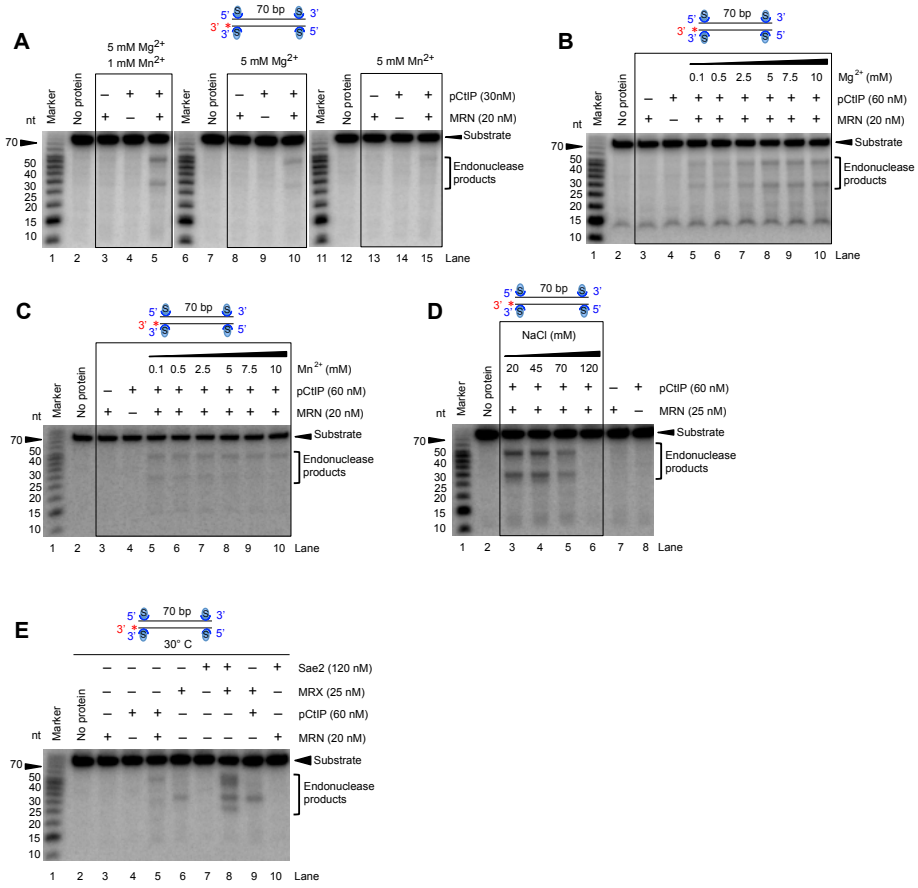

Supplementary Figure 3 (related to Figure 3)

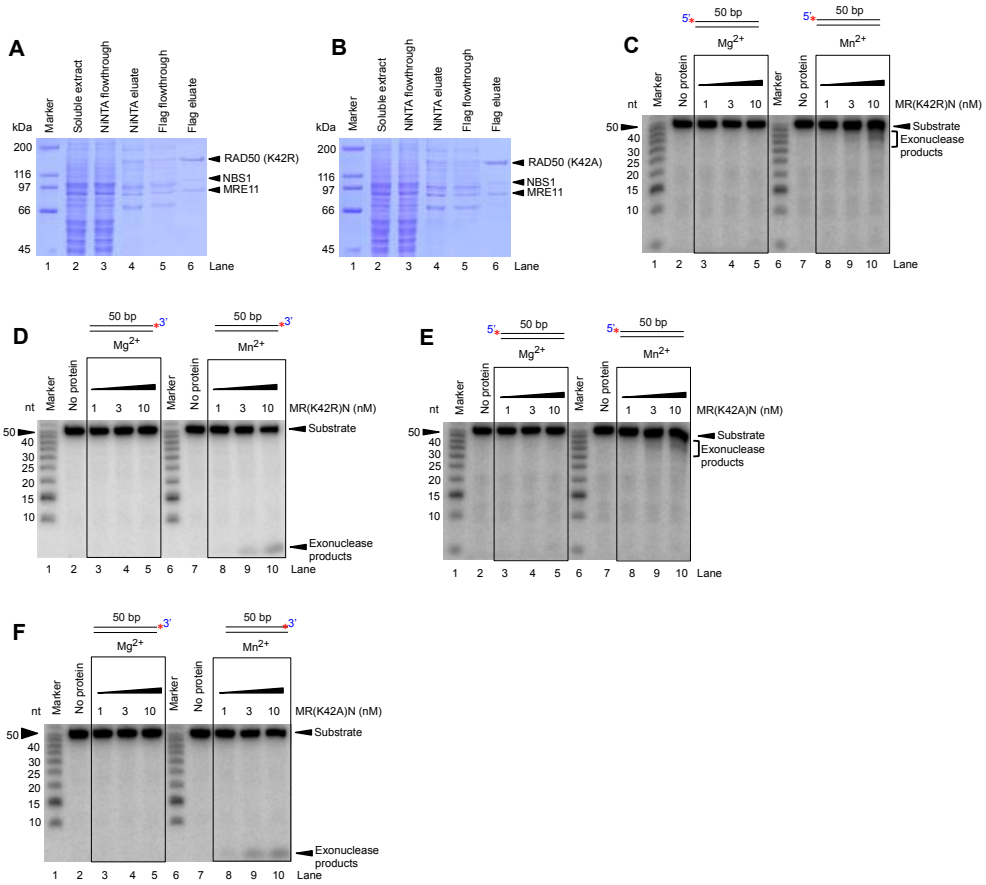

Supplementary Figure 4 (related to Figure 4)

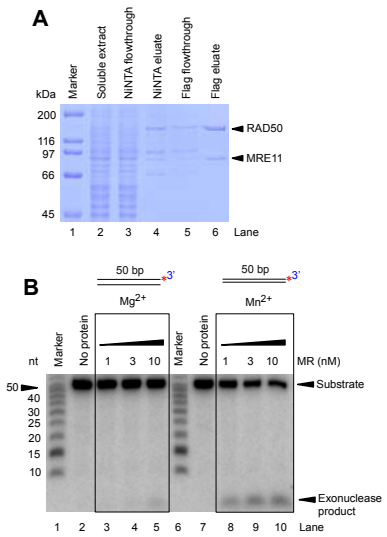

Supplementary Figure 5 (related to Figure 5)

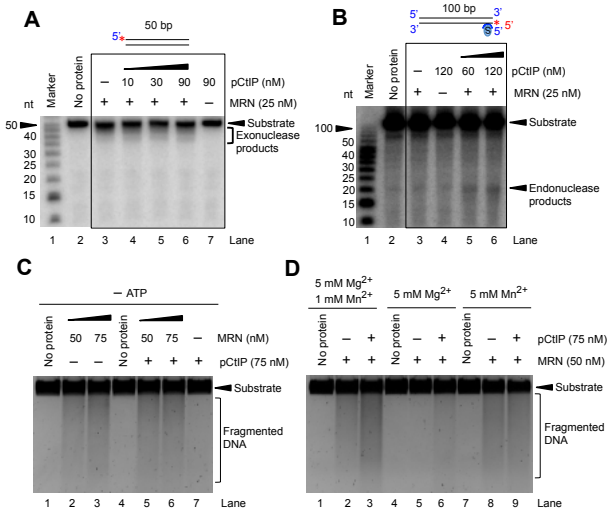

Supplementary Figure 6 (related to Figure 6)

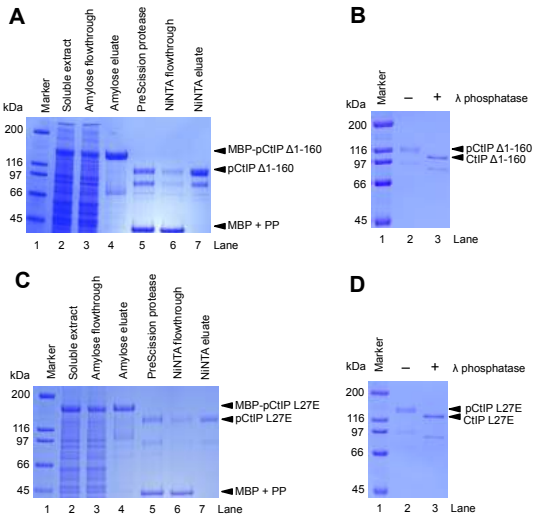

2.2 The *Saccharomyces cerevisiae* Mlh1-Mlh3 heterodimer is an endonuclease that preferentially binds to Holliday junctions

Lepakshi Ranjha, **Roopesh Anand** and Petr Cejka[1]

Article published in *The Journal of Biological Chemistry*, 2014

I contributed to this study by expressing and purifying human MLH1-MLH3 and performing hMLH1-hMLH3 DNA binding analysis. I also analysed the human data with other authors.

THE JOURNAL OF BIOLOGICAL CHEMISTRY VOL. 289, NO. 9, pp. 5674–5686, February 28, 2014

The *Saccharomyces cerevisiae* Mlh1-Mlh3 Heterodimer Is an Endonuclease That Preferentially Binds to Holliday Junctions*[S]

Received for publication, November 13, 2013, and in revised form, January 16, 2014 Published, JBC Papers in Press, January 17, 2014, DOI 10.1074/jbc.M113.533810

Lepakshi Ranjha, Roopesh Anand, and Petr Cejka[1]

From the Institute of Molecular Cancer Research, University of Zurich, Winterthurerstrasse 190, 8057 Zurich, Switzerland

Background: Mlh1-Mlh3 is required for meiotic interference-dependent crossovers.
Results: We produced recombinant Mlh1-Mlh3 and show that it is an endonuclease that binds specifically Holliday junctions.
Conclusion: Mlh1-Mlh3 prefers to bind the open conformation of Holliday junctions, which infers that it acts as part of a larger complex to process Holliday junctions in meiosis.
Significance: Recombinant Mlh1-Mlh3 complexes will be invaluable for further studies.

MutLγ, a heterodimer of the MutL homologues Mlh1 and Mlh3, plays a critical role during meiotic homologous recombination. The meiotic function of Mlh3 is fully dependent on the integrity of a putative nuclease motif DQHAX_2EX_4E, inferring that the anticipated nuclease activity of Mlh1-Mlh3 is involved in the processing of joint molecules to generate crossover recombination products. Although a vast body of genetic and cell biological data regarding Mlh1-Mlh3 is available, mechanistic insights into its function have been lacking due to the unavailability of the recombinant protein complex. Here we expressed the yeast Mlh1-Mlh3 heterodimer and purified it into near homogeneity. We show that recombinant MutLγ is a nuclease that nicks double-stranded DNA. We demonstrate that MutLγ binds DNA with a high affinity and shows a marked preference for Holliday junctions. We also expressed the human MLH1-MLH3 complex and show that preferential binding to Holliday junctions is a conserved capacity of eukaryotic MutLγ complexes. Specific DNA recognition has never been observed with any other eukaryotic MutL homologue. MutLγ thus represents a new paradigm for the function of the eukaryotic MutL protein family. We provide insights into the mode of Holliday junction recognition and show that Mlh1-Mlh3 prefers to bind the open unstacked Holliday junction form. This further supports the model where MutLγ is part of a complex acting on joint molecules to generate crossovers in meiosis.

DNA repair mechanisms safeguard genome stability and ensure correct passage of genetic information during DNA replication. By preventing mutagenesis, DNA repair pathways represent a barrier to cellular transformation to prevent carcinogenesis and delay aging (1). These pathways repair accidental DNA damage caused by a variety of exogenous and endogenous agents or replication errors. Double-strand DNA (dsDNA) breaks represent one of the most cytotoxic and dangerous lesions and are repaired by either non-homologous end-joining or homologous recombination pathways. During meiosis, programmed chromosome breakage and subsequent dsDNA break repair by homologous recombination help to ensure correct chromosome segregation and promote genetic diversity of the progeny (2, 3).

The post-replicative mismatch repair (MMR)[2] corrects DNA polymerases errors that escape their proofreading activity. In *Escherichia coli*, mismatches are detected by the MutS homodimer. Upon mismatch recognition, the ADP-bound MutS is converted into an ATP-bound sliding clamp, which recruits the MutL homodimer, and both MutS and MutL proteins complexed with ATP then activate the MutH endonuclease. MutH incises the newly synthesized DNA strand at non-methylated d(GATC) sites, and this provides entry points for a DNA helicase and one of several exonucleases that degrades the error-containing strand (4). In eukaryotes the MutS and MutL homologues are represented by heterodimers (5, 6). The Msh2-Msh6 (MutSα) and Msh2-Msh3 (MutSβ) complexes recognize base-base mismatches or insertion-deletion loops, respectively. The main MutL complex involved in *Saccharomyces cerevisiae* MMR is the Mlh1-Pms1 heterodimer (MutLα, MLH1-PMS2 in humans). The other major MutL homologue complex, MutLγ (Mlh1-Mlh3), has a key function during meiotic homologous recombination (see below) but also a minor MMR role in the repair of insertion-deletion loops alongside Msh2-Msh3 (7–11). Unlike in *E. coli*, there are no MutH homologues in eukaryotes. However, MutLα has been shown to possess a cryptic endonuclease activity, which is dependent on the integrity of the DQHAX_2EX_4E motif within human PMS2 or yeast Pms1 (12–15). In contrast to MutSα and MutSβ, MutLα has very low affinity for DNA and shows no preference for mismatches (16, 17). In the reconstituted system, it was shown that the latent MutLα endonuclease is activated in a concerted reaction dependent on a preexisting nick, mismatch, MutSα, replication factor C (RFC), and proliferating cell nuclear antigen (PCNA). Likely, these factors help to trigger a conformational change in MutLα that licenses the endonuclease (18). MutLα incises the discontinuous strand and generates new entry points for the

* This work was supported by Swiss National Science Foundation Grants PP00P3 133636 (to P. C.) and PDFMP3 141759 (to J. Jiricny (University of Zurich) and P. C.).
[S] This article contains supplemental Table 1.
[1] To whom correspondence should be addressed. Tel.: 41-44-635-4786; E-mail: cejka@imcr.uzh.ch.

[2] The abbreviations used are: MMR, mismatch repair; HJ, Holliday junction; PCNA, proliferating cell nuclear antigen; RFC, replication factor C; MBP, maltose-binding protein; scDNA, supercoiled DNA; Exo1, Exonuclease 1.

5′-3′ dsDNA-specific Exonuclease 1 (Exo1) to degrade the strand containing the misincorporated nucleotide. Thus, the endonucleolytic activity of MutLα is critically important for MMR, which is in agreement with high mutation rates caused by point mutations (*e.g. pms1E707K*) within the *PMS1* nuclease motif (13).

Meiosis is a specialized cell division that results in the production of spores or gametes. Programmed Spo11-dependent double-strand breaks activate homologous recombination, which facilitates proper pairing of homologous chromosomes and their subsequent segregation (19). Furthermore, by crossing over, or exchanging of DNA sequences between the broken chromosome and a homologous template, homologous recombination contributes to the generation of genetic diversity during sexual reproduction (2). Meiotic crossovers are dependent on the functionally diverse group of proteins belonging to the ZMM family. These factors help to form and stabilize intermediates termed single end invasions and facilitate their conversion into double Holliday junctions (HJs) that are prerequisite for crossover formation (20–24). Both MutS and MutL family proteins have critical functions in meiotic recombination. The Msh4-Msh5 complex is a member of the ZMM group and likely has both early and late roles in meiotic recombination. Msh4-Msh5 localizes as early as leptotene to the chromosome axis, and mutant mice are defective in synapsis (25). Later in pachytene, Msh4-Msh5 might recruit Mlh1-Mlh3 (MutLγ) via its HJ binding and protein-protein interaction (26, 27). MutLγ is, together with the ZMM proteins, essential for meiotic interference-dependent crossovers (28). Joint molecule formation occurs normally in yeast *mlh1 mlh3* mutants, but crossing over is impaired, which suggests that MutLγ functions only in a late step of meiotic recombination to promote a crossover outcome (29–32). Similarly in mice, Mlh1 or Mlh3 foci on pachytene chromosomes mark future crossover sites (33–36). Mlh3 also contains the DQHAX_2EX_4E metal binding motif that is critical for the MMR function of yeast Pms1 or human PMS2 (12). The pro-crossover function of MutLγ is absolutely dependent on the integrity of this motif, and *mlh3D523N* mutation that disrupts the motif confers joint molecule resolution defect that is identical to *mlh3* null mutants (29, 31). This infers that MutLγ and its nuclease activity is an integral part of a meiotic resolution pathway. The absence of other resolution activities including Mus81-Mms4 (MUS81-EME1 in humans), Yen1 (GEN1 in humans), and Slx1-Slx4 had only a modest impact on joint molecule resolution, which together with other data shows that Mlh1-Mlh3 is responsible for the majority of interference-dependent meiotic crossovers (29, 31). Furthermore, the disruption of the metal binding motif in Mlh3 resulted in a modest mutator phenotype in mitotic cells, suggesting that the anticipated endonuclease activity of Mlh3 is required for both its meiotic and MMR functions (31).

In contrast to MutLα, the analysis of the Mlh1-Mlh3 behavior was hindered by the fact that previous attempts to prepare recombinant MutLγ have been unsuccessful. Here we demonstrate the expression and purification of both yeast and human Mlh1-Mlh3/MLH1-MLH3 heterodimers from Sf9 cells. We show that yeast MutLγ is indeed a DNA endonuclease as anticipated by genetic studies. We demonstrate that MutLγ has a strong DNA binding activity with a marked preference for Holliday junctions. These recombinant complexes will be invaluable for further studies of MutLγ biochemistry.

EXPERIMENTAL PROCEDURES

Preparation of Expression Plasmids and Purification of Recombinant Proteins—The sequence of all primers is listed in supplemental Table 1. The yeast *MLH3* sequence was amplified from pEAE220 (E. Alani, Cornell University) using primers 245 and 246 (31). The PCR product was digested with ApaI and XhoI restriction endonucleases and cloned into ApaI and XhoI sites of pFB-MBP-SGS1-His (37), creating pFB-MBP-MLH3-his. Similarly, the sequence of yeast *MLH1* was amplified from pEAA109 (E. Alani, Cornell University) using primers 251 and 252. The PCR product was digested by NheI and XhoI restriction endonucleases and cloned into NheI and XhoI sites of pFB-GST-TOP3 (38), creating pFB-GST-MLH1. The cloned genes were verified by sequencing. The viruses were produced using a Bac-to-Bac system (Invitrogen) according to manufacturers' recommendations. *Spodoptera frugiperda* Sf9 cells were then co-infected with optimal ratios of both viruses, and the cells were harvested 52 h after infection, washed with phosphate-buffered saline, frozen in liquid nitrogen, and kept at −80 °C until use.

Typical purification was performed with cell pellets from 3.6 liters of culture. All subsequent steps were carried out at 0–4 °C. Cells were resuspended in 3 volumes of lysis buffer (50 mM Tris-HCl, pH 7.5, 1 mM DTT, 1 mM EDTA, 1:500 (v/v) Sigma protease inhibitory mixture (P8340), 1 mM phenylmethylsulfonyl fluoride, 30 μg/ml leupeptin). Sample was stirred slowly for 15 min. Then, glycerol was added (16% final concentration). Finally, 5 M NaCl was added to 325 mM (final concentration), and the sample was stirred for 30 min. Cell suspension was centrifuged at 50,000 × *g* for 30 min to obtain soluble extract. The cleared extract was bound to pre-equilibrated amylose resin (8 ml, New England Biolabs) for 1 h batch-wise. The resin was washed extensively with wash buffer (50 mM Tris-HCl, pH 7.5, 2 mM β-mercaptoethanol, 250 mM NaCl, 10% glycerol, 1 mM phenylmethylsulfonyl fluoride, 10 μg/ml leupeptin). MBP-Mlh3 and glutathione *S*-transferase (GST)-Mlh1 complex was eluted in wash buffer containing 10 mM maltose. Next, the maltose-binding protein (MBP) and GST tags were cleaved by PreScission protease (1 h) (the GST tag on Mlh1 did not improve our purification; therefore, we did not utilize it in our final protocol). The sample was applied on pre-equilibrated nickel nitriloacetic acid resin (0.7 ml, Qiagen) during 45 min of incubation in the wash buffer supplemented with 20 mM imidazole. The resin was washed with wash buffer containing 40 mM imidazole and eluted in the same buffer but with 400 mM imidazole. Pooled fractions were dialyzed against dialysis buffer (50 mM Tris-HCl, pH 7.5, 5 mM β-mercaptoethanol, 300 mM NaCl, 10% glycerol, 0.5 mM phenylmethylsulfonyl fluoride). The sample was aliquoted, frozen in liquid nitrogen, and stored at −80 °C. The sequence coding for the nuclease-deficient Mlh1-Mlh3 (D523N) mutant was amplified from plasmid pEAE282 (E. Alani, Cornell University) (31) and prepared in the same way as the wild type complex. To verify that the C-terminal His tag on Mlh3 does not affect its biochemical function reported here,

a recombinant wild type MutLγ with a His tag on the N terminus of Mlh1 rather than the C terminus of Mlh3 was also prepared. Both constructs behaved very similarly in our assays. Only the data obtained using the former construct are shown in this work. The construct for the expression of Mlh1 (N35A) was prepared using oligonucleotides 325 and 326, and the construct for the expression of Mlh3 (N35A) was prepared using oligonucleotides 327 and 328 by QuikChange site-directed mutagenesis (Agilent Technologies) following manufacturers' instructions.

The sequence of human MLH3 was amplified using primers 288 and 289 from pFB-MLH3 (11), digested with NheI and XmaI restriction endonucleases, and cloned into NheI and XmaI sites of pFB-MBP-SGS1-his, creating pFB-MBP-hMLH3-His. The pFB-MLH1 was described previously (39). The human MLH1-MLH3 complex was expressed and purified using the same procedure as the yeast homologue.

Recombinant Exo1 (D173A) was prepared as described previously (40). PCNA and RFC were expressed and purified from *E. coli* by minor modifications of previously established procedures (41, 42). We thank Robert Bambara (University of Rochester) and Manju Hingorani (Wesleyan University) for the expression plasmids.

DNA Substrates for Nuclease and Binding Assays—The oligonucleotide-based substrates were prepared as described previously (37). The sequences of all oligonucleotides used here are listed in supplemental Table 1. The oligonucleotides used for the respective substrate were: HJ (1253, 1254, 1255, 1256); dsDNA (1253, 1253C); Y-structure (1253, 1254); Nicked HJ (1253, 1254, 1255, 312, 314); Open HJ (1253, 1254, 316, 317), 3-Way junction (1253, 1254, 1255), ssDNA (1253). For endonuclease assays, negatively supercoiled pUC19 dsDNA (scDNA) was used.

Electrophoretic Mobility Shift Assays—The binding reactions (15 μl volume) were carried out in 25 mM Tris acetate, pH 7.5, 1 mM DTT, 100 μg/ml BSA (New England Biolabs), DNA substrate (1 nM, molecules), and either 3 mM EDTA or 2 mM magnesium acetate as indicated ($-Mg^{2+}$ or $+Mg^{2+}$, respectively). Where indicated, the reactions were supplemented with competitors, either dsDNA (pUC19), 3.3 ng/μl, or poly(dI-dC), 1.3 ng/μl. This corresponded to 50-fold molar excess (in nucleotides) over HJ for dsDNA competitor and a 20-fold molar excess (in nucleotides) for poly(dI-dC) competitor. Finally, the recombinant proteins were added. All reactions were assembled on ice. The reactions were then incubated for 30 min at 30 °C (yeast heterodimer) or 37 °C (human heterodimer). Upon adding 5 μl of 50% glycerol with bromphenol blue (0.25%) into each reaction, the products were separated by electrophoresis in 6% polyacrylamide gel (ratio acrylamide:bisacrylamide 19:1, Bio-Rad) at 4 °C. Gels were dried on DE81 chromatography paper (Whatman), exposed to storage phosphor screens (GE Healthcare), and analyzed by Typhoon FLA 9500 (GE Healthcare). The reactions were quantified using Image Quant software. The K_d corresponds to MutLγ concentration when 50% of the respective DNA substrate was protein-bound. The K_d is only reported when at least 90% substrate saturation was reached.

Nuclease Assays—The nuclease assays (15 μl volume) were carried out unless indicated otherwise in 25 mM Tris acetate, pH 7.5, 5 mM manganese acetate, 0.1 mM EDTA, 1 mM DTT, 100 μg/ml BSA (New England Biolabs), DNA substrate (200 ng, pUC19), and recombinant proteins as indicated. The reactions were incubated for 1 h at 30 °C and stopped with 5 μl of stop solution (150 mM EDTA, 2% SDS, 30% glycerol, 0.25% bromphenol blue) and 1 μl of Proteinase K (14–22 mg/ml, Roche Applied Science) for 15 min at 30 °C. The products were separated by 1% agarose gel electrophoresis, and DNA was visualized by staining with ethidium bromide (0.1 μg/ml) using the Alpha InnoTec imaging station.

RESULTS

Expression and Purification of S. cerevisiae and Homo sapiens MutLγ—The sequences coding for yeast Mlh3 and Mlh1 proteins were cloned into pFastBac1 vectors behind MBP or GST affinity tags, respectively (Fig. 1*A*). The heterodimer was expressed in *S. frugiperda* Sf9 cells and purified to near homogeneity (Fig. 1*B*). During purification, the MBP and GST tags were cleaved off by the PreScission protease (see "Experimental Procedures" for details). Using an identical procedure, we also prepared the Mlh1-Mlh3 (D523N) mutant with a disrupted putative endonuclease active site (Fig. 1*C*). The typical yield of the recombinant yeast Mlh1-Mlh3 heterodimers was ~ 0.5–1 mg from 3.6 liters of Sf9 culture, and the protein concentration was ~5 μM.

MutLγ Is an Endonuclease—We first set out to test whether MutLγ has an intrinsic endonuclease activity, as anticipated based on the presence of the metal binding DQHAX_2EX_4E motif within *MLH3* and on the phenotype of the putative nuclease site mutants (12, 13, 29, 31). Because MutLα exhibited a Mn^{2+}-ATP-dependent endonuclease activity on supercoiled dsDNA (13), we set out to test for a similar activity of MutLγ (Fig. 2*A*). We show here that Mlh1-Mlh3 does nick supercoiled dsDNA, whereas mutant Mlh1-Mlh3 (D523N) is devoid of this activity (Fig. 2*B*). The mutant MutLγ was prepared in exactly the same way as the wild type complex, and as we show below, both wild type and mutant complexes behave similarly with regard to DNA binding. We thus conclude that the endonuclease activity is inherent to MutLγ. As with MutLα, the endonuclease activity was dependent on manganese, as we observed almost no activity when manganese was substituted with magnesium (Fig. 2*B*). The optimal activity required at least 3–5 mM manganese (Fig. 2*C*), and magnesium added in addition to manganese had neither stimulatory nor inhibitory effect on the endonuclease activity of MutLγ (Fig. 2*D*). The endonuclease activity was inhibited by elevated levels of sodium or potassium chloride, as expected (Fig. 2*E*). We also found that MutLγ exhibits optimal endonuclease activity at pH 7.5– 8.5 (Fig. 2*F*).

ATP binding and hydrolysis by MutLα are required for mismatch repair, and the endonuclease activity is strongly stimulated by ATP (13). As ATP binding and hydrolysis are equally important for the meiotic and mismatch repair functions of MutLγ in genetic assays (44), we set out to test the effect of ATP on its endonuclease activity. Initially, we observed that ATP inhibited the cleavage of scDNA by MutLγ (Fig. 2*G*). However, ATP is known to chelate divalent cations such as Mn^{2+} or Mg^{2+}. To distinguish whether ATP has a direct effect on the MutLγ endonuclease or affects it indirectly via reducing the

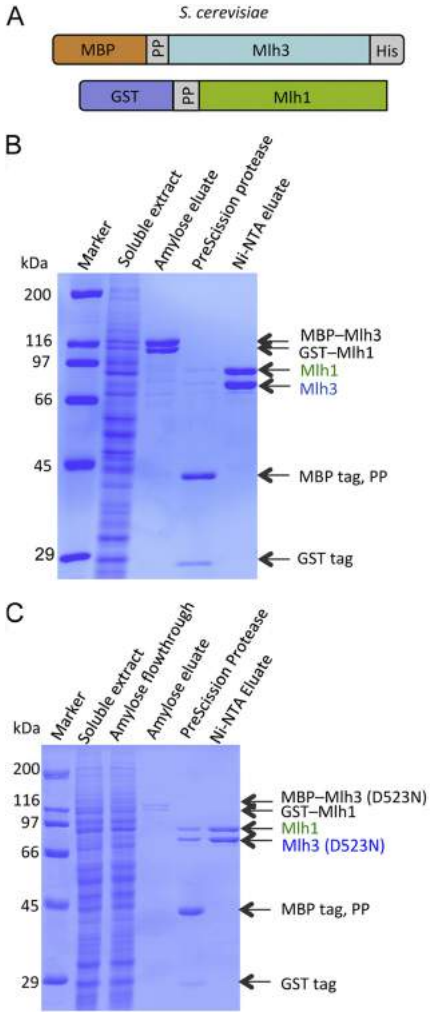

FIGURE 1. **Purification of recombinant yeast MutLγ.** *A*, a diagram of *S. cerevisiae* Mlh1 and Mlh3 constructs. *PP*, PreScission protease cleavage site. *B*, a representative Mlh1-Mlh3 purification showing fractions analyzed by SDS-PAGE. The mass of molecular weight markers is indicated on the *left*, and the positions of the respective recombinant constructs are indicated on the right. The gel was photographed upon staining with Coomassie Brilliant Blue. *C*, a representative purification as in *panel B* but with the nuclease-deficient Mlh1-Mlh3 (D523N) mutant.

free manganese concentration, we supplemented the reactions with ATP as well as an equimolar concentration of manganese acetate (Fig. 2*G*). The simultaneous addition of Mn^{2+} largely, but not completely, negated the inhibitory effect of ATP. Thus, in contrast to MutLα, ATP does not promote the endonuclease activity of MutLγ, indicating that MutLα and MutLγ nucleases are regulated differently. Furthermore, we found out that ATP binding is important for the stability of the MutLγ heterodimer. Mutations that disrupt ATP binding in Mlh1 (Mlh1 (N35A)) or are predicted to confer the same defect on Mlh3 (Mlh3 (N35A)) (44) resulted in nearly complete protein degradation in Sf9 cells (Fig. 2*H*). ATP binding was previously found to be important for the stability of human MutLα (45), and we show here that it is similar for MutLγ.

Yeast Exo1 was found in genetic assays to be required for all Mlh1-Mlh3-dependent meiotic crossovers. Surprisingly, the direct protein-protein interaction between Exo1 and Mlh1, but not the nuclease activity of Exo1, was essential for this effect (30). We set out to test whether the nuclease-deficient Exo1 (D173A) mutant stimulated the endonuclease activity of Mlh1-Mlh3 on dsDNA (46). We show in Fig. 3*A* that this was not the case; Exo1 (D173A) did not stimulate the Mlh1-Mlh3 endonuclease. Rather, we observed a decrease of the MutLγ endonuclease activity. The reason for this effect is not known; nevertheless, we point out that Mn^{2+}-dependent nicking of scDNA is unlikely the physiological condition for the MutLγ endonuclease. Therefore, we cannot exclude that Exo1 (D173A) might have a very different role on other substrates and/or under different experimental conditions.

Furthermore, the nuclease activity of MutLα was strongly promoted by RFC and PCNA in both yeast and human systems (12, 13). The effect of these proteins on the meiotic function of Mlh1-Mlh3 is unknown due to the inviability of the respective mutants. We show here that in contrast to MutLα, the endonuclease of MutLγ was not promoted by the recombinant yeast RFC and PCNA proteins (Fig. 3, *B* and *C*), not even in combination with Exo1 (D173A) (Fig. 3*D*). We also show that our preparations of RFC and PCNA were active, as demonstrated by their capacity to stimulate the endonuclease of hMutLα (Fig. 3*E*). Furthermore, we observed no magnesium-dependent endonuclease activity on either scDNA or a plasmid-based DNA substrate containing a cruciform structure resembling a Holliday junction (data not shown (43)). In summary, we demonstrate here that Mlh1-Mlh3 is indeed an endonuclease as anticipated from biochemical studies. Its activation in the context of meiotic recombination is likely to be regulated in a different manner than the nuclease of MutLα in MMR.

Mlh1-Mlh3 Preferentially Binds Holliday Junctions—Having shown that our preparation of yeast MutLγ is active as a nuclease, we next set out to analyze its DNA binding activity. To this end, we used a variety of oligonucleotide-based DNA structures and monitored DNA binding by electrophoretic mobility shift assays. In contrast to what was observed for MutLα, we show in Fig. 4*A* that MutLγ binds DNA with a very high affinity (K_d for dsDNA, Y-structure, and HJ ~1–2 nM and for ssDNA ~3 nM). Yeast MutLα was initially described to lack DNA binding activity (17). Later, DNA binding of MutLα was observed, but the apparent affinity was very low, with K_d values for oligonucleotide-based DNA in the high nanomolar or micromolar range (47–49). Initially, we did not observe significant differences between the various structures tested, and the DNA-bound Mlh1-Mlh3 complex was mostly trapped in the

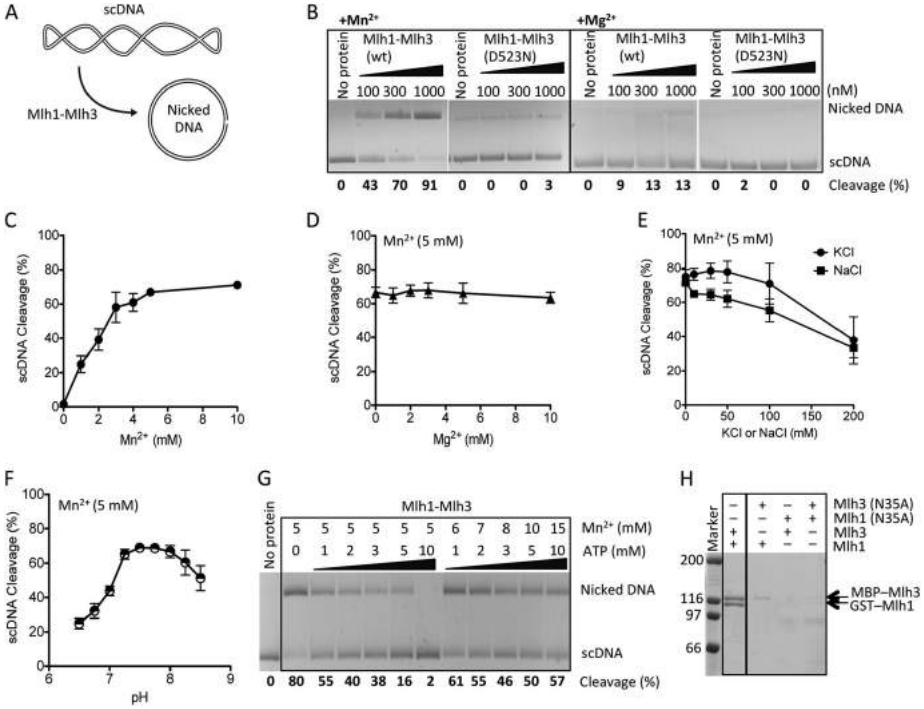

FIGURE 2. **Yeast Mlh1-Mlh3 is an endonuclease that cleaves dsDNA.** *A*, a scheme of the endonuclease assay. *B*, endonuclease assay was carried out with wild type or mutant Mlh1-Mlh3 (D523N), in a reaction buffer containing either 5 mM manganese acetate (*left side*) or 5 mM magnesium acetate (*right side*) as indicated. *Cleavage (%)*, the average value from two independent experiments. *C*, endonuclease assay with Mlh1-Mlh3 (300 nM) was carried out in the presence of various concentrations of manganese acetate as indicated. The results are based on two independent experiments; *error bars*, S.E. *D*, endonuclease assay with Mlh1-Mlh3 (300 nM) was carried out in the presence of 5 mM manganese acetate and various concentrations of magnesium acetate as indicated. The results are based on two independent experiments; *error bars*, S.E. *E*, the effect of sodium and potassium chloride on the endonuclease activity of Mlh1-Mlh3 (300 nM). The results are based on two independent experiments; *error bars*, S.E. *F*, the effect of pH on the endonuclease activity of Mlh1-Mlh3 (300 nM) in Tris acetate-based reaction buffers. The results are based on three independent experiments; *error bars*, S.E. *G*, the effect of ATP on the endonuclease activity of Mlh1-Mlh3 (300 nM). *Cleavage (%)*, the average value from two independent experiments. *H*, ATP binding is required for the stability of MutLγ in Sf9 cells. Amylose pulldown assays were carried out using extracts from Sf9 cells infected with a combination of baculoviruses coding for wild type or mutant Mlh1 or Mlh3 proteins.

wells of the polyacrylamide gels, which was suggestive of a cooperative binding or aggregation (data not shown). Thus, similarly to MutLα, the DNA binding appeared to be rather unspecific (47). The only exception was the HJ substrate, where we observed a minor protein-bound DNA species that entered the gel (data not shown).

We next supplemented the reactions with competitor DNA (pUC19 dsDNA, 3.3 ng/μl) and repeated the binding analyses. The presence of the DNA competitor lowered the apparent DNA binding affinity (Fig. 4*B*). Importantly, we could now observe a clear preference for the HJ substrate (Fig. 4, *B* and *C*). The apparent K_d for HJ was ~16 nM, which was about 5-fold lower than that for dsDNA (K_d ~ 82 nM) and 11-fold lower than for ssDNA (K_d ~ 180 nM). Furthermore, the protein-bound DNA species that entered the polyacrylamide gel was very prominent and was observed only in the case of the HJ substrate (Fig. 4*C*, indicated by a *red arrow*). We believe that this species represents the Mlh1-Mlh3 heterodimer bound specifically to the HJ structure. At higher concentrations and in the case of other DNA substrates such as dsDNA and ssDNA, the DNA was bound rather unspecifically, likely by multiple MutLγ heterodimers, and the complexes then became too large to enter the polyacrylamide gels (Fig. 4*C* and data not shown).

DNA binding by MutLγ decreased as a function of NaCl concentration, indicating that DNA binding was mediated primarily via ionic interactions (data not shown). Next we supplemented the reactions with Tween 20, which is a non-ionic detergent that reduces hydrophobic interactions that may be responsible for protein-protein aggregation. The inclusion of Tween 20 (0.5%) in the binding buffer increased the selectivity

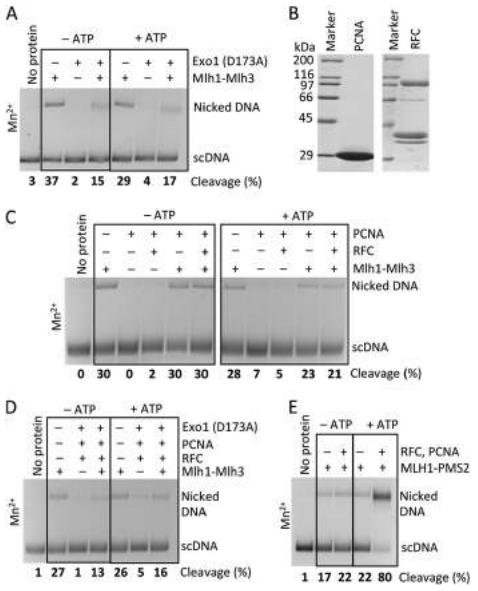

FIGURE 3. **The endonuclease activity of yeast Mlh1-Mlh3 is not promoted by either Exo1 or RFC/PCNA.** *A*, the effect of nuclease-dead yeast Exo1 (D173A, 100 nM) on the endonuclease activity of yeast Mlh1-Mlh3 (100 nM). ATP was present in the reaction buffer where indicated (1 mM). *Cleavage (%)*, the average value from two independent experiments. *B*, purified recombinant yeast PCNA and yeast RFC proteins used in this study. The gel was photographed upon staining with Coomassie Brilliant Blue. *C*, the effect of yeast PCNA (100 nM) and yeast RFC (100 nM) on the endonuclease activity of yeast Mlh1-Mlh3 (100 nM). ATP was present in the reaction buffer where indicated (1 mM). *Cleavage (%)*, the average value from two independent experiments. *D*, the effect of yeast PCNA, yeast RFC, and yeast Exo1 (D173A) on the endonuclease activity of yeast Mlh1-Mlh3 (all proteins 100 nM). ATP was present in the reaction buffer where indicated (1 mM). *Cleavage (%)*, the average value from two independent experiments. *E*, the effect of yeast PCNA (90 nM) and yeast RFC (27 nM) on the endonuclease activity of human MLH1-PMS2 (60 nM). ATP was present in the reaction buffer where indicated (1 mM). *Cleavage (%)*, the average value from two independent experiments.

of MutLγ binding to HJ (Fig. 4*E*). Tween 20 reduced the binding affinity to dsDNA about 2-fold ($K_d \sim 160$ nM), whereas it had a minimal effect on the apparent K_d for HJ ($K_d \sim 20$ nM). Thus, in the presence of Tween 20, MutLγ preferred HJ over dsDNA >8-fold. Based on these results, we conclude that DNA binding by MutLγ is mainly ionic in nature and that unspecific DNA binding is promoted by protein aggregation mediated largely by hydrophobic interactions. Next we analyzed the DNA binding in the presence of the synthetic polymer poly(dI-dC) (1.3 ng/μl). When using both poly(dI-dC) competitor and 0.5% Tween 20, MutLγ preferred binding to HJ >10-fold over dsDNA (Fig. 4, *D* and *F*). We also show that the fraction of the specifically bound HJs was very prominent (up to about 70% of the DNA substrate) and was apparent over a wide range of Mlh1-Mlh3 concentrations (Fig. 4*F*). In contrast, no specific binding to dsDNA was observed. Such binding selectivity is in agreement with the anticipated role of MutLγ in the processing of meiotic double Holliday junctions. It, however, stands in contrast with the behavior of MutLα, which shows no specific binding to mismatched DNA (17). Such behavior is rather reminiscent of MutSα or MutSβ factors, which show a similar binding preference for mismatched over homoduplex DNA (50, 51). We also analyzed DNA binding of the Mlh1-Mlh3 (D523N) mutant. As shown in Fig. 4, *G* and *H*, the mutant preferred to bind HJs similarly to the wild type protein. Although the binding affinity was lower than that of the wild type protein, the experiment shows that the integrity of the putative endonuclease active site does not affect the DNA binding selectivity. In summary, MutLγ has a strong affinity for DNA and exhibits a striking preference for binding to Holliday junctions.

Mlh1-Mlh3 Prefers to Bind the Unstacked Form of a Holliday Junction—We next analyzed the DNA binding by Mlh1-Mlh3 in a reaction buffer supplemented with magnesium. The inclusion of magnesium had a relatively modest effect on the binding affinity to dsDNA ($K_d \sim 155$ nM *versus* ~ 82 nM, decrease of binding affinity less than 2-fold). In contrast, magnesium lowered the binding affinity to HJ ~8-fold ($K_d \sim 130$ *versus* ~ 16 nM). Thus, in the presence of magnesium, the binding preference of MutLγ to HJ-like structures was strongly reduced (data not shown). The loss of binding preference to HJ in the presence of magnesium was, however, not complete, as revealed by a competition experiment. We prebound MutLγ to a ^{32}P-labeled HJ and then challenged the complex with an excess of either unlabeled HJ or dsDNA. As shown in Fig. 5*A*, the HJ competitor was more effective in disrupting the MutLγ-HJ complex than the dsDNA competitor. Preference for binding HJs in reactions with magnesium was further revealed in the presence of poly(dI-dC) competitor and Tween 20. Under these conditions, MutLγ preferred binding to HJs over dsDNA ~3-fold (Fig. 5, *B* and *C*). We could also clearly detect the specific MutLγ-HJ complex (Fig. 5, *B* and *C*). Nevertheless, the ~3-fold preference for HJs over dsDNA was still significantly smaller than that observed in the absence of magnesium (Fig. 4, *D* and *F*, ~10-fold). Supplementing the reaction with ATP affected neither the affinity for DNA nor the preference for binding HJs by Mlh1-Mlh3 (Fig. 5, *E* and *F*).

We believe that the lower preference for binding HJs in the presence of magnesium reflects an altered HJ structure. Holliday junctions are known to exist in two major conformations. In the absence of metal ions such as Mg^{2+}, HJ adopts an open planar structure with a 4-fold symmetry. In the presence of Mg^{2+}, HJ stacks into a closed antiparallel structure with a 2-fold symmetry (52, 53). Under our experimental conditions, HJ adopts the open or closed conformation depending on the presence of magnesium (data not shown) as expected. Our observation that Mlh1-Mlh3 shows a stronger preference for HJs in the absence of magnesium suggests that MutLγ prefers to bind the open unfolded HJ or a similar structure.

To characterize the binding selectivity of MutLγ in greater detail, we constructed additional oligonucleotide-based DNA substrates, including a three-way junction, a nicked HJ, and a four-way junction with a non-complementary core (open HJ). We next performed electrophoretic mobility shift assays in the presence or absence of magnesium. The most notable results

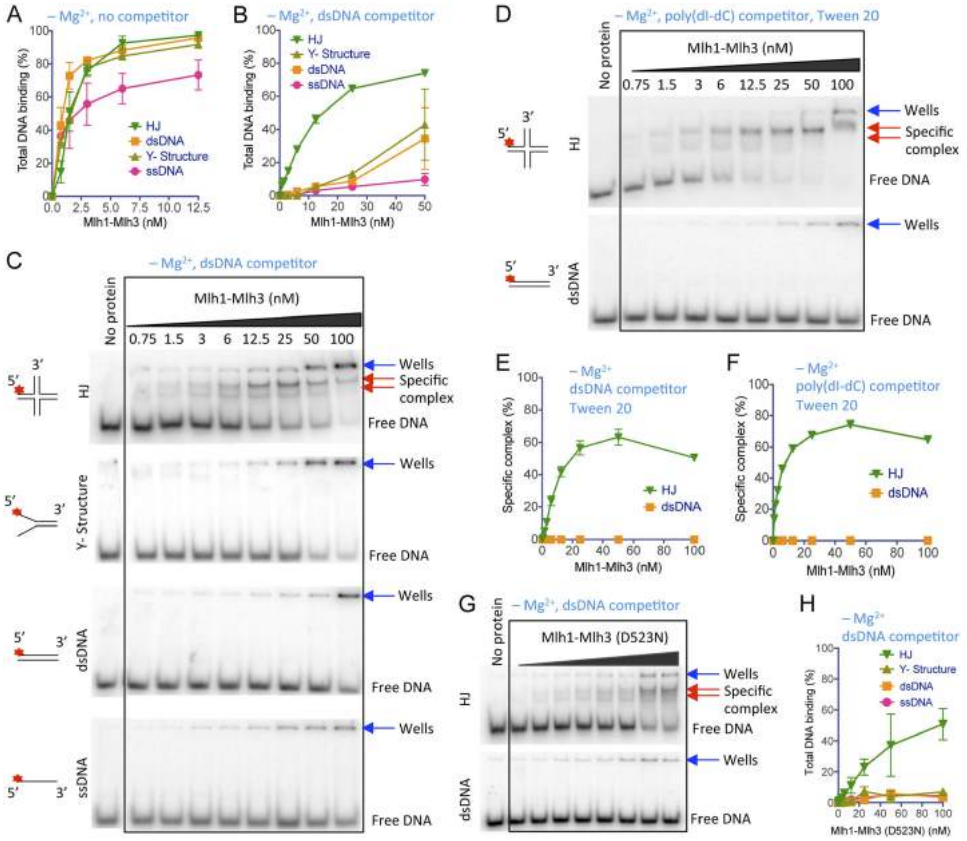

FIGURE 4. **Yeast Mlh1-Mlh3 has a high affinity for DNA and prefers to bind Holliday junctions.** Electrophoretic mobility shift assays were carried out with oligonucleotide-based DNA substrates, as indicated. All oligonucleotides were 50-nucleotides long. *A*, quantitation of assays carried out in a buffer containing 3 mM EDTA and no DNA competitor. The curves show the disappearance of the substrate band and are based on three independent experiments; *error bars*, S.E. *B*, electrophoretic mobility shift assays were carried out in a buffer containing 3 mM EDTA and a dsDNA competitor. The curves show the disappearance of the substrate band and are based on two independent experiments; *error bars*, S.E. *C*, representative experiments from the condition described in *panel B*. The species representing Mlh1-Mlh3 bound specifically to the Holliday junction is indicated by an *arrow* and denoted as *Specific complex*. A *blue arrow* indicates the position of wells. *D*, non-ionic detergent increases the fraction of specifically bound HJ by Mlh1-Mlh3. An electrophoretic mobility shift assay was carried out as in *panel C* but in a buffer supplemented with 0.5% Tween 20 and poly(dI-dC) competitor instead of dsDNA. Shown are representative experiments. The species representing Mlh1-Mlh3 bound specifically to the Holliday junction is indicated by an *arrow* and denoted as *Specific complex*. A *blue arrow* indicates the position of wells. *E*, quantitation of the fraction of specifically bound DNA from experiments carried out in a buffer containing 3 mM EDTA, dsDNA competitor, and 0.5% Tween 20. Results are based on two independent experiments, and *error bars* show S.E. *F*, quantitation of the specific complex from *panel D*. Results are based on two independent experiments, and *error bars* show S.E. *G*, representative experiments such as in *panel C* but with the nuclease-deficient Mlh1-Mlh3 (D523N) mutant (0.8–100 nM). The species representing Mlh1-Mlh3 (D523N) bound specifically to the Holliday junction is indicated by an *arrow* and is denoted as *Specific complex*. A *blue arrow* indicates the position of wells. *H*, quantitation of total DNA binding from assays such as in *panel G*. Results are based on two independent experiments, and *error bars* show S.E.

were obtained with the non-complementary core junction (open HJ). As shown in Fig. 6, *A* and *B*, in the absence of magnesium, the open junction was as good a substrate for MutLγ as the HJ substrate ($K_d \sim 10$ nM). Upon the inclusion of magnesium (Fig. 6, *C* and *D*), the open junction, which cannot stack due to a lack of complementarity, became the preferred substrate for MutLγ binding ($K_d \sim 35$ nM). In summary, we demonstrate here that the binding preference of MutLγ to HJs is reduced in the presence of magnesium that stacks HJs into a closed conformation. Our results indicate that MutLγ prefers to bind the unstacked form of HJs. By inference, we believe that MutLγ *in vivo* acts in a complex with other factors that facilitate its access to the junction under physiological conditions when magnesium is present (see "Discussion").

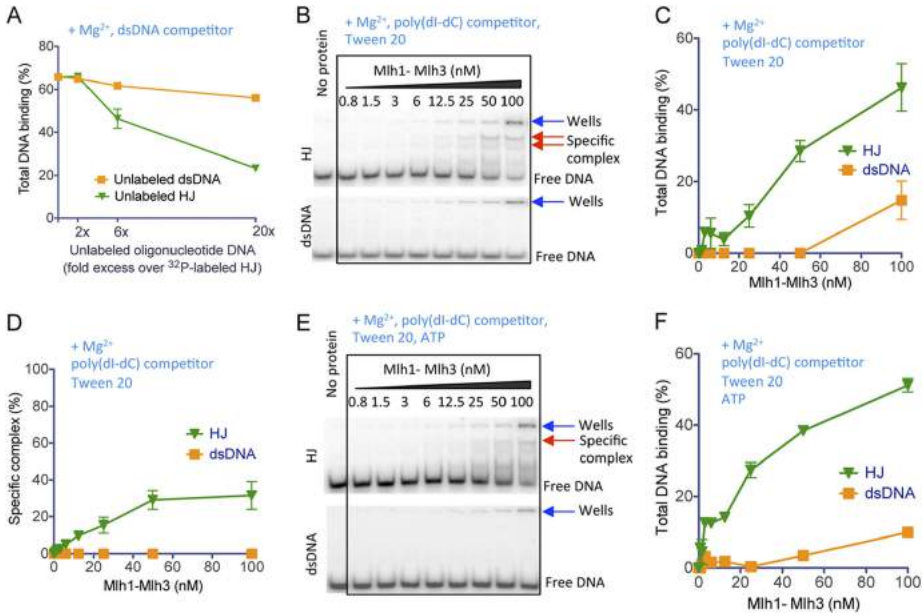

FIGURE 5. **Magnesium lowers the specificity of yeast Mlh1-Mlh3 binding to Holliday junctions.** *A*, HJ is effective as a DNA competitor in the presence of magnesium. The Mlh1-Mlh3 heterodimer (100 nM) was prebound for 15 min to ^{32}P-labeled HJ in a buffer containing 2 mM Mg^{2+}. The complex was then challenged with an excess of unlabeled dsDNA or HJ as indicated and incubated for an additional 15 min. The reaction products were then analyzed by electrophoresis. Results are based on two independent experiments, and *error bars* show S.E. *B*, electrophoretic mobility shift assays were carried out in a buffer with 2 mM Mg^{2+}, 0.5% Tween 20, and poly(dI-dC) competitor. Shown are representative experiments. The species representing Mlh1-Mlh3 bound specifically to Holliday junction is indicated by an *arrow* and denoted as *Specific complex*. A *blue arrow* indicates the position of wells. *C*, quantitation of the experiments such as shown in *panel B*, based on the disappearance of the substrate band. Three independent experiments were done, and *error bars* show S.E. *D*, quantitation of the fraction of specifically bound DNA from experiments such as shown in *panel B*. Results are based on three independent experiments, and *error bars* show S.E. *E*, assays were as in B but additionally supplemented with ATP (1 mM). Representative experiments are shown. The species representing Mlh1-Mlh3 bound specifically to the Holliday junction is indicated by an *arrow* and denoted as *Specific complex*. A *blue arrow* indicates the position of wells. *F*, quantitation of the experiments such as shown in *panel E*, based on the disappearance of the substrate band. Three independent experiments were done, and *error bars* show S.E.

Specific Holliday Junction Binding Is a Conserved Property of Eukaryotic MutLγ Proteins—To test whether the preference for HJ binding is conserved in evolution, we expressed the human MutLγ heterodimer. The sequence coding for hMLH3 was cloned behind a MBP affinity tag (Fig. 7*A*) and co-expressed with untagged hMLH1 in Sf9 cells. The typical yield of the human recombinant heterodimer was ~0.1 mg from 3.6 L Sf9 cells, and the protein concentration was ~645 nM (Fig. 7*B*). Next, we analyzed its DNA binding activity. In the absence of magnesium, the human complex also clearly preferred binding to HJs and related structures (Fig. 7, *C* and *D*). Upon supplementing the reaction buffer with magnesium, the apparent affinity to DNA was decreased, and the complex clearly preferred binding to the open junction structure with the non-complementary core, similarly to the yeast homologue (Fig. 7, *C* and *E*). In contrast to the yeast protein, however, the human MutLγ-bound DNA species remained trapped in the wells of the acrylamide gel, which likely reflects a greater propensity of hMutLγ to multimerize upon DNA binding (Fig. 7*C*). The lower protein concentration of our human MLH1-MLH3 preparation did not allow us to reliably establish the apparent K_d values for all substrates tested; however, the data presented here strongly suggest that the human and yeast MutLγ complexes behave similarly with regard to preferred HJ binding.

DISCUSSION

Here we present the first biochemical characterization of Mlh1-Mlh3. We show that the heterodimer can be expressed in Sf9 cells and purified to near homogeneity. Our analysis reveals that MutLγ has an unexpectedly strong affinity for DNA with a marked preference for Holliday junctions. This behavior stands in sharp contrast to the MMR-specific MutLα (Mlh1-Pms1 in yeast or MLH1-PMS2 in humans) and defines a novel paradigm for a function of a MutL homologue in eukaryotes. We also demonstrate that yeast Mlh1-Mlh3 endonucleolytically cleaves dsDNA and that the regulation of this endonuclease activity is distinct from that of MutLα.

A vast body of *in vivo* data from a number of organisms including yeast, mice, and humans identified MutLγ as a central player in meiotic homologous recombination (26, 29,

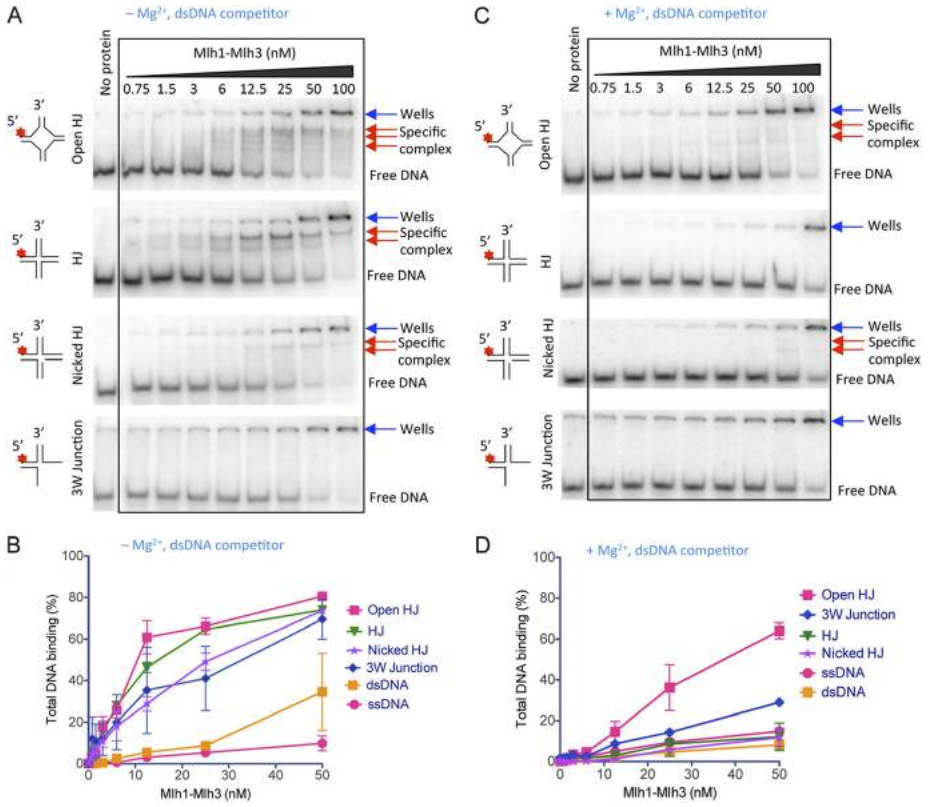

FIGURE 6. **Yeast Mlh1-Mlh3 prefers to bind the open conformation of a Holliday junction.** *A*, an electrophoretic mobility shift assay was carried out in a buffer containing 3 mM EDTA ($-Mg^{2+}$), dsDNA competitor, the respective DNA substrate as indicated on the left, and a range of Mlh1-Mlh3 concentrations. Shown are representative experiments. The image showing Mlh1-Mlh3 binding to HJ is the same as in Fig. 4*C* and is shown here again for reference. The species representing Mlh1-Mlh3 bound specifically to DNA is indicated by an *arrow* and denoted as *Specific complex*. A *blue arrow* indicates the position of wells. *B*, quantitation of the experiments such as shown in *panel A*. The curves show the disappearance of the substrate band and are based on two independent experiments; *error bars*, S.E. *C*, an electrophoretic mobility shift assay was carried out as in *panel A* but with 2 mM magnesium acetate ($+Mg^{2+}$) instead of 3 mM EDTA. The species representing Mlh1-Mlh3 bound specifically to DNA is indicated by an *arrow* and denoted as *Specific complex*. A *blue arrow* indicates the position of wells. *D*, quantitation of the experiments such as shown in *panel C*. The curves show the disappearance of the substrate band and are based on two independent experiments; *error bars*, S.E.

31–34, 54, 55). Available evidence infers a late function, likely in the processing of joint molecules such as double Holliday junctions into crossover recombination products. It was shown that MutLγ is responsible for the majority of meiotic crossovers (29). In addition, MutLγ likely has a minor role in post-replicative MMR (7–11). Understanding the molecular mechanism of MutLγ function is a major challenge, as this complex has been very difficult to obtain. The analysis of the full-length recombinant MutLγ heterodimer presented here thus represents a major step toward that goal.

As first shown by Kunkel and co-workers (16, 47), the MMR-specific yeast MutLα is a DNA-binding protein. However, the affinity of Mlh1-Pms1 for DNA is very low. In the absence of a DNA competitor, the apparent K_d is in the high nanomolar or micromolar range, which represents 2–3 orders of magnitude lower affinity than what we demonstrate here for MutLγ. Although the MutLα heterodimer shows a modest preference for binding to ssDNA, the binding is lost upon supplementing the reaction with a competitor (47). The complex shows no preference for binding either mismatched DNA or a Holliday junction (17, 47). Thus, the DNA binding by MutLα is believed to be unspecific, and it has no direct role in mismatch recognition. This function is carried out by either the MutSα or the MutSβ heterodimers. Although MutLα may increase the affinity of MutSα or MutSβ for mismatched DNA (17, 56), MutLα is not believed to come into contact with the heteroduplex. Yet

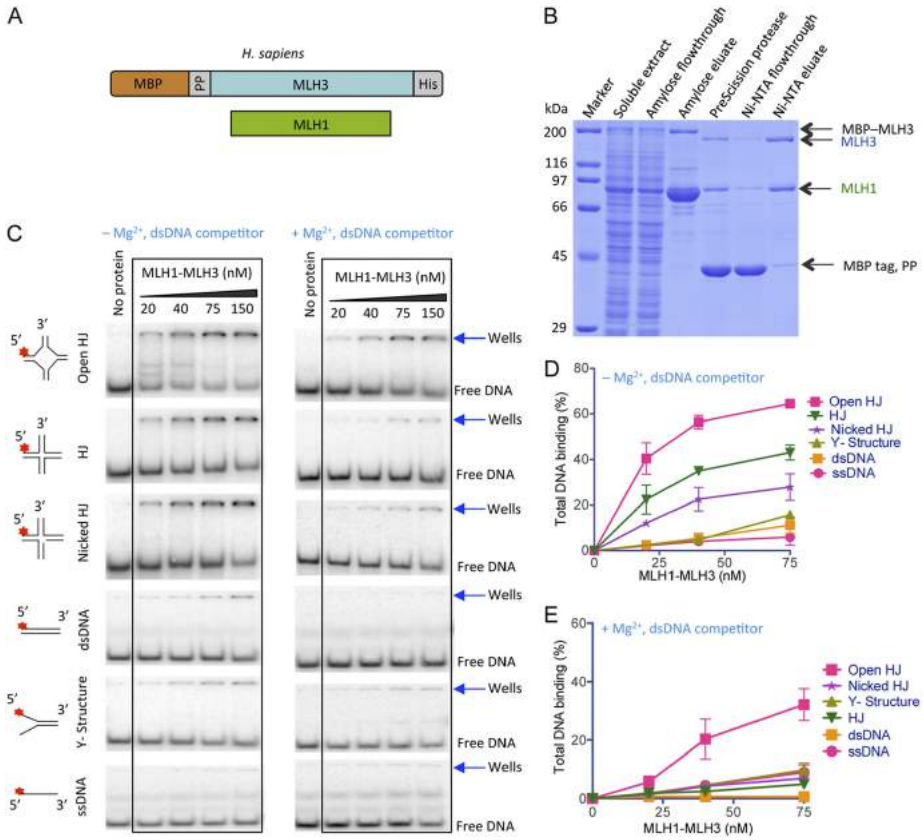

FIGURE 7. **Human MLH1-MLH3 prefers to bind Holliday junctions.** *A*, a diagram of *H. sapiens* MLH1 and MLH3 constructs. *PP*, PreScission protease cleavage site. *B*, a representative MLH1-MLH3 purification showing fractions analyzed by SDS-PAGE. The mass of molecular weight markers is indicated on the *left*, and the positions of the respective recombinant constructs on the *right*. The gel was photographed upon staining with Coomassie Brilliant Blue. *PP*, PreScission protease. *C*, an electrophoretic mobility shift assay was carried out in a buffer containing 3 mM EDTA ($-Mg^{2+}$) or 2 mM Mg^{2+} ($+Mg^{2+}$) as indicated, pUC19 dsDNA competitor, the respective DNA substrate as depicted on the *left*, and a range of MLH1-MLH3 concentrations. Shown are representative experiments. *D*, quantitation of the experiments with 3 mM EDTA such as shown in *panel C*. The curves show the disappearance of the substrate band and are based on three independent experiments; *error bars*, S.E. *E*, quantitation of the experiments with 2 mM Mg^{2+} such as shown in *panel C*. The curves show disappearance of the substrate band and are based on three independent experiments; *error bars*, S.E.

the modest DNA binding activity of MutLα is important *in vivo* as revealed by mutator phenotypes of *mlh1* and *pms1* mutants lacking the DNA binding capacity (16, 49). It may be important downstream of mismatch recognition for the movement of MutLα along the DNA contour before engagement of its endonuclease activity (57, 58).

The strong and specific binding of HJ substrates by MutLγ reported here contrasts with the behavior of MutLα. We demonstrate that MutLγ shows up to a 10-fold preference for binding HJs over dsDNA. This value is very similar to the reported preference of either MutSα (Msh2-Msh6) or MutSβ (Msh2-Msh3) toward binding heteroduplex over homoduplex dsDNA in the presence of the same competitor (50, 51). Analysis of the human MLH1-MLH3 complex further reveals that specific HJ binding by MutLγ is conserved in evolution. This infers that, during meiosis, MutLγ may directly contact HJs. Together with previously published compelling genetic data, our results further support the hypothesis that MutLγ is part of a meiosis-specific HJ resolvase (29, 31, 32).

The conformation of HJs is strongly dependent on the presence of divalent metal ions such as magnesium. In the absence of magnesium, HJs assume an open, 4-fold symmetrical structure. In the presence of magnesium, the core of the HJ folds into a stacked, X-like structure (52). We observed that the prefer-

ence of Mlh1-Mlh3 binding to HJ over dsDNA was greater in the absence (up to ~10-fold; Fig. 4) than in the presence of magnesium (up to ~3-fold; Fig. 5). This revealed that Mlh1-Mlh3 prefers to bind the unstacked, open form of a Holliday junction. This was further supported by the analysis of Mlh1-Mlh3 binding to a HJ structure with a non-complementary core. We show that Mlh1-Mlh3 bound this structure with a high affinity even in the presence of magnesium, showing that the conformation of the HJ, and not the absence of magnesium, results in the high binding affinity. The affinity of MutLγ to ssDNA is very low (Fig. 4); thus the preferred binding to the unstacked form of a HJ cannot be explained by binding to exposed ssDNA. Furthermore, no specific binding was observed to a 3-way junction, showing that a junction with all four arms is the favored substrate of MutLγ (Fig. 6).

Preferred binding to the open conformation is rather unusual for HJ resolvases. Typically, as it has been observed with *e.g.* the canonical *E. coli* resolvase RuvC or the mitochondrial *S. cerevisiae* resolvase Cce1, these enzymes bind equally well the stacked and the unstacked forms of HJs (59, 60). Upon binding, however, these proteins open the core of the HJ so that the resolvase-bound HJ in the presence of magnesium resembles more the conformation of the protein-free structure observed without magnesium rather than the stacked structure (59, 60). We believe that the simplest explanation of our results is that Mlh1-Mlh3 does not bind HJs alone but rather in complex with other factors, such as Exo1, Msh4-Msh5, or Sgs1, which may facilitate its access to HJs. Msh4-Msh5 is an obvious candidate for this role. The human heterodimer was shown to form a complex with HJs that was stable in the presence of magnesium. Upon HJ binding and ADP → ATP exchange, the MSH4-MSH5 complex turns into a sliding clamp that slides away from the HJ (27, 61). It remains to be established whether MSH4-MSH5 makes the HJ more accessible for MLH1-MLH3 binding and whether yeast Msh4-Msh5 behaves similarly. Furthermore, Sgs1 and its helicase activity is part of the crossover-specific pathway together with Mlh1-Mlh3[3] (29, 32). As Sgs1 shows a preference for unwinding HJs and it interacts with Mlh3 during meiosis (37, 62), it is possible also that the Sgs1 helicase may act in complex with Mlh1-Mlh3 to melt the HJ structure. Finally, Exo1 has a non-catalytic role in promoting joint molecule resolution by Mlh1-Mlh3. However, the molecular mechanism of this function remains unknown (30). We anticipate that some of these proteins, possibly in combination with yet-unidentified factors, may help to recruit MutLγ to the joint molecules.

During MMR, human and yeast MutLα exhibit a Mg^{2+}-dependent endonuclease activity that nicks dsDNA and that is activated in a concerted reaction requiring a pre-existing strand discontinuity (*i.e.* a nick), a mismatch, and the MutSα, RFC, and PCNA proteins. In addition, MutLα exhibits a rather unspecific Mn^{2+}-dependent endonuclease activity that nicks supercoiled dsDNA. The presence of manganese bypasses the requirement for the presence of the above reaction components (12, 13). Thus, the analysis of the Mn^{2+}-dependent nuclease reveals elements of the specific reaction. To this point, it was demonstrated that the MutLα endonuclease is strongly stimulated by ATP as well as by RFC and PCNA. We show here that MutLγ exhibits a similar, Mn^{2+}-dependent endonuclease activity. We show that, similarly to MutLα, ATP binding by either Mlh1 or Mlh3 is required for the stability of the MutLγ heterodimer. In contrast to MutLα, however, ATP does not stimulate the endonuclease of MutLγ. We also show that RFC and PCNA also do not promote the MutLγ endonuclease. Thus, the endonucleases of MutLα and MutLγ differ dramatically with regard to how their activity is regulated in a physiological context.

It is anticipated that the physiological substrate for the MutLγ endonuclease are double HJs. As MutLγ and its partners process these structures into specifically crossovers, the key question is what determines the crossover-specific resolution. Double HJs may not be fully matured (*i.e.* ligated), and the position of nicks may indicate the directionality of cleavage. Furthermore, asymmetric protein binding (such as Msh4-Msh5 or other ZMM family members, Exo1, Sgs1) may direct MutLγ cleavage. Finally, it is possible that the structure of the double HJ itself, in particular when both HJs are in close proximity, may activate MutLγ in a structure-specific manner. The availability of recombinant MutLγ will prove instrumental toward further understanding of this important and evolutionarily conserved pathway.

Acknowledgments—We thank J. Jiricny (University of Zurich), U. Rass (FMI Basel), E. Alani (Cornell University), R. Bambara (University of Rochester), W. Heyer (UC Davis), and M. Hingorani (Wesleyan University) for reagents. We thank E. Alani (Cornell University) and N. Hunter (UC Davis) for discussing unpublished data. We thank to J. Jiricny, M. Levikova, L. Mlejnkova, E. Cannavo (all University of Zurich), and C. Pinto (ETH Zurich) for helpful comments on the manuscript and M. Awad (University of Virginia) for technical assistance.

REFERENCES

1. Jackson, S. P., and Bartek, J. (2009) The DNA-damage response in human biology and disease. *Nature* **461,** 1071–1078
2. Phadnis, N., Hyppa, R. W., and Smith, G. R. (2011) New and old ways to control meiotic recombination. *Trends Genet.* **27,** 411–421
3. Zickler, D. (2006) From early homologue recognition to synaptonemal complex formation. *Chromosoma* **115,** 158–174
4. Acharya, S., Foster, P. L., Brooks, P., and Fishel, R. (2003) The coordinated functions of the *E. coli* MutS and MutL proteins in mismatch repair. *Mol. Cell* **12,** 233–246
5. Jiricny, J. (2013) Postreplicative mismatch repair. *Cold Spring Harb. Perspect. Biol.* **5,** a012633
6. Kunkel, T. A., and Erie, D. A. (2005) DNA mismatch repair. *Annu. Rev. Biochem.* **74,** 681–710
7. Flores-Rozas, H., and Kolodner, R. D. (1998) The *Saccharomyces cerevisiae* MLH3 gene functions in MSH3-dependent suppression of frameshift mutations. *Proc. Natl. Acad. Sci. U.S.A.* **95,** 12404–12409
8. Harfe, B. D., Minesinger, B. K., and Jinks-Robertson, S. (2000) Discrete *in vivo* roles for the MutL homologs Mlh2p and Mlh3p in the removal of frameshift intermediates in budding yeast. *Curr. Biol.* **10,** 145–148
9. Lipkin, S. M., Wang, V., Jacoby, R., Banerjee-Basu, S., Baxevanis, A. D., Lynch, H. T., Elliott, R. M., and Collins, F. S. (2000) MLH3: A DNA mismatch repair gene associated with mammalian microsatellite instability. *Nat. Genet.* **24,** 27–35
10. Wang, T. F., Kleckner, N., and Hunter, N. (1999) Functional specificity of MutL homologs in yeast. Evidence for three Mlh1-based heterocomplexes with distinct roles during meiosis in recombination and mismatch correc-

[3] N. Hunter, UC Davis, personal communication.

tion. *Proc. Natl. Acad. Sci. U.S.A.* **96,** 13914–13919
11. Cannavo, E., Marra, G., Sabates-Bellver, J., Menigatti, M., Lipkin, S. M., Fischer, F., Cejka, P., and Jiricny, J. (2005) Expression of the MutL homologue hMLH3 in human cells and its role in DNA mismatch repair. *Cancer Res.* **65,** 10759–10766
12. Kadyrov, F. A., Dzantiev, L., Constantin, N., and Modrich, P. (2006) Endonucleolytic function of MutLα in human mismatch repair. *Cell* **126,** 297–308
13. Kadyrov, F. A., Holmes, S. F., Arana, M. E., Lukianova, O. A., O'Donnell, M., Kunkel, T. A., and Modrich, P. (2007) *Saccharomyces cerevisiae* MutLα is a mismatch repair endonuclease. *J. Biol. Chem.* **282,** 37181–37190
14. Guarné, A. (2012) The functions of MutL in mismatch repair. The power of multitasking. *Prog. Mol. Biol. Transl. Sci.* **110,** 41–70
15. Gueneau, E., Dherin, C., Legrand, P., Tellier-Lebegue, C., Gilquin, B., Bonnesoeur, P., Londino, F., Quemener, C., Le Du, M. H., Márquez, J. A., Moutiez, M., Gondry, M., Boiteux, S., and Charbonnier, J. B. (2013) Structure of the MutLα C-terminal domain reveals how Mlh1 contributes to Pms1 endonuclease site. *Nat. Struct. Mol. Biol.* **20,** 461–468
16. Hall, M. C., Shcherbakova, P. V., Fortune, J. M., Borchers, C. H., Dial, J. M., Tomer, K. B., and Kunkel, T. A. (2003) DNA binding by yeast Mlh1 and Pms1. Implications for DNA mismatch repair. *Nucleic Acids Res.* **31,** 2025–2034
17. Habraken, Y., Sung, P., Prakash, L., and Prakash, S. (1997) Enhancement of MSH2-MSH3-mediated mismatch recognition by the yeast MLH1-PMS1 complex. *Curr. Biol.* **7,** 790–793
18. Pillon, M. C., Lorenowicz, J. J., Uckelmann, M., Klocko, A. D., Mitchell, R. R., Chung, Y. S., Modrich, P., Walker, G. C., Simmons, L. A., Friedhoff, P., and Guarné, A. (2010) Structure of the endonuclease domain of MutL. Unlicensed to cut. *Mol. Cell* **39,** 145–151
19. Keeney, S. (2008) Spo11 and the formation of DNA double-strand breaks in meiosis. *Genome Dyn. Stab.* **2,** 81–123
20. Lynn, A., Soucek, R., and Börner, G. V. (2007) ZMM proteins during meiosis. Crossover artists at work. *Chromosome Res.* **15,** 591–605
21. Börner, G. V., Kleckner, N., and Hunter, N. (2004) Crossover/noncrossover differentiation, synaptonemal complex formation, and regulatory surveillance at the leptotene/zygotene transition of meiosis. *Cell* **117,** 29–45
22. Hunter, N., and Kleckner, N. (2001) The single-end invasion. An asymmetric intermediate at the double-strand break to double-holliday junction transition of meiotic recombination. *Cell* **106,** 59–70
23. Argueso, J. L., Wanat, J., Gemici, Z., and Alani, E. (2004) Competing crossover pathways act during meiosis in *Saccharomyces cerevisiae*. *Genetics* **168,** 1805–1816
24. de los Santos, T., Hunter, N., Lee, C., Larkin, B., Loidl, J., and Hollingsworth, N. M. (2003) The Mus81/Mms4 endonuclease acts independently of double-Holliday junction resolution to promote a distinct subset of crossovers during meiosis in budding yeast. *Genetics* **164,** 81–94
25. Kneitz, B., Cohen, P. E., Avdievich, E., Zhu, L., Kane, M. F., Hou, H., Jr., Kolodner, R. D., Kucherlapati, R., Pollard, J. W., and Edelmann, W. (2000) MutS homolog 4 localization to meiotic chromosomes is required for chromosome pairing during meiosis in male and female mice. *Genes Dev.* **14,** 1085–1097
26. Santucci-Darmanin, S., Neyton, S., Lespinasse, F., Saunières, A., Gaudray, P., and Paquis-Flucklinger, V. (2002) The DNA mismatch-repair MLH3 protein interacts with MSH4 in meiotic cells, supporting a role for this MutL homolog in mammalian meiotic recombination. *Hum. Mol. Genet.* **11,** 1697–1706
27. Snowden, T., Acharya, S., Butz, C., Berardini, M., and Fishel, R. (2004) hMSH4-hMSH5 recognizes Holliday junctions and forms a meiosis-specific sliding clamp that embraces homologous chromosomes. *Mol. Cell* **15,** 437–451
28. Lenzi, M. L., Smith, J., Snowden, T., Kim, M., Fishel, R., Poulos, B. K., and Cohen, P. E. (2005) Extreme heterogeneity in the molecular events leading to the establishment of chiasmata during meiosis i in human oocytes. *Am. J. Hum. Genet.* **76,** 112–127
29. Zakharyevich, K., Tang, S., Ma, Y., and Hunter, N. (2012) Delineation of joint molecule resolution pathways in meiosis identifies a crossover-specific resolvase. *Cell* **149,** 334–347
30. Zakharyevich, K., Ma, Y., Tang, S., Hwang, P. Y., Boiteux, S., and Hunter, N. (2010) Temporally and biochemically distinct activities of Exo1 during meiosis. Double-strand break resection and resolution of double Holliday junctions. *Mol. Cell* **40,** 1001–1015
31. Nishant, K. T., Plys, A. J., and Alani, E. (2008) A mutation in the putative MLH3 endonuclease domain confers a defect in both mismatch repair and meiosis in *Saccharomyces cerevisiae*. *Genetics* **179,** 747–755
32. De Muyt, A., Jessop, L., Kolar, E., Sourirajan, A., Chen, J., Dayani, Y., and Lichten, M. (2012) BLM helicase ortholog Sgs1 is a central regulator of meiotic recombination intermediate metabolism. *Mol. Cell* **46,** 43–53
33. Kolas, N. K., Svetlanov, A., Lenzi, M. L., Macaluso, F. P., Lipkin, S. M., Liskay, R. M., Greally, J., Edelmann, W., and Cohen, P. E. (2005) Localization of MMR proteins on meiotic chromosomes in mice indicates distinct functions during prophase I. *J. Cell Biol.* **171,** 447–458
34. Marcon, E., and Moens, P. (2003) MLH1p and MLH3p localize to precociously induced chiasmata of okadaic acid-treated mouse spermatocytes. *Genetics* **165,** 2283–2287
35. Baker, S. M., Plug, A. W., Prolla, T. A., Bronner, C. E., Harris, A. C., Yao, X., Christie, D. M., Monell, C., Arnheim, N., Bradley, A., Ashley, T., and Liskay, R. M. (1996) Involvement of mouse Mlh1 in DNA mismatch repair and meiotic crossing over. *Nat. Genet.* **13,** 336–342
36. Barlow, A. L., and Hultén, M. A. (1998) Crossing over analysis at pachytene in man. *Eur. J. Hum. Genet.* **6,** 350–358
37. Cejka, P., and Kowalczykowski, S. C. (2010) The full-length *Saccharomyces cerevisiae* Sgs1 protein is a vigorous DNA helicase that preferentially unwinds holliday junctions. *J. Biol. Chem.* **285,** 8290–8301
38. Cejka, P., Plank, J. L., Dombrowski, C. C., and Kowalczykowski, S. C. (2012) Decatenation of DNA by the *S. cerevisiae* Sgs1-Top3-Rmi1 and RPA complex. A mechanism for disentangling chromosomes. *Mol. Cell* **47,** 886–896
39. Räschle, M., Marra, G., Nyström-Lahti, M., Schär, P., and Jiricny, J. (1999) Identification of hMutLβ, a heterodimer of hMLH1 and hPMS1. *J. Biol. Chem.* **274,** 32368–32375
40. Cannavo, E., Cejka, P., and Kowalczykowski, S. C. (2013) Relationship of DNA degradation by *Saccharomyces cerevisiae* exonuclease 1 and its stimulation by RPA and Mre11-Rad50-Xrs2 to DNA end resection. *Proc. Natl. Acad. Sci. U.S.A.* **110,** E1661–E1668
41. Biswas, E. E., Chen, P. H., and Biswas, S. B. (1995) Overexpression and rapid purification of biologically active yeast proliferating cell nuclear antigen. *Protein Expr. Purif.* **6,** 763–770
42. Finkelstein, J., Antony, E., Hingorani, M. M., and O'Donnell, M. (2003) Overproduction and analysis of eukaryotic multiprotein complexes in *Escherichia coli* using a dual-vector strategy. *Anal. Biochem.* **319,** 78–87
43. Rass, U., Compton, S. A., Matos, J., Singleton, M. R., Ip, S. C., Blanco, M. G., Griffith, J. D., and West, S. C. (2010) Mechanism of Holliday junction resolution by the human GEN1 protein. *Genes Dev.* **24,** 1559–1569
44. Sonntag Brown, M., Lim, E., Chen, C., Nishant, K. T., and Alani, E. (2013) Genetic analysis of mlh3 mutations reveals interactions between crossover promoting factors during meiosis in baker's yeast. *G3* **3,** 9–22
45. Räschle, M., Dufner, P., Marra, G., and Jiricny, J. (2002) Mutations within the hMLH1 and hPMS2 subunits of the human MutLα mismatch repair factor affect its ATPase activity but not its ability to interact with hMutSα. *J. Biol. Chem.* **277,** 21810–21820
46. Tran, P. T., Erdeniz, N., Dudley, S., and Liskay, R. M. (2002) Characterization of nuclease-dependent functions of Exo1p in *Saccharomyces cerevisiae*. *DNA Repair* **1,** 895–912
47. Hall, M. C., Wang, H., Erie, D. A., and Kunkel, T. A. (2001) High affinity cooperative DNA binding by the yeast Mlh1-Pms1 heterodimer. *J. Mol. Biol.* **312,** 637–647
48. Hall, M. C., Shcherbakova, P. V., and Kunkel, T. A. (2002) Differential ATP binding and intrinsic ATP hydrolysis by amino-terminal domains of the yeast Mlh1 and Pms1 proteins. *J. Biol. Chem.* **277,** 3673–3679
49. Plys, A. J., Rogacheva, M. V., Greene, E. C., and Alani, E. (2012) The unstructured linker arms of Mlh1-Pms1 are important for interactions with DNA during mismatch repair. *J. Mol. Biol.* **422,** 192–203
50. Marsischky, G. T., and Kolodner, R. D. (1999) Biochemical characterization of the interaction between the *Saccharomyces cerevisiae* MSH2-

MSH6 complex and mispaired bases in DNA. *J. Biol. Chem.* **274,** 26668–26682
51. Gradia, S., Acharya, S., and Fishel, R. (1997) The human mismatch recognition complex hMSH2-hMSH6 functions as a novel molecular switch. *Cell* **91,** 995–1005
52. Lilley, D. M., and Clegg, R. M. (1993) The structure of the four-way junction in DNA. *Annu. Rev. Biophys. Biomol. Struct.* **22,** 299–328
53. Duckett, D. R., Murchie, A. I., Diekmann, S., von Kitzing, E., Kemper, B., and Lilley, D. M. (1988) The structure of the Holliday junction, and its resolution. *Cell* **55,** 79–89
54. Lipkin, S. M., Moens, P. B., Wang, V., Lenzi, M., Shanmugarajah, D., Gilgeous, A., Thomas, J., Cheng, J., Touchman, J. W., Green, E. D., Schwartzberg, P., Collins, F. S., and Cohen, P. E. (2002) Meiotic arrest and aneuploidy in MLH3-deficient mice. *Nat. Genet.* **31,** 385–390
55. Svetlanov, A., Baudat, F., Cohen, P. E., and de Massy, B. (2008) Distinct functions of MLH3 at recombination hot spots in the mouse. *Genetics* **178,** 1937–1945
56. Habraken, Y., Sung, P., Prakash, L., and Prakash, S. (1998) ATP-dependent assembly of a ternary complex consisting of a DNA mismatch and the yeast MSH2-MSH6 and MLH1-PMS1 protein complexes. *J. Biol. Chem.* **273,** 9837–9841
57. Gorman, J., Plys, A. J., Visnapuu, M. L., Alani, E., and Greene, E. C. (2010) Visualizing one-dimensional diffusion of eukaryotic DNA repair factors along a chromatin lattice. *Nat. Struct. Mol. Biol.* **17,** 932–938
58. Hombauer, H., Campbell, C. S., Smith, C. E., Desai, A., and Kolodner, R. D. (2011) Visualization of eukaryotic DNA mismatch repair reveals distinct recognition and repair intermediates. *Cell* **147,** 1040–1053
59. White, M. F., and Lilley, D. M. (1997) The resolving enzyme CCE1 of yeast opens the structure of the four-way DNA junction. *J. Mol. Biol.* **266,** 122–134
60. Bennett, R. J., and West, S. C. (1995) Structural analysis of the RuvC-Holliday junction complex reveals an unfolded junction. *J. Mol. Biol.* **252,** 213–226
61. Snowden, T., Shim, K. S., Schmutte, C., Acharya, S., and Fishel, R. (2008) hMSH4-hMSH5 adenosine nucleotide processing and interactions with homologous recombination machinery. *J. Biol. Chem.* **283,** 145–154
62. Wang, T. F., and Kung, W. M. (2002) Supercomplex formation between Mlh1-Mlh3 and Sgs1-Top3 heterocomplexes in meiotic yeast cells. *Biochem. Biophys. Res. Commun.* **296,** 949–953

Supplementary Table 1

Oligonucleotide	Sequence 5-3'
1253	TGGGTCAACGTGGGCAAAGATGTCCTAGCAATGTAATCGTCTATGACGTT
1254	TGCCGAATTCTACCAGTGCCAGTGATGGACATCTTTGCCCACGTTGACCC
1255	GTCGGATCCTCTAGACAGCTCCATGATCACTGGCACTGGTAGAATTCGGC
1256	CAACGTCATAGACGATTACATTGCTACATGGAGCTGTCTAGAGGATCCGA
1253C	AACGTCATAGACGATTACATTGCTAGGACATCTTTGCCCACGTTGACCCA
312	AACGTCATAGACGATTACATTGCTA
314	CATGGAGCTGTCTAGAGGATCCGAC
316	TGCCGAATTCTACCAGTGCCGGCAGCAAGTCGCTTTGCCCACGTTGACCC
317	CAACGTCATAGACGATTACAGTTAGGTCGAAGGCTGTCTAGAGGATCCGA
288	GGCTAGCTGCTAGCGGATCCATGATCAAGTGCTTGTCAGTTG
289	CGCAAATCCTCGAGCCCGGGTGGTGGCTCACAGGGAGGCATG
245	GGCTAGCT GGGCCC GCTAGC GGATCC ATGAGCCAGCATATTAGGAAATTAG
246	CGCAAATC CTCGAG CCCGGG CTTCAATTCTGCAATGGGTACC
251	GGCTAGCT GCTAGC GGATCC ATGTCTCTCAGAATAAAAGCAC
252	CGCAAATC CTCGAG CCCGGG TTAACACCTCTCAAAAACTTTGTATAG
325	CTCTCAAA GAAATGATGG AGGCCTCCAT CGATGCGAAT GCTAC
326	GTAGC ATTCGCATCG ATGGAGGCCT CCATCATTTC TTTGAGAG
327	CGGTTAGA GAAATAGTTC AAGCCTCTGT AGATGCACAC GCTAC
328	GTAGC GTGTGCATCT ACAGAGGCTT GAACTATTTC TCTAACCG

Table 1. **Oligonucleotide sequences.** Sequences of all deoxyribonucleotides used in this study are listed in a 5' to 3' orientation.

2.3 RECQL4 promotes DNA end resection in repair of DNA double-strand breaks

Huiming Lu, Raghavendra A. Shamanna, Guido Keijzers, **Roopesh Anand**, Lene Juel Rasmussen, Petr Cejka, Deborah L. Croteau, and Vilhelm A. Bohr

Article published in *Cell Reports, 2016*

I contributed to this study by expressing and purifying human MRN complex.

Article

Cell Reports

RECQL4 Promotes DNA End Resection in Repair of DNA Double-Strand Breaks

Graphical Abstract

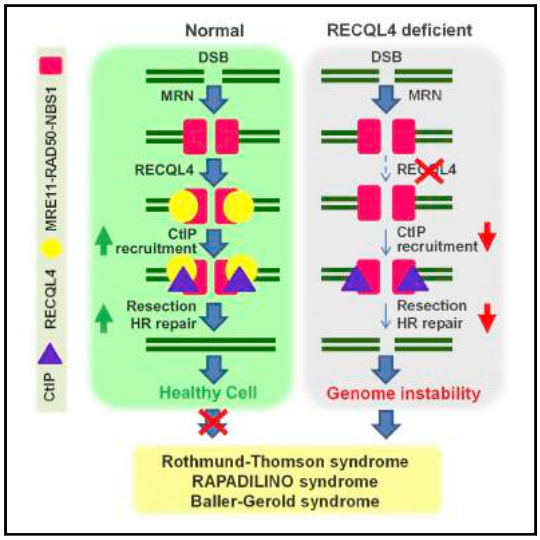

Highlights

- RECQL4 promotes 5′ end resection at DSBs
- RECQL4 recruitment to DSBs depends on MRE11
- RECQL4 promotes recruitment of CtIP to DSBs
- RECQL4 helicase activity is required for 5′ DNA end resection

Authors

Huiming Lu, Raghavendra A. Shamanna, Guido Keijzers, ..., Petr Cejka, Deborah L. Croteau, Vilhelm A. Bohr

Correspondence

vbohr@nih.gov

In Brief

RECQL4, a RecQ helicase mutated in Rothmund-Thomson syndrome, is a guardian of genome stability and repairs DNA, but the underlying mechanisms remain unclear. Lu et al. show that RECQL4 plays a role in homologous recombination repair of DNA double-strand breaks (DSBs). RECQL4 promotes 5′ DNA end resection through the MRE11-RAD50-NBS1 and CtIP complexes.

Lu et al., 2016, Cell Reports *16*, 161–173
June 28, 2016
http://dx.doi.org/10.1016/j.celrep.2016.05.079

CellPress

Cell Reports
Article

RECQL4 Promotes DNA End Resection in Repair of DNA Double-Strand Breaks

Huiming Lu,[1,4] Raghavendra A. Shamanna,[1,4] Guido Keijzers,[2] Roopesh Anand,[3] Lene Juel Rasmussen,[2] Petr Cejka,[3] Deborah L. Croteau,[1] and Vilhelm A. Bohr[1,2,*]
[1]Laboratory of Molecular Gerontology, National Institute on Aging, National Institutes of Health, Baltimore, MD 21224, USA
[2]Center for Healthy Aging and Department of Cellular and Molecular Medicine, University of Copenhagen, 2200 Copenhagen, Denmark
[3]Institute of Molecular Cancer Research, University of Zurich, Winterthurerstrasse 190, 8057 Zurich, Switzerland
[4]Co-first author
*Correspondence: vbohr@nih.gov
http://dx.doi.org/10.1016/j.celrep.2016.05.079

SUMMARY

The RecQ helicase RECQL4, mutated in Rothmund-Thomson syndrome, regulates genome stability, aging, and cancer. Here, we identify a crucial role for RECQL4 in DNA end resection, which is the initial and an essential step of homologous recombination (HR)-dependent DNA double-strand break repair (DSBR). Depletion of RECQL4 severely reduces HR-mediated repair and 5′ end resection in vivo. RECQL4 physically interacts with MRE11-RAD50-NBS1 (MRN), which senses DSBs and initiates DNA end resection with CtIP. The MRE11 exonuclease regulates the retention of RECQL4 at laser-induced DSBs. RECQL4 also directly interacts with CtIP via its N-terminal domain and promotes CtIP recruitment to the MRN complex at DSBs. Moreover, inactivation of RECQL4's helicase activity impairs DNA end processing and HR-dependent DSBR without affecting its interaction with MRE11 and CtIP, suggesting an important role for RECQL4's unwinding activity in the process. Thus, we report that RECQL4 is an important participant in HR-dependent DSBR.

INTRODUCTION

DNA double-strand breaks (DSBs) are generated by exogenous stress, endogenous replication, and programmed recombination events. Improperly repaired DSBs can lead to genome instability, chromosomal rearrangements, and/or cell death (Symington, 2014). DSBs are usually repaired by one of two major pathways: homologous recombination (HR) and non-homologous end joining (NHEJ) (Aparicio et al., 2014). HR-dependent DSBR is mostly error free, but it requires a sister or non-sister chromatid as template and is only active during the S and G2 phases of the cell cycle. In contrast, NHEJ-dependent DSBR is error prone, DNA template-independent, and active during all phases of the cell cycle.

HR-dependent DSBR is initiated by 5′ end resection of the DSBs, which generates 3′ protruding single-strand DNA (ssDNA) tails (Chen et al., 2013; Zhu et al., 2008). RPA coats the ssDNA, and then RAD51 replaces RPA to promote strand invasion. This is followed by repair synthesis, dissolution, and resolution of Holliday junctions and ligation of the ends (Prakash et al., 2015). It is generally considered that DNA end resection occurs in two steps (Cejka et al., 2010; Gravel et al., 2008; Mimitou and Symington, 2008; Nimonkar et al., 2011; Niu et al., 2010; Zhu et al., 2008). The first step is the initial resection by Mre11-Rad50-Xrs2 (MRX) and Sae2 at the DSB in yeast (Cannavo and Cejka, 2014; Mimitou and Symington, 2008) or by MRE11-RAD50-NBS1 (MRN) and CtIP (CtBP-interacting protein) in human cells (Sartori et al., 2007; You et al., 2009). This is followed by extensive resection by either exonuclease1 (EXO1) or DNA2/BLM/TOP3/RMI1/2 (Dna2/Sgs1/Top3/Rmi1 in yeast) (Cejka et al., 2010; Gravel et al., 2008; Mimitou and Symington, 2008; Nimonkar et al., 2008, 2011; Niu et al., 2010; Zhu et al., 2008).

RECQL4 is one of five RecQ helicase proteins in mammalian cells. Defects in human RECQL4 are associated with three genetic diseases: Rothmund-Thomson syndrome (RTS), RAPADILINO, and Baller-Gerold syndrome (Siitonen et al., 2009) as well as several cancers (Fang et al., 2013; Lu et al., 2014b; Su et al., 2010). It is well established that RECQL4 is required for the assembly of the DNA replication initiation machinery (Im et al., 2009; Sangrithi et al., 2005; Xu et al., 2009). However, the role of RECQL4 in DNA repair is less clear (Croteau et al., 2014). Lack of RECQL4 increases persistent DNA damage and triggers cellular senescence in human and mouse primary fibroblasts (Lu et al., 2014a). RECQL4 is recruited to laser-induced DSBs and RTS fibroblasts are sensitive to ionizing radiation (IR), suggesting that RECQL4 plays a role in DSBR (Singh et al., 2010). Recently, we showed that depletion of RECQL4 inhibits NHEJ in U2OS cells (Shamanna et al., 2014). Nevertheless, RECQL4 is highly expressed during S phase (Singh et al., 2012; Xu et al., 2009), when HR-dependent DSBR dominates. Thus, we explore the possibility that RECQL4 also plays a role in HR-dependent DSBR. We find that RECQL4 promotes DNA end resection and HR-dependent DSBR by stimulating the association of CtIP with MRN at DSBs and that the helicase activity of RECQL4 is necessary for DNA end resection. Together, these

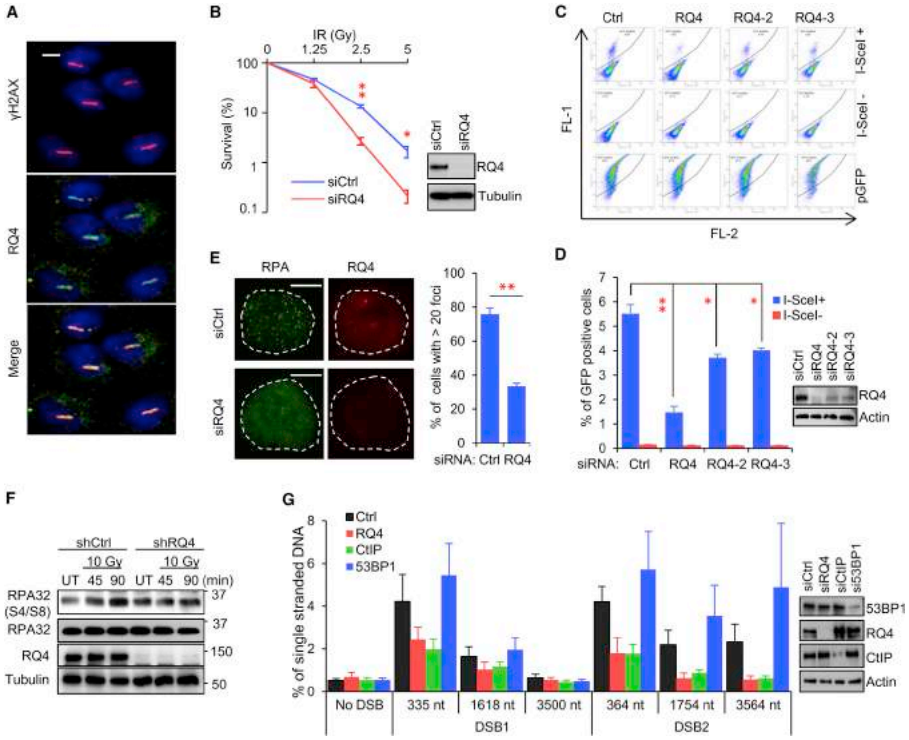

Figure 1. RECQL4 Is Required for HR-Mediated Repair and DNA End Resection

(A) Co-localization of endogenous RECQL4 and γH2AX at laser-induced DSB tracks. Scale bar represents 10 μm.

(B) Clonogenic survival of siRQ4-transfected U2OS cells treated with γ radiation.

(C) Representative dot-plot images of DR-GFP U2OS cells showing in vivo HR.

(D) Quantification of HR repair.

(E) RPA foci in U2OS cells treated with control or *RECQL4* siRNA 1 hr after 10 Gy IR. Scale bar represents 10 μm.

(F) IR-induced RPA32 phosphorylation on serine 4 and 8. U2OS cells expressing control or *RECQL4* shRNA were exposed to 10 Gy of IR then allowed to recover for the indicated time. UT, untreated.

(G) Quantification of ssDNA generated by 5′ end resection at two AsiSI-induced DSBs in AID-DIvA U2OS cells.

All graphs show mean ± SEM from at least three biological repeats. p values (*$p < 0.05$; **$p < 0.01$) was determined by Student's t test. See also Figures S1 and S2.

findings suggest that RECQL4 plays an important role in the DNA end resection step of HR-mediated DSBR in human cells.

RESULTS

RECQL4 Promotes DNA End Resection during HR-Dependent DSBR

Endogenous RECQL4 co-localized with γH2AX at laser-induced DSBs in U2OS cells (Figure 1A) and depletion of RECQL4 caused U2OS and HeLa cells to be significantly more sensitive to IR (Figures 1B and S1A). Since DSB repair pathway choice is cell-cycle regulated (Aparicio et al., 2014), we first examined the effect of RECQL4 depletion on cell-cycle progression. Knockdown of RECQL4 did not perturb cell-cycle progression significantly in U2OS or HEK293T cells and did not alter expression of cell-cycle marker proteins Cyclin A and Cyclin D1 (Figure S2), which is consistent with a previous finding in HEK293 cells (Park et al., 2006).

The role of RECQL4 in HR-dependent DSBR was then investigated in DR-GFP U2OS cells, which can be scored for efficiency of HR-mediated repair of an I-SceI endonuclease-induced DSB by measuring the fraction of GFP-positive cells (Pierce et al., 1999; Wang et al., 2014). DR-GFP U2OS cells were transfected with one of three RECQL4-targeted small interfering RNAs (siRNAs). The efficiency of RECQL4 knockdown was about 90%, 60%, and 50% for siRQ4, siRQ4-2, and siRQ4-3, respectively (Figure 1D). Given that siRQ4 produced the greatest knockdown it was used in all subsequent experiments. Depletion of RECQL4 by siRQ4 significantly reduced the proportion of GFP-positive cells by 73%, from 5.5% in control cells to 1.47% in knockdown cells (Figures 1C and 1D), suggesting that RECQL4 plays a crucial role in HR-dependent DSBR. The other two siRNAs, siRQ4-2 and siRQ4-3, also significantly reduced the proportions of GFP-positive cells to 3.71% and 4.0%, respectively (Figures 1C and 1D). These data show that knockdown efficiency of RECQL4 correlates with a decrease of HR-mediated DSBR.

RECQL4 is rapidly recruited to laser-induced DSBs where it is retained for a short time (Singh et al., 2010). Thus, we speculated that it plays a role in the early stages of HR repair. As mentioned above, the first step of HR-mediated DSBR is 5′-3′ end resection of the DSBs to generate 3′ protruding ssDNA tails, which are rapidly coated by RPA to form a nuclease-resistant protective protein-DNA filament (Chen et al., 2013). We then examined RPA foci formation in RECQL4-depleted cells. After exposure to 10 Gy of IR, the fraction of cells with >20 RPA foci was ~33.6% in the siRQ4-treated U2OS cells, significantly less than 75.8% in the control cells (Figure 1E). Depletion of RECQL4 also repressed RPA foci formation after IR in HeLa cells (Figure S1B). Consistent with these results, the abundance of phosphorylated RPA32 on serine 4 and serine 8, a maker of ssDNA-bound RPA (Shao et al., 1999), was increased in IR-treated control U2OS and HEK293T cells, but not in RECQL4 knockdown cells (Figures 1F and S1C).

AID-DIvA U2OS cells have been used to directly quantify ssDNA generated by 5′ end resection at two AsiSI-induced DSBs (Aymard et al., 2014). With addition of 4-hydroxytamoxifen (4-OHT), the AsiSI endonuclease fused to an estrogen receptor ligand binding domain translocates from the cytoplasm to the nucleus to induce DSBs (Aymard et al., 2014). Genomic DNA from these cells was prepared and analyzed for ssDNA at two DSBs by TaqMan qPCR, as previously described (Aymard et al., 2014; Zhou et al., 2014). Consistent with a previous report (Zhou et al., 2014), we observed notably lower ssDNA in cells treated with CtIP siRNA because CtIP stimulates DNA end resection (Sartori et al., 2007). On the contrary, depletion of 53BP1 increased the amount of ssDNA (Figure 1G), since 53BP1 inhibits resection (Bunting et al., 2010). To investigate the role of RECQL4 in 5′ end resection, ssDNA content was measured in siRQ4-transfected AID-DIvA U2OS cells. Interestingly, the amount of ssDNA generated at position 335 nt from DSB1 was 40.2% lower than that in siCtrl-treated cells, and similar to the reduction caused by CtIP depletion. At DSB2, depletion of RECQL4 reduced ssDNA content by 57.2%, 70.1%, and 75.2% at positions 364, 1,754, and 3,574 nt, respectively. Together, these results demonstrate that RECQL4 is important for HR by promoting 5′ end resection of DSBs.

Retention of RECQL4 at DSBs Depends on MRE11

To explore the function of RECQL4 in 5′ end resection, we used mass spectroscopy to analyze proteins captured by co-immunoprecipitation (IP) with RECQL4-3xFLAG from irradiated HEK293T cells in the presence of benzonase. MRN components MRE11 and RAD50 and other DNA resection proteins BLM, EXO1, and DNA2 were identified (Figure S3A; Table S1), and their interactions with RECQL4 were independently confirmed by IP with GFP-RECQL4 in the presence of benzonase (Figure S3B) or ethidium bromide (Figure S3C). We found that RECQL4 co-localized with MRE11 at DSBs and that the RECQL4-MRN interaction is stimulated by IR (Figures 2A and 2B). Purified recombinant RECQL4 also immunoprecipitated recombinant MRE11, RAD50, and NBS1 (Figure 2C), indicating complex formation between RECQL4 and MRN. To map the interaction region of RECQL4 with MRE11, purified RECQL4-3xFLAG and truncation fragments were incubated with purified YFP-MRE11 bound to GFP agarose beads. YFP-MRE11 pulled down full-length and the N-terminal domain of RECQL4 (Figure 2D), indicating that the N-terminal fragment of RECQL4 is responsible for the interaction with MRE11. To determine whether the interaction between RECQL4 and MRN is functional, we measured the nuclease activity of MRN on closed-circular single-strand PhiX174 DNA in the presence of RECQL4 in vitro as previously reported (Sartori et al., 2007). Wild-type MRN and nuclease-dead MRN-ND (H129L/D130V) (Stracker et al., 2002) as well as RECQL4 and its helicase-dead mutant RQ4KM were used (Figure S4A). We found that RECQL4 slightly stimulated the nuclease activity of MRN on closed-circular single-strand PhiX174 DNA (Figure 2E).

Both RECQL4 and MRE11 are rapidly recruited to DSB (Haince et al., 2008; Singh et al., 2010), and thus we evaluated whether RECQL4 and MRE11 affected each other's recruitment to DNA damage. GFP-RECQL4 was recruited significantly less to laser-induced DSBs in siMRE11-treated U2OS cells than in control cells (Figure 2F), and there is less chromatin-bound RECQL4 in siMRE11-treated U2OS cells than in control cells after IR (Figure S4B). However, depletion of RECQL4 did not affect the recruitment of YFP-MRE11 to laser-induced DSB (Figure S4C), suggesting that recruitment of RECQL4 to DSBs requires MRE11, but not vice versa.

Given that MRE11 nuclease regulates the pathway choice between NHEJ and HR (Shibata et al., 2014), the dynamics of GFP-RECQL4 recruitment was also evaluated in cells exposed to mirin, which specifically inhibits the MRE11 exonuclease but does not inhibit MRN complex formation (Dupré et al., 2008). RECQL4 was still rapidly recruited to laser-induced DSBs in mirin-treated cells (Figure 2G), indicating that the recruitment of RECQL4 does not depend on the exonuclease activity of MRE11. However, GFP-RECQL4 was retained at DSBs for a significantly shorter time after mirin treatment (Figure 2G). This suggests that retention of RECQL4 at DSBs is regulated by MRE11 nuclease activity.

When ssDNA was measured at AsiSI-induced DSB in AID-DIvA U2OS cells pre-treated with mirin, siRQ4 or siMRE11, a

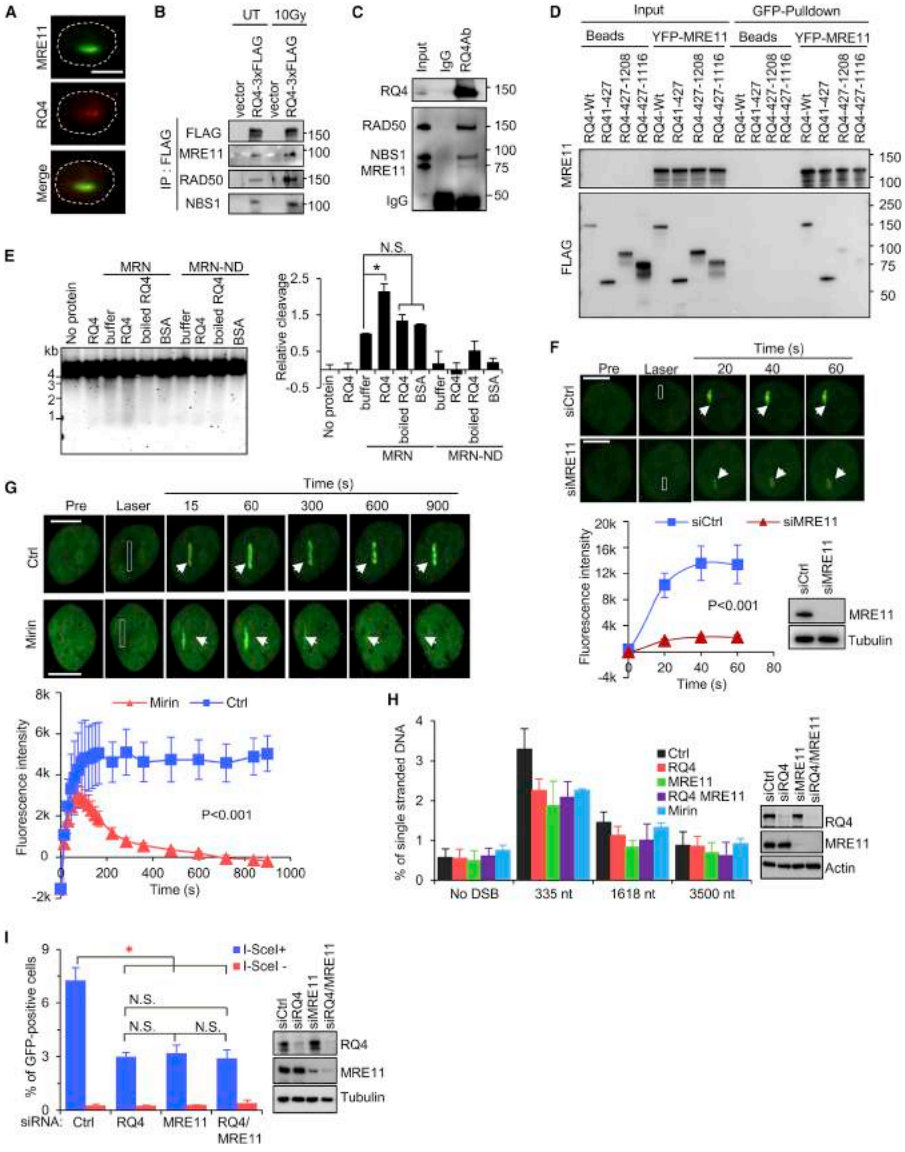

(legend on next page)

lower amount of ssDNA was detected (Figure 2H). However, the effect was not additive (Figure 2H). Using the DR-GFP reporter system, it was observed that pre-treatment with siRQ4 or siMRE11 significantly reduced HR-mediated DSBR, but the effect was also not additive (Figure 2I). These results suggest that RECQL4 functions downstream of MRN to promote DNA 5′ end resection and HR-dependent DSBR.

RECQL4 Promotes Recruitment of CtIP to DSBs

CtIP is required for initiation of MRN-catalyzed 5′ end resection at DSBs (Chen et al., 2008; Sartori et al., 2007; Yuan and Chen, 2009). Here, we found that RECQL4 co-localized with CtIP at laser-induced DSBs (Figure 3A) and interacted with CtIP in irradiated HEK293T cells (Figures 3B, S3B, and S3C). The interaction between CtIP and RECQL4 appeared to be stronger in IR-treated cells (Figure 3B). CoIP of recombinant RECQL4 and CtIP suggests that RECQL4 interacts directly with CtIP (Figure 3C), and the N terminus of RECQL4 was mapped as the interacting region with CtIP (Figure 3D).

Recruitment of RECQL4 reaches its peak about 1 min after laser damage (Figure 2G), while CtIP needs much longer (Wang et al., 2013). Considering the direct interaction between RECQL4 and CtIP, it is possible that RECQL4 promotes CtIP recruitment to DSBs. To test this hypothesis, we first measured the abundance of chromatin-bound CtIP in control and RECQL4 knockdown U2OS cells after IR and found that IR increased chromatin-bound CtIP in the control cells but not in RECQL4-depleted cells (Figure 3E). Interestingly, more mobility shift of chromatin-bound CtIP was detected in control cells that in RECQL4-depleted cells after IR (Figure 3E), indicating that RECQL4 promotes IR-induced posttranslational modification of CtIP. Also, IR-treated control U2OS cells had an average of 22.6 GFP-CtIP foci per cell, significantly higher than that in siRQ4-treated cells (Figure 3F). Furthermore, in the RECQL4 knockdown U2OS cells, recruitment of GFP-CtIP was significantly slower and less efficient than that in control cells (Figure 3G). Together these data suggest that RECQL4 promotes stable CtIP recruitment to DSBs.

Given that RECQL4 promotes recruitment of CtIP to DSBs, we asked whether RECQL4 is required for MRN-CtIP complex formation after IR. Pull-down assays were conducted in control and RECQL4 knockdown HEK293T cells expressing YFP-MRE11 or GFP-CtIP. Expression levels of MRE11, RAD50, NBS1, and CtIP proteins were similar in control and RECQL4 knockdown cells (input of Figure 3H). Cell-cycle status was not significantly different between RECQL4-depleted and control HEK293T cells (Figures S2D and S2E). IP of YFP-MRE11 efficiently pulled down similar amounts of RAD50 and NBS1 from control and RECQL4 knockdown cells. In contrast, the interaction between MRE11 and CtIP was inhibited by knockdown of RECQL4 (Figure 3H). In the reverse experiments with GFP-CtIP-expressing cells, GFP-CtIP efficiently co-immunoprecipitated MRE11, RAD50, and NBS1 from control cells but much less from RECQL4 knockdown cells (Figure 3H). These data are consistent with the idea that RECQL4 promotes the interaction between MRN and CtIP in human cells.

Depletion of RECQL4 or CtIP significantly reduced ssDNA generation at DSB1 in AID-DIvA cells (Figure 3I). However, there were no differences among RECQL4 or CtIP-depleted cells and RECQL4/CtIP double-knockdown cells. A similar result was obtained from the experiments measuring the HR efficiency (Figure 3J). These results imply that RECQL4 and CtIP both play a role in HR-dependent DSBR and that RECQL4 promotes recruitment of CtIP to DSBs.

BLM and EXO1 Act Downstream of RECQL4 during HR-Mediated DSBR

5′ resection, initiated by the MRN-CtIP complex, is extended by BLM/DNA2 and EXO1 via two alternative pathways (Cejka, 2015; Symington, 2014). Recruitment of both BLM and EXO1 to DSBs requires CtIP (Wang et al., 2013). Since RECQL4 promotes CtIP recruitment to DSBs, we tested whether removal of RECQL4 could result in failure of the two extensive resection pathways. We found that BLM, DNA2, and EXO1 interact with RECQL4 in irradiated HEK293T cells (Figure S3). In addition, the retention of GFP-BLM at DSBs was reduced in U2OS cells after RECQL4 knockdown (Figure 4A), suggesting that RECQL4 stimulates retention of BLM at IR-induced DSBs. In addition, knockdown of BLM, RECQL4, or both inhibited 5′ resection to a similar extent at DSB1 in AID-DIvA U2OS cells (Figure 4B). In the HR assay, knockdown of BLM, RECQL4, or both significantly reduced HR by 40%, 60%, or 60%, respectively (Figure 4C). These findings

Figure 2. MRE11 Mediates Recruitment of RECQL4 to DSBs to Promote HR Repair

(A) Co-localization of endogenous RECQL4 and MRE11 at laser-induced DSB tracks in U2OS cells. Scale bar represents 10 μm.

(B) RECQL4 interacts with MRN complex in vivo. FLAG-IP was carried out using extracts prepared from vector and RQ4-3xFLAG expressing HEK293T cells treated with a 10-Gy IR and recovered for 10 min.

(C) CoIP of recombinant MRE11, RAD50, and NBS1 with RECQL4.

(D) N-terminal domain of RECQL4 interacts with MRE11.

(E) Nuclease of MRN is stimulated by RECQL4 on closed circular single-strand PhiX174 DNA. MRN (20 nM) or the nuclease-dead mutant, MRN-ND, was incubated with 20 nM RECQL4, boiled RECQL4, or BSA. Buffer, nuclease reaction buffer.

(F) MRE11 promotes RECQL4 recruitment to DSBs in U2OS cells. The recruitment of GFP-RECQL4 to DSB tracks, generated with a 435-nm laser, was monitored in the control and MRE11-depleted U2OS cells, and the fluorescence intensity was quantified. n = 27. Scale bar represents 10 μm.

(G) Retention of RECQL4 at DSBs depends on the exonuclease activity of MRE11. U2OS cells were treated with 100 μM mirin. Graphic quantification below images, n = 21. Scale bar represents 10 μm.

(H) RECQL4 and MRE11 regulate resection at DSBs. Bar graph showing percent of ssDNA content generated at DSB1 in siRNA- or mirin-treated cells. Error bars represent SEM from four biological repeats.

(I) HR repair assay and western blots from RECQL4 and MRE11 knockdown DR-GFP cells.

All data are presented as mean ± SEM from at least three independent experiments with p value calculated with Student's t test. *$p < 0.05$. See also Figures S3 and S4 and Table S1.

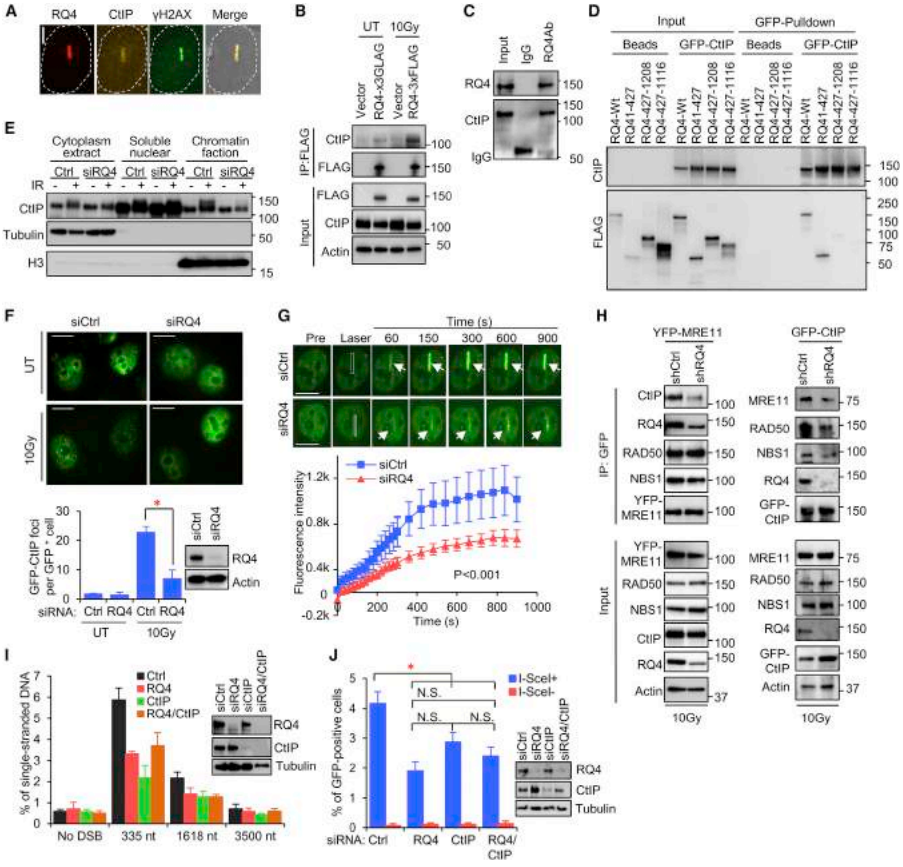

Figure 3. RECQL4 Promotes CtIP Recruitment to DSBs for DNA End Resection and HR Repair

(A) Co-localization of endogenous RECQL4 and CtIP at laser-induced DSB tracks. Scale bar represents 5 μm

(B) CoIP of CtIP with RECQL4 in response to IR.

(C) In vitro coIP analysis of recombinant RECQL4 and CtIP.

(D) The N terminus of RECQL4 interacts with CtIP.

(E) Subcellular distribution of CtIP in control and RECQL4-depleted U2OS cells 10 min after IR.

(F) GFP-CtIP foci in the control and RECQL4-depeted U2OS cells 30 min after IR. Scale bar represents 10 μm.

(G) Recruitment of GFP-CtIP to DSB tracks in control and RECQL4-depeted U2OS cells. n = 29. Scale bar represents 10 μm.

(H) RECQL4 supports the interaction between MRN and CtIP. Western analysis of indicated proteins pulled down with YFP-MRE11 or GFP-CtIP from control and RECQL4 knockdown HEK293T cells 10 min after IR.

(I) Quantification of ssDNA generated at DSB1 in AID-DIvA U2OS cells after knockdown of RECQL4 and CtIP.

(J) HR repair assay after knockdown of RECQL4 and CtIP in DR-GFP U2OS cells.

Error bars for (I) and (J) represent SEM from three independent experiments. The IR dose is 10 Gy. See also Figures S2 and S3 and Table S1.

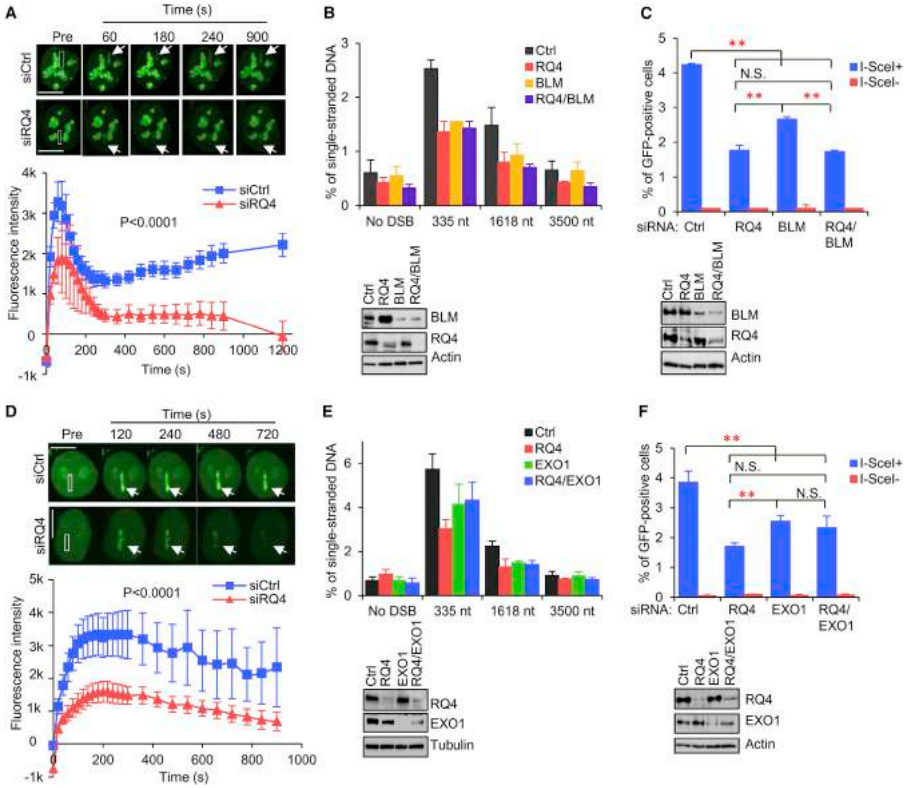

Figure 4. RECQL4 Promotes Recruitment of BLM and EXO1 to Laser-Induced DSBs

(A) Recruitment of GFP-BLM in control and RECQL4-depeted U2OS cells. n = 22. Scale bar represents 10 μm.

(B) Quantification of ssDNA content generated at DSB1 in AID-DIvA U2OS cells depleted for RECQL4 and BLM.

(C) Quantification of GFP-positive cells from the HR repair in control, RECQL4, and BLM knockdown cells.

(D) Recruitment of GFP-EXO1 in control and RECQL4 knockdown U2OS cells. n = 27. Scale bar represents 10 μm.

(E) Quantification of the ssDNA generated from resection at DSB1 in cells with knockdown for RECQL4 and EXO1.

(F) HR assay from EXO1 and RECQL4 knockdown DR-GFP cells. Data are presented as mean ± SEM from three biological repeats. See also Figure S3 and Table S1.

suggest that RECQL4 promotes retention of BLM at DSBs to stimulate HR.

We also evaluated the impact of RECQL4 loss on EXO1-mediated resection. RECQL4 co-localized with EXO1 at laser-induced DSBs in U2OS cells (Figure S3E) and co-immunoprecipitated endogenous EXO1 in irradiated U2OS cells but not in untreated cells (Figure S3F). GFP-EXO1 was rapidly recruited to DSBs in U2OS cells, but significantly more slowly in siRQ4-treated U2OS cells (Figure 4D), indicating that RECQL4 also promotes EXO1 function at DSBs. Knockdown of EXO1 reduced the amount of 5′-end-resected DSBs in AID-DIvA U2OS cells (Figure 4E), which is consistent with previous findings (Zhou et al., 2014). However, EXO1 and RECQL4 double knockdown was not additive in resection of DSBs (Figure 4E). EXO1 knockdown reduced HR by about 31.4% but did not significantly exacerbate the reduction of HR in combination with RECQL4 depletion (Figure 4F). These data support a model in which RECQL4 acts upstream of DNA2/BLM and EXO1 in HR-dependent DSBR.

RECQL4 Helicase Activity Is Required for DNA End Resection during HR-Mediated Repair

The RecQ proteins share a conserved RecQ helicase domain and possess 3′-5′ DNA unwinding activity (Croteau et al., 2014). The helicase activity of human RECQL4 is weak compared to the others in vitro (Rossi et al., 2010; Xu and Liu, 2009). However, mutations in the helicase domain have been identified in many reported RECQL4-asscociated syndrome patients (Siitonen et al., 2009), indicating the importance of the helicase domain in vivo. To explore whether RECQL4 helicase activity is involved in DNA end resection and HR repair, we transfected siRQ4-resistant plasmids to ectopically express 3xFLAG-tagged wild-type (WT) RECQL4 or the helicase-dead mutant RECQL4-KM in siRQ4-treated AID-DIvA U2OS or DR-GFP U2OS cells. Western blots showed that endogenous RECQL4 was depleted by siRQ4 and that 3xFLAG-tagged RECQL4 and RECQL4-KM were expressed in AID-DIvA U2OS cells (Figure 5A). Depletion of RECQL4 resulted in a reduction of ssDNA generated by DNA resection at the DSB1 site, and overexpression of RECQL4-3xFLAG completely restored the loss of 5′ end resection in siRQ4-transfected cells, whereas overexpression of RECQL4-KM-3xFLAG did not (Figure 5A). These results indicate that the RECQL4 helicase activity is required for DNA end resection.

In the HR repair assay, DSBs were generated by transfection of I-SceI-expressing plasmid into DR-GFP U2OS cells (Pierce et al., 1999). To reduce competition with I-SceI-expressing plasmid, the amount of pCMVtag4A-RQ4-siR, pCMVtag4A-RQ4KM-siR or vector was reduced to 0.5 μg for 2×10^6 cells, which resulted in a low expression level of 3xFLAG-tagged RECQL4 and the mutant. However, this level of RECQL4-3xFLAG still significantly increased the percentage of GFP-positive cells, depleted for endogenous RECQL4 (Figure 5B). This is consistent with our observation that RECQL4 levels correlate with HR repair (Figures 1C and 1D). The RECQL4-KM-3xFLAG expression was higher than that of WT RECQL4 but did not significantly rescue the loss of HR repair after RECQL4 depletion. These data suggest that the RECQL4's helicase activity is important for DNA end resection and HR-dependent DSBR.

Given that RECQL4 promotes complex formation between CtIP and MRN by interacting with these proteins, we then measured whether inactivation of the helicase impairs RECQL4's ability to interact with CtIP and MRE11. RECQL4-KM-3xFLAG was pulled down with YFP-MRE11 to the same extent as RECQL4-3xFLAG (Figure 5C). Similarly, helicase-dead RECQL4 also interacted with CtIP as well as WT RECQL4 did (Figure 5D). These findings suggests that inactivation of the helicase domain of RECQL4 does not affect the interaction between RECQL4 and MRE11 or CtIP. Additionally, we found that both helicase-dead and WT RECQL4 proteins were able to stimulate the nuclease activity of MRN on closed circle single-strand PhiX174 DNA (Figure 5E). Taken together, the DNA unwinding activity of RECQL4 is required to promote DNA end resection and HR repair.

RPA-Mediated Displacement of RECQL4 from ssDNA

Unlike BLM and WRN, RECQL4 remains at DSB sites for only a short time (Singh et al., 2010), suggesting that it falls off or is displaced. After DNA end resection, RPA coats the ssDNA tails for protection, which supported by the observation that RPA recruitment to DSBs increases continuously in 1 hr (Figure S5A), as previously reported (Costelloe et al., 2012). Thus, we used an in vitro RECQL4 displacement assay to determine whether RPA could remove RECQL4 from ssDNA. Biotin-labeled ssDNA, dsDNA, or 3′ tailed dsDNA substrates were first incubated with RECQL4 and then with either RPA or BSA. RPA-mediated RECQL4 displacement was detected by visualization of RECQL4 in the supernatant (Figure 5F). Consistent with previous findings (Jensen et al., 2012; Keller et al., 2014), RECQL4 binds to ssDNA, dsDNA, and 3′ tailed dsDNA substrates (Figure 5F). RPA prefers to bind DNA substrates with longer ssDNA (Figures S5C and S5D). When RPA was added to the RECQL4 coated 80-nt-long ssDNA G80, RECQL4 was displaced as RPA bound to this substrate (Figure 5F). A similar phenomenon was observed using GC40 and GC60 DNA substrates, which contain 40 or 20 nucleotide 3′ tails, respectively (Figure 5F). However, very little RECQL4 was replaced by RPA from the blunt-ended dsDNA GC80 or from the 6-nt-tailed dsDNA G80/C74 (Figure 5F). BSA, our negative control, did not displace RECQL4 from the tested DNA substrates (Figure 5F). Together, these data imply that RPA can displace RECQL4 from ssDNA or 3′ tailed dsDNA in vitro but not duplex DNA.

DISCUSSION

DNA end resection generates 3′ tailed ssDNA, which is critical for launching HR repair. The MRN complex initiates 5′ end resection with CtIP, and then extensive resection is carried out by the nucleases EXO1 or DNA2 in two alternative pathways (Cejka, 2015; Symington, 2014). In the present work, we establish that RECQL4 is required for robust DNA end resection by regulating the interaction between MRN and CtIP and further that the helicase activity of RECQL4 is required for the process. We show that depletion of RECQL4 results in loss of HR repair as a result of diminished 5′ resection. IR enhances the physical interaction of RECQL4 with MRN and CtIP. The nuclease activity of MRE11 regulates the retention of RECQL4 at DSBs, and RECQL4 promotes recruitment of CtIP, as well as downstream players like BLM, DNA2, and EXO1, which participate in the extensive resection step of HR. Thus, this work ascribes a hitherto unrecognized role for RECQL4 as an important regulator of DNA end resection in HR repair.

The data presented here indicate that rapid recruitment of RECQL4 to laser-induced DSBs depends on prior recruitment of MRN while RECQL4 is not required for recruitment of MRN to IR-induced DSBs. Additionally, RECQL4 interacts physically with the MRN complex in living cells and under cell-free conditions in vitro (Figures 2A–2D). RECQL4 and MRN function in the same pathway during 5′ end resection in HR repair (Figures 2H and 2I). These findings suggest that RECQL4 functions downstream of MRN in HR DSBR. Combining these findings with the previous reports that both MRE11 and RECQL4 immediately gather at laser-induced DSB (Haince et al., 2008; Singh et al., 2010), it is likely that MRN and RECQL4 act sequentially and cooperatively at DSBs to promote 5′ end resection at DNA DSBs.

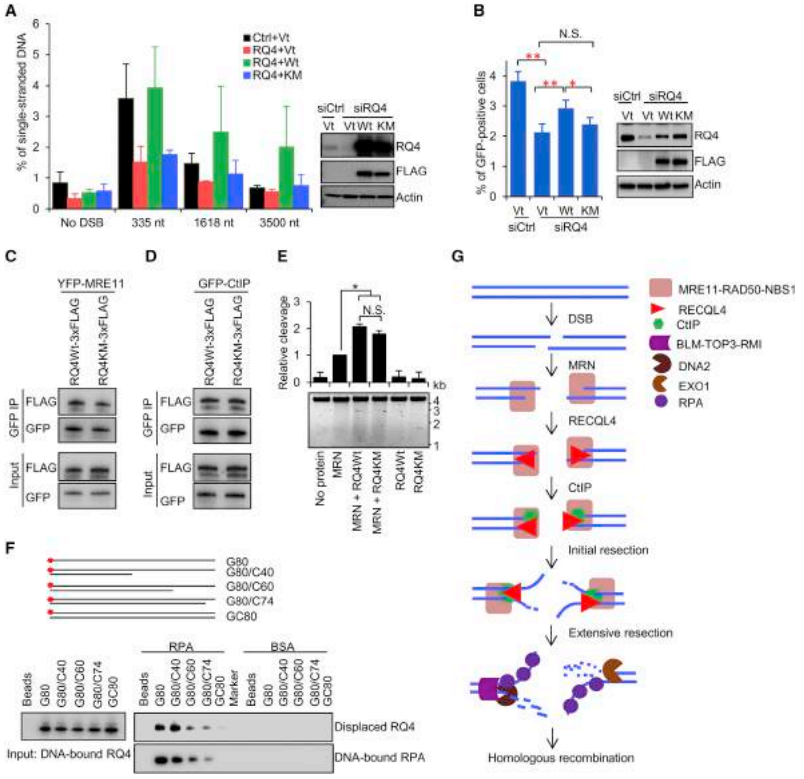

Figure 5. Helicase Activity of RECQL4 Is Required for RECQL4 to Function in DNA Resection and HR Repair

(A) Quantification of the ssDNA generated from resection at DSB1 after endogenous RECQL4 depletion of AID-DIvA U2OS cells but complementation with RECQL4-WT-3xFLAG or RECQL4-KM-3xFLAG. Data presented are mean ± SEM from three biological repeats.

(B) HR repair assay after endogenous RECLQ4 depletion in DR-GFP U2OS cells expressing wild-type or helicase dead mutant RECQL4. Error bars represent SEM from four independent experiments. N.S., no significance.

(C and D) Pull-down assay using YFP-MRE11 (C) or GFP-CtIP (D) with RQ4Wt-3xFLAG and RQ4KM-3xFLAG in vitro.

(E) Both WT and helicase-dead mutant RECQL4 significantly stimulate nuclease of MRN on closed circular single-strand PhiX174 DNA. The concentration of MRN, RECQL4 and RQ4KM were 20 nM. Error bars represent SEM from three repeats with p value by Student's t test.

(F) RPA displaces RECQL4 from ssDNA. Various substrates as shown were pre-incubated with RECQL4 then RPA or BSA were added to compete off RECQL4. Detection of displaced RECQL4 and DNA-bound RPA were visualized by western blotting.

(G) Model showing RECQL4's role in DNA end resection of HR-mediated repair. MRN complex recognizes and binds to DSBs and recruits RECQL4 to the sites of damage. In turn, RECQL4 promotes the stable recruitment of CtIP to DSBs and performs unwinding at the DNA ends thereby promoting resection.

See also Figure S5.

Retention of RECQL4 at DSBs is dramatically reduced in the presence of mirin (Figure 2G). Mirin inhibits MRE11 exonuclease and also represses MRN-dependent ATM activation (Dupré et al., 2008). After recruitment by MRN, RECQL4 is likely retained at DSBs by the resected DNA, which depends on the exonuclease activity of MRE11. Meanwhile, RECQL4 stimulates the nuclease activity of MRN in vitro and promotes MRN-CtIP complex formation after IR, which is required for initiation of DNA resection (Sartori et al., 2007; You et al., 2009). Therefore, it is possible that RECQL4 promotes MRE11-mediated resection at a limited level, which further stimulates retention of RECQL4 at DSBs. Meanwhile, initially resected DNA also leads to limited

ATR activation and ATR-dependent phosphorylation of CtIP, and in turn promotes stable chromatin association of CtIP for robust resection (Peterson et al., 2013). With 5′ resection ongoing, RPA binds to long ssDNA and disassociates RECQL4. Therefore, MRN, RECQL4, CtIP, and checkpoint kinases can function in a feedback loop during DNA end processing at DSBs.

Recruitment of CtIP to DSBs depends on MRN and ATM (You et al., 2009). MRN is recruited earlier than CtIP to DSBs; therefore, MRN may not directly recruit CtIP (You et al., 2009). This study reports that RECQL4 physically interacts with CtIP and promotes stable recruitment of CtIP to DSBs. However, the kinetics of the accumulation of CtIP differs from that of RECQL4. CtIP reaches its peak of abundance at laser-induced DSBs around 15 min after microirradiation (Figure 3G), as previously reported (Wang et al., 2013; You et al., 2009). However, RECQL4 only needs about 1 min to reach its recruitment peak (Figure 2G). Therefore, it is possible that RECQL4 recruits CtIP directly to initiate DNA resection, which further promotes more recruitment of CtIP due to checkpoint activation. RECQL4 also facilitates formation of an MRN-CtIP complex in vivo after IR (Figure 3H). In summary, the data are consistent with the model that RECQL4 promotes CtIP recruitment to DSBs and thereby directly promotes end processing and HR-dependent DSBR.

BLM/DNA2 and EXO1 are required for extensive 5′-end-resection step during HR-dependent DSBR (Symington, 2014). In contrast to RECQL4, BLM appears to play a somewhat more complex role during HR in human cells, possibly at two steps, once during end processing and a second time during dissolution of Holliday junctions together with TopoIIIα/RMI1/2 (Croteau et al., 2014). Here, we show that RECQL4 plays a role in recruiting and retaining BLM and EXO1 at DSBs and that RECQL4 acts in the same pathway as BLM and EXO1 (Figure 4). Since MRE11 and CtIP are required to recruit/retain BLM/EXO1 at DSBs (Eid et al., 2010; Truong et al., 2013; Wang et al., 2013), this lack of retention of BLM/EXO1 on DSBs in RECQL4-depleted cells is probably a consequence of the inhibition of CtIP recruitment caused by loss of RECQL4. Another possibility is that RECQL4 directly recruits BLM and EXO1 in order to switch from initial resection to extensive resection.

RECQL4 is unlikely to be directly involved in the extensive resection step with DNA2/BLM or EXO1, although it interacts with the all of them. Short retention of RECQL4 at DSBs reduces the possibility that RECQL4 works together with DNA2/BLM or EXO1 in extensive resection. Second, BLM, but not RECQL4, specifically stimulates the nuclease activities of both DNA2 and EXO1 in vitro (Nimonkar et al., 2008, 2011). Moreover, RPA displaces RECQL4 from ssDNA (Figure 5F). However, it is possible that RECQL4 after interacting with MRN and CtIP remains bound to the ssDNA long enough to interact with DNA2/BLM and EXO1 and promotes their recruitment and chromatin association, which may activate the switch from initial resection to extensive resection.

Here, we found that depletion of either BLM or EXO1 reduces DNA resection and HR (Figure 4). In yeast, absence of Exo1 reduced resection 1–5 kb from the DSB (Llorente and Symington, 2004; Mimitou and Symington, 2008). Dysfunction of sgs1 also markedly reduced the DNA resection rate and efficiency (Zhu et al., 2008). However, co-depletion of sgs1 and exo1 caused more dramatic loss of DNA resection (Mimitou and Symington, 2008; Zhu et al., 2008). In human cells, depletion of EXO1, DNA2, or BLM reduced 5′ DNA resection in U2OS cells (Grabarz et al., 2013; Gravel et al., 2008; Myler et al., 2016; Tomimatsu et al., 2012; Zhou et al., 2014). DNA2/BLM (Dna2/sgs1) and EXO1 can compensate for each other in extensive resection (Symington, 2014). However, dysfunction of either pathway could affect efficiency of DNA resection in vivo.

The helicase-dead mutant RECQL4-KM did not rescue the loss of either DNA end resection or HR repair (Figure 5), demonstrating that the helicase activity of RECQL4 is required for DNA end resection and HR repair. RECQL4-KM was generated by replacing lysine 508 in the Walker A motif of the SFII helicase domain with methionine, and the mutation eliminates 3′-5′ DNA unwinding activity and ATPase of RECQL4 but not its annealing activity (Rossi et al., 2010). The expression of RECQL4-KM only partially restored the ability of RECQL4 to prevent cellular senescence in primary human fibroblasts with depletion of the endogenous RECQL4, indicating the importance of helicase activity in vivo (Lu et al., 2014a). However, the helicase activity is neither involved in the physical interaction between RECQL4 and MRN and CtIP, nor in the stimulation of the nuclease activity of MRN. In vivo DSBs are complex due to chromatin organization and DSB binding proteins competing at the site. RECQL4 has several activities. The failure of RECQL4-KM to rescue the resection and HR in endogenous RECQL4-depleted cells may reflect that it acts as a dominant-negative. RECQL4 can unwind dsDNA, dsDNA with 3′ overhang (not 5′ overhang), bubble-structured dsDNA, Y-structured duplex, and D-loop (Ghosh et al., 2012; Rossi et al., 2010; Xu and Liu, 2009). Thus, these activities might also help resolve secondary structures near the DNA ends to facilitate the initiation or extensive steps of DNA end resection.

A model for 5′ DNA resection is presented in Figure 5G, which highlights the role of RECQL4 in initiating 5′ end resection at a nascent DSB. DSB arise due to endo- or exogenous insults, which are first sensed by the MRN complex. RECQL4 is recruited by MRN, and RECQL4 possibly promotes a limited resection with MRN, which also promotes retention of RECQL4 at DSB. The MRN-RECQL4 complex then promotes recruitment of CtIP to DSBs. After CtIP enters the complex, the nuclease activity of MRN is greatly stimulated (Sartori et al., 2007). The resultant short ssDNA strands then may also promote greater retention of RECQL4 and CtIP. This feedback loop would then facilitate recruitment of proteins involved in the extensive end resection step like BLM/DNA2 and EXO1. We are proposing that an activity of RECQL4 may remove DNA secondary structure barriers near the ends of the DNA to promote MRN-mediated DNA resection. After some length of resection, RPA binds the ssDNA and promotes displacement of RECQL4 allowing it to be recycled for use at other dsDNA break sites.

EXPERIMENTAL PROCEDURES

Cell Culture, Knockdown, DNA Transfection, γ Radiation, and Survival Assay

U2OS, HEK293T, and HeLa cell lines were cultured in DMEM medium with 10% fetal bovine serum (Sigma-Aldrich), 1 × penicillin/streptomycin (Gibco). All cells were cultured in an atmosphere of 5% CO_2 at 37°C. Lentivirus-mediated small hairpin RNA (shRNA) knockdown and siRNA knockdown were

performed as reported (Lu et al., 2014a). The sequences of siRNA and shRNA are listed in Table S2. Polyplus JetPrime was used for DNA transfection. γ rays were generated using a cesium-137 source (Gammacell Exactor 40, Best Theratronics). Radiation dose is 10 Gy, and post-irradiation recovery time is indicated in the figure legends. For the colony formation assay, cells were irradiated and then stained with 2% methylene blue in 5% ethanol 10 days after IR. The colonies with over 50 cells were counted. The results are presented as mean ± SEM from three independent experiments with p value by Student's t test.

Laser-Induced DNA Damage and Real-Time Recruitment of Fluorescence Proteins

Laser-induced DSB and the recruitment of GFP-RECQL4, GFP-CtIP, GFP-BLM, GFP-EXO1, and GFP-RPA were performed as described (Singh et al., 2010). For mirin treatment, U2OS cells expressing GFP-RECQL4 were pre-incubated with 100 μM mirin for 4 hr before laser microirradiation. The results are presented as mean ± SEM with p value by Student's t test.

HR Assay

RECQL4 and other target proteins were knocked down by siRNA in the DR-GFP U2OS cells (a gift from Prof. Xiaofan Wang), and, 72 hr after siRNA transfection, the HR assay was performed as reported (Pierce et al., 1999; Wang et al., 2014). The siRQ4-resistant plasmids, pCMVTag4A-RQ4-siR and pCMVTag4A-RQ4KM-siR, expressing 3xFLAG-tagged wild-type RECQL4 and helicase-dead mutant RECQL4KM, respectively, were generated by PCR with primers RQ4-siR-PF and RQ4-siR-PR (Table S2). 0.5 μg vector, pCMVTag4A-RQ4-siR, or pCMVTag4A-RQ4KM-siR were transfected into 5 × 10^5 siRQ4-treated DR-GFP U2OS cells. 24 hr later, cells were then processed for HR assay. The results are presented as mean ± SEM from three independent experiments with p value by Student's t test.

5′ Resection Assay

In vivo 5′ end resection was measured in AID-DIvA U2OS cells (a gift from Dr. Gaëlle Legube), as previously described (Zhou et al., 2014). For the rescue assay, 5 μg pCMVTag4A-RQ4-siR, pCMVTag4A-RQ4KM-siR, or control vector was transfected into 2 × 10^6 RECQL4 siRQ4-treated cells. 45 hr later, cells were treated with 4-OHT and then processed for the resection assay. At least three biological repeats were performed, and data are presented as the mean ± SEM.

Subcellular Fractionation, Western Blotting, and Immunofluorescence Microscopy

Subcellular fractions were isolated using a subcellular protein fractionation kit (Thermo Fisher Scientific) according to the manufacturer's instructions, and the resultant fractions were analyzed with western blotting. Western blot and immunofluorescence microscopy were performed as previously described (Lu et al., 2014a). Antibodies used in this study are listed in the Supplemental Experimental Procedures.

Protein Purification

The MRE11-RAD50-NBS1 complex was purified from insect cells as previously described (Cheng et al., 2004). Purification of recombinant RECQL4 and helicase-dead mutant RECQL4-KM were performed as described (Rossi et al., 2010). RPA purification was performed as described (Henricksen et al., 1994). The details of CtIP purification and 3xFLAG-tagged RECQL4 and its truncation fragments are provided in the Supplemental Experimental Procedures.

IP, Pull-Down Assay, Silver Staining, and Protein Identification

Control and γ-irradiated cells were incubated for 10 min and then sonicated on ice in IP Lysis Buffer 2 containing 40 mM Tris-HCl (pH 7.4), 150 mM NaCl, 2 mM $MgCl_2$, 0.2% NP-40, 0.4% Triton 100, 1 × protease inhibitor cocktail (Thermo Fisher Scientific), 1× phosphatase inhibitor cocktail 2 and 3 (Sigma-Aldrich), and 20 U/ml benzonase (Novagen). 50 μg/ml ethidium bromide was added in lysate where it was indicated. For coIP with RECQL4 antibody, 2 mg protein was incubated with 2 μg of RECQL4 antibody (Lu et al., 2014a) or normal rabbit immunoglobulin G (IgG) (Thermo Fisher Scientific). For FLAG IP, the cell lysate was incubated with M2 FLAG-magnetic beads (Sigma-Aldrich). For GFP IP, GFP-TRAP beads (ChromoTek) were used to capture GFP-RECQL4 or YFP-MRE11. The beads were washed with cold washing buffer 4 (20 mM Tris-HCl [pH 7.4], 150 mM NaCl, 0.2% Triton X-100) five times and then subjected to western blotting, silver staining, or mass spectrometry analysis by Harvard Taplin Mass Spectrometry Facility. The details of mass spectrometry are listed in Table S1.

For in vitro IP, purified RECQL4 was incubated with recombinant MRN complex or CtIP in Binding Buffer 1 (20 mM Tris-HCl [pH 7.4], 100 mM NaCl, 0.2% Triton X-100) for 2 hr at 4°C and then incubated with anti-RECQL4 antibody or normal rabbit IgG. After washing with Binding Buffer, the proteins remained on the beads were analyzed by western blotting.

Nuclease Assay

Nuclease assays were carried out with 20 nM MRN or nuclease-dead MRN-ND in the presence of 20 nM wild-type RECQL4 or helicase-dead RECQL4 RQ4KM on 50 ng closed circular single-stranded PhiX174 DNA in the resection buffer containing 20 mM MOPS (pH 7.2), 1 mM DTT, 5 mM $MgCl_2$, 5 mM $MnCl_2$, 1 mM ATP, as previously described (Sartori et al., 2007). After 3 hr incubation at 37°C, DNA was separated in 0.8% agarose gel, further stained with SYBR Gold, visualized with Chemidoc XRS+ system (Bio-Rad) and quantified with Bio-Rad Image Lab (v.3.0). Data were presented as mean ± SEM from three repeats.

Displacement Assay

A biotin-labeled oligonucleotide (G80) was annealed with C80, C74, C60, and C40 and resulted in dsDNA GC80 and 3′ tailed dsDNA GC74, GC60, and GC40, respectively (see the sequences in Table S2). RECQL4 (200 nM) was incubated with 20 nM DNA substrates bound to M280-streptavidin beads (Life Technologies) in the binding buffer (20 mM HEPES [pH 7.4], 100 mM NaCl, 1 mM $MgCl_2$, 0.1% Triton X-100, and 200 ng/ml BSA) at room temperature (RT) for 15 min. After washing with the binding buffer, the beads were incubated with 200 nM RPA or 200 ng/ml BSA at RT for 15 min. The supernatants and beads were then collected for detecting displaced RECQL4 and DNA-bound RPA by western blotting.

SUPPLEMENTAL INFORMATION

Supplemental Information includes Supplemental Experimental Procedures, five figures, and two tables and can be found with this article online at http://dx.doi.org/10.1016/j.celrep.2016.05.079.

AUTHOR CONTRIBUTIONS

Conceptualization: H.L., R.A.S., D.L.C., and V.A.B.; Methodology: H.L. and R.A.S.; Investigation: H.L. and R.A.S.; Writing–Original Draft, H.L. and R.A.S.; Review & Editing, H.L., R.A.S., L.J.R., P.C., D.L.C., and V.A.B.; Funding Acquisition, V.A.B.; Resources, G.K., R.A., L.J.R., and P.C.; Supervision, D.L.C. and V.A.B.

ACKNOWLEDGMENTS

AID-DIVA U2OS is under MTA between Dr. Gaëlle Legube and NIA. We thank Dr. Xiaofan Wang for DR-GFP U2OS, Drs. Dik van Gent and Roland Kanaar for YFP-MRE11 plasmid, Dr. Marc Wold for the GFP-RPA plasmids, Dr. Binghui Shen for FLAG-DNA2 plasmid, Dr. Tomasz Kulikowicz and Christopher Dunn for RECQL4 protein, Tomasz Kulikowicz and Alfred May for IR operation, and Drs. Morten Scheibye-Knudsen and Jaya Sarkar for their critical comments. This research was supported entirely by the Intramural Research Program of the NIH, National Institute on Aging.

Received: January 29, 2016
Revised: April 25, 2016
Accepted: May 19, 2016
Published: June 16, 2016

REFERENCES

Aparicio, T., Baer, R., and Gautier, J. (2014). DNA double-strand break repair pathway choice and cancer. DNA Repair (Amst.) *19*, 169–175.

Aymard, F., Bugler, B., Schmidt, C.K., Guillou, E., Caron, P., Briois, S., Iacovoni, J.S., Daburon, V., Miller, K.M., Jackson, S.P., and Legube, G. (2014). Transcriptionally active chromatin recruits homologous recombination at DNA double-strand breaks. Nat. Struct. Mol. Biol. *21*, 366–374.

Bunting, S.F., Callén, E., Wong, N., Chen, H.T., Polato, F., Gunn, A., Bothmer, A., Feldhahn, N., Fernandez-Capetillo, O., Cao, L., et al. (2010). 53BP1 inhibits homologous recombination in Brca1-deficient cells by blocking resection of DNA breaks. Cell *141*, 243–254.

Cannavo, E., and Cejka, P. (2014). Sae2 promotes dsDNA endonuclease activity within Mre11-Rad50-Xrs2 to resect DNA breaks. Nature *514*, 122–125.

Cejka, P. (2015). DNA end resection: nucleases team up with the right partners to initiate homologous recombination. J. Biol. Chem. *290*, 22931–22938.

Cejka, P., Cannavo, E., Polaczek, P., Masuda-Sasa, T., Pokharel, S., Campbell, J.L., and Kowalczykowski, S.C. (2010). DNA end resection by Dna2-Sgs1-RPA and its stimulation by Top3-Rmi1 and Mre11-Rad50-Xrs2. Nature *467*, 112–116.

Chen, L., Nievera, C.J., Lee, A.Y., and Wu, X. (2008). Cell cycle-dependent complex formation of BRCA1.CtIP.MRN is important for DNA double-strand break repair. J. Biol. Chem. *283*, 7713–7720.

Chen, H., Lisby, M., and Symington, L.S. (2013). RPA coordinates DNA end resection and prevents formation of DNA hairpins. Mol. Cell *50*, 589–600.

Cheng, W.H., von Kobbe, C., Opresko, P.L., Arthur, L.M., Komatsu, K., Seidman, M.M., Carney, J.P., and Bohr, V.A. (2004). Linkage between Werner syndrome protein and the Mre11 complex via Nbs1. J. Biol. Chem. *279*, 21169–21176.

Costelloe, T., Louge, R., Tomimatsu, N., Mukherjee, B., Martini, E., Khadaroo, B., Dubois, K., Wiegant, W.W., Thierry, A., Burma, S., et al. (2012). The yeast Fun30 and human SMARCAD1 chromatin remodellers promote DNA end resection. Nature *489*, 581–584.

Croteau, D.L., Popuri, V., Opresko, P.L., and Bohr, V.A. (2014). Human RecQ helicases in DNA repair, recombination, and replication. Annu. Rev. Biochem. *83*, 519–552.

Dupré, A., Boyer-Chatenet, L., Sattler, R.M., Modi, A.P., Lee, J.H., Nicolette, M.L., Kopelovich, L., Jasin, M., Baer, R., Paull, T.T., and Gautier, J. (2008). A forward chemical genetic screen reveals an inhibitor of the Mre11-Rad50-Nbs1 complex. Nat. Chem. Biol. *4*, 119–125.

Eid, W., Steger, M., El-Shemerly, M., Ferretti, L.P., Peña-Diaz, J., König, C., Valtorta, E., Sartori, A.A., and Ferrari, S. (2010). DNA end resection by CtIP and exonuclease 1 prevents genomic instability. EMBO Rep. *11*, 962–968.

Fang, H., Nie, L., Chi, Z., Liu, J., Guo, D., Lu, X., Hei, T.K., Balajee, A.S., and Zhao, Y. (2013). RecQL4 helicase amplification is involved in human breast tumorigenesis. PLoS ONE *8*, e69600.

Ghosh, A.K., Rossi, M.L., Singh, D.K., Dunn, C., Ramamoorthy, M., Croteau, D.L., Liu, Y., and Bohr, V.A. (2012). RECQL4, the protein mutated in Rothmund-Thomson syndrome, functions in telomere maintenance. J. Biol. Chem. *287*, 196–209.

Grabarz, A., Guirouilh-Barbat, J., Barascu, A., Pennarun, G., Genet, D., Rass, E., Germann, S.M., Bertrand, P., Hickson, I.D., and Lopez, B.S. (2013). A role for BLM in double-strand break repair pathway choice: prevention of CtIP/Mre11-mediated alternative nonhomologous end-joining. Cell Rep. *5*, 21–28.

Gravel, S., Chapman, J.R., Magill, C., and Jackson, S.P. (2008). DNA helicases Sgs1 and BLM promote DNA double-strand break resection. Genes Dev. *22*, 2767–2772.

Haince, J.F., McDonald, D., Rodrigue, A., Déry, U., Masson, J.Y., Hendzel, M.J., and Poirier, G.G. (2008). PARP1-dependent kinetics of recruitment of MRE11 and NBS1 proteins to multiple DNA damage sites. J. Biol. Chem. *283*, 1197–1208.

Henricksen, L.A., Umbricht, C.B., and Wold, M.S. (1994). Recombinant replication protein A: expression, complex formation, and functional characterization. J. Biol. Chem. *269*, 11121–11132.

Im, J.S., Ki, S.H., Farina, A., Jung, D.S., Hurwitz, J., and Lee, J.K. (2009). Assembly of the Cdc45-Mcm2-7-GINS complex in human cells requires the Ctf4/And-1, RecQL4, and Mcm10 proteins. Proc. Natl. Acad. Sci. USA *106*, 15628–15632.

Jensen, M.B., Dunn, C.A., Keijzers, G., Kulikowicz, T., Rasmussen, L.J., Croteau, D.L., and Bohr, V.A. (2012). The helicase and ATPase activities of RECQL4 are compromised by mutations reported in three human patients. Aging (Albany, N.Y.) *4*, 790–802.

Keller, H., Kiosze, K., Sachsenweger, J., Haumann, S., Ohlenschläger, O., Nuutinen, T., Syväoja, J.E., Görlach, M., Grosse, F., and Pospiech, H. (2014). The intrinsically disordered amino-terminal region of human RecQL4: multiple DNA-binding domains confer annealing, strand exchange and G4 DNA binding. Nucleic Acids Res. *42*, 12614–12627.

Llorente, B., and Symington, L.S. (2004). The Mre11 nuclease is not required for 5′ to 3′ resection at multiple HO-induced double-strand breaks. Mol. Cell. Biol. *24*, 9682–9694.

Lu, H., Fang, E.F., Sykora, P., Kulikowicz, T., Zhang, Y., Becker, K.G., Croteau, D.L., and Bohr, V.A. (2014a). Senescence induced by RECQL4 dysfunction contributes to Rothmund-Thomson syndrome features in mice. Cell Death Dis. *5*, e1226.

Lu, L., Jin, W., Liu, H., and Wang, L.L. (2014b). RECQ DNA helicases and osteosarcoma. Adv. Exp. Med. Biol. *804*, 129–145.

Mimitou, E.P., and Symington, L.S. (2008). Sae2, Exo1 and Sgs1 collaborate in DNA double-strand break processing. Nature *455*, 770–774.

Myler, L.R., Gallardo, I.F., Zhou, Y., Gong, F., Yang, S.H., Wold, M.S., Miller, K.M., Paull, T.T., and Finkelstein, I.J. (2016). Single-molecule imaging reveals the mechanism of Exo1 regulation by single-stranded DNA binding proteins. Proc. Natl. Acad. Sci. USA *113*, E1170–E1179.

Nimonkar, A.V., Ozsoy, A.Z., Genschel, J., Modrich, P., and Kowalczykowski, S.C. (2008). Human exonuclease 1 and BLM helicase interact to resect DNA and initiate DNA repair. Proc. Natl. Acad. Sci. USA *105*, 16906–16911.

Nimonkar, A.V., Genschel, J., Kinoshita, E., Polaczek, P., Campbell, J.L., Wyman, C., Modrich, P., and Kowalczykowski, S.C. (2011). BLM-DNA2-RPA-MRN and EXO1-BLM-RPA-MRN constitute two DNA end resection machineries for human DNA break repair. Genes Dev. *25*, 350–362.

Niu, H., Chung, W.H., Zhu, Z., Kwon, Y., Zhao, W., Chi, P., Prakash, R., Seong, C., Liu, D., Lu, L., et al. (2010). Mechanism of the ATP-dependent DNA end-resection machinery from Saccharomyces cerevisiae. Nature *467*, 108–111.

Park, S.J., Lee, Y.J., Beck, B.D., and Lee, S.H. (2006). A positive involvement of RecQL4 in UV-induced S-phase arrest. DNA Cell Biol. *25*, 696–703.

Peterson, S.E., Li, Y., Wu-Baer, F., Chait, B.T., Baer, R., Yan, H., Gottesman, M.E., and Gautier, J. (2013). Activation of DSB processing requires phosphorylation of CtIP by ATR. Mol. Cell *49*, 657–667.

Pierce, A.J., Johnson, R.D., Thompson, L.H., and Jasin, M. (1999). XRCC3 promotes homology-directed repair of DNA damage in mammalian cells. Genes Dev. *13*, 2633–2638.

Prakash, R., Zhang, Y., Feng, W., and Jasin, M. (2015). Homologous recombination and human health: the roles of BRCA1, BRCA2, and associated proteins. Cold Spring Harb. Perspect. Biol. *7*, a016600.

Rossi, M.L., Ghosh, A.K., Kulikowicz, T., Croteau, D.L., and Bohr, V.A. (2010). Conserved helicase domain of human RecQ4 is required for strand annealing-independent DNA unwinding. DNA Repair (Amst.) *9*, 796–804.

Sangrithi, M.N., Bernal, J.A., Madine, M., Philpott, A., Lee, J., Dunphy, W.G., and Venkitaraman, A.R. (2005). Initiation of DNA replication requires the RECQL4 protein mutated in Rothmund-Thomson syndrome. Cell *121*, 887–898.

Sartori, A.A., Lukas, C., Coates, J., Mistrik, M., Fu, S., Bartek, J., Baer, R., Lukas, J., and Jackson, S.P. (2007). Human CtIP promotes DNA end resection. Nature *450*, 509–514.

Shamanna, R.A., Singh, D.K., Lu, H., Mirey, G., Keijzers, G., Salles, B., Croteau, D.L., and Bohr, V.A. (2014). RECQ helicase RECQL4 participates in non-homologous end joining and interacts with the Ku complex. Carcinogenesis *35*, 2415–2424.

Shao, R.G., Cao, C.X., Zhang, H., Kohn, K.W., Wold, M.S., and Pommier, Y. (1999). Replication-mediated DNA damage by camptothecin induces phosphorylation of RPA by DNA-dependent protein kinase and dissociates RPA:DNA-PK complexes. EMBO J. *18*, 1397–1406.

Shibata, A., Moiani, D., Arvai, A.S., Perry, J., Harding, S.M., Genois, M.M., Maity, R., van Rossum-Fikkert, S., Kertokalio, A., Romoli, F., et al. (2014). DNA double-strand break repair pathway choice is directed by distinct MRE11 nuclease activities. Mol. Cell *53*, 7–18.

Siitonen, H.A., Sotkasiira, J., Biervliet, M., Benmansour, A., Capri, Y., Cormier-Daire, V., Crandall, B., Hannula-Jouppi, K., Hennekam, R., Herzog, D., et al. (2009). The mutation spectrum in RECQL4 diseases. Eur. J. Hum. Genet. *17*, 151–158.

Singh, D.K., Karmakar, P., Aamann, M., Schurman, S.H., May, A., Croteau, D.L., Burks, L., Plon, S.E., and Bohr, V.A. (2010). The involvement of human RECQL4 in DNA double-strand break repair. Aging Cell *9*, 358–371.

Singh, D.K., Popuri, V., Kulikowicz, T., Shevelev, I., Ghosh, A.K., Ramamoorthy, M., Rossi, M.L., Janscak, P., Croteau, D.L., and Bohr, V.A. (2012). The human RecQ helicases BLM and RECQL4 cooperate to preserve genome stability. Nucleic Acids Res. *40*, 6632–6648.

Stracker, T.H., Carson, C.T., and Weitzman, M.D. (2002). Adenovirus oncoproteins inactivate the Mre11-Rad50-NBS1 DNA repair complex. Nature *418*, 348–352.

Su, Y., Meador, J.A., Calaf, G.M., Proietti De-Santis, L., Zhao, Y., Bohr, V.A., and Balajee, A.S. (2010). Human RecQL4 helicase plays critical roles in prostate carcinogenesis. Cancer Res. *70*, 9207–9217.

Symington, L.S. (2014). End resection at double-strand breaks: mechanism and regulation. Cold Spring Harb. Perspect. Biol. *6*, a016436.

Tomimatsu, N., Mukherjee, B., Deland, K., Kurimasa, A., Bolderson, E., Khanna, K.K., and Burma, S. (2012). Exo1 plays a major role in DNA end resection in humans and influences double-strand break repair and damage signaling decisions. DNA Repair (Amst.) *11*, 441–448.

Truong, L.N., Li, Y., Shi, L.Z., Hwang, P.Y., He, J., Wang, H., Razavian, N., Berns, M.W., and Wu, X. (2013). Microhomology-mediated End Joining and Homologous Recombination share the initial end resection step to repair DNA double-strand breaks in mammalian cells. Proc. Natl. Acad. Sci. USA *110*, 7720–7725.

Wang, H., Shi, L.Z., Wong, C.C., Han, X., Hwang, P.Y., Truong, L.N., Zhu, Q., Shao, Z., Chen, D.J., Berns, M.W., et al. (2013). The interaction of CtIP and Nbs1 connects CDK and ATM to regulate HR-mediated double-strand break repair. PLoS Genet. *9*, e1003277.

Wang, Q., Goldstein, M., Alexander, P., Wakeman, T.P., Sun, T., Feng, J., Lou, Z., Kastan, M.B., and Wang, X.F. (2014). Rad17 recruits the MRE11-RAD50-NBS1 complex to regulate the cellular response to DNA double-strand breaks. EMBO J. *33*, 862–877.

Xu, X., and Liu, Y. (2009). Dual DNA unwinding activities of the Rothmund-Thomson syndrome protein, RECQ4. EMBO J. *28*, 568–577.

Xu, X., Rochette, P.J., Feyissa, E.A., Su, T.V., and Liu, Y. (2009). MCM10 mediates RECQ4 association with MCM2-7 helicase complex during DNA replication. EMBO J. *28*, 3005–3014.

You, Z., Shi, L.Z., Zhu, Q., Wu, P., Zhang, Y.W., Basilio, A., Tonnu, N., Verma, I.M., Berns, M.W., and Hunter, T. (2009). CtIP links DNA double-strand break sensing to resection. Mol. Cell *36*, 954–969.

Yuan, J., and Chen, J. (2009). N terminus of CtIP is critical for homologous recombination-mediated double-strand break repair. J. Biol. Chem. *284*, 31746–31752.

Zhou, Y., Caron, P., Legube, G., and Paull, T.T. (2014). Quantitation of DNA double-strand break resection intermediates in human cells. Nucleic Acids Res. *42*, e19.

Zhu, Z., Chung, W.H., Shim, E.Y., Lee, S.E., and Ira, G. (2008). Sgs1 helicase and two nucleases Dna2 and Exo1 resect DNA double-strand break ends. Cell *134*, 981–994.

2.4 Additional results

2.4.1 Biochemical characterisation of human MLH1-MLH3 and its interplay with human MSH4-MSH5

Human MLH1-MLH3 is an endonuclease

Introduction: Human MLH1-MLH3 (MutLγ) has been strongly implicated as a putative endonuclease in meiosis, which is responsible for the formation of majority of meiotic COs (Zakharyevich et al., 2012). Many genetic studies carried out in various organisms found that an inactivation of hMLH1-hMLH3 leads to drastic reduction in COs (Wang et al., 1999). However, all such studies have mostly used genetic and cytological approach to investigate the function of hMutLγ. Until recently, no biochemical characterization was available for MutLγ from any species due to the technical challenges encountered in purifying the recombinant protein. Previously, we succeeded in purifying the recombinant *S. cerevisiae* MutLγ and could show that it is an endonuclease(Ranjha et al., 2014). Simultaneously, another group (E. Alani, Cornell University) could also confirm the same findings (Rogacheva et al., 2014). In my PhD project, I was interested in studying the biochemical behaviour of hMutLγ. Therefore, I purified recombinant hMLH1-hMLH3 from *Sf9* cells, which was equally challenging as it was for the yeast protein.

MutLγ is a member of the MutL family of MMR proteins. MutLα, another member of the MutL family, has already been well established as endonuclease, which shares the same nuclease motif as MutLγ. For MutLα, it was shown that it is a cryptic endonuclease, which requires mismatch, MutSα, proliferating cell nuclear antigen (PCNA), replication factor C (RFC) and ATP for its latent nuclease activity in reconstituted system (Kadyrov et al., 2006). Interestingly, MutLα showed Mn^{2+} dependent nicking activity on super-coiled dsDNA in the absence of minimal required components of reconstituted system, hence bypassing their requirements. I therefore I took a cue from the already defined MutLα biochemistry and performed nicking assay under similar conditions.

Results and conclusion: The constructs used for purifying human MutLγ was slightly modified from the ones reported previously. For yeast MutLα (yMlh1-yPms1), it was shown that mutation of the last residue of yMlh1 (Cys769) abolishes the yMutLα activity without affecting the dimerization of yMlh1 and yPms1. Therefore, in the newly prepared constructs of hMLH3, the His tag was removed from the C-terminus of MLH3, while the MBP tag at the N-terminus of MLH3 was preserved. A Flag tag was inserted at the N-terminus of MLH1. hMLH1-hMLH3 purified from the new construct (Figure 1A and B) behaved similarly in DNA binding as the previous construct as reported previously (data not shown). A nuclease assay was performed with this "new" hMLH1-hMLH3 preparation and super-coiled dsDNA as a substrate in the presence of either Mn^{2+} or Mg^{2+}. hMLH1-hMLH3 nicked the substrate and produced the linear species of DNA in the presence of Mn^{2+} (Figure 1C) while no activity was observed with Mg^{2+} (Figure 1D). To exclude the possibility that observed nicking activity was due to a nuclease contamination in our protein preparation, we next purified nuclease inactive variant of hMLH1-hMLH3 by introducing the point mutation (D1223N) in the nuclease motif of the MLH3 subunit (Figure 1E). As anticipated, this point mutation in MLH3 abolished the nuclease activity of hMLH1-hMLH3, showing clearly that the observed nicking observed was intrinsic to hMLH1-hMLH3 (Figure 1F). Further analysis revealed that ATP slightly stimulates the hMLH1-hMLH3 nicking activity, whereas no such stimulation was observed upon supplementing the reaction with hMSH4-hMSH5 (Figure 1G and H). Additionally, hMLH1-hMLH3 did not show any cleavage activity with or without hMSH4-hMSH5 on oligonucleotide-based HJ (Figure 1I). In summary, I could show that hMLH1-hMLH3 possesses an endonuclease activity, which is slightly stimulated by ATP. No HJ cleavage by hMLH1-hMLH3 with our without hMSH4-hMSH5was observed, indicating the likely requirement for additional factors, which were missing in our reactions.

Human MSH4-MSH5 prefers binding to HJs that is decreased in the presence of ATP

Introduction: MutSγ plays a significant role in the production of interference dependent COs. Deletion of either MSH4 or MSH5 subunit leads to a severe reduction in CO levels (Lynn et al., 2007; Ross-Macdonald and Roeder, 1994). Moreover *in S. cerevisiae,* MutSγ and MutLγ have been shown to function in the same pathway. In addition to its early role, MutSγ may function with MutLγ at a late stage of meiotic HR. More than a decade earlier, a biochemical characterization of human MSH4-MSH5 showed that it preferably binds to HJs and similar structures and slides on the HJ arms upon ATP binding (Snowden et al., 2004). The sliding was independent of ATP hydrolysis. These findings compelled us to study the interplay of hMSH4-hMSH5with hMutLγ. Therefore I purified recombinant hMSH4-hMSH5and tested its DNA binding capacity and its dependence on ATP to make sure that our purified protein is active and conforms to previously reported characteristics.

Results and conclusion: I expressed and purified the recombinant human MutSγ (MSH4-Strep-MSH5-His) in *Sf9* cells using the baculovirus system. The single baculovirus of hMSH4-hMSH5 was prepared from the plasmid containing both MSH4 and MSH5 genes. It was kindly provided by Eva R Hoffmann (University of Copenhagen). Both his and strep tags were utilized sequentially for purification (Figure 2A and B). To test the DNA binding capacity and preference of hMutSγ, in collaboration with Nicolas Weyland, a master student in our laboratory, we performed electrophoretic mobility shift assays (EMSA) using first polyacrylamide gels. hMSH4-hMSH5 did indeed prefer binding HJs over dsDNA (Figure 2C). Without Mg^{2+}, hMSH4-hMSH5 binding to HJ was stronger, which could be attributed to the un-stacked form of HJ in the absence of Mg^{2+} (Figure 2D). We further investigated the influence of ATP on hMSH4-hMSH5 DNA binding. The addition of ATP in the EMSA reaction decreased hMutSγ's binding to HJ though not to a very large extent (Figure 2E-G). It indicated a negative influence of ATP on DNA binding by hMSH4-hMSH5, in agreement with previous reports. However, it was not clear that whether hMSH4-hMSH5 simply falls off the HJ arms upon ATP binding or whether it slides along the HJ arms to ultimately fall off at the ends of the arms. To distinguish between these two

scenarios, I prepared an oligonucleotide-based HJ with biotin labels at each end of the fours arms. Streptavidin was used to block all DNA ends of the HJ substrate (Figure 2H). With this quadruple blocked HJ, hMSH4-hMSH5 did not show any decrease in DNA binding upon ATP addition, indicating that it slides along the HJ arms when ATP is present (Figure 2I-K). The binding was specific to the HJ structure, as I also prepared blocked dsDNA, and did not observe any specific DNA binding (Figure 2L). To summarise, I could purify an active preparation of recombinant hMSH4-hMSH5, which showed DNA binding preference to HJs and exhibited sliding on HJ arms upon ATP binding.

Human MLH1-MLH3 physically interacts with human MSH4-MSH5

Introduction: MutSγ has been shown to be necessary for the formation of interference dependent COs in meiosis (Lynn et al., 2007). It has been postulated to function at an early stage of HR by antagonizing the Sgs1 anti-CO activity and thus stabilizing the single end invasion (SEI) structures (Borner et al., 2004). Other than its early role, MutSγ is also believed to function at later stages of HR due to the co-localization of MSH4 in human with Mlh1 and Mlh3 in mid pachynema (Oliver-Bonet et al., 2005). In other observations, MSH4 co-immunoprecipitates with MLH3 in mouse meiotic cell extract and hMSH4-hMSH5 binds HJ *in vitro* (Santucci-Darmanin et al., 2002; Snowden et al., 2004). This evidence indicates that MutSγ functions together with MutLγ, which may be facilitated by direct protein-protein interactions. Previously, recombinant human MSH4 has been shown to interact with human MLH3 (Santucci-Darmanin et al., 2002). However, MLH3 used for the testing was *in vitro* translated and only single subunits of both heterodimers were used. Here, we set out to study the physical interaction between both heterodimers by using recombinant hMSH4-hMSH5 and hMLH1-hMLH3.

Results and conclusion: To study the interaction between hMSH4-hMSH5 and hMLH1-hMLH3, I designed the interaction assays, which were performed in the collaboration with Nicolas Weyland. In brief, either anti-His (for MSH4-Strep-MSH5-His) or anti-Flag (for Flag-MLH1-MLH3) antibodies were captured on

protein G. Subsequently, recombinant proteins with the appropriate tags were further immobilized on protein-G-antibodies complex. Finally, second recombinant protein was added and incubated, followed by an extensive washing and elution. The eluted products were analysed by silver staining. With these assay, we could show that hMSH4-hMSH5 interacts directly with hMLH1-hMLH3 *in vitro* (Figure 3A). To confirm this interaction further, we performed the reverse of the previous assay where we captured hMLH1-hMLH3 with immobilized hMSH4-hMSH5 (Figure 3B). These results further prove that both complexes directly interact with each other.

Human MLH1-MLH3 binds cooperatively to HJs with hMSH4-hMSH5.

Introduction: MutSγ has been proposed to function with MutLγ in CO formation. In fact, hMSH4-hMSH5 itself binds to the core of oligonucleotide-based HJs. Recently, we showed that hMLH1-hMLH3 prefers binding to the HJs and similar structures. We specifically showed a binding preference to the un-stacked form of HJs. As both MutSγ and MutLγ complexes binds to HJs, we were wondering about the possibility that hMSH4-hMSH5 could stimulate the binding of hMLH1-hMLH3 to HJs. Such speculation was based on the proposed model where hMSH4-hMSH5, upon ATP binding, may form sliding clamp and vacate the sites for hMLH1-hMLH3 binding. In such a scenario, it is also possible that hMLH1-hMLH3 may inhibit hMSH4-hMSH5 binding to the DNA structure preventing its further loading.

Result and conclusion: EMSAs were used to test for cooperativity between hMSH4-hMSH5 and hMLH1-hMLH3 in HJ binding. These assays were also carried out in collaboration with Nicolas Weyland. Instead of standard polyacrylamide gels, we used 0.6% agarose gels as both hMLH1-hMLH3 and hMSH4-hMSH5 remain stuck in the wells of polyacrylamide gels, which hindered us to detect any super-shift produced by their (potential) cooperativity. We also modified our reaction conditions from our previous DNA binding analysis to include salt and ATP to further optimize the reactions so that complex can enter the gel. We performed these EMSAs in both presence and absence of Mg^{2+}. Under these

modified conditions, while hMSH4-hMSH5 alone did not bind at all to either dsDNA or HJ, hMLH1-hMLH3 only bound to HJs and migrated as distinct band with additional smearing below, indicating that the DNA-protein complex is rather unstable (Figure 4A). When both proteins were added together with the HJ substrate, we observed a slight but consistent shift (super-shift) protein-bound DNA band. The limited extent of observed super-shift with these proteins can likely be attributed to the limited resolution capacity of the agarose gel. Interestingly, both proteins together also showed a slight reduction in the band smearing, indicating the stabilization of the MutLγ-HJ complex by hMSH4-hMSH5. In the absence of Mg^{2+}, the super-shift was still observed and effect was more prominent than with Mg^{2+} (Figure 4B), most likely due to enhanced protein-DNA binding. This effect was specific for HJs, as no dsDNA binding was observed under any condition (Figure 4C and D). Hence, taken together, these data indicate further that hMLH1-hMLH3 functions together with hMSH4-hMSH5 *in vivo* as it shows a cooperative binding to HJs with hMSH4-hMSH5.

Human MLH1-MLH3 does not show cooperative binding to HJ with non-cognate yeast Msh4-Msh5 (yMutSγ)

Introduction: The cooperative binding to HJs by hMLH1-hMLH3 with hMSH4-hMSH5 encouraged us to further investigation the nature of this cooperativity. As shown previously, both complexes bind to HJ. Therefore, it was possible that both proteins are binding to the HJ separately and hence produce the super-shift. To determine the mechanism, we used yeast Msh4-Msh5 (L. Ranjha, unpublished), which also binds to HJs but is not a cognate partner of hMLH1-hMLH3.

Results and conclusion: I collaborated with Lepakshi Ranjha to provide yMutSγ and to perform this assay. Importantly, yMutSγ with hMLH1-hMLH3,
did not show any cooperativity in HJ binding (Figure 5A and B). Unlike human MutSγ, yMutSγ alone bound to HJs, which indicates that observed lack of cooperativity in between yMutSγ and human MLH1-MLH3 was not due to

inactive yMutSγ. Therefore, we conclude that the super-shift observed with human MLH1-MLH3 and hMSH4-hMSH5 is based on a cognate, species-specific interactions between both heterodimers.

Figure legends

Figure 1. Human MLH1-MLH3 is an endonuclease.

A. Schematic representation of human MLH1-MLH3 constructs used in experiments shown as additional results. **B.** Samples from a representative purification of hMLH1-hMLH3 analysed by 10% polyacrylamide gel. The gel was stained with Coomassie brilliant blue. MBP, maltose-binding protein; PP, PreScission protease; Flag flowthrough and eluate, flowthrough and eluate from anti-Flag affinity resin. **C**. Agarose gel (1%) showing the nuclease assay with hMLH1-hMLH3 on super-coiled dsDNA (sc-dsDNA) plasmid with Mn^{2+}(5 mM). **D**. Nuclease assay with hMLH1-hMLH3 on sc-dsDNA with Mg^{2+}(5 mM).

E. Samples from a representative purification of nuclease deficient variant of hMLH1-hMLH3 (D1223N) analysed by 10% polyacrylamide gel. The gel was stained with Coomassie brilliant blue. MBP, maltose-binding protein; PP, PreScission protease; Flag flowthrough and eluate, flowthrough and eluate from anti-Flag affinity resin. **F.** Nuclease assay with nuclease deficient hMLH1-hMLH3 (D1223N) on sc-dsDNA with Mn^{2+}(5 mM). **G.** Nuclease assay with hMLH1-hMLH3 on sc-dsDNA and with various concentration of ATP. **H.** Nuclease assay with hMLH1-hMLH3 and hMSH4-hMSH5 on sc-dsDNA. **I.** Denaturing polyacrylamide gel showing the nuclease assay with hMLH1-hMLH3 and hMSH4-hMSH5 on a 5'-end labeled HJ (50-mer). (*) denotes the position of radioactive ^{32}P on DNA substrate.

Figure 2. Human MSH4-MSH5 prefers binding to Holliday junction and slides on its arms upon ATP binding.

A. Schematic representation of human MSH4-MSH5 constructs used in this study. **B.** Samples from a representative purification of hMSH4-hMSH5 analysed by 10% polyacrylamide gel. The gel was stained with Coomassie brilliant blue. Ni-NTA flowthrough and eluate, flowthrough and eluate from nickel-nitrilotriacetic acid (Ni-NTA) resin; Strep flowthrough and eluate, flowthrough and eluate from StrepTactin sepharose resin. **C.** Representative 6% native polyacrylamide gel

showing the DNA binding affinity of various concentrations of hMSH4-hMSH5 to radioactive labeled HJ and dsDNA by electrophoretic mobility shift assay (EMSA) in the presence of Mg^{2+}. Below, quantitation of experiments shown in this panel; n=2, error bars, SEM. **D.** Representative EMSA showing DNA binding of various concentrations of hMSH4-hMSH5 to HJ and dsDNA in the absence of Mg^{2+}. Below, quantitation of experiments shown in this panel; n=2, error bars, SEM. **E.** Representative EMSA showing DNA binding of various concentrations of hMSH4-hMSH5 to HJ in the presence of ATP. **F.** Representative EMSA showing DNA binding of various concentrations of hMSH4-hMSH5 to HJ in the absence of ATP. **G.** Quantitation showing the hMSH4-hMSH5 binding to HJ such as shown in panel D and E; n=2, error bars, SEM. **H.** Schematic representation of quadruple streptavidin-blocked HJ. Representative EMSA showing DNA binding of various concentrations of hMSH4-hMSH5 with quadruple-blocked HJ in the presence of ATP. **I.** Representative EMSA showing DNA binding of various concentrations of hMSH4-hMSH5 with quadruple-blocked HJ in the absence of ATP. **J.** Quantitation showing the hMSH4-hMSH5 binding to quadruple-blocked HJ such as shown in panel G and H; n=2, error bars, SEM. **K.** Quantitation showing the hMSH4-hMSH5 binding to quadruple-blocked HJ and double-blocked dsDNA (gels not shown); n=2, error bars, SEM.

Figure 3. Human MLH1-MLH3 physically interacts with hMSH4-hMSH5.

A. Silver stained 10% polyacrylamide gel showing the pull down of hMSH4-hMSH5 by hMLH1-hMLH3, immobilized on Protein-G beads with anti-MLH1 antibody, indicating the interaction between both complexes. **B.** Pull down of hMLH1-hMLH3 by hMSH4-hMSH5, immobilized on protein-G beads with anti-His antibody, further confirming the interaction between both heterodimers.

Figure 4. Human MLH1-MLH3 cooperatively binds to HJ with hMSH4-hMSH5.

A. EMSA with 0.6% agarose gel showing the DNA binding of multiple concentrations of hMLH1-hMLH3 and hMSH4-hMSH5 to HJ in the presence of Mg^{2+}. **B.** EMSA showing the DNA binding of multiple concentrations of hMLH1-

hMLH3 and hMSH4-hMSH5 to HJ in the absence of Mg^{2+}. **C.** EMSA showing the DNA binding of multiple concentrations of hMLH1-hMLH3 and hMSH4-hMSH5 to dsDNA in the presence of Mg^{2+}. **D.** EMSA showing the DNA binding of multiple concentrations of hMLH1-hMLH3 and hMSH4-hMSH5 to dsDNA in the absence of Mg^{2+}.

Figure 5. Human MLH1-MLH3 does not show cooperative binding to Holliday junction with non-cognate yeast Mlh1-Mlh3

A. EMSA showing the DNA binding of hMLH1-hMLH3, hMSH4-hMSH5 and yMsh4-yMsh5 to HJ in the presence of Mg^{2+}. **B.** EMSA showing the DNA binding of hMLH1-hMLH3, hMSH4-hMSH5 and yMsh4-yMsh5 to HJ in the absence of Mg^{2+}.

Figure 1

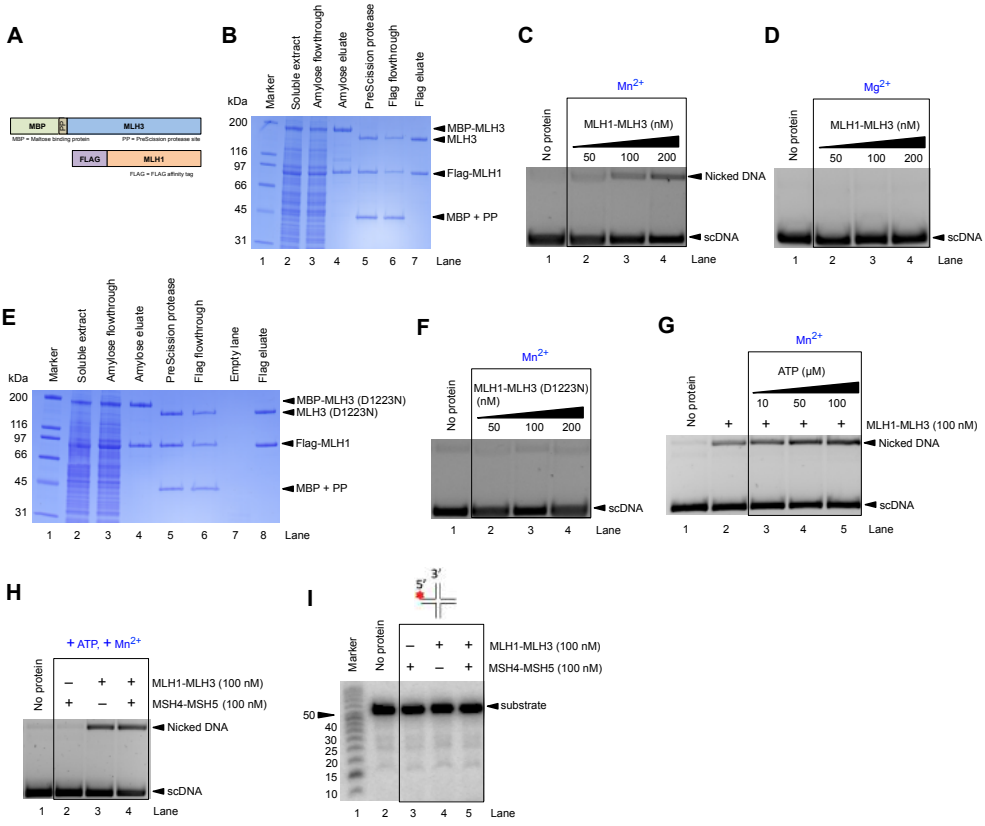
A
MBP
PP
MLH3
MBP = Maltose binding protein
PP = PreScission protease site
FLAG
MLH1
FLAG = FLAG affinity tag
B
kDa
Marker
Soluble extract
Amylose flowthrough
Amylose eluate
PreScission protease
Flag flowthrough
Flag eluate
200
116
97
66
45
31
MBP-MLH3
MLH3
Flag-MLH1
MBP + PP
1 2 3 4 5 6 7 Lane
C
Mn2+
No protein
MLH1-MLH3 (nM)
50 100 200
Nicked DNA
scDNA
1 2 3 4 Lane
D
Mg2+
No protein
MLH1-MLH3 (nM)
50 100 200
scDNA
1 2 3 4 Lane
E
kDa
Marker
Soluble extract
Amylose flowthrough
Amylose eluate
PreScission protease
Flag flowthrough
Empty lane
Flag eluate
200
116
97
66
45
31
MBP-MLH3 (D1223N)
MLH3 (D1223N)
Flag-MLH1
MBP + PP
1 2 3 4 5 6 7 8 Lane
F
Mn2+
No protein
MLH1-MLH3 (D1223N) (nM)
50 100 200
scDNA
1 2 3 4 Lane
G
Mn2+
No protein
ATP (μM)
10 50 100
+ + + +
MLH1-MLH3 (100 nM)
Nicked DNA
scDNA
1 2 3 4 5 Lane
H
+ ATP, + Mn2+
No protein
– + +
+ – +
MLH1-MLH3 (100 nM)
MSH4-MSH5 (100 nM)
Nicked DNA
scDNA
1 2 3 4 Lane
I
5′
3′
Marker
No protein
– + +
+ – +
MLH1-MLH3 (100 nM)
MSH4-MSH5 (100 nM)
50
40
30
25
20
15
10
substrate
1 2 3 4 5 Lane

Figure 2

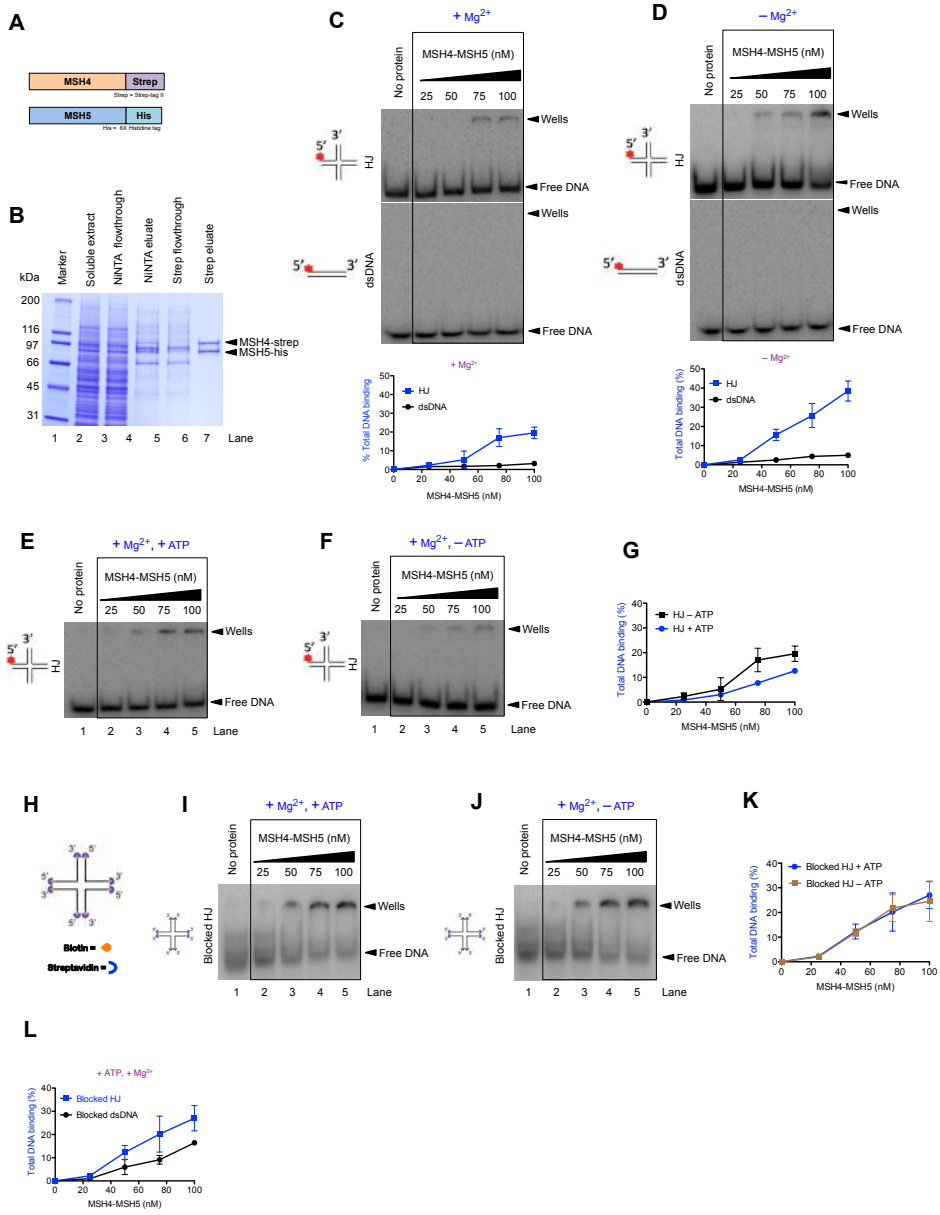
A
MSH4
Strep
MSH5
His
B
kDa
Marker
Soluble extract
NINTA flowthrough
NINTA eluate
Strep flowthrough
Strep eluate
200
116
97
66
45
31
MSH4-strep
MSH5-his
1 2 3 4 5 6 7 Lane
C
+ Mg2+
No protein
MSH4-MSH5 (nM)
25 50 75 100
HJ
dsDNA
Wells
Free DNA
% Total DNA binding
MSH4-MSH5 (nM)
D
– Mg2+
Total DNA binding (%)
E
+ Mg2+, + ATP
F
+ Mg2+, – ATP
1 2 3 4 5 Lane
G
HJ – ATP
HJ + ATP
H
Biotin
Streptavidin
I
Blocked HJ
J
K
Blocked HJ + ATP
Blocked HJ – ATP
L
+ ATP, + Mg2+
Blocked HJ
Blocked dsDNA

Figure 3

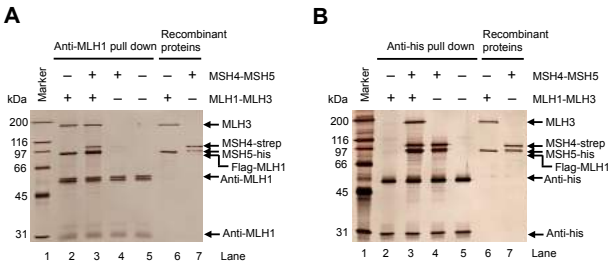
A
Anti-MLH1 pull down
Recombinant proteins
Marker
MSH4-MSH5
MLH1-MLH3
kDa
200
116
97
66
45
31
MLH3
MSH4-strep
MSH5-his
Flag-MLH1
Anti-MLH1
Anti-MLH1
1 2 3 4 5 6 7 Lane
B
Anti-his pull down
Recombinant proteins
Marker
MSH4-MSH5
MLH1-MLH3
kDa
200
116
97
66
45
31
MLH3
MSH4-strep
MSH5-his
Flag-MLH1
Anti-his
Anti-his
1 2 3 4 5 6 7 Lane

Figure 4

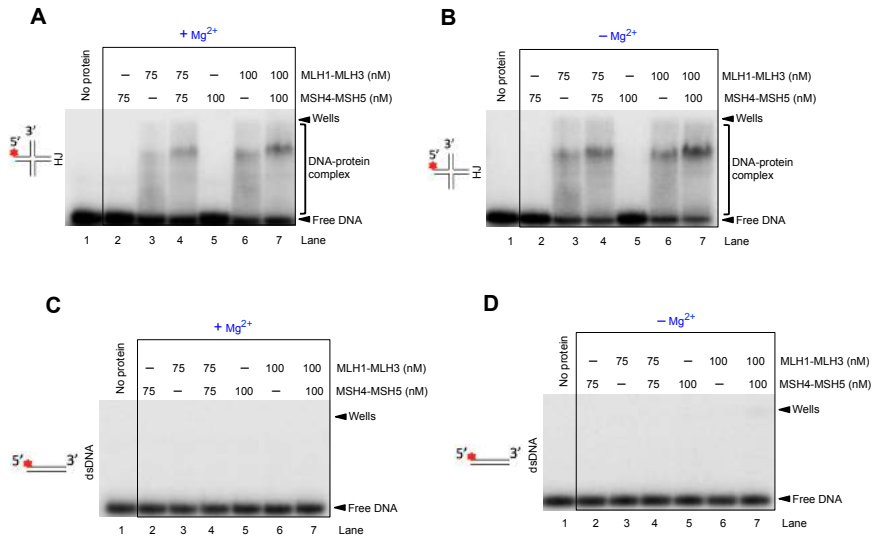
A
+ Mg2+
No protein
– 75 75 – 100 100 MLH1-MLH3 (nM)
75 – 75 100 – 100 MSH4-MSH5 (nM)
Wells
DNA-protein complex
Free DNA
5′ 3′
HJ
1 2 3 4 5 6 7 Lane
B
– Mg2+
No protein
– 75 75 – 100 100 MLH1-MLH3 (nM)
75 – 75 100 – 100 MSH4-MSH5 (nM)
Wells
DNA-protein complex
Free DNA
5′ 3′
HJ
1 2 3 4 5 6 7 Lane
C
+ Mg2+
No protein
– 75 75 – 100 100 MLH1-MLH3 (nM)
75 – 75 100 – 100 MSH4-MSH5 (nM)
Wells
Free DNA
5′ 3′
dsDNA
1 2 3 4 5 6 7 Lane
D
– Mg2+
No protein
– 75 75 – 100 100 MLH1-MLH3 (nM)
75 – 75 100 – 100 MSH4-MSH5 (nM)
Wells
Free DNA
5′ 3′
dsDNA
1 2 3 4 5 6 7 Lane

Figure 5

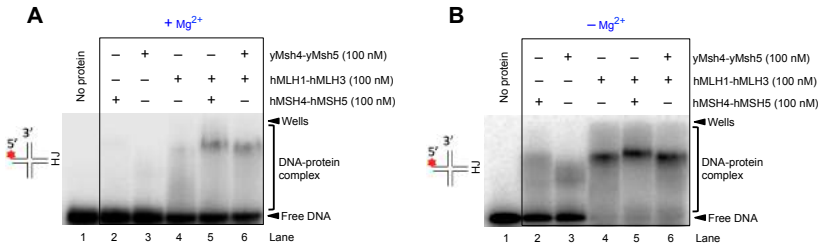
A
+ Mg2+
No protein
yMsh4-yMsh5 (100 nM)
hMLH1-hMLH3 (100 nM)
hMSH4-hMSH5 (100 nM)
Wells
DNA-protein complex
Free DNA
HJ
5′
3′
1 2 3 4 5 6 Lane
B
– Mg2+
No protein
yMsh4-yMsh5 (100 nM)
hMLH1-hMLH3 (100 nM)
hMSH4-hMSH5 (100 nM)
Wells
DNA-protein complex
Free DNA
HJ
5′
3′
1 2 3 4 5 6 Lane

Experimental procedures

Cloning, expression and purification of recombinant proteins

Recombinant hMutLγ was prepared from the codon-optimized (for insect cells) constructs of hMLH1 and hMLH3 for expression in *Spodoptera frugiperda* (*Sf*9) cells. The single plasmid pFL-MLH1co/His-MLH3co (co; codon optimized) containing both genes was kindly provided by Jean-Baptiste Charbonnier (Institut de Biologie et Technologies de Saclay, France). I modified the previously reported constructs of hMutLγ from MBP-hMLH3-his to MBP-hMLH3co and hMLH1 to Flag-hMLH1co (Ranjha et al., 2014). To prepare the pFB-MBP-MLH3co, hMLH3 gene was amplified by PCR using pFL-MLH1co/His-MLH3co as template with forward primer MLH3co_F and reverse primer MLH3co_R. The amplified product was digested with NheI and XmaI and cloned into pFB-MBP-MLH3-his. The reverse primer MLH3co_R contained stop codon, which resulted in its insertion between MLH3 gene and his tag and hence forming plasmid pFB-MBP-hMLH3co. Similarly, Flag tag was inserted at N-terminus of pFB-hMLH1 by amplification of hMLH1 from pFL-MLH1co/His-MLH3co by PCR using forward primer reverse primer Flag_MLH1co_F and MLH1co_R. The amplified product was digested with BamHI and XbaI and cloned into pFB-MBP-MLH3co giving rise to pFB-Flag-MLH1co. To prepare the nuclease deficient variant of MLH3, aspartic acid (D) at position 1223 in MLH3 was mutated to asparagine (N) by QuikChangeII site-directed mutagenesis kit (Agilent Techonologies) using primers MLH3co_ND_F and MLH3co_ND_R by following the manufacturer's instructions.

All cloned genes were verified by sequencing. Bacmids, primary and secondary baculoviruses were prepared by Bac-to-Bac system (Invitrogen) according to manufacturer's recommendations. The transfection of *Sf*9 cells was carried out using Trans-IT insect reagent (Mirus Bio).

For the large-scale expression and purification of hMLH1-hMLH3, 3.2 litres *Sf*9 cells were seeded at 0.5×10^6 per ml and co-infected 16 hours later with equal amount of secondary baculoviruses of MLH3 and MLH1. Cells were further incubated for 52 hours at 27° C with constant agitation. The cells were harvested

by centrifuging them for 10 minutes at 500 X g and washed once with phosphate buffered saline (PBS). The collected pellets were snap frozen and stored at –80° C. All subsequent steps during purification were carried out at 4° C or on ice. Cell pellets were re-suspended in 3 volumes of lysis buffer (Tris-HCl, pH 7.5, 50 mM; dithiothreitol, 1 mM; EDTA, 1 mM; Protease inhibitory cocktail, Sigma P8340, 1:400; phenylmethylsulfonyl fluoride (PMSF), 1 mM; leupeptin, 30 μg/ml; NaCl, 300 mM; glycerol, 10%) and incubated for 20 minutes with continuous mixing. Glycerol was added to 16% (v/v) concentration followed by (slow) addition of NaCl to reach the final concentration of 305 mM. The cell suspension was further incubated for 30 minutes with continuous stirring. Total cell suspension was centrifuged at 57'800 X g for 30 min to obtain soluble extract. Pre-equilibrated amylose resin (Qiagen) was added to cleared soluble extract and incubated for 1 hour with continuous mixing. The soluble extract with amylose resin was centrifuged for 2 minutes at 2000 X g to separate the resin with the supernatant. The resin was washed extensively with wash buffer (Tris-HCl, pH 7.5, 50 mM; β-mercaptoethanol, 2 mM; NaCl, 300 mM; glycerol, 10%; PMSF, 1 mM) batch wise as well as on disposable columns (ThermoFisher Scientific). The protein was eluted from the resin with wash buffer containing 10 mM maltose (Sigma). The eluates were further treated with PreScission protease for 1 hour to cleave the maltose binding protein affinity tag (MBP). The eluate was further incubated with anti-FLAG M2 Affinity Gel (A2220, Sigma) for 1 h with continuous mixing. The FLAG-resin was then washed extensively on disposable column with FLAG wash buffer (Tris-HCl, pH 7.5, 50 mM; NaCl, 150 mM; glycerol, 10%; PMSF, 1 mM; β-mercaptoethanol, 1 mM). Finally, recombinant hMLH1-hMLH3 was eluted with FLAG wash buffer containing 3xFLAG peptide (200 μg/ml, Sigma, F4799) in multiple fractions. Fractions with proteins were pooled, aliquoted, snap frozen and stored at –80° C. The purification of nuclease deficient variant of hMLH1-hMLH3 (D1223N) was carried out with the identical expression and purification procedure as wild type hMLH1-hMLH3.

To express and purify hMSH4-hMSH5 at large-scale, primary virus for hMSH4-hMSH5, received from Eva R Hoffman (University of Copenhagen), was amplified to prepare secondary virus. The *Sf9* cells were seeded at $0.5x10^6$ per ml and 16

hours later infected with single secondary virus of hMSH4-hMSH5. The cells were incubated for 52 hours at 27° C with constant agitation. The infected cells were harvested by centrifugation (10 minutes, 500 g) and washed once with PBS. The collected pellets were snap frozen and stored at –80° C. All subsequent steps of purification were carried out either at 4° C or on ice. The pellets were re-suspended with 3 volumes of lysis buffer (Tris-HCl, pH 7.5, 50 mM; β-mercaptoethanol, 2 mM; ethylenediaminetetraacetic acid (EDTA), 1 mM; Protease inhibitory cocktail, Sigma P8340, 1:400; phenylmethylsulfonyl fluoride (PMSF), 1 mM; leupeptin, 30 μg/ml; imidazole, 20 mM) and incubated for 20 minutes with continuous mixing. After incubation, glycerol was added to 16% (v/v) concentration, followed by slow addition of NaCl to reach the final concentration of 305 mM. The cell suspension was further incubated for 30 min with continuous stirring. The suspension was centrifuged at 57'800 g for 30 min to obtain the soluble extract. Pre-equilibrated nickel-nitrilotriacetic acid (Ni-NTA) agarose resin (Qiagen) was added to the soluble extract and incubated for 1 hour with continuous mixing. The Ni-NTA resin was separated from the soluble extract by centrifugation at 2'000 g for 2 min and washed extensively with Ni-NTA wash buffer (Tris-HCl, pH 7.5, 50 mM; β-mercaptoethanol, 2 mM; NaCl, 300 mM; glycerol, 10%; PMSF, 1 mM; imidazole, 20 mM) batch wise as well as on disposable columns (Thermo Scientific). The protein was eluted with Ni-NTA wash buffer containing 250 mM Imidazole. The eluted protein was mixed and incubated with *Strep*-Tactin Superflow resin (Qiagen) for 1 hour with continues mixing. The *Strep*-Tactin resin was washed extensively with Strep wash buffer (Tris-HCl, pH 7.5, 50 mM; β-mercaptoethanol, 2 mM; NaCl, 300 mM; glycerol, 10%; PMSF, 1 mM) on disposable column (Thermo Scientific). In the last step, recombinant hMSH4-hMSH5 was eluted in fractions with strep wash buffer containing 150 mM NaCl (instead of 300 mM) and 2.5 mM desthiobiotin (Sigma). The fractions containing proteins were pooled, aliquoted, snap frozen and stored at –80° C.

Nuclease assay

Nuclease assays were carried out in 15 μL volume with buffer containing Tris-acetate pH 7.5, 25 mM; manganese or magnesium acetate (or as indicated), 5

mM; dithiothreitol, 1 mM; EDTA, 100 μM; bovine serum albumin, (New England Biolabs), 0.1 mg/ml; DNA substrate, 100 μg (pUC19) on ice. Additionally, ATP (100 μM) was added to the reactions wherever indicated. Recombinant proteins were then added to the reactions on ice and samples were incubated for 1 hour at 37° C. Reactions were stopped with 5 μL of stop solution (EDTA, 150 mM; SDS (Sodium dodecyl sulfate), 2%; glycerol, 30%; bromophenol blue, 0.25%) and 1μL Proteinase K (14-22 mg/mL, Roche) for 30 minutes at 37° C. Finally, products were separated by electrophoresis on 1% agarose gel electrophoresis and DNA was visualized by staining with ethidium bromide (0.1 μg/ml) using the Alpha InnoTec imaging station.

Nuclease assays with radioactive labeled ^{32}P substrates were carried in 15 μL volume with buffer containing Tris-acetate pH 7.5, 25 mM; manganese acetate, 1 mM; magnesium acetate, 5 mM; dithiothreitol, 1 mM; ATP, 1 mM; bovine serum albumin, (New England Biolabs), 0.25 mg/ml; phosphoenolpyruvate, 1 mM; pyruvate kinase, (Sigma), 80 U/ml and oligonucleotide-based DNA substrate (50-mer), 1 nM (in molecules) on ice. Recombinant proteins were added to the reactions and incubated for 30 minutes at 37° C. Reactions were stopped with 0.5 μl Proteinase K (20.6 mg/mL, Roche); and 1 μL solution containing 5% SDS and 0.25 M EDTA for 30 minutes at 37°C. Finally, 16.5 μL loading buffer (95% formamide, 20 mM EDTA and bromophenol blue) was added to all the samples and the products were separated on 15% polyacrylamide denaturing urea gels (19:1 acrylamide-bisacrylamide, BioRad). The gels were fixed in a solution containing 40% methanol, 10% acetic acid and 5% glycerol for 30 minutes at room temperature and dried on a 3 mm CHR paper (Whatman). The dried gels were exposed to storage phosphor screens (GE Healthcare) and scanned by Typhoon Phosphor imager (FLA 9500, GE Healthcare)

DNA substrates

The radioactive labeled (^{32}P) oligonucleotide-based Holliday junction (HJ) or double stranded DNA (dsDNA) substrates were prepared and used as described previously. To prepare the blocked substrates, oligonucleotides with the attached biotin at both ends were purchased from the Microsynth AG. The

sequences of biotinylated oligonucleotides were identical to the non-biotinylated oligonucleotides used for preparing non-blocked dsDNA and HJ.

Electrophoretic mobility shift assay (EMSA)

The DNA binding assays were carried out in 15 µL volume with buffer containing HEPES pH 7.8, 25 mM; magnesium chloride, 2 mM or EDTA, 3 mM (in – Mg^{2+} assays); glycerol, 5%; dithiothreitol, 1 mM; bovine serum albumin, (New England Biolabs), 0.05 mg/ml; DNA substrate (non- or biotinylated), 0.5 nM (in molecules); dsDNA (50-mer, "cold" oligonucleotide used as competitor DNA), 3.3 ng/uL (corresponded to ~ 200 molar fold excess); ATP, 1 mM (wherever indicated) on ice. In super-shift assays (as shown in Figure 4 and 5), ATP (10 µM) and NaCl (75 mM) were also included in the reactions. Wherever blocked substrates are indicated, reactions were supplemented with streptavidin (15 nM, Sigma) and pre-incubated at room temperature for 5 minutes. Recombinant proteins were added and incubated for 15 minutes on ice. Next, 5 µL loading buffer [50% glycerol with bromophenol blue (0.25%)] was added to each sample and products were separated by electrophoresis in 6% polyacrylamide gel (ratio acrylamide:bisacrylamide 19:1, Bio-Rad) at 4 °C. Wherever indicated, 0.6% agarose gels were used for separating the larger complexes. Gels were dried on DE-81 chromatography paper (Whatman) and were exposed to storage phosphor screens (GE Healthcare) and scanned by a Typhoon Phosphor imager (FLA 9500, GE Healthcare).

Pull down interaction assays

Interaction assays were carried out in collaboration with Nicolas Weyland, master student in our lab. The anti-MLH1 or anti-His (GenScript) antibodies were re-suspended in 50 µL PBS-T (PBS-Tween 0.2%) and incubated with 60 µL magnetic Dynabead Protein-G (ThermoFisher Scientific) for 60 minutes at 4 C. The supernatant was discarded and beads were washed 3 times with 150 µL PBS-T on magnetic rack and again re-suspended in 60 µL PBS-T. Beads with immobilized antibodies were transferred to microtubes equally (15 µL). Recombinant proteins hMLH1-hMLH3 (220 nM) and hMSH4-hMSH5 (220 nM) either alone or together were re-suspended in 50 uL binding buffer containing

HEPES pH 7.8, 25 mM; EDTA, 3 mM; DTT, 1 mM; BSA, 0.05 µg/mL; NaCl, 80 mM; transferred and incubated with 15 µL washed beads for 45 minutes at 4° C with regular gentle tapping. Beads were washed 3X with 150 µL binding buffer additionally containing 0.1% Triton-X100. Proteins were eluted by adding SDS buffer (0.25 % bromophenol blue, 0.5 M DTT, 50% glycerol and 10% SDS) to each tube and boiling them for 3 minutes at 95 C. The boiled samples were analysed by polyacrylamide gel electrophoresis (PAGE) and stained with silver staining.

3. Discussion

DSB repair by HR is an essential process to repair accidental DNA breaks where its task is to maintain genomic integrity (Aparicio et al., 2014). Cells also utilize HR to produce genetic diversity during meiosis (Hunter, 2015). DNA end resection represents a critical key step in the repair of DSB by suppressing NHEJ while facilitating HR. In my PhD, I investigated the key steps of HR, which included DNA end resection and the resolution of recombination intermediate produced during meiosis.

In recent past, various studies have firmly established that DNA end resection occurs in 5' to 3' direction (Symington, 2014a). It is initiated by the MRE11 nuclease with RAD50 and NBS1 along with CtIP. However, MRE11 exhibits the opposite exonuclease polarity (3' to 5') and shows nicking activity only on ssDNA (Paull and Gellert, 1998). The first project of my PhD thesis specifically focused on the elucidation of mechanism of DNA end resection by MRN and CtIP. Here, I could show that phosphorylated CtIP (pCtIP) promotes MRN endonuclease activity on dsDNA. This stimulation of MRN is strongly dependent on phosphorylation of CtIP as *in vitro* phosphatase treatment of CtIP incapacitates it to stimulate MRN activity. The phosphorylation of certain sites in CtIP is cell cycle regulated, which is mediated by CDK (Huertas and Jackson, 2009). In particular, highly conserved CDK site T847 is important for the HR function of CtIP. The nonphosphorylatable mutation CtIP T847A abolishes its capacity to promote the clipping activity of MRN. The failure of CtIP T847A mutant to promote MRN activity explains the DNA end resection deficiency of CtIP T847A *in vivo* (Huertas and Jackson, 2009). I could also demonstrate that the nuclease activity responsible for observed MRN-pCtIP clipping activity is integral to MRE11, as nuclease-deficient variant of MRE11 (MRE11 H129L D130V) does not show any clipping activity. The ability of phosphorylated CtIP to stimulate MRN is independent of its DNA binding capacity, as pCtIP binds less to dsDNA substrate than CtIP, which was expressed and purified without phosphatase inhibitors and is unable to stimulate MRN. Recently, it was shown

that yeast Sae2 promotes MRX endonuclease activity (Cannavo and Cejka, 2014). The cross-species analysis of MRN and CtIP with MRX and Sae2 demonstrates that the stimulation of MRN or MRX is specific to their cognate protein partners, and infers the requirement for direct protein-protein interactions.

The RAD50 ATPase activity is essential for MRN function (Luo et al., 1999) (Paull and Deshpande, 2014). The mutation of the Rad50 ATPase motif in yeast exhibits the same HR defects as *rad50* null mutants (Alani et al., 1990). To investigate the contribution of RAD50 ATPase activity, I prepared RAD50 variants, which were deficient in either ATP binding (K42A) or ATP hydrolysis (K42R) but still showed the efficient exonucleolytic ssDNA degradation. I could clearly demonstrate that not only ATP binding but also ATP hydrolysis by RAD50 is essential for MRN-pCtIP clipping activity. In accordance, the exclusion of ATP from the reactions containing wild type proteins results in the failure of MRN stimulation by pCtIP. In addition, ATP cannot be replaced by either ADP or ATPγS, which further states the importance of ATP hydrolysis for MRN-pCtIP activity. This data explains the functional importance of ATP motif of RAD50 during HR. Furthermore; I also found that while MRE11 is Mn^{2+} -dependent exonuclease, both Mg^{2+} and Mn^{2+} are essential for MRN-pCtIP activity. Specifically, we observed that more Mg^{2+} is required than Mn^{2+} for optimal clipping activity, which roughly represents the cellular physiological condition where Mg^{2+} is more abundant in comparison to Mn^{2+}.

The NBS1 is not highly conserved in evolution and it is present only in higher eukaryotes (Saito and Komatsu, 2015). In yeast and humans, both Xrs2 and NBS1 contain nuclear localization signal (NLS), which is required for MR function. Besides nuclear localization of MR, Xrs2/NBS1 also play an important role in checkpoint signalling and coordinating the interactions with various mediator proteins(Thompson, 2012). In yeast, Xrs2 has been shown to be dispensable for MR stimulation by Sae2 (Oh et al., 2016). Surprisingly, NBS1 in humans is required for MRN stimulation by pCtIP, as MR with pCtIP fails to show any clipping activity. The exonuclease activity of MR is proficient and hence not negatively influenced by the absence of NBS1. It indicates the direct participation

of NBS1 in resection other than its mediator functions. I also discovered that the blocking of DNA ends is important to observe the clipping activity as exclusion of streptavidin in the reactions inhibited DNA cleavage. It is not clear which physiological protein blocks stimulate MRN-pCtIP activity in vivo, although Spo11 in meiosis is an excellent candidate as MRN-pCtIP nicking activity is required to remove Sae2 proteins prior to resection. In yeast, HO- or I-SceI mediated "clean" DSBs can be resected even in the absence of the Mre11 nuclease or Sae2, which support my finding (Symington, 2016). By varying the position of P^{32} label on dsDNA, I could demonstrate that MRN-pCtIP nicks at ~ 20 nt away from the 5' end, which corroborates well with the 5' end resection in HR. Additionally, the length of total DNA substrate, at least in our reconstituted system, does not influence the position of cleavage. While pCtIP does not affect MRN exonuclease activity on dsDNA, it surprisingly enhances the MRN nicking activity of circular ssDNA, in contrast to yeast system (Cannavo and Cejka, 2014). Although circular ssDNA is a poorly defined substrate, it provides hints that pCtIP is likely to be capable to stimulate MRN cleavage of yet unknown secondary structures. In yeast, it was shown that inverted Alu-repeats, which can create hairpins or other secondary structures, require MRX and Sae2 for mitotic recombination (Lobachev et al., 2002).

CtIP exists as tetramer *in vivo* and this oligomeric state is important for its HR functions (Davies et al., 2015). Recent analysis from Davies and colleagues showed that CtIP acquires tetrameric state in a dimer of dimers configuration, which associate with each other in head to head association through their N-termini. To examine the effect of the CtIP oligomeric state on MRN clipping activity, I initially constructed and purified N-terminal truncated pCtIP Δ1-160, which is unable to form dimers and hence consequently, no tetramers. The stimulation capacity of pCtIP Δ1-160 is strongly impaired in comparison to wild type pCtIP. Additionally, we also prepared the pCtIP L27E mutant, which abolishes the tetrameric form while retaining the dimeric state of CtIP (Davies et al., 2015; Kowalczykowski, 2015). My investigation with pCtIP L27E showed that while it does promote MRN activity, the comparative analysis with wild type revealed that pCtIP L27E is less proficient than pCtIP in MRN stimulation. This

observation partially explains the impaired resection phenotype of CtIP L27E cells. It is important to note here that pCtIP L27E fails to form foci at DSBs indicating its impaired localization at break sites. Collectively, our data show that the disruption of CtIP oligomeric state negatively affects MRN stimulation.

Meiosis is a key process required for the generation of genetic diversity demanded by evolution. In meiosis, diploid germ cells recombine DNA sequences between homologous chromosomes, which gives rise to the new set of chromosomes with a sequence that differs from the original parental chromosomes. During genetic recombination, various recombination intermediates are produced including the dHJ. The specific processing of dHJs by various enzymes give rise to either COs or NCOs or both products. MutLγ, an endonuclease, which exclusively produces COs, has been strongly implicated in the production of obligate COs in meiosis. Disruption or deletion of MutLγ in many organisms reduces CO levels significantly (Lipkin et al., 2002; Nishant et al., 2008; Wang et al., 1999; Zakharyevich et al., 2012). In addition to MutLγ, MutSγ has also been shown to function as a pro-CO factor within same pathway as MutLγ. Most of the evidence for MutLγ being the main putative endonuclease for HJ processing required for the majority of COs have come from genetic or cytological studies. Especially for human MutLγ, no information on its biochemical behavior is available in the literature. Therefore, in my second PhD project, I set out to biochemically characterize human MutLγ and its interplay with human MutSγ.

Initially, we showed that human MutLγ prefers binding to HJs and similar structures over dsDNA, ssDNA and Y-structures (Ranjha et al., 2014). We could also show that hMutLγ binding to HJs is reduced in the presence of Mg^{2+} presumably due to the stacked configuration of HJ, which likely prevents the hMutLγ access to the core of HJ. MutLα, another member of MutL family of MMR pathway, is capable of incising the super-coiled dsDNA (sc-dsDNA) in the presence of Mn^{2+}, hence bypassing the requirement of otherwise requisite factors (Kadyrov et al., 2006). Therefore, I also tested the nicking activity of hMutLγ under the similar conditions and found that hMutLγ does incise sc-

dsDNA in the presence of Mn^{2+}. No nicking activity by the nuclease deficient mutant of hMutLγ (hMLH1-hMLH3D1223N) further confirmed our findings. Hence, I could show that hMutLγ is indeed an endonuclease, which shows Mn^{2+} dependent non-specific dsDNA nicking activity. This result added a piece into the puzzle of formation of biased COs in meiosis by human MutLγ. However, the nicking activity was only observed in Mn^{2+} and was missing in Mg^{2+}, which does not represent the physiological environment of the cells where Mg^{2+} is much more abundant than Mn^{2+}. Furthermore, MutLγ did not show any cleavage activity on oligonucleotide-based HJs. Double HJs are believed to be hMutLγ's ideal substrate *in vivo*. No enhancement of hMutLγ nicking activity by hMutSγ, was not surprising, as sc-dsDNA does not represent the structure upon which these complexes are likely to function *in vivo.* The failure of yMutLγ to cleave HJs *in vitro* further suggests that a specific structure or additional activators are required for MutLγ specific nuclease activity. It is strongly believed that a specific configuration of the DNA substrate will be one of the key requirements to understand the specific MutLγ mediated cleavage. These findings collectively provide hints about the complexity of MutLγ nuclease action and its regulation *in vivo*. MutLγ exclusively generates COs only, which indicates the controlled biased cleavage mechanism in place for MutLγ to function. Similar to MutLα, MutLγ may also possess a latent Mg^{2+}-dependent endonuclease activity, which is promoted by other known or yet unknown factors, which are missing in our reconstituted reactions. Therefore, it will be imperative to study other pro-CO proteins (which may directly interact with MutLγ), post-translation modifications and to use a better DNA substrate to more closely mimic the *in vivo* substrate to understand the behavior of MutLγ in meiosis.

To further study the interplay between hMutLγ and hMutSγ, I expressed and purified recombinant hMutSγ in *Sf*9 cells. Previously, hMutSγ was shown to bind to the core of HJs and it showed sliding on HJ arms (Snowden et al., 2004). This was dependent on ATP binding but independent of its hydrolysis. To test whether our purified recombinant hMutSγ shows a similar behaviour, I performed DNA binding analysis of hMutSγ. Expectedly, hMutSγ does exhibit DNA binding preference for HJs over dsDNA, confirming that purified MutSγ is

active and behaves similarly as reported previously. Moreover, I could show that hMutSγ binding to HJ decreases when ATP is present in the reaction. In further experiments, I could also confirm that MutSγ does indeed slide on the HJ arms rather than simply falls off upon DNA binding. Although hMutSγ behaved similarly as characterized earlier, the total DNA binding affinity of hMutSγ to HJ was lower than previously reported. This could be due to ATP that may co-purify with our recombinant protein. In such a case, it would also explain the relatively minor decrease of hMutSγ binding to HJs upon ATP addition. Therefore, it will be important to test for the presence of ATP in our purified hMutSγ.

4. Outlook

The focus of my first PhD project was to elucidate the mechanism involved in DNA end resection in HR. Specifically, how MRE11 plays a central role in 5' to 3' DNA end resection despite its opposite nuclease polarity. Here, I could demonstrate that hyper-phosphorylated CtIP promotes MRN endonuclease activity on dsDNA. This main finding provides the supporting evidence for the proposed bidirectional resection mechanism.

Although I could clearly establish the essential role of CtIP phosphorylation in MRN-pCtIP clipping activity, how exactly does CtIP phosphorylation activate MRN on the mechanistic level remains unanswered. I believe that the key to answering this question will require learning about the interactions between MRN and both phospho- and non-phosphorylated CtIP variants. CtIP has been known to interact with each of the individual subunits of the MRN complex (Sartori et al., 2007; Yuan and Chen, 2009). It will be useful to study these interactions to map the exact position of residues required for the interaction. Upon interaction mapping, various non-interacting mutants of MRN and/or CtIP can be prepared, which are likely to provide further hints about the mechanism. It is highly conceivable that phosphorylation of CtIP on certain sites changes its confirmation. Therefore the structural analysis of wild type and various CtIP mutants is greatly desirable. It can also be used for in-depth analysis of MRN and CtIP interactions. However, the low yields of recombinant CtIP and MRN obtained during purification can be limiting.

The important role of NBS1 in MRN-pCtIP clipping activity was surprising as Xrs2 is dispensable in the yeast-reconstituted system (Oh et al., 2016). CtIP has been shown to interact with NBS1 at its N-terminal FHA domain as well as the C-terminus (Wang et al., 2013b). The FHA domain in various proteins has been described as phospho-peptide binding domain, and the phosphorylation of CtIP allows its binding to the FHA domain of NBS1. It will be interesting to disrupt the pCtIP-(FHA)-NBS1 interaction by mutating the FHA domain and to determine its

effects on the MRN-pCtIP activity. Another challenging future direction will be to identify the physiological protein blocks capable of stimulating the MRN-pCtIP activity. It is possible that SPO11, the Ku heterodimer or stalled topoisomerase-DNA complexes can all serve as the protein blocks in different scenarios. To investigate such possibilities, it will require the production of mentioned recombinant proteins, which by itself will be a challenging task. In our current study, the usage of artificial block yields a specific pattern of MRN-pCtIP cleavage. It will be intriguing to see the nature of MRN-pCtIP cleavage with physiological protein blocks (if any) and whether the nicking pattern changes or it remains the same.

According to the bidirectional resection model, the MRN-pCtIP nicks the dsDNA near to DSB, which is followed by the degradation of ssDNA in 3' to 5' direction towards breaks by MRE11exonucelolytic activity. Multiple *in vivo* studies carried out in yeast supports this proposed model (Symington, 2016). However, no such exonucleolytic degradation was observed in our reconstituted assay after MRN-CtIP clipping of dsDNA substrate. This important piece of information is therefore still missing from the puzzle. Moreover, the overall nicking activity of MRN-pCtIP is not very efficient. Recently, the roles of various proteins like MCM8-MCM9, EXD2, the SOSS complex and RECLQ4 have been identified in DNA end resection as positive regulators (Broderick et al., 2016; Lee et al., 2015; Lu et al., 2016b; Yang et al., 2013). It is therefore possible that these proteins may enhance MRN-pCtIP activity. It will be insightful to express and purify these recombinant proteins to see their effect on MRN-pCtIP clipping activity.

In my second PhD project, I set out to study the mechanism of recombination intermediates resolution in humans by the putative endonuclease hMutLγ. Using a biochemical approach, I could establish that hMutLγ is indeed an endonuclease that binds preferentially to HJ like structures (Ranjha et al., 2014). Additionally, I could I also demonstrate that human MSH4-MSH5 positively influences hMutLγ binding to HJ. Despite of these findings, the exact mechanism of action of hMutLγ to process HJ remains elusive. The failure to detect any specific nuclease activity by hMLH1-hMLH3 on HJ likely indicates the complexity of the underlying

mechanism. In the future, multiple approaches can be followed to better learn about the anticipated HJ cleavage mechanism. It is strongly believed that the "correct" structure of recombination intermediate will be one of the most crucial aspects of hMutLγ mediated biased resolution. Therefore it will be important to construct the dHJ structure, which can be either oligonucleotide- or plasmid based, and test hMLH1-hMLH3 nuclease activity on these structures. Another possibility is the regulation of hMutLγ activity by yet-unidentified post-translation modification(s) (PTM). To test this possibility, hMutLγ can be treated with various mediators/effectors of different PTMs *in vitro* and this modified hMLH1-hMLH3 (if any) can be used again in nuclease assay. Additionally, the mass spectrometry analysis of hMutLγ can be used to identify the potential PTMs sites during meiotic recombination. Although hMSH4-hMSH5 did not stimulate hMutLγ nuclease activity on supercoiled dsDNA, it is possible that other stimulatory factors are missing from the reaction. For instance, the activation of nuclease activity of hMLH1-PMS2 requires the ensemble of various proteins. It is highly probable that the same is true for hMutLγ as well. The hMutLγ only showed Mn^{2+}-dependent nicking activity whereas no such activity was observed in Mg^{2+}. As Mg^{2+} is more abundant than Mn^{2+} in physiological condition, it will be useful to study the apparent lack of activity of hMutLγ in Mg^{2+}. The DNA binding analysis data showed that while ATP slightly stimulates hMutLγ binding to HJ, hMSH4-hMSH5 binding to HJ decreases with ATP. It will be interesting to study the specific effect of ATP in more details on both heterodimers separately as well as in combination. Similar to hMutLγ, it will be important to learn about the posttranslational modifications of hMSH4-hMSH5 and apply the knowledge to further elucidate the mechanism. The understanding of the process of biased resolution by hMLH1-hMLH3 may require any of the processes described above or their combination.

5. Bibliography

Ahnesorg, P., Smith, P., and Jackson, S.P. (2006). XLF interacts with the XRCC4-DNA ligase IV complex to promote DNA nonhomologous end-joining. Cell *124*, 301-313.

Alani, E., Padmore, R., and Kleckner, N. (1990). Analysis of wild-type and rad50 mutants of yeast suggests an intimate relationship between meiotic chromosome synapsis and recombination. Cell *61*, 419-436.

Alberts, B., Johnson, A., Lewis, J., Morgan, D., Raff, M., Roberts, K., and Walter, P. (2015). Molecular Biology of the Cell, Sixth Edition. Molecular Biology of the Cell, Sixth Edition, 1-1342.

Allers, T., and Lichten, M. (2001). Differential timing and control of noncrossover and crossover recombination during meiosis. Cell *106*, 47-57.

Andersen, S.L., and Sekelsky, J. (2010). Meiotic versus mitotic recombination: two different routes for double-strand break repair: the different functions of meiotic versus mitotic DSB repair are reflected in different pathway usage and different outcomes. BioEssays : news and reviews in molecular, cellular and developmental biology *32*, 1058-1066.

Anderson, D.G., and Kowalczykowski, S.C. (1997). The translocating RecBCD enzyme stimulates recombination by directing RecA protein onto ssDNA in a chi-regulated manner. Cell *90*, 77-86.

Andres, S.N., Appel, C.D., Westmoreland, J.W., Williams, J.S., Nguyen, Y., Robertson, P.D., Resnick, M.A., and Williams, R.S. (2015). Tetrameric Ctp1 coordinates DNA binding and DNA bridging in DNA double-strand-break repair. Nat Struct Mol Biol *22*, 158-166.

Andres, S.N., and Junop, M.S. (2011). Crystallization and preliminary X-ray diffraction analysis of the human XRCC4-XLF complex. Acta Crystallogr Sect F Struct Biol Cryst Commun *67*, 1399-1402.

Antonarakis, S.E. (1991). Parental origin of the extra chromosome in trisomy 21 as indicated by analysis of DNA polymorphisms. Down Syndrome Collaborative Group. N Engl J Med *324*, 872-876.

Antonarakis, S.E., Petersen, M.B., McInnis, M.G., Adelsberger, P.A., Schinzel, A.A., Binkert, F., Pangalos, C., Raoul, O., Slaugenhaupt, S.A., Hafez, M.*, et al.* (1992). The meiotic stage of nondisjunction in trisomy 21: determination by using DNA polymorphisms. Am J Hum Genet *50*, 544-550.

Arana, M.E., and Kunkel, T.A. (2010). Mutator phenotypes due to DNA replication infidelity. Semin Cancer Biol *20*, 304-311.

Araujo, S.J., Nigg, E.A., and Wood, R.D. (2001). Strong functional interactions of TFIIH with XPC and XPG in human DNA nucleotide excision repair, without a preassembled repairosome. Mol Cell Biol *21*, 2281-2291.

Araujo, S.J., Tirode, F., Coin, F., Pospiech, H., Syvaoja, J.E., Stucki, M., Hubscher, U., Egly, J.M., and Wood, R.D. (2000). Nucleotide excision repair of DNA with recombinant human proteins: definition of the minimal set of factors, active forms of TFIIH, and modulation by CAK. Genes Dev *14*, 349-359.

Argueso, J.L., Wanat, J., Gemici, Z., and Alani, E. (2004). Competing crossover pathways act during meiosis in Saccharomyces cerevisiae. Genetics *168*, 1805-1816.

Arthur, L.M., Gustausson, K., Hopfner, K.P., Carson, C.T., Stracker, T.H., Karcher, A., Felton, D., Weitzman, M.D., Tainer, J., and Carney, J.P. (2004). Structural and functional analysis of Mre11-3. Nucleic Acids Res *32*, 1886-1893.

Audebert, M., Salles, B., and Calsou, P. (2004). Involvement of poly(ADP-ribose) polymerase-1 and XRCC1/DNA ligase III in an alternative route for DNA double-strand breaks rejoining. J Biol Chem *279*, 55117-55126.

Aylon, Y., Liefshitz, B., and Kupiec, M. (2004). The CDK regulates repair of double-strand breaks by homologous recombination during the cell cycle. The EMBO journal *23*, 4868-4875.

Badie, S., Carlos, A.R., Folio, C., Okamoto, K., Bouwman, P., Jonkers, J., and Tarsounas, M. (2015). BRCA1 and CtIP promote alternative non-homologous end-joining at uncapped telomeres. Embo J *34*, 410-424.

Bae, S.H., Bae, K.H., Kim, J.A., and Seo, Y.S. (2001). RPA governs endonuclease switching during processing of Okazaki fragments in eukaryotes. Nature *412*, 456-461.

Baker, S.M., Plug, A.W., Prolla, T.A., Bronner, C.E., Harris, A.C., Yao, X., Christie, D.M., Monell, C., Arnheim, N., Bradley, A*., et al.* (1996). Involvement of mouse Mlh1 in DNA mismatch repair and meiotic crossing over. Nat Genet *13*, 336-342.

Barlow, J.H., Lisby, M., and Rothstein, R. (2008). Differential regulation of the cellular response to DNA double-strand breaks in G1. Mol Cell *30*, 73-85.

Barnes, D.E., and Lindahl, T. (2004). Repair and genetic consequences of endogenous DNA base damage in mammalian cells. Annual review of genetics *38*, 445-476.

Bascom-Slack, C.A., Ross, L.O., and Dawson, D.S. (1997). Chiasmata, crossovers, and meiotic chromosome segregation. Adv Genet *35*, 253-284.

Bassing, C.H., Swat, W., and Alt, F.W. (2002). The mechanism and regulation of chromosomal V(D)J recombination. Cell *109 Suppl*, S45-55.

Beard, W.A., Prasad, R., and Wilson, S.H. (2006). Activities and mechanism of DNA polymerase beta. Methods Enzymol *408*, 91-107.

Becker, E., Meyer, V., Madaoui, H., and Guerois, R. (2006). Detection of a tandem BRCT in Nbs1 and Xrs2 with functional implications in the DNA damage response. Bioinformatics *22*, 1289-1292.

Berchowitz, L.E., Francis, K.E., Bey, A.L., and Copenhaver, G.P. (2007). The role of AtMUS81 in interference-insensitive crossovers in A. thaliana. PLoS Genet *3*, e132.

Bergerat, A., de Massy, B., Gadelle, D., Varoutas, P.C., Nicolas, A., and Forterre, P. (1997). An atypical topoisomerase II from Archaea with implications for meiotic recombination. Nature *386*, 414-417.

Bernstein, H., and Bernstein, C. (2010). Evolutionary Origin of Recombination during Meiosis. Bioscience *60*, 498-505.

Bernstein, N.K., Williams, R.S., Rakovszky, M.L., Cui, D., Green, R., Karimi-Busheri, F., Mani, R.S., Galicia, S., Koch, C.A., Cass, C.E.*, et al.* (2005). The molecular architecture of the mammalian DNA repair enzyme, polynucleotide kinase. Mol Cell *17*, 657-670.

Bishop, D.K., Park, D., Xu, L., and Kleckner, N. (1992). DMC1: a meiosis-specific yeast homolog of E. coli recA required for recombination, synaptonemal complex formation, and cell cycle progression. Cell *69*, 439-456.

Bishop, D.K., and Zickler, D. (2004). Early decision; meiotic crossover interference prior to stable strand exchange and synapsis. Cell *117*, 9-15.

Bizard, A.H., and Hickson, I.D. (2014). The dissolution of double Holliday junctions. Cold Spring Harb Perspect Biol *6*, a016477.

Blackwood, J.K., Rzechorzek, N.J., Bray, S.M., Maman, J.D., Pellegrini, L., and Robinson, N.P. (2013). End-resection at DNA double-strand breaks in the three domains of life. Biochem Soc Trans *41*, 314-320.

Blanco, M.G., and Matos, J. (2015). Hold your horSSEs: controlling structure-selective endonucleases MUS81 and Yen1/GEN1. Frontiers in genetics *6*, 253.

Blanco, M.G., Matos, J., and West, S.C. (2014). Dual control of Yen1 nuclease activity and cellular localization by Cdk and Cdc14 prevents genome instability. Mol Cell *54*, 94-106.

Boboila, C., Alt, F.W., and Schwer, B. (2012). Classical and alternative end-joining pathways for repair of lymphocyte-specific and general DNA double-strand breaks. Adv Immunol *116*, 1-49.

Boddy, M.N., Gaillard, P.H., McDonald, W.H., Shanahan, P., Yates, J.R., 3rd, and Russell, P. (2001). Mus81-Eme1 are essential components of a Holliday junction resolvase. Cell *107*, 537-548.

Bogue, M.A., Jhappan, C., and Roth, D.B. (1998). Analysis of variable (diversity) joining recombination in DNAdependent protein kinase (DNA-PK)-deficient mice reveals DNA-PK-independent pathways for both signal and coding joint formation. Proc Natl Acad Sci U S A *95*, 15559-15564.

Boland, C.R., and Goel, A. (2010). Microsatellite instability in colorectal cancer. Gastroenterology *138*, 2073-2087 e2073.

Bonetti, D., Clerici, M., Manfrini, N., Lucchini, G., and Longhese, M.P. (2010). The MRX complex plays multiple functions in resection of Yku- and Rif2-protected DNA ends. PLoS One *5*, e14142.

Borde, V., and de Massy, B. (2013). Programmed induction of DNA double strand breaks during meiosis: setting up communication between DNA and the chromosome structure. Current opinion in genetics & development *23*, 147-155.

Borner, G.V., Kleckner, N., and Hunter, N. (2004). Crossover/noncrossover differentiation, synaptonemal complex formation, and regulatory surveillance at the leptotene/zygotene transition of meiosis. Cell *117*, 29-45.

Bothmer, A., Robbiani, D.F., Di Virgilio, M., Bunting, S.F., Klein, I.A., Feldhahn, N., Barlow, J., Chen, H.T., Bosque, D., Callen, E.*, et al.* (2011). Regulation of DNA end joining, resection, and immunoglobulin class switch recombination by 53BP1. Mol Cell *42*, 319-329.

Bothmer, A., Robbiani, D.F., Feldhahn, N., Gazumyan, A., Nussenzweig, A., and Nussenzweig, M.C. (2010). 53BP1 regulates DNA resection and the choice between classical and alternative end joining during class switch recombination. The Journal of experimental medicine *207*, 855-865.

Botuyan, M.V., Lee, J., Ward, I.M., Kim, J.E., Thompson, J.R., Chen, J., and Mer, G. (2006). Structural basis for the methylation state-specific recognition of histone H4-K20 by 53BP1 and Crb2 in DNA repair. Cell *127*, 1361-1373.

Boulton, S.J., and Jackson, S.P. (1998). Components of the Ku-dependent non-homologous end-joining pathway are involved in telomeric length maintenance and telomeric silencing. The EMBO journal *17*, 1819-1828.

Bouwman, P., Aly, A., Escandell, J.M., Pieterse, M., Bartkova, J., van der Gulden, H., Hiddingh, S., Thanasoula, M., Kulkarni, A., Yang, Q.*, et al.* (2010). 53BP1 loss rescues BRCA1 deficiency and is associated with triple-negative and BRCA-mutated breast cancers. Nat Struct Mol Biol *17*, 688-695.

Bressan, D.A., Olivares, H.A., Nelms, B.E., and Petrini, J.H. (1998). Alteration of N-terminal phosphoesterase signature motifs inactivates Saccharomyces cerevisiae Mre11. Genetics *150*, 591-600.

Broderick, R., Nieminuszczy, J., Baddock, H.T., Deshpande, R.A., Gileadi, O., Paull, T.T., McHugh, P.J., and Niedzwiedz, W. (2016). EXD2 promotes homologous recombination by facilitating DNA end resection. Nat Cell Biol *18*, 271-280.

Brown, M.S., and Bishop, D.K. (2015). DNA strand exchange and RecA homologs in meiosis. Cold Spring Harb Perspect Biol *7*, a016659.

Buis, J., Wu, Y., Deng, Y., Leddon, J., Westfield, G., Eckersdorff, M., Sekiguchi, J.M., Chang, S., and Ferguson, D.O. (2008). Mre11 nuclease activity has essential roles in DNA repair and genomic stability distinct from ATM activation. Cell *135*, 85-96.

Bunick, C.G., Miller, M.R., Fuller, B.E., Fanning, E., and Chazin, W.J. (2006). Biochemical and structural domain analysis of xeroderma pigmentosum complementation group C protein. Biochemistry *45*, 14965-14979.

Bunting, S.F., Callen, E., Kozak, M.L., Kim, J.M., Wong, N., Lopez-Contreras, A.J., Ludwig, T., Baer, R., Faryabi, R.B., Malhowski, A.*, et al.* (2012). BRCA1 functions independently of homologous recombination in DNA interstrand crosslink repair. Mol Cell *46*, 125-135.

Bunting, S.F., Callen, E., Wong, N., Chen, H.T., Polato, F., Gunn, A., Bothmer, A., Feldhahn, N., Fernandez-Capetillo, O., Cao, L.*, et al.* (2010). 53BP1 inhibits homologous recombination in Brca1-deficient cells by blocking resection of DNA breaks. Cell *141*, 243-254.

Buscemi, G., Savio, C., Zannini, L., Micciche, F., Masnada, D., Nakanishi, M., Tauchi, H., Komatsu, K., Mizutani, S., Khanna, K.*, et al.* (2001). Chk2 activation dependence on Nbs1 after DNA damage. Molecular and cellular biology *21*, 5214-5222.

Bzymek, M., Thayer, N.H., Oh, S.D., Kleckner, N., and Hunter, N. (2010). Double Holliday junctions are intermediates of DNA break repair. Nature *464*, 937-941.

Cadet, J., and Wagner, J.R. (2013). DNA base damage by reactive oxygen species, oxidizing agents, and UV radiation. Cold Spring Harb Perspect Biol *5*.

Caldecott, K.W. (2008). Single-strand break repair and genetic disease. Nat Rev Genet *9*, 619-631.

Callen, E., Di Virgilio, M., Kruhlak, M.J., Nieto-Soler, M., Wong, N., Chen, H.T., Faryabi, R.B., Polato, F., Santos, M., Starnes, L.M.*, et al.* (2013). 53BP1 mediates productive and mutagenic DNA repair through distinct phosphoprotein interactions. Cell *153*, 1266-1280.

Camenisch, U., Dip, R., Schumacher, S.B., Schuler, B., and Naegeli, H. (2006). Recognition of helical kinks by xeroderma pigmentosum group A protein triggers DNA excision repair. Nat Struct Mol Biol *13*, 278-284.

Cannavo, E., and Cejka, P. (2014). Sae2 promotes dsDNA endonuclease activity within Mre11-Rad50-Xrs2 to resect DNA breaks. Nature *514*, 122-125.

Cannavo, E., Cejka, P., and Kowalczykowski, S.C. (2013). Relationship of DNA degradation by Saccharomyces cerevisiae exonuclease 1 and its stimulation by

RPA and Mre11-Rad50-Xrs2 to DNA end resection. Proc Natl Acad Sci U S A *110*, E1661-1668.

Carney, J.P., Maser, R.S., Olivares, H., Davis, E.M., Le Beau, M., Yates, J.R., 3rd, Hays, L., Morgan, W.F., and Petrini, J.H. (1998). The hMre11/hRad50 protein complex and Nijmegen breakage syndrome: linkage of double-strand break repair to the cellular DNA damage response. Cell *93*, 477-486.

Carson, C.T., Schwartz, R.A., Stracker, T.H., Lilley, C.E., Lee, D.V., and Weitzman, M.D. (2003). The Mre11 complex is required for ATM activation and the G2/M checkpoint. Embo J *22*, 6610-6620.

Cary, R.B., Peterson, S.R., Wang, J., Bear, D.G., Bradbury, E.M., and Chen, D.J. (1997). DNA looping by Ku and the DNA-dependent protein kinase. Proc Natl Acad Sci U S A *94*, 4267-4272.

Castor, D., Nair, N., Declais, A.C., Lachaud, C., Toth, R., Macartney, T.J., Lilley, D.M., Arthur, J.S., and Rouse, J. (2013). Cooperative control of holliday junction resolution and DNA repair by the SLX1 and MUS81-EME1 nucleases. Mol Cell *52*, 221-233.

Ceccaldi, R., Rondinelli, B., and D'Andrea, A.D. (2016). Repair Pathway Choices and Consequences at the Double-Strand Break. Trends Cell Biol *26*, 52-64.

Cejka, P. (2015). DNA end resection: nucleases team up with the right partners to initiate homologous recombination. J Biol Chem.

Cejka, P., Cannavo, E., Polaczek, P., Masuda-Sasa, T., Pokharel, S., Campbell, J.L., and Kowalczykowski, S.C. (2010a). DNA end resection by Dna2-Sgs1-RPA and its stimulation by Top3-Rmi1 and Mre11-Rad50-Xrs2. Nature *467*, 112-116.

Cejka, P., and Kowalczykowski, S.C. (2010). The full-length Saccharomyces cerevisiae Sgs1 protein is a vigorous DNA helicase that preferentially unwinds holliday junctions. J Biol Chem *285*, 8290-8301.

Cejka, P., Plank, J.L., Bachrati, C.Z., Hickson, I.D., and Kowalczykowski, S.C. (2010b). Rmi1 stimulates decatenation of double Holliday junctions during dissolution by Sgs1-Top3. Nat Struct Mol Biol *17*, 1377-1382.

Cejka, P., Plank, J.L., Dombrowski, C.C., and Kowalczykowski, S.C. (2012). Decatenation of DNA by the S. cerevisiae Sgs1-Top3-Rmi1 and RPA complex: a mechanism for disentangling chromosomes. Mol Cell *47*, 886-896.

Chaganti, R.S., Schonberg, S., and German, J. (1974). A manyfold increase in sister chromatid exchanges in Bloom's syndrome lymphocytes. Proc Natl Acad Sci U S A *71*, 4508-4512.

Chan, Y.W., and West, S.C. (2014). Spatial control of the GEN1 Holliday junction resolvase ensures genome stability. Nat Commun *5*, 4844.

Chang, M., Bellaoui, M., Zhang, C., Desai, R., Morozov, P., Delgado-Cruzata, L., Rothstein, R., Freyer, G.A., Boone, C., and Brown, G.W. (2005). RMI1/NCE4, a suppressor of genome instability, encodes a member of the RecQ helicase/Topo III complex. Embo J *24*, 2024-2033.

Chapman, J.R., Barral, P., Vannier, J.B., Borel, V., Steger, M., Tomas-Loba, A., Sartori, A.A., Adams, I.R., Batista, F.D., and Boulton, S.J. (2013). RIF1 is essential for 53BP1-dependent nonhomologous end joining and suppression of DNA double-strand break resection. Mol Cell *49*, 858-871.

Chapman, J.R., and Jackson, S.P. (2008). Phospho-dependent interactions between NBS1 and MDC1 mediate chromatin retention of the MRN complex at sites of DNA damage. EMBO reports *9*, 795-801.

Chapman, J.R., Sossick, A.J., Boulton, S.J., and Jackson, S.P. (2012). BRCA1-associated exclusion of 53BP1 from DNA damage sites underlies temporal control of DNA repair. Journal of cell science *125*, 3529-3534.

Chen, J.M., Cooper, D.N., Chuzhanova, N., Ferec, C., and Patrinos, G.P. (2007). Gene conversion: mechanisms, evolution and human disease. Nat Rev Genet *8*, 762-775.

Chen, L., Nievera, C.J., Lee, A.Y., and Wu, X. (2008a). Cell cycle-dependent complex formation of BRCA1.CtIP.MRN is important for DNA double-strand break repair. J Biol Chem *283*, 7713-7720.

Chen, L., Nievera, C.J., Lee, A.Y., and Wu, X. (2008b). Cell cycle-dependent complex formation of BRCA1.CtIP.MRN is important for DNA double-strand break repair. J Biol Chem *283*, 7713-7720.

Chen, L., Trujillo, K.M., Van Komen, S., Roh, D.H., Krejci, L., Lewis, L.K., Resnick, M.A., Sung, P., and Tomkinson, A.E. (2005). Effect of amino acid substitutions in the rad50 ATP binding domain on DNA double strand break repair in yeast. J Biol Chem *280*, 2620-2627.

Chen, S.Y., Tsubouchi, T., Rockmill, B., Sandler, J.S., Richards, D.R., Vader, G., Hochwagen, A., Roeder, G.S., and Fung, J.C. (2008c). Global analysis of the meiotic crossover landscape. Dev Cell *15*, 401-415.

Chiruvella, K.K., Liang, Z., and Wilson, T.E. (2013). Repair of double-strand breaks by end joining. Cold Spring Harb Perspect Biol *5*, a012757.

Chistiakov, D.A., Voronova, N.V., and Chistiakov, A.P. (2009). Ligase IV syndrome. European journal of medical genetics *52*, 373-378.

Ciccia, A., Constantinou, A., and West, S.C. (2003). Identification and characterization of the human mus81-eme1 endonuclease. J Biol Chem *278*, 25172-25178.

Ciccia, A., McDonald, N., and West, S.C. (2008). Structural and functional relationships of the XPF/MUS81 family of proteins. Annu Rev Biochem *77*, 259-287.

Claverys, J.P., and Lacks, S.A. (1986). Heteroduplex deoxyribonucleic acid base mismatch repair in bacteria. Microbiol Rev *50*, 133-165.

Clerici, M., Mantiero, D., Guerini, I., Lucchini, G., and Longhese, M.P. (2008). The Yku70-Yku80 complex contributes to regulate double-strand break processing and checkpoint activation during the cell cycle. EMBO reports *9*, 810-818.

Cloud, V., Chan, Y.L., Grubb, J., Budke, B., and Bishop, D.K. (2012). Rad51 is an accessory factor for Dmc1-mediated joint molecule formation during meiosis. Science *337*, 1222-1225.

Coin, F., Oksenych, V., and Egly, J.M. (2007). Distinct roles for the XPB/p52 and XPD/p44 subcomplexes of TFIIH in damaged DNA opening during nucleotide excision repair. Mol Cell *26*, 245-256.

Compe, E., and Egly, J.M. (2012). TFIIH: when transcription met DNA repair. Nat Rev Mol Cell Biol *13*, 343-354.

Connelly, J.C., de Leau, E.S., and Leach, D.R. (2003). Nucleolytic processing of a protein-bound DNA end by the E. coli SbcCD (MR) complex. DNA Repair (Amst) *2*, 795-807.

Constantinou, A., Chen, X.B., McGowan, C.H., and West, S.C. (2002). Holliday junction resolution in human cells: two junction endonucleases with distinct substrate specificities. Embo J *21*, 5577-5585.

Cortes Ledesma, F., El Khamisy, S.F., Zuma, M.C., Osborn, K., and Caldecott, K.W. (2009). A human 5'-tyrosyl DNA phosphodiesterase that repairs topoisomerase-mediated DNA damage. Nature *461*, 674-678.

Costantini, S., Woodbine, L., Andreoli, L., Jeggo, P.A., and Vindigni, A. (2007). Interaction of the Ku heterodimer with the DNA ligase IV/Xrcc4 complex and its regulation by DNA-PK. DNA Repair (Amst) *6*, 712-722.

Cruz-Garcia, A., Lopez-Saavedra, A., and Huertas, P. (2014). BRCA1 accelerates CtIP-mediated DNA-end resection. Cell reports *9*, 451-459.

D'Amours, D., and Jackson, S.P. (2001). The yeast Xrs2 complex functions in S phase checkpoint regulation. Genes & development *15*, 2238-2249.

Daley, J.M., and Sung, P. (2014). 53BP1, BRCA1, and the choice between recombination and end joining at DNA double-strand breaks. Mol Cell Biol *34*, 1380-1388.

Davies, O.R., Forment, J.V., Sun, M., Belotserkovskaya, R., Coates, J., Galanty, Y., Demir, M., Morton, C.R., Rzechorzek, N.J., Jackson, S.P.*, et al.* (2015). CtIP tetramer

assembly is required for DNA-end resection and repair. Nature structural & molecular biology *22*, 150-157.

Davis, A.J., and Chen, D.J. (2013). DNA double strand break repair via non-homologous end-joining. Transl Cancer Res *2*, 130-143.

Davis, A.P., and Symington, L.S. (2001). The yeast recombinational repair protein Rad59 interacts with Rad52 and stimulates single-strand annealing. Genetics *159*, 515-525.

Dayani, Y., Simchen, G., and Lichten, M. (2011). Meiotic recombination intermediates are resolved with minimal crossover formation during return-to-growth, an analogue of the mitotic cell cycle. PLoS Genet *7*, e1002083.

de Jager, M., van Noort, J., van Gent, D.C., Dekker, C., Kanaar, R., and Wyman, C. (2001). Human Rad50/Mre11 is a flexible complex that can tether DNA ends. Mol Cell *8*, 1129-1135.

de los Santos, T., Hunter, N., Lee, C., Larkin, B., Loidl, J., and Hollingsworth, N.M. (2003). The Mus81/Mms4 endonuclease acts independently of double-Holliday junction resolution to promote a distinct subset of crossovers during meiosis in budding yeast. Genetics *164*, 81-94.

de los Santos, T., Loidl, J., Larkin, B., and Hollingsworth, N.M. (2001). A role for MMS4 in the processing of recombination intermediates during meiosis in Saccharomyces cerevisiae. Genetics *159*, 1511-1525.

De Muyt, A., Jessop, L., Kolar, E., Sourirajan, A., Chen, J., Dayani, Y., and Lichten, M. (2012). BLM helicase ortholog Sgs1 is a central regulator of meiotic recombination intermediate metabolism. Mol Cell *46*, 43-53.

de Vries, S.S., Baart, E.B., Dekker, M., Siezen, A., de Rooij, D.G., de Boer, P., and te Riele, H. (1999). Mouse MutS-like protein Msh5 is required for proper chromosome synapsis in male and female meiosis. Genes Dev *13*, 523-531.

Deng, C., Brown, J.A., You, D., and Brown, J.M. (2005). Multiple endonucleases function to repair covalent topoisomerase I complexes in Saccharomyces cerevisiae. Genetics *170*, 591-600.

Desai-Mehta, A., Cerosaletti, K.M., and Concannon, P. (2001). Distinct functional domains of nibrin mediate Mre11 binding, focus formation, and nuclear localization. Molecular and cellular biology *21*, 2184-2191.

Deshpande, R.A., Williams, G.J., Limbo, O., Williams, R.S., Kuhnlein, J., Lee, J.H., Classen, S., Guenther, G., Russell, P., Tainer, J.A.*, et al.* (2014). ATP-driven Rad50 conformations regulate DNA tethering, end resection, and ATM checkpoint signaling. Embo J *33*, 482-500.

Di Virgilio, M., Callen, E., Yamane, A., Zhang, W., Jankovic, M., Gitlin, A.D., Feldhahn, N., Resch, W., Oliveira, T.Y., Chait, B.T.*, et al.* (2013). Rif1 prevents

resection of DNA breaks and promotes immunoglobulin class switching. Science *339*, 711-715.

Di Virgilio, M., and Gautier, J. (2005). Repair of double-strand breaks by nonhomologous end joining in the absence of Mre11. The Journal of cell biology *171*, 765-771.

Dillingham, M.S., and Kowalczykowski, S.C. (2008). RecBCD enzyme and the repair of double-stranded DNA breaks. Microbiol Mol Biol Rev *72*, 642-671, Table of Contents.

Dillingham, M.S., Spies, M., and Kowalczykowski, S.C. (2003). RecBCD enzyme is a bipolar DNA helicase. Nature *423*, 893-897.

Dixon, D.A., and Kowalczykowski, S.C. (1993). The recombination hotspot chi is a regulatory sequence that acts by attenuating the nuclease activity of the E. coli RecBCD enzyme. Cell *73*, 87-96.

Doe, C.L., Ahn, J.S., Dixon, J., and Whitby, M.C. (2002). Mus81-Eme1 and Rqh1 involvement in processing stalled and collapsed replication forks. J Biol Chem *277*, 32753-32759.

Dupre, A., Boyer-Chatenet, L., Sattler, R.M., Modi, A.P., Lee, J.H., Nicolette, M.L., Kopelovich, L., Jasin, M., Baer, R., Paull, T.T.*, et al.* (2008). A forward chemical genetic screen reveals an inhibitor of the Mre11-Rad50-Nbs1 complex. Nat Chem Biol *4*, 119-125.

Dzantiev, L., Constantin, N., Genschel, J., Iyer, R.R., Burgers, P.M., and Modrich, P. (2004). A defined human system that supports bidirectional mismatch-provoked excision. Mol Cell *15*, 31-41.

Edelmann, W., Cohen, P.E., Kneitz, B., Winand, N., Lia, M., Heyer, J., Kolodner, R., Pollard, J.W., and Kucherlapati, R. (1999). Mammalian MutS homologue 5 is required for chromosome pairing in meiosis. Nat Genet *21*, 123-127.

Eissler, C.L., Mazon, G., Powers, B.L., Savinov, S.N., Symington, L.S., and Hall, M.C. (2014). The Cdk/cDc14 module controls activation of the Yen1 holliday junction resolvase to promote genome stability. Mol Cell *54*, 80-93.

Eliezer, Y., Argaman, L., Rhie, A., Doherty, A.J., and Goldberg, M. (2009). The direct interaction between 53BP1 and MDC1 is required for the recruitment of 53BP1 to sites of damage. J Biol Chem *284*, 426-435.

Ellis, N.A., and German, J. (1996). Molecular genetics of Bloom's syndrome. Hum Mol Genet *5 Spec No*, 1457-1463.

Escribano-Diaz, C., Orthwein, A., Fradet-Turcotte, A., Xing, M., Young, J.T., Tkac, J., Cook, M.A., Rosebrock, A.P., Munro, M., Canny, M.D.*, et al.* (2013). A cell cycle-dependent regulatory circuit composed of 53BP1-RIF1 and BRCA1-CtIP controls DNA repair pathway choice. Mol Cell *49*, 872-883.

Evans, E., Fellows, J., Coffer, A., and Wood, R.D. (1997). Open complex formation around a lesion during nucleotide excision repair provides a structure for cleavage by human XPG protein. Embo J *16*, 625-638.

Fagbemi, A.F., Orelli, B., and Scharer, O.D. (2011). Regulation of endonuclease activity in human nucleotide excision repair. DNA Repair (Amst) *10*, 722-729.

Fan, Q.Q., Xu, F., White, M.A., and Petes, T.D. (1997). Competition between adjacent meiotic recombination hotspots in the yeast Saccharomyces cerevisiae. Genetics *145*, 661-670.

Farah, J.A., Cromie, G.A., and Smith, G.R. (2009). Ctp1 and Exonuclease 1, alternative nucleases regulated by the MRN complex, are required for efficient meiotic recombination. Proc Natl Acad Sci U S A *106*, 9356-9361.

Fattah, F.J., Lichter, N.F., Fattah, K.R., Oh, S., and Hendrickson, E.A. (2008). Ku70, an essential gene, modulates the frequency of rAAV-mediated gene targeting in human somatic cells. Proc Natl Acad Sci U S A *105*, 8703-8708.

Fei, J., and Chen, J. (2012). KIAA1530 protein is recruited by Cockayne syndrome complementation group protein A (CSA) to participate in transcription-coupled repair (TCR). J Biol Chem *287*, 35118-35126.

Feldmann, E., Schmiemann, V., Goedecke, W., Reichenberger, S., and Pfeiffer, P. (2000). DNA double-strand break repair in cell-free extracts from Ku80-deficient cells: implications for Ku serving as an alignment factor in non-homologous DNA end joining. Nucleic Acids Res *28*, 2585-2596.

Finkelstein, I.J., Visnapuu, M.L., and Greene, E.C. (2010). Single-molecule imaging reveals mechanisms of protein disruption by a DNA translocase. Nature *468*, 983-987.

Foster, S.S., Balestrini, A., and Petrini, J.H. (2011). Functional interplay of the Mre11 nuclease and Ku in the response to replication-associated DNA damage. Mol Cell Biol *31*, 4379-4389.

Fraga, C.G., Shigenaga, M.K., Park, J.W., Degan, P., and Ames, B.N. (1990). Oxidative damage to DNA during aging: 8-hydroxy-2'-deoxyguanosine in rat organ DNA and urine. Proc Natl Acad Sci U S A *87*, 4533-4537.

Frit, P., Barboule, N., Yuan, Y., Gomez, D., and Calsou, P. (2014). Alternative end-joining pathway(s): bricolage at DNA breaks. DNA Repair (Amst) *17*, 81-97.

Furuse, M., Nagase, Y., Tsubouchi, H., Murakami-Murofushi, K., Shibata, T., and Ohta, K. (1998). Distinct roles of two separable in vitro activities of yeast Mre11 in mitotic and meiotic recombination. The EMBO journal *17*, 6412-6425.

Gallo-Fernandez, M., Saugar, I., Ortiz-Bazan, M.A., Vazquez, M.V., and Tercero, J.A. (2012). Cell cycle-dependent regulation of the nuclease activity of Mus81-Eme1/Mms4. Nucleic Acids Res *40*, 8325-8335.

Gangloff, S., McDonald, J.P., Bendixen, C., Arthur, L., and Rothstein, R. (1994). The yeast type I topoisomerase Top3 interacts with Sgs1, a DNA helicase homolog: a potential eukaryotic reverse gyrase. Mol Cell Biol *14*, 8391-8398.

Garcia, V., Phelps, S.E., Gray, S., and Neale, M.J. (2011). Bidirectional resection of DNA double-strand breaks by Mre11 and Exo1. Nature *479*, 241-244.

Garner, E., Kim, Y., Lach, F.P., Kottemann, M.C., and Smogorzewska, A. (2013). Human GEN1 and the SLX4-associated nucleases MUS81 and SLX1 are essential for the resolution of replication-induced Holliday junctions. Cell Rep *5*, 207-215.

Ghezraoui, H., Piganeau, M., Renouf, B., Renaud, J.B., Sallmyr, A., Ruis, B., Oh, S., Tomkinson, A.E., Hendrickson, E.A., Giovannangeli, C.*, et al.* (2014). Chromosomal translocations in human cells are generated by canonical nonhomologous end-joining. Mol Cell *55*, 829-842.

Gilljam, K.M., Muller, R., Liabakk, N.B., and Otterlei, M. (2012). Nucleotide excision repair is associated with the replisome and its efficiency depends on a direct interaction between XPA and PCNA. PloS one *7*, e49199.

Girard, P.M., Riballo, E., Begg, A.C., Waugh, A., and Jeggo, P.A. (2002). Nbs1 promotes ATM dependent phosphorylation events including those required for G1/S arrest. Oncogene *21*, 4191-4199.

Gong, Y., Zhu, D., Ding, J., Dou, C.N., Ren, X., Gu, L., Jiang, T., and Wang, D.C. (2011). Crystal structures of aprataxin ortholog Hnt3 reveal the mechanism for reversal of 5'-adenylated DNA. Nat Struct Mol Biol *18*, 1297-1299.

Goodwin, A., Wang, S.W., Toda, T., Norbury, C., and Hickson, I.D. (1999). Topoisomerase III is essential for accurate nuclear division in Schizosaccharomyces pombe. Nucleic Acids Res *27*, 4050-4058.

Gottlieb, T.M., and Jackson, S.P. (1993). The DNA-dependent protein kinase: requirement for DNA ends and association with Ku antigen. Cell *72*, 131-142.

Gravel, S., Chapman, J.R., Magill, C., and Jackson, S.P. (2008). DNA helicases Sgs1 and BLM promote DNA double-strand break resection. Genes & development *22*, 2767-2772.

Grawunder, U., Wilm, M., Wu, X., Kulesza, P., Wilson, T.E., Mann, M., and Lieber, M.R. (1997). Activity of DNA ligase IV stimulated by complex formation with XRCC4 protein in mammalian cells. Nature *388*, 492-495.

Grossman, L., Caron, P.R., Mazur, S.J., and Oh, E.Y. (1988). Repair of DNA-containing pyrimidine dimers. FASEB journal : official publication of the Federation of American Societies for Experimental Biology *2*, 2696-2701.

Grundy, G.J., Rulten, S.L., Zeng, Z., Arribas-Bosacoma, R., Iles, N., Manley, K., Oliver, A., and Caldecott, K.W. (2013). APLF promotes the assembly and activity of non-homologous end joining protein complexes. Embo J *32*, 112-125.

Gu, J., Lu, H., Tippin, B., Shimazaki, N., Goodman, M.F., and Lieber, M.R. (2007). XRCC4:DNA ligase IV can ligate incompatible DNA ends and can ligate across gaps. Embo J *26*, 1010-1023.

Gu, Y., Seidl, K.J., Rathbun, G.A., Zhu, C., Manis, J.P., van der Stoep, N., Davidson, L., Cheng, H.L., Sekiguchi, J.M., Frank, K.*, et al.* (1997). Growth retardation and leaky SCID phenotype of Ku70-deficient mice. Immunity *7*, 653-665.

Guarne, A. (2012). The functions of MutL in mismatch repair: the power of multitasking. Progress in molecular biology and translational science *110*, 41-70.

Guillon, H., Baudat, F., Grey, C., Liskay, R.M., and de Massy, B. (2005). Crossover and noncrossover pathways in mouse meiosis. Mol Cell *20*, 563-573.

Gunz, D., Hess, M.T., and Naegeli, H. (1996). Recognition of DNA adducts by human nucleotide excision repair. Evidence for a thermodynamic probing mechanism. J Biol Chem *271*, 25089-25098.

Guttinger, S., Laurell, E., and Kutay, U. (2009). Orchestrating nuclear envelope disassembly and reassembly during mitosis. Nat Rev Mol Cell Biol *10*, 178-191.

Haber, J.E., and Hearn, M. (1985). Rad52-independent mitotic gene conversion in Saccharomyces cerevisiae frequently results in chromosomal loss. Genetics *111*, 7-22.

Hakem, R., de la Pompa, J.L., and Mak, T.W. (1998). Developmental studies of Brca1 and Brca2 knock-out mice. J Mammary Gland Biol Neoplasia *3*, 431-445.

Hakem, R., de la Pompa, J.L., Sirard, C., Mo, R., Woo, M., Hakem, A., Wakeham, A., Potter, J., Reitmair, A., Billia, F.*, et al.* (1996). The tumor suppressor gene Brca1 is required for embryonic cellular proliferation in the mouse. Cell *85*, 1009-1023.

Hammel, M., Yu, Y., Fang, S., Lees-Miller, S.P., and Tainer, J.A. (2010). XLF regulates filament architecture of the XRCC4.ligase IV complex. Structure *18*, 1431-1442.

Han, E.S., Cooper, D.L., Persky, N.S., Sutera, V.A., Jr., Whitaker, R.D., Montello, M.L., and Lovett, S.T. (2006). RecJ exonuclease: substrates, products and interaction with SSB. Nucleic Acids Res *34*, 1084-1091.

Handa, N., Morimatsu, K., Lovett, S.T., and Kowalczykowski, S.C. (2009). Reconstitution of initial steps of dsDNA break repair by the RecF pathway of E. coli. Genes Dev *23*, 1234-1245.

Handa, N., Yang, L., Dillingham, M.S., Kobayashi, I., Wigley, D.B., and Kowalczykowski, S.C. (2012). Molecular determinants responsible for recognition of the single-stranded DNA regulatory sequence, chi, by RecBCD enzyme. Proc Natl Acad Sci U S A *109*, 8901-8906.

Hartsuiker, E., Mizuno, K., Molnar, M., Kohli, J., Ohta, K., and Carr, A.M. (2009a). Ctp1CtIP and Rad32Mre11 nuclease activity are required for Rec12Spo11

removal, but Rec12Spo11 removal is dispensable for other MRN-dependent meiotic functions. Molecular and cellular biology *29*, 1671-1681.

Hartsuiker, E., Neale, M.J., and Carr, A.M. (2009b). Distinct requirements for the Rad32(Mre11) nuclease and Ctp1(CtIP) in the removal of covalently bound topoisomerase I and II from DNA. Mol Cell *33*, 117-123.

Heyer, W.D. (2004). Recombination: Holliday junction resolution and crossover formation. Curr Biol *14*, R56-58.

Heyer, W.D., Ehmsen, K.T., and Liu, J. (2010). Regulation of homologous recombination in eukaryotes. Annual review of genetics *44*, 113-139.

Hicks, W.M., Kim, M., and Haber, J.E. (2010). Increased mutagenesis and unique mutation signature associated with mitotic gene conversion. Science *329*, 82-85.

Hillers, K.J. (2004). Crossover interference. Curr Biol *14*, R1036-1037.

Hillers, K.J., and Villeneuve, A.M. (2003). Chromosome-wide control of meiotic crossing over in C. elegans. Curr Biol *13*, 1641-1647.

Hinz, J.M., Yamada, N.A., Salazar, E.P., Tebbs, R.S., and Thompson, L.H. (2005). Influence of double-strand-break repair pathways on radiosensitivity throughout the cell cycle in CHO cells. DNA Repair (Amst) *4*, 782-792.

HJ, M. (1916). The mechanism of crossing-over. Am Nat *50*, 193–221.

Hoffmann, E.R., and Borts, R.H. (2004). Meiotic recombination intermediates and mismatch repair proteins. Cytogenetic and genome research *107*, 232-248.

Hohl, M., Kwon, Y., Galvan, S.M., Xue, X., Tous, C., Aguilera, A., Sung, P., and Petrini, J.H. (2011). The Rad50 coiled-coil domain is indispensable for Mre11 complex functions. Nature structural & molecular biology *18*, 1124-1131.

Hollingsworth, N.M., Ponte, L., and Halsey, C. (1995). MSH5, a novel MutS homolog, facilitates meiotic reciprocal recombination between homologs in Saccharomyces cerevisiae but not mismatch repair. Genes Dev *9*, 1728-1739.

Hong, S., Sung, Y., Yu, M., Lee, M., Kleckner, N., and Kim, K.P. (2013). The logic and mechanism of homologous recombination partner choice. Mol Cell *51*, 440-453.

Hopfner, K.P., Craig, L., Moncalian, G., Zinkel, R.A., Usui, T., Owen, B.A., Karcher, A., Henderson, B., Bodmer, J.L., McMurray, C.T.*, et al.* (2002). The Rad50 zinc-hook is a structure joining Mre11 complexes in DNA recombination and repair. Nature *418*, 562-566.

Hopfner, K.P., Karcher, A., Craig, L., Woo, T.T., Carney, J.P., and Tainer, J.A. (2001). Structural biochemistry and interaction architecture of the DNA double-strand break repair Mre11 nuclease and Rad50-ATPase. Cell *105*, 473-485.

Hopfner, K.P., Karcher, A., Shin, D., Fairley, C., Tainer, J.A., and Carney, J.P. (2000a). Mre11 and Rad50 from Pyrococcus furiosus: cloning and biochemical characterization reveal an evolutionarily conserved multiprotein machine. Journal of bacteriology *182*, 6036-6041.

Hopfner, K.P., Karcher, A., Shin, D.S., Craig, L., Arthur, L.M., Carney, J.P., and Tainer, J.A. (2000b). Structural biology of Rad50 ATPase: ATP-driven conformational control in DNA double-strand break repair and the ABC-ATPase superfamily. Cell *101*, 789-800.

Huang, J., and Dynan, W.S. (2002). Reconstitution of the mammalian DNA double-strand break end-joining reaction reveals a requirement for an Mre11/Rad50/NBS1-containing fraction. Nucleic acids research *30*, 667-674.

Huang, J.C., Svoboda, D.L., Reardon, J.T., and Sancar, A. (1992). Human nucleotide excision nuclease removes thymine dimers from DNA by incising the 22nd phosphodiester bond 5' and the 6th phosphodiester bond 3' to the photodimer. Proc Natl Acad Sci U S A *89*, 3664-3668.

Huertas, P., Cortes-Ledesma, F., Sartori, A.A., Aguilera, A., and Jackson, S.P. (2008). CDK targets Sae2 to control DNA-end resection and homologous recombination. Nature *455*, 689-692.

Huertas, P., and Jackson, S.P. (2009). Human CtIP mediates cell cycle control of DNA end resection and double strand break repair. J Biol Chem *284*, 9558-9565.

Huffman, J.L., Sundheim, O., and Tainer, J.A. (2005). DNA base damage recognition and removal: new twists and grooves. Mutation research *577*, 55-76.

Hunter, N., and Borts, R.H. (1997). Mlh1 is unique among mismatch repair proteins in its ability to promote crossing-over during meiosis. Genes Dev *11*, 1573-1582.

Hunter, N., and Kleckner, N. (2001). The single-end invasion: an asymmetric intermediate at the double-strand break to double-holliday junction transition of meiotic recombination. Cell *106*, 59-70.

Iliakis, G. (2009). Backup pathways of NHEJ in cells of higher eukaryotes: cell cycle dependence. Radiother Oncol *92*, 310-315.

Iliakis, G., Murmann, T., and Soni, A. (2015). Alternative end-joining repair pathways are the ultimate backup for abrogated classical non-homologous end-joining and homologous recombination repair: Implications for the formation of chromosome translocations. Mutat Res Genet Toxicol Environ Mutagen *793*, 166-175.

Interthal, H., and Heyer, W.D. (2000). MUS81 encodes a novel helix-hairpin-helix protein involved in the response to UV- and methylation-induced DNA damage in Saccharomyces cerevisiae. Molecular & general genetics : MGG *263*, 812-827.

Ira, G., Pellicioli, A., Balijja, A., Wang, X., Fiorani, S., Carotenuto, W., Liberi, G., Bressan, D., Wan, L., Hollingsworth, N.M., *et al.* (2004). DNA end resection, homologous recombination and DNA damage checkpoint activation require CDK1. Nature *431*, 1011-1017.

Ivanov, E.L., Sugawara, N., Fishman-Lobell, J., and Haber, J.E. (1996). Genetic requirements for the single-strand annealing pathway of double-strand break repair in Saccharomyces cerevisiae. Genetics *142*, 693-704.

Jackson, S.P., and Bartek, J. (2009). The DNA-damage response in human biology and disease. Nature *461*, 1071-1078.

Jacobs, A.L., and Schar, P. (2012). DNA glycosylases: in DNA repair and beyond. Chromosoma *121*, 1-20.

Jasin, M., and Rothstein, R. (2013). Repair of strand breaks by homologous recombination. Cold Spring Harb Perspect Biol *5*, a012740.

Jeggo, P.A., and Lobrich, M. (2015). How cancer cells hijack DNA double-strand break repair pathways to gain genomic instability. The Biochemical journal *471*, 1-11.

Jiricny, J. (2006). The multifaceted mismatch-repair system. Nat Rev Mol Cell Biol *7*, 335-346.

Jiricny, J. (2013). Postreplicative mismatch repair. Cold Spring Harb Perspect Biol *5*, a012633.

Jones, G.H. (1984). The control of chiasma distribution. Symp Soc Exp Biol *38*, 293-320.

Jung, D., and Alt, F.W. (2004). Unraveling V(D)J recombination; insights into gene regulation. Cell *116*, 299-311.

Kabotyanski, E.B., Gomelsky, L., Han, J.O., Stamato, T.D., and Roth, D.B. (1998). Double-strand break repair in Ku86- and XRCC4-deficient cells. Nucleic Acids Res *26*, 5333-5342.

Kadyk, L.C., and Hartwell, L.H. (1992). Sister chromatids are preferred over homologs as substrates for recombinational repair in Saccharomyces cerevisiae. Genetics *132*, 387-402.

Kadyrov, F.A., Dzantiev, L., Constantin, N., and Modrich, P. (2006). Endonucleolytic function of MutLalpha in human mismatch repair. Cell *126*, 297-308.

Kaliraman, V., Mullen, J.R., Fricke, W.M., Bastin-Shanower, S.A., and Brill, S.J. (2001). Functional overlap between Sgs1-Top3 and the Mms4-Mus81 endonuclease. Genes Dev *15*, 2730-2740.

Karanam, K., Kafri, R., Loewer, A., and Lahav, G. (2012). Quantitative live cell imaging reveals a gradual shift between DNA repair mechanisms and a maximal use of HR in mid S phase. Mol Cell *47*, 320-329.

Keeney, S. (2008). Spo11 and the Formation of DNA Double-Strand Breaks in Meiosis. Genome Dyn Stab *2*, 81-123.

Keeney, S., Giroux, C.N., and Kleckner, N. (1997). Meiosis-specific DNA double-strand breaks are catalyzed by Spo11, a member of a widely conserved protein family. Cell *88*, 375-384.

Kelly, K.O., Dernburg, A.F., Stanfield, G.M., and Villeneuve, A.M. (2000). Caenorhabditis elegans msh-5 is required for both normal and radiation-induced meiotic crossing over but not for completion of meiosis. Genetics *156*, 617-630.

Kim, H., Chen, J., and Yu, X. (2007). Ubiquitin-binding protein RAP80 mediates BRCA1-dependent DNA damage response. Science *316*, 1202-1205.

Kneitz, B., Cohen, P.E., Avdievich, E., Zhu, L., Kane, M.F., Hou, H., Jr., Kolodner, R.D., Kucherlapati, R., Pollard, J.W., and Edelmann, W. (2000). MutS homolog 4 localization to meiotic chromosomes is required for chromosome pairing during meiosis in male and female mice. Genes Dev *14*, 1085-1097.

Kobayashi, J., Tauchi, H., Sakamoto, S., Nakamura, A., Morishima, K., Matsuura, S., Kobayashi, T., Tamai, K., Tanimoto, K., and Komatsu, K. (2002). NBS1 localizes to gamma-H2AX foci through interaction with the FHA/BRCT domain. Curr Biol *12*, 1846-1851.

Kohl, K.P., and Sekelsky, J. (2013). Meiotic and mitotic recombination in meiosis. Genetics *194*, 327-334.

Kolodkin, A.L., Klar, A.J., and Stahl, F.W. (1986). Double-strand breaks can initiate meiotic recombination in S. cerevisiae. Cell *46*, 733-740.

Kosugi, S., Hasebe, M., Tomita, M., and Yanagawa, H. (2009). Systematic identification of cell cycle-dependent yeast nucleocytoplasmic shuttling proteins by prediction of composite motifs. Proc Natl Acad Sci U S A *106*, 10171-10176.

Kotnis, A., Du, L., Liu, C., Popov, S.W., and Pan-Hammarstrom, Q. (2009). Non-homologous end joining in class switch recombination: the beginning of the end. Philosophical transactions of the Royal Society of London Series B, Biological sciences *364*, 653-665.

Kousholt, A.N., Fugger, K., Hoffmann, S., Larsen, B.D., Menzel, T., Sartori, A.A., and Sorensen, C.S. (2012). CtIP-dependent DNA resection is required for DNA damage checkpoint maintenance but not initiation. The Journal of cell biology *197*, 869-876.

Kowalczykowski, S.C. (2015). An Overview of the Molecular Mechanisms of Recombinational DNA Repair. Cold Spring Harb Perspect Biol *7*.

Kragelund, B.B., Weterings, E., Hartmann-Petersen, R., and Keijzers, G. (2016). The Ku70/80 ring in Non-Homologous End-Joining: easy to slip on, hard to remove. Front Biosci (Landmark Ed) *21*, 514-527.

Krejci, L., Altmannova, V., Spirek, M., and Zhao, X. (2012). Homologous recombination and its regulation. Nucleic Acids Res *40*, 5795-5818.

Krogh, B.O., Llorente, B., Lam, A., and Symington, L.S. (2005). Mutations in Mre11 phosphoesterase motif I that impair Saccharomyces cerevisiae Mre11-Rad50-Xrs2 complex stability in addition to nuclease activity. Genetics *171*, 1561-1570.

Krokan, H.E., and Bjoras, M. (2013). Base excision repair. Cold Spring Harb Perspect Biol *5*, a012583.

Kusumoto, R., Dawut, L., Marchetti, C., Wan Lee, J., Vindigni, A., Ramsden, D., and Bohr, V.A. (2008). Werner protein cooperates with the XRCC4-DNA ligase IV complex in end-processing. Biochemistry *47*, 7548-7556.

Lafrance-Vanasse, J., Williams, G.J., and Tainer, J.A. (2015). Envisioning the dynamics and flexibility of Mre11-Rad50-Nbs1 complex to decipher its roles in DNA replication and repair. Progress in biophysics and molecular biology *117*, 182-193.

Lamarche, B.J., Orazio, N.I., and Weitzman, M.D. (2010). The MRN complex in double-strand break repair and telomere maintenance. FEBS letters *584*, 3682-3695.

Lammens, K., Bemeleit, D.J., Mockel, C., Clausing, E., Schele, A., Hartung, S., Schiller, C.B., Lucas, M., Angermuller, C., Soding, J.*, et al.* (2011). The Mre11:Rad50 structure shows an ATP-dependent molecular clamp in DNA double-strand break repair. Cell *145*, 54-66.

Langerak, P., Mejia-Ramirez, E., Limbo, O., and Russell, P. (2011). Release of Ku and MRN from DNA ends by Mre11 nuclease activity and Ctp1 is required for homologous recombination repair of double-strand breaks. PLoS Genet *7*, e1002271.

Lao, J.P., Cloud, V., Huang, C.C., Grubb, J., Thacker, D., Lee, C.Y., Dresser, M.E., Hunter, N., and Bishop, D.K. (2013). Meiotic crossover control by concerted action of Rad51-Dmc1 in homolog template bias and robust homeostatic regulation. PLoS Genet *9*, e1003978.

Lao, J.P., and Hunter, N. (2010). Trying to avoid your sister. PLoS biology *8*, e1000519.

Lee, K.Y., Im, J.S., Shibata, E., Park, J., Handa, N., Kowalczykowski, S.C., and Dutta, A. (2015). MCM8-9 complex promotes resection of double-strand break ends by MRE11-RAD50-NBS1 complex. Nat Commun *6*, 7744.

Lee-Theilen, M., Matthews, A.J., Kelly, D., Zheng, S., and Chaudhuri, J. (2011). CtIP promotes microhomology-mediated alternative end joining during class-switch recombination. Nat Struct Mol Biol *18*, 75-79.

Lengsfeld, B.M., Rattray, A.J., Bhaskara, V., Ghirlando, R., and Paull, T.T. (2007). Sae2 is an endonuclease that processes hairpin DNA cooperatively with the Mre11/Rad50/Xrs2 complex. Mol Cell *28*, 638-651.

Li, H., Vogel, H., Holcomb, V.B., Gu, Y., and Hasty, P. (2007). Deletion of Ku70, Ku80, or both causes early aging without substantially increased cancer. Mol Cell Biol *27*, 8205-8214.

Li, L., Elledge, S.J., Peterson, C.A., Bales, E.S., and Legerski, R.J. (1994). Specific association between the human DNA repair proteins XPA and ERCC1. Proc Natl Acad Sci U S A *91*, 5012-5016.

Li, S., Ting, N.S., Zheng, L., Chen, P.L., Ziv, Y., Shiloh, Y., Lee, E.Y., and Lee, W.H. (2000). Functional link of BRCA1 and ataxia telangiectasia gene product in DNA damage response. Nature *406*, 210-215.

Li, W., and Wang, J.C. (1998). Mammalian DNA topoisomerase IIIalpha is essential in early embryogenesis. Proc Natl Acad Sci U S A *95*, 1010-1013.

Li, X., Stith, C.M., Burgers, P.M., and Heyer, W.D. (2009). PCNA is required for initiation of recombination-associated DNA synthesis by DNA polymerase delta. Mol Cell *36*, 704-713.

Lieber, M.R. (2008). The mechanism of human nonhomologous DNA end joining. J Biol Chem *283*, 1-5.

Lieber, M.R. (2010). The mechanism of double-strand DNA break repair by the nonhomologous DNA end-joining pathway. Annu Rev Biochem *79*, 181-211.

Lieber, M.R., Gu, J., Lu, H., Shimazaki, N., and Tsai, A.G. (2010). Nonhomologous DNA end joining (NHEJ) and chromosomal translocations in humans. Subcell Biochem *50*, 279-296.

Lim, C.T., Lai, P.J., Leach, D.R., Maki, H., and Furukohri, A. (2015). A novel mode of nuclease action is revealed by the bacterial Mre11/Rad50 complex. Nucleic Acids Res *43*, 9804-9816.

Lim, D.S., and Hasty, P. (1996). A mutation in mouse rad51 results in an early embryonic lethal that is suppressed by a mutation in p53. Mol Cell Biol *16*, 7133-7143.

Lim, D.S., Kim, S.T., Xu, B., Maser, R.S., Lin, J., Petrini, J.H., and Kastan, M.B. (2000). ATM phosphorylates p95/nbs1 in an S-phase checkpoint pathway. Nature *404*, 613-617.

Lim, H.S., Kim, J.S., Park, Y.B., Gwon, G.H., and Cho, Y. (2011). Crystal structure of the Mre11-Rad50-ATPgammaS complex: understanding the interplay between Mre11 and Rad50. Genes Dev *25*, 1091-1104.

Lindahl, T. (1993). Instability and decay of the primary structure of DNA. Nature *362*, 709-715.

Lindahl, T., and Nyberg, B. (1972). Rate of depurination of native deoxyribonucleic acid. Biochemistry *11*, 3610-3618.

Lipkin, S.M., Moens, P.B., Wang, V., Lenzi, M., Shanmugarajah, D., Gilgeous, A., Thomas, J., Cheng, J., Touchman, J.W., Green, E.D.*, et al.* (2002). Meiotic arrest and aneuploidy in MLH3-deficient mice. Nat Genet *31*, 385-390.

Lisby, M., Barlow, J.H., Burgess, R.C., and Rothstein, R. (2004). Choreography of the DNA damage response: spatiotemporal relationships among checkpoint and repair proteins. Cell *118*, 699-713.

Liu, C., Pouliot, J.J., and Nash, H.A. (2002). Repair of topoisomerase I covalent complexes in the absence of the tyrosyl-DNA phosphodiesterase Tdp1. Proc Natl Acad Sci U S A *99*, 14970-14975.

Liu, L.F., Desai, S.D., Li, T.K., Mao, Y., Sun, M., and Sim, S.P. (2000). Mechanism of action of camptothecin. Annals of the New York Academy of Sciences *922*, 1-10.

Liu, Y., Reeves, D., Kropachev, K., Cai, Y., Ding, S., Kolbanovskiy, M., Kolbanovskiy, A., Bolton, J.L., Broyde, S., Van Houten, B.*, et al.* (2011). Probing for DNA damage with beta-hairpins: similarities in incision efficiencies of bulky DNA adducts by prokaryotic and human nucleotide excision repair systems in vitro. DNA Repair (Amst) *10*, 684-696.

Llorente, B., and Symington, L.S. (2004). The Mre11 nuclease is not required for 5' to 3' resection at multiple HO-induced double-strand breaks. Mol Cell Biol *24*, 9682-9694.

Lloyd, J., Chapman, J.R., Clapperton, J.A., Haire, L.F., Hartsuiker, E., Li, J., Carr, A.M., Jackson, S.P., and Smerdon, S.J. (2009). A supramodular FHA/BRCT-repeat architecture mediates Nbs1 adaptor function in response to DNA damage. Cell *139*, 100-111.

Lobachev, K.S., Gordenin, D.A., and Resnick, M.A. (2002). The Mre11 complex is required for repair of hairpin-capped double-strand breaks and prevention of chromosome rearrangements. Cell *108*, 183-193.

Loeb, L.A., and Monnat, R.J., Jr. (2008). DNA polymerases and human disease. Nat Rev Genet *9*, 594-604.

Lomax, M.E., Folkes, L.K., and O'Neill, P. (2013). Biological consequences of radiation-induced DNA damage: relevance to radiotherapy. Clin Oncol (R Coll Radiol) *25*, 578-585.

Lu, H., Pannicke, U., Schwarz, K., and Lieber, M.R. (2007). Length-dependent binding of human XLF to DNA and stimulation of XRCC4.DNA ligase IV activity. J Biol Chem *282*, 11155-11162.

Lu, H., Shamanna4, R.A., Keijzers, G., Anand, R., Rasmussen, L.J., Cejka, P., Croteau, D.L., and Bohr, V.A. (2016). RECQL4 Promotes DNA End Resection in Repair of DNA Double-Strand Breaks. Cell Rep *In press*.

Lynn, A., Soucek, R., and Borner, G.V. (2007). ZMM proteins during meiosis: crossover artists at work. Chromosome research : an international journal on the molecular, supramolecular and evolutionary aspects of chromosome biology *15*, 591-605.

Ma, Y., Lu, H., Tippin, B., Goodman, M.F., Shimazaki, N., Koiwai, O., Hsieh, C.L., Schwarz, K., and Lieber, M.R. (2004). A biochemically defined system for mammalian nonhomologous DNA end joining. Mol Cell *16*, 701-713.

Ma, Y., Pannicke, U., Schwarz, K., and Lieber, M.R. (2002). Hairpin opening and overhang processing by an Artemis/DNA-dependent protein kinase complex in nonhomologous end joining and V(D)J recombination. Cell *108*, 781-794.

Maftahi, M., Han, C.S., Langston, L.D., Hope, J.C., Zigouras, N., and Freyer, G.A. (1999). The top3(+) gene is essential in Schizosaccharomyces pombe and the lethality associated with its loss is caused by Rad12 helicase activity. Nucleic Acids Res *27*, 4715-4724.

Mahadevaiah, S.K., Turner, J.M., Baudat, F., Rogakou, E.P., de Boer, P., Blanco-Rodriguez, J., Jasin, M., Keeney, S., Bonner, W.M., and Burgoyne, P.S. (2001). Recombinational DNA double-strand breaks in mice precede synapsis. Nat Genet *27*, 271-276.

Mailand, N., Bekker-Jensen, S., Faustrup, H., Melander, F., Bartek, J., Lukas, C., and Lukas, J. (2007). RNF8 ubiquitylates histones at DNA double-strand breaks and promotes assembly of repair proteins. Cell *131*, 887-900.

Makharashvili, N., Tubbs, A.T., Yang, S.H., Wang, H., Barton, O., Zhou, Y., Deshpande, R.A., Lee, J.H., Lobrich, M., Sleckman, B.P.*, et al.* (2014). Catalytic and noncatalytic roles of the CtIP endonuclease in double-strand break end resection. Mol Cell *54*, 1022-1033.

Malkova, A., Klein, F., Leung, W.Y., and Haber, J.E. (2000). HO endonuclease-induced recombination in yeast meiosis resembles Spo11-induced events. Proc Natl Acad Sci U S A *97*, 14500-14505.

Maloisel, L., Fabre, F., and Gangloff, S. (2008). DNA polymerase delta is preferentially recruited during homologous recombination to promote heteroduplex DNA extension. Mol Cell Biol *28*, 1373-1382.

Malu, S., Malshetty, V., Francis, D., and Cortes, P. (2012). Role of non-homologous end joining in V(D)J recombination. Immunol Res *54*, 233-246.

Mancera, E., Bourgon, R., Brozzi, A., Huber, W., and Steinmetz, L.M. (2008). High-resolution mapping of meiotic crossovers and non-crossovers in yeast. Nature *454*, 479-485.

Manfrini, N., Guerini, I., Citterio, A., Lucchini, G., and Longhese, M.P. (2010). Processing of meiotic DNA double strand breaks requires cyclin-dependent kinase and multiple nucleases. J Biol Chem *285*, 11628-11637.

Mao, Z., Bozzella, M., Seluanov, A., and Gorbunova, V. (2008). DNA repair by nonhomologous end joining and homologous recombination during cell cycle in human cells. Cell cycle *7*, 2902-2906.

Mari, P.O., Florea, B.I., Persengiev, S.P., Verkaik, N.S., Bruggenwirth, H.T., Modesti, M., Giglia-Mari, G., Bezstarosti, K., Demmers, J.A., Luider, T.M.*, et al.* (2006). Dynamic assembly of end-joining complexes requires interaction between Ku70/80 and XRCC4. Proc Natl Acad Sci U S A *103*, 18597-18602.

Martini, E., Diaz, R.L., Hunter, N., and Keeney, S. (2006). Crossover homeostasis in yeast meiosis. Cell *126*, 285-295.

Mathiasen, D.P., and Lisby, M. (2014). Cell cycle regulation of homologous recombination in Saccharomyces cerevisiae. FEMS microbiology reviews *38*, 172-184.

Matos, J., Blanco, M.G., Maslen, S., Skehel, J.M., and West, S.C. (2011). Regulatory control of the resolution of DNA recombination intermediates during meiosis and mitosis. Cell *147*, 158-172.

Matos, J., Blanco, M.G., and West, S.C. (2013). Cell-cycle kinases coordinate the resolution of recombination intermediates with chromosome segregation. Cell Rep *4*, 76-86.

Matos, J., and West, S.C. (2014). Holliday junction resolution: regulation in space and time. DNA Repair (Amst) *19*, 176-181.

McKinnon, P.J., and Caldecott, K.W. (2007). DNA strand break repair and human genetic disease. Annu Rev Genomics Hum Genet *8*, 37-55.

McMahill, M.S., Sham, C.W., and Bishop, D.K. (2007). Synthesis-dependent strand annealing in meiosis. PLoS biology *5*, e299.

Mehrotra, S., and McKim, K.S. (2006). Temporal analysis of meiotic DNA double-strand break formation and repair in Drosophila females. PLoS Genet *2*, e200.

Mehta, A., and Haber, J.E. (2014). Sources of DNA double-strand breaks and models of recombinational DNA repair. Cold Spring Harb Perspect Biol *6*, a016428.

Meneely, P.M., Farago, A.F., and Kauffman, T.M. (2002). Crossover distribution and high interference for both the X chromosome and an autosome during

oogenesis and spermatogenesis in Caenorhabditis elegans. Genetics *162*, 1169-1177.

Milman, N., Higuchi, E., and Smith, G.R. (2009). Meiotic DNA double-strand break repair requires two nucleases, MRN and Ctp1, to produce a single size class of Rec12 (Spo11)-oligonucleotide complexes. Molecular and cellular biology *29*, 5998-6005.

Mimitou, E.P., and Symington, L.S. (2008). Sae2, Exo1 and Sgs1 collaborate in DNA double-strand break processing. Nature *455*, 770-774.

Mimitou, E.P., and Symington, L.S. (2009). DNA end resection: many nucleases make light work. DNA repair *8*, 983-995.

Mimitou, E.P., and Symington, L.S. (2010). Ku prevents Exo1 and Sgs1-dependent resection of DNA ends in the absence of a functional MRX complex or Sae2. The EMBO journal *29*, 3358-3369.

Missura, M., Buterin, T., Hindges, R., Hubscher, U., Kasparkova, J., Brabec, V., and Naegeli, H. (2001). Double-check probing of DNA bending and unwinding by XPA-RPA: an architectural function in DNA repair. Embo J *20*, 3554-3564.

Mladenov, E., Magin, S., Soni, A., and Iliakis, G. (2016). DNA double-strand-break repair in higher eukaryotes and its role in genomic instability and cancer: Cell cycle and proliferation-dependent regulation. Semin Cancer Biol *37-38*, 51-64.

Moens, P.B., Kolas, N.K., Tarsounas, M., Marcon, E., Cohen, P.E., and Spyropoulos, B. (2002). The time course and chromosomal localization of recombination-related proteins at meiosis in the mouse are compatible with models that can resolve the early DNA-DNA interactions without reciprocal recombination. Journal of cell science *115*, 1611-1622.

Mol, C.D., Hosfield, D.J., and Tainer, J.A. (2000). Abasic site recognition by two apurinic/apyrimidinic endonuclease families in DNA base excision repair: the 3' ends justify the means. Mutation research *460*, 211-229.

Moreau, S., Ferguson, J.R., and Symington, L.S. (1999). The nuclease activity of Mre11 is required for meiosis but not for mating type switching, end joining, or telomere maintenance. Molecular and cellular biology *19*, 556-566.

Moreau, S., Morgan, E.A., and Symington, L.S. (2001). Overlapping functions of the Saccharomyces cerevisiae Mre11, Exo1 and Rad27 nucleases in DNA metabolism. Genetics *159*, 1423-1433.

Moreno-Herrero, F., de Jager, M., Dekker, N.H., Kanaar, R., Wyman, C., and Dekker, C. (2005). Mesoscale conformational changes in the DNA-repair complex Rad50/Mre11/Nbs1 upon binding DNA. Nature *437*, 440-443.

Moser, J., Kool, H., Giakzidis, I., Caldecott, K., Mullenders, L.H., and Fousteri, M.I. (2007). Sealing of chromosomal DNA nicks during nucleotide excision repair

requires XRCC1 and DNA ligase III alpha in a cell-cycle-specific manner. Mol Cell *27*, 311-323.

Moynahan, M.E., and Jasin, M. (2010). Mitotic homologous recombination maintains genomic stability and suppresses tumorigenesis. Nat Rev Mol Cell Biol *11*, 196-207.

Mullen, J.R., Kaliraman, V., Ibrahim, S.S., and Brill, S.J. (2001). Requirement for three novel protein complexes in the absence of the Sgs1 DNA helicase in Saccharomyces cerevisiae. Genetics *157*, 103-118.

Mullen, J.R., Nallaseth, F.S., Lan, Y.Q., Slagle, C.E., and Brill, S.J. (2005). Yeast Rmi1/Nce4 controls genome stability as a subunit of the Sgs1-Top3 complex. Mol Cell Biol *25*, 4476-4487.

Munz, P. (1994). An analysis of interference in the fission yeast Schizosaccharomyces pombe. Genetics *137*, 701-707.

Murakami, H., and Keeney, S. (2008). Regulating the formation of DNA double-strand breaks in meiosis. Genes Dev *22*, 286-292.

Myung, K., Datta, A., Chen, C., and Kolodner, R.D. (2001). SGS1, the Saccharomyces cerevisiae homologue of BLM and WRN, suppresses genome instability and homeologous recombination. Nat Genet *27*, 113-116.

Myung, K., and Kolodner, R.D. (2002). Suppression of genome instability by redundant S-phase checkpoint pathways in Saccharomyces cerevisiae. Proc Natl Acad Sci U S A *99*, 4500-4507.

Nairz, K., and Klein, F. (1997). mre11S--a yeast mutation that blocks double-strand-break processing and permits nonhomologous synapsis in meiosis. Genes & development *11*, 2272-2290.

Nakada, D., Matsumoto, K., and Sugimoto, K. (2003). ATM-related Tel1 associates with double-strand breaks through an Xrs2-dependent mechanism. Genes & development *17*, 1957-1962.

Nakamura, K., Kogame, T., Oshiumi, H., Shinohara, A., Sumitomo, Y., Agama, K., Pommier, Y., Tsutsui, K.M., Tsutsui, K., Hartsuiker, E.*, et al.* (2010). Collaborative action of Brca1 and CtIP in elimination of covalent modifications from double-strand breaks to facilitate subsequent break repair. PLoS Genet *6*, e1000828.

Neale, M.J., Pan, J., and Keeney, S. (2005). Endonucleolytic processing of covalent protein-linked DNA double-strand breaks. Nature *436*, 1053-1057.

Nelms, B.E., Maser, R.S., MacKay, J.F., Lagally, M.G., and Petrini, J.H. (1998). In situ visualization of DNA double-strand break repair in human fibroblasts. Science *280*, 590-592.

Nick McElhinny, S.A., Havener, J.M., Garcia-Diaz, M., Juarez, R., Bebenek, K., Kee, B.L., Blanco, L., Kunkel, T.A., and Ramsden, D.A. (2005). A gradient of template

dependence defines distinct biological roles for family X polymerases in nonhomologous end joining. Mol Cell *19*, 357-366.

Nick McElhinny, S.A., Snowden, C.M., McCarville, J., and Ramsden, D.A. (2000). Ku recruits the XRCC4-ligase IV complex to DNA ends. Mol Cell Biol *20*, 2996-3003.

Nickoloff, J.A., and Brenneman, M.A. (2004). Analysis of recombinational repair of DNA double-strand breaks in mammalian cells with I-SceI nuclease. Methods Mol Biol *262*, 35-52.

Nicolette, M.L., Lee, K., Guo, Z., Rani, M., Chow, J.M., Lee, S.E., and Paull, T.T. (2010a). Mre11-Rad50-Xrs2 and Sae2 promote 5' strand resection of DNA double-strand breaks. Nat Struct Mol Biol *17*, 1478-1485.

Nicolette, M.L., Lee, K., Guo, Z., Rani, M., Chow, J.M., Lee, S.E., and Paull, T.T. (2010b). Mre11-Rad50-Xrs2 and Sae2 promote 5' strand resection of DNA double-strand breaks. Nat Struct Mol Biol *17*, 1478-1485.

Nimonkar, A.V., Genschel, J., Kinoshita, E., Polaczek, P., Campbell, J.L., Wyman, C., Modrich, P., and Kowalczykowski, S.C. (2011). BLM-DNA2-RPA-MRN and EXO1-BLM-RPA-MRN constitute two DNA end resection machineries for human DNA break repair. Genes Dev *25*, 350-362.

Nimonkar, A.V., Ozsoy, A.Z., Genschel, J., Modrich, P., and Kowalczykowski, S.C. (2008). Human exonuclease 1 and BLM helicase interact to resect DNA and initiate DNA repair. Proceedings of the National Academy of Sciences of the United States of America *105*, 16906-16911.

Nishant, K.T., Plys, A.J., and Alani, E. (2008). A mutation in the putative MLH3 endonuclease domain confers a defect in both mismatch repair and meiosis in Saccharomyces cerevisiae. Genetics *179*, 747-755.

Niu, H., Chung, W.H., Zhu, Z., Kwon, Y., Zhao, W., Chi, P., Prakash, R., Seong, C., Liu, D., Lu, L.*, et al.* (2010). Mechanism of the ATP-dependent DNA end-resection machinery from Saccharomyces cerevisiae. Nature *467*, 108-111.

Nocentini, S., Coin, F., Saijo, M., Tanaka, K., and Egly, J.M. (1997). DNA damage recognition by XPA protein promotes efficient recruitment of transcription factor II H. J Biol Chem *272*, 22991-22994.

Nussenzweig, A., Chen, C., da Costa Soares, V., Sanchez, M., Sokol, K., Nussenzweig, M.C., and Li, G.C. (1996). Requirement for Ku80 in growth and immunoglobulin V(D)J recombination. Nature *382*, 551-555.

O'Driscoll, M. (2012). Diseases associated with defective responses to DNA damage. Cold Spring Harb Perspect Biol *4*.

Ogi, T., and Lehmann, A.R. (2006). The Y-family DNA polymerase kappa (pol kappa) functions in mammalian nucleotide-excision repair. Nat Cell Biol *8*, 640-642.

Oh, S.D., Lao, J.P., Hwang, P.Y., Taylor, A.F., Smith, G.R., and Hunter, N. (2007). BLM ortholog, Sgs1, prevents aberrant crossing-over by suppressing formation of multichromatid joint molecules. Cell *130*, 259-272.

Oh, S.D., Lao, J.P., Taylor, A.F., Smith, G.R., and Hunter, N. (2008). RecQ helicase, Sgs1, and XPF family endonuclease, Mus81-Mms4, resolve aberrant joint molecules during meiotic recombination. Mol Cell *31*, 324-336.

Oliver-Bonet, M., Turek, P.J., Sun, F., Ko, E., and Martin, R.H. (2005). Temporal progression of recombination in human males. Mol Hum Reprod *11*, 517-522.

Onoda, F., Seki, M., Miyajima, A., and Enomoto, T. (2000). Elevation of sister chromatid exchange in Saccharomyces cerevisiae sgs1 disruptants and the relevance of the disruptants as a system to evaluate mutations in Bloom's syndrome gene. Mutation research *459*, 203-209.

Orthwein, A., Noordermeer, S.M., Wilson, M.D., Landry, S., Enchev, R.I., Sherker, A., Munro, M., Pinder, J., Salsman, J., Dellaire, G.*, et al.* (2015). A mechanism for the suppression of homologous recombination in G1 cells. Nature *528*, 422-426.

Palmbos, P.L., Wu, D., Daley, J.M., and Wilson, T.E. (2008). Recruitment of Saccharomyces cerevisiae Dnl4-Lif1 complex to a double-strand break requires interactions with Yku80 and the Xrs2 FHA domain. Genetics *180*, 1809-1819.

Pannunzio, N.R., Manthey, G.M., and Bailis, A.M. (2010). RAD59 and RAD1 cooperate in translocation formation by single-strand annealing in Saccharomyces cerevisiae. Current genetics *56*, 87-100.

Paques, F., and Haber, J.E. (1999). Multiple pathways of recombination induced by double-strand breaks in Saccharomyces cerevisiae. Microbiol Mol Biol Rev *63*, 349-404.

Park, C.H., Mu, D., Reardon, J.T., and Sancar, A. (1995). The general transcription-repair factor TFIIH is recruited to the excision repair complex by the XPA protein independent of the TFIIE transcription factor. J Biol Chem *270*, 4896-4902.

Paull, T.T. (2010). Making the best of the loose ends: Mre11/Rad50 complexes and Sae2 promote DNA double-strand break resection. DNA Repair (Amst) *9*, 1283-1291.

Paull, T.T., and Gellert, M. (1998). The 3' to 5' exonuclease activity of Mre 11 facilitates repair of DNA double-strand breaks. Mol Cell *1*, 969-979.

Paull, T.T., and Gellert, M. (1999). Nbs1 potentiates ATP-driven DNA unwinding and endonuclease cleavage by the Mre11/Rad50 complex. Genes Dev *13*, 1276-1288.

Pecina, A., Smith, K.N., Mezard, C., Murakami, H., Ohta, K., and Nicolas, A. (2002). Targeted stimulation of meiotic recombination. Cell *111*, 173-184.

Persky, N.S., and Lovett, S.T. (2008). Mechanisms of recombination: lessons from E. coli. Crit Rev Biochem Mol Biol *43*, 347-370.

Plank, J.L., Chu, S.H., Pohlhaus, J.R., Wilson-Sali, T., and Hsieh, T.S. (2005). Drosophila melanogaster topoisomerase IIIalpha preferentially relaxes a positively or negatively supercoiled bubble substrate and is essential during development. J Biol Chem *280*, 3564-3573.

Plank, J.L., Wu, J., and Hsieh, T.S. (2006). Topoisomerase IIIalpha and Bloom's helicase can resolve a mobile double Holliday junction substrate through convergent branch migration. Proc Natl Acad Sci U S A *103*, 11118-11123.

Polato, F., Callen, E., Wong, N., Faryabi, R., Bunting, S., Chen, H.T., Kozak, M., Kruhlak, M.J., Reczek, C.R., Lee, W.H*., et al.* (2014). CtIP-mediated resection is essential for viability and can operate independently of BRCA1. The Journal of experimental medicine *211*, 1027-1036.

Pomerantz, R.T., Kurth, I., Goodman, M.F., and O'Donnell, M.E. (2013). Preferential D-loop extension by a translesion DNA polymerase underlies error-prone recombination. Nat Struct Mol Biol *20*, 748-755.

Pouliot, J.J., Yao, K.C., Robertson, C.A., and Nash, H.A. (1999). Yeast gene for a Tyr-DNA phosphodiesterase that repairs topoisomerase I complexes. Science *286*, 552-555.

Povirk, L.F., Zhou, T., Zhou, R., Cowan, M.J., and Yannone, S.M. (2007). Processing of 3'-phosphoglycolate-terminated DNA double strand breaks by Artemis nuclease. J Biol Chem *282*, 3547-3558.

Prakash, R., Zhang, Y., Feng, W., and Jasin, M. (2015). Homologous recombination and human health: the roles of BRCA1, BRCA2, and associated proteins. Cold Spring Harb Perspect Biol *7*, a016600.

Pray, L. (2008). DNA Replication and Causes of Mutation. Nature Education

Quennet, V., Beucher, A., Barton, O., Takeda, S., and Lobrich, M. (2011). CtIP and MRN promote non-homologous end-joining of etoposide-induced DNA double-strand breaks in G1. Nucleic Acids Res *39*, 2144-2152.

Ramadan, K., Shevelev, I.V., Maga, G., and Hubscher, U. (2004). De novo DNA synthesis by human DNA polymerase lambda, DNA polymerase mu and terminal deoxyribonucleotidyl transferase. J Mol Biol *339*, 395-404.

Ranjha, L., Anand, R., and Cejka, P. (2014). The Saccharomyces cerevisiae Mlh1-Mlh3 heterodimer is an endonuclease that preferentially binds to Holliday junctions. J Biol Chem *289*, 5674-5686.

Rass, E., Grabarz, A., Plo, I., Gautier, J., Bertrand, P., and Lopez, B.S. (2009a). Role of Mre11 in chromosomal nonhomologous end joining in mammalian cells. Nat Struct Mol Biol *16*, 819-824.

Rass, E., Grabarz, A., Plo, I., Gautier, J., Bertrand, P., and Lopez, B.S. (2009b). Role of Mre11 in chromosomal nonhomologous end joining in mammalian cells. Nature structural & molecular biology *16*, 819-824.

Ray Chaudhuri, A., Hashimoto, Y., Herrador, R., Neelsen, K.J., Fachinetti, D., Bermejo, R., Cocito, A., Costanzo, V., and Lopes, M. (2012). Topoisomerase I poisoning results in PARP-mediated replication fork reversal. Nat Struct Mol Biol *19*, 417-423.

Raynard, S., Bussen, W., and Sung, P. (2006). A double Holliday junction dissolvasome comprising BLM, topoisomerase IIIalpha, and BLAP75. J Biol Chem *281*, 13861-13864.

Reardon, J.T., and Sancar, A. (2003). Recognition and repair of the cyclobutane thymine dimer, a major cause of skin cancers, by the human excision nuclease. Genes Dev *17*, 2539-2551.

Renkawitz, J., Lademann, C.A., and Jentsch, S. (2014). Mechanisms and principles of homology search during recombination. Nat Rev Mol Cell Biol *15*, 369-383.

Rich, T., Allen, R.L., and Wyllie, A.H. (2000). Defying death after DNA damage. Nature *407*, 777-783.

Richard, D.J., Savage, K., Bolderson, E., Cubeddu, L., So, S., Ghita, M., Chen, D.J., White, M.F., Richard, K., Prise, K.M.*, et al.* (2011). hSSB1 rapidly binds at the sites of DNA double-strand breaks and is required for the efficient recruitment of the MRN complex. Nucleic Acids Res *39*, 1692-1702.

Riedl, T., Hanaoka, F., and Egly, J.M. (2003). The comings and goings of nucleotide excision repair factors on damaged DNA. Embo J *22*, 5293-5303.

Robert, T., Nore, A., Brun, C., Maffre, C., Crimi, B., Bourbon, H.M., and de Massy, B. (2016). The TopoVIB-Like protein family is required for meiotic DNA double-strand break formation. Science *351*, 943-949.

Robine, N., Uematsu, N., Amiot, F., Gidrol, X., Barillot, E., Nicolas, A., and Borde, V. (2007). Genome-wide redistribution of meiotic double-strand breaks in Saccharomyces cerevisiae. Mol Cell Biol *27*, 1868-1880.

Rocco, V., de Massy, B., and Nicolas, A. (1992). The Saccharomyces cerevisiae ARG4 initiator of meiotic gene conversion and its associated double-strand DNA breaks can be inhibited by transcriptional interference. Proc Natl Acad Sci U S A *89*, 12068-12072.

Rogacheva, M.V., Manhart, C.M., Chen, C., Guarne, A., Surtees, J., and Alani, E. (2014). Mlh1-Mlh3, a meiotic crossover and DNA mismatch repair factor, is a Msh2-Msh3-stimulated endonuclease. J Biol Chem *289*, 5664-5673.

Roots, R., Kraft, G., and Gosschalk, E. (1985). The formation of radiation-induced DNA breaks: the ratio of double-strand breaks to single-strand breaks. International journal of radiation oncology, biology, physics *11*, 259-265.

Rositsa Dueva, G.I. (2013). Alternative pathways of non-homologous end joining (NHEJ) in genomic instability and cancer. Transl Cancer Res *Vol 2*.

Ross-Macdonald, P., and Roeder, G.S. (1994). Mutation of a meiosis-specific MutS homolog decreases crossing over but not mismatch correction. Cell *79*, 1069-1080.

Rothkamm, K., Kruger, I., Thompson, L.H., and Lobrich, M. (2003). Pathways of DNA double-strand break repair during the mammalian cell cycle. Mol Cell Biol *23*, 5706-5715.

Rydberg, B., and Lindahl, T. (1982). Nonenzymatic methylation of DNA by the intracellular methyl group donor S-adenosyl-L-methionine is a potentially mutagenic reaction. Embo J *1*, 211-216.

San Filippo, J., Sung, P., and Klein, H. (2008). Mechanism of eukaryotic homologous recombination. Annu Rev Biochem *77*, 229-257.

Santivasi, W.L., and Xia, F. (2014). Ionizing radiation-induced DNA damage, response, and repair. Antioxid Redox Signal *21*, 251-259.

Santucci-Darmanin, S., Neyton, S., Lespinasse, F., Saunieres, A., Gaudray, P., and Paquis-Flucklinger, V. (2002). The DNA mismatch-repair MLH3 protein interacts with MSH4 in meiotic cells, supporting a role for this MutL homolog in mammalian meiotic recombination. Hum Mol Genet *11*, 1697-1706.

Sarbajna, S., and West, S.C. (2014). Holliday junction processing enzymes as guardians of genome stability. Trends Biochem Sci *39*, 409-419.

Sartori, A.A., Lukas, C., Coates, J., Mistrik, M., Fu, S., Bartek, J., Baer, R., Lukas, J., and Jackson, S.P. (2007). Human CtIP promotes DNA end resection. Nature *450*, 509-514.

Scharer, O.D. (2013). Nucleotide excision repair in eukaryotes. Cold Spring Harb Perspect Biol *5*, a012609.

Scharer, O.D., and Campbell, A.J. (2009). Wedging out DNA damage. Nat Struct Mol Biol *16*, 102-104.

Schiller, C.B., Lammens, K., Guerini, I., Coordes, B., Feldmann, H., Schlauderer, F., Mockel, C., Schele, A., Strasser, K., Jackson, S.P.*, et al.* (2012). Structure of Mre11-Nbs1 complex yields insights into ataxia-telangiectasia-like disease mutations and DNA damage signaling. Nature structural & molecular biology *19*, 693-700.

Schiller, C.B., Seifert, F.U., Linke-Winnebeck, C., and Hopfner, K.P. (2014). Structural studies of DNA end detection and resection in homologous recombination. Cold Spring Harb Perspect Biol *6*, a017962.

Schwacha, A., and Kleckner, N. (1997). Interhomolog bias during meiotic recombination: meiotic functions promote a highly differentiated interhomolog-only pathway. Cell *90*, 1123-1135.

Schwartz, E.K., and Heyer, W.D. (2011). Processing of joint molecule intermediates by structure-selective endonucleases during homologous recombination in eukaryotes. Chromosoma *120*, 109-127.

Sebesta, M., Burkovics, P., Juhasz, S., Zhang, S., Szabo, J.E., Lee, M.Y., Haracska, L., and Krejci, L. (2013). Role of PCNA and TLS polymerases in D-loop extension during homologous recombination in humans. DNA Repair (Amst) *12*, 691-698.

Sfeir, A., and Symington, L.S. (2015). Microhomology-Mediated End Joining: A Back-up Survival Mechanism or Dedicated Pathway? Trends Biochem Sci *40*, 701-714.

Sharma, S., Javadekar, S.M., Pandey, M., Srivastava, M., Kumari, R., and Raghavan, S.C. (2015). Homology and enzymatic requirements of microhomology-dependent alternative end joining. Cell death & disease *6*, e1697.

Sharp, L.W. (1921). An introduction to cytology, 1st edn (New York etc., McGraw-Hill book company, inc.).

Shibata, A., Moiani, D., Arvai, A.S., Perry, J., Harding, S.M., Genois, M.M., Maity, R., van Rossum-Fikkert, S., Kertokalio, A., Romoli, F.*, et al.* (2014). DNA double-strand break repair pathway choice is directed by distinct MRE11 nuclease activities. Mol Cell *53*, 7-18.

Shim, E.Y., Chung, W.H., Nicolette, M.L., Zhang, Y., Davis, M., Zhu, Z., Paull, T.T., Ira, G., and Lee, S.E. (2010). Saccharomyces cerevisiae Mre11/Rad50/Xrs2 and Ku proteins regulate association of Exo1 and Dna2 with DNA breaks. The EMBO journal *29*, 3370-3380.

Shinohara, A., Ogawa, H., and Ogawa, T. (1992). Rad51 protein involved in repair and recombination in S. cerevisiae is a RecA-like protein. Cell *69*, 457-470.

Shinohara, M., Shita-Yamaguchi, E., Buerstedde, J.M., Shinagawa, H., Ogawa, H., and Shinohara, A. (1997). Characterization of the roles of the Saccharomyces cerevisiae RAD54 gene and a homologue of RAD54, RDH54/TID1, in mitosis and meiosis. Genetics *147*, 1545-1556.

Shivji, M.K., Podust, V.N., Hubscher, U., and Wood, R.D. (1995). Nucleotide excision repair DNA synthesis by DNA polymerase epsilon in the presence of PCNA, RFC, and RPA. Biochemistry *34*, 5011-5017.

Shrivastav, M., De Haro, L.P., and Nickoloff, J.A. (2008). Regulation of DNA double-strand break repair pathway choice. Cell research *18*, 134-147.

Sinha, S., Villarreal, D., Shim, E.Y., and Lee, S.E. (2016). Risky business: Microhomology-mediated end joining. Mutation research *788*, 17-24.

Smith, J., Baldeyron, C., De Oliveira, I., Sala-Trepat, M., and Papadopoulo, D. (2001). The influence of DNA double-strand break structure on end-joining in human cells. Nucleic Acids Res *29*, 4783-4792.

Smith, J., Riballo, E., Kysela, B., Baldeyron, C., Manolis, K., Masson, C., Lieber, M.R., Papadopoulo, D., and Jeggo, P. (2003). Impact of DNA ligase IV on the fidelity of end joining in human cells. Nucleic Acids Res *31*, 2157-2167.

Snowden, T., Acharya, S., Butz, C., Berardini, M., and Fishel, R. (2004). hMSH4-hMSH5 recognizes Holliday Junctions and forms a meiosis-specific sliding clamp that embraces homologous chromosomes. Mol Cell *15*, 437-451.

Sobhian, B., Shao, G., Lilli, D.R., Culhane, A.C., Moreau, L.A., Xia, B., Livingston, D.M., and Greenberg, R.A. (2007). RAP80 targets BRCA1 to specific ubiquitin structures at DNA damage sites. Science *316*, 1198-1202.

Spies, M., Bianco, P.R., Dillingham, M.S., Handa, N., Baskin, R.J., and Kowalczykowski, S.C. (2003). A molecular throttle: the recombination hotspot chi controls DNA translocation by the RecBCD helicase. Cell *114*, 647-654.

Spies, M., and Fishel, R. (2015). Mismatch repair during homologous and homeologous recombination. Cold Spring Harb Perspect Biol *7*, a022657.

Stahl, F.W., Foss, H.M., Young, L.S., Borts, R.H., Abdullah, M.F., and Copenhaver, G.P. (2004). Does crossover interference count in Saccharomyces cerevisiae? Genetics *168*, 35-48.

Stark, J.M., and Jasin, M. (2003). Extensive loss of heterozygosity is suppressed during homologous repair of chromosomal breaks. Mol Cell Biol *23*, 733-743.

Stark, J.M., Pierce, A.J., Oh, J., Pastink, A., and Jasin, M. (2004). Genetic steps of mammalian homologous repair with distinct mutagenic consequences. Mol Cell Biol *24*, 9305-9316.

Stavnezer, J., Guikema, J.E., and Schrader, C.E. (2008). Mechanism and regulation of class switch recombination. Annual review of immunology *26*, 261-292.

Stewart, G.S., Maser, R.S., Stankovic, T., Bressan, D.A., Kaplan, M.I., Jaspers, N.G., Raams, A., Byrd, P.J., Petrini, J.H., and Taylor, A.M. (1999). The DNA double-strand break repair gene hMRE11 is mutated in individuals with an ataxia-telangiectasia-like disorder. Cell *99*, 577-587.

Stracker, T.H., and Petrini, J.H. (2011). The MRE11 complex: starting from the ends. Nature reviews Molecular cell biology *12*, 90-103.

Sturzenegger, A., Burdova, K., Kanagaraj, R., Levikova, M., Pinto, C., Cejka, P., and Janscak, P. (2014). DNA2 cooperates with the WRN and BLM RecQ helicases to mediate long-range DNA end resection in human cells. J Biol Chem *289*, 27314-27326.

Sugasawa, K., Ng, J.M., Masutani, C., Iwai, S., van der Spek, P.J., Eker, A.P., Hanaoka, F., Bootsma, D., and Hoeijmakers, J.H. (1998). Xeroderma pigmentosum group C protein complex is the initiator of global genome nucleotide excision repair. Mol Cell *2*, 223-232.

Sugasawa, K., Okamoto, T., Shimizu, Y., Masutani, C., Iwai, S., and Hanaoka, F. (2001). A multistep damage recognition mechanism for global genomic nucleotide excision repair. Genes Dev *15*, 507-521.

Sugasawa, K., Okuda, Y., Saijo, M., Nishi, R., Matsuda, N., Chu, G., Mori, T., Iwai, S., Tanaka, K., and Hanaoka, F. (2005). UV-induced ubiquitylation of XPC protein mediated by UV-DDB-ubiquitin ligase complex. Cell *121*, 387-400.

Sugawara, N., Paques, F., Colaiacovo, M., and Haber, J.E. (1997). Role of Saccharomyces cerevisiae Msh2 and Msh3 repair proteins in double-strand break-induced recombination. Proc Natl Acad Sci U S A *94*, 9214-9219.

Sun, H., Treco, D., and Szostak, J.W. (1991). Extensive 3'-overhanging, single-stranded DNA associated with the meiosis-specific double-strand breaks at the ARG4 recombination initiation site. Cell *64*, 1155-1161.

Suzuki, A., de la Pompa, J.L., Hakem, R., Elia, A., Yoshida, R., Mo, R., Nishina, H., Chuang, T., Wakeham, A., Itie, A.*, et al.* (1997). Brca2 is required for embryonic cellular proliferation in the mouse. Genes Dev *11*, 1242-1252.

Svilar, D., Goellner, E.M., Almeida, K.H., and Sobol, R.W. (2011). Base excision repair and lesion-dependent subpathways for repair of oxidative DNA damage. Antioxid Redox Signal *14*, 2491-2507.

Swuec, P., and Costa, A. (2014). Molecular mechanism of double Holliday junction dissolution. Cell Biosci *4*, 36.

Sym, M., Engebrecht, J.A., and Roeder, G.S. (1993). ZIP1 is a synaptonemal complex protein required for meiotic chromosome synapsis. Cell *72*, 365-378.

Symington, L.S. (2002). Role of RAD52 epistasis group genes in homologous recombination and double-strand break repair. Microbiol Mol Biol Rev *66*, 630-670, table of contents.

Symington, L.S. (2014a). End resection at double-strand breaks: mechanism and regulation. Cold Spring Harb Perspect Biol *6*.

Symington, L.S. (2014b). End resection at double-strand breaks: mechanism and regulation. Cold Spring Harbor perspectives in biology *6*.

Symington, L.S. (2016). Mechanism and regulation of DNA end resection in eukaryotes. Crit Rev Biochem Mol Biol *51*, 195-212.

Symington, L.S., and Gautier, J. (2011). Double-strand break end resection and repair pathway choice. Annual review of genetics *45*, 247-271.

Szakal, B., and Branzei, D. (2013). Premature Cdk1/Cdc5/Mus81 pathway activation induces aberrant replication and deleterious crossover. Embo J *32*, 1155-1167.

Szankasi, P., and Smith, G.R. (1992). A DNA exonuclease induced during meiosis of Schizosaccharomyces pombe. J Biol Chem *267*, 3014-3023.

Szankasi, P., and Smith, G.R. (1995). A role for exonuclease I from S. pombe in mutation avoidance and mismatch correction. Science *267*, 1166-1169.

Szekvolgyi, L., Ohta, K., and Nicolas, A. (2015). Initiation of meiotic homologous recombination: flexibility, impact of histone modifications, and chromatin remodeling. Cold Spring Harb Perspect Biol *7*.

Takata, M., Sasaki, M.S., Sonoda, E., Morrison, C., Hashimoto, M., Utsumi, H., Yamaguchi-Iwai, Y., Shinohara, A., and Takeda, S. (1998). Homologous recombination and non-homologous end-joining pathways of DNA double-strand break repair have overlapping roles in the maintenance of chromosomal integrity in vertebrate cells. Embo J *17*, 5497-5508.

Takeda, S., Hoa, N.N., and Sasanuma, H. (2016). The role of the Mre11-Rad50-Nbs1 complex in double-strand break repair-facts and myths. Journal of radiation research.

Tauchi, H., Kobayashi, J., Morishima, K., Matsuura, S., Nakamura, A., Shiraishi, T., Ito, E., Masnada, D., Delia, D., and Komatsu, K. (2001). The forkhead-associated domain of NBS1 is essential for nuclear foci formation after irradiation but not essential for hRAD50[middle dot]hMRE11[middle dot]NBS1 complex DNA repair activity. J Biol Chem *276*, 12-15.

Tauchi, H., Kobayashi, J., Morishima, K., van Gent, D.C., Shiraishi, T., Verkaik, N.S., vanHeems, D., Ito, E., Nakamura, A., Sonoda, E.*, et al.* (2002a). Nbs1 is essential for DNA repair by homologous recombination in higher vertebrate cells. Nature *420*, 93-98.

Tauchi, H., Matsuura, S., Kobayashi, J., Sakamoto, S., and Komatsu, K. (2002b). Nijmegen breakage syndrome gene, NBS1, and molecular links to factors for genome stability. Oncogene *21*, 8967-8980.

Taylor, A.F., and Smith, G.R. (2003). RecBCD enzyme is a DNA helicase with fast and slow motors of opposite polarity. Nature *423*, 889-893.

Thangavel, S., Berti, M., Levikova, M., Pinto, C., Gomathinayagam, S., Vujanovic, M., Zellweger, R., Moore, H., Lee, E.H., Hendrickson, E.A.*, et al.* (2015). DNA2 drives processing and restart of reversed replication forks in human cells. J Cell Biol *208*, 545-562.

Thiagalingam, S., Laken, S., Willson, J.K., Markowitz, S.D., Kinzler, K.W., Vogelstein, B., and Lengauer, C. (2001). Mechanisms underlying losses of heterozygosity in human colorectal cancers. Proc Natl Acad Sci U S A *98*, 2698-2702.

Tholey, G., Ledig, M., Mandel, P., Sargentini, L., Frivold, A.H., Leroy, M., Grippo, A.A., and Wedler, F.C. (1988). Concentrations of physiologically important metal ions in glial cells cultured from chick cerebral cortex. Neurochem Res *13*, 45-50.

Tomita, K., Matsuura, A., Caspari, T., Carr, A.M., Akamatsu, Y., Iwasaki, H., Mizuno, K., Ohta, K., Uritani, M., Ushimaru, T.*, et al.* (2003). Competition between the Rad50 complex and the Ku heterodimer reveals a role for Exo1 in processing double-strand breaks but not telomeres. Molecular and cellular biology *23*, 5186-5197.

Tomkinson, A.E., Bardwell, A.J., Bardwell, L., Tappe, N.J., and Friedberg, E.C. (1993). Yeast DNA repair and recombination proteins Rad1 and Rad10 constitute a single-stranded-DNA endonuclease. Nature *362*, 860-862.

Tounekti, O., Kenani, A., Foray, N., Orlowski, S., and Mir, L.M. (2001). The ratio of single- to double-strand DNA breaks and their absolute values determine cell death pathway. Br J Cancer *84*, 1272-1279.

Tran, P.T., Erdeniz, N., Symington, L.S., and Liskay, R.M. (2004a). EXO1-A multi-tasking eukaryotic nuclease. DNA repair *3*, 1549-1559.

Tran, P.T., Erdeniz, N., Symington, L.S., and Liskay, R.M. (2004b). EXO1-A multi-tasking eukaryotic nuclease. DNA Repair (Amst) *3*, 1549-1559.

Trujillo, K.M., and Sung, P. (2001). DNA structure-specific nuclease activities in the Saccharomyces cerevisiae Rad50*Mre11 complex. J Biol Chem *276*, 35458-35464.

Trujillo, K.M., Yuan, S.S., Lee, E.Y., and Sung, P. (1998). Nuclease activities in a complex of human recombination and DNA repair factors Rad50, Mre11, and p95. J Biol Chem *273*, 21447-21450.

Tsubouchi, H., and Ogawa, H. (2000). Exo1 roles for repair of DNA double-strand breaks and meiotic crossing over in Saccharomyces cerevisiae. Molecular biology of the cell *11*, 2221-2233.

Tsukamoto, Y., Mitsuoka, C., Terasawa, M., Ogawa, H., and Ogawa, T. (2005). Xrs2p regulates Mre11p translocation to the nucleus and plays a role in telomere elongation and meiotic recombination. Molecular biology of the cell *16*, 597-608.

Tsuzuki, T., Fujii, Y., Sakumi, K., Tominaga, Y., Nakao, K., Sekiguchi, M., Matsushiro, A., Yoshimura, Y., and MoritaT (1996). Targeted disruption of the Rad51 gene leads to lethality in embryonic mice. Proc Natl Acad Sci U S A *93*, 6236-6240.

Tumbale, P., Appel, C.D., Kraehenbuehl, R., Robertson, P.D., Williams, J.S., Krahn, J., Ahel, I., and Williams, R.S. (2011). Structure of an aprataxin-DNA complex with insights into AOA1 neurodegenerative disease. Nat Struct Mol Biol *18*, 1189-1195.

Uematsu, N., Weterings, E., Yano, K., Morotomi-Yano, K., Jakob, B., Taucher-Scholz, G., Mari, P.O., van Gent, D.C., Chen, B.P., and Chen, D.J. (2007). Autophosphorylation of DNA-PKCS regulates its dynamics at DNA double-strand breaks. J Cell Biol *177*, 219-229.

Usui, T., Ohta, T., Oshiumi, H., Tomizawa, J., Ogawa, H., and Ogawa, T. (1998). Complex formation and functional versatility of Mre11 of budding yeast in recombination. Cell *95*, 705-716.

Uziel, T., Lerenthal, Y., Moyal, L., Andegeko, Y., Mittelman, L., and Shiloh, Y. (2003). Requirement of the MRN complex for ATM activation by DNA damage. Embo J *22*, 5612-5621.

Vermeulen, W., and Fousteri, M. (2013). Mammalian transcription-coupled excision repair. Cold Spring Harb Perspect Biol *5*, a012625.

Volker, M., Mone, M.J., Karmakar, P., van Hoffen, A., Schul, W., Vermeulen, W., Hoeijmakers, J.H., van Driel, R., van Zeeland, A.A., and Mullenders, L.H. (2001). Sequential assembly of the nucleotide excision repair factors in vivo. Mol Cell *8*, 213-224.

Wakasugi, M., Kasashima, H., Fukase, Y., Imura, M., Imai, R., Yamada, S., Cleaver, J.E., and Matsunaga, T. (2009). Physical and functional interaction between DDB and XPA in nucleotide excision repair. Nucleic Acids Res *37*, 516-525.

Walles, S.A., Zhou, R., and Liliemark, E. (1996). DNA damage induced by etoposide; a comparison of two different methods for determination of strand breaks in DNA. Cancer letters *105*, 153-159.

Wang, B., Matsuoka, S., Ballif, B.A., Zhang, D., Smogorzewska, A., Gygi, S.P., and Elledge, S.J. (2007). Abraxas and RAP80 form a BRCA1 protein complex required for the DNA damage response. Science *316*, 1194-1198.

Wang, H., Li, Y., Truong, L.N., Shi, L.Z., Hwang, P.Y., He, J., Do, J., Cho, M.J., Li, H., Negrete, A.*, et al.* (2014). CtIP maintains stability at common fragile sites and inverted repeats by end resection-independent endonuclease activity. Mol Cell *54*, 1012-1021.

Wang, H., Shao, Z., Shi, L.Z., Hwang, P.Y., Truong, L.N., Berns, M.W., Chen, D.J., and Wu, X. (2012). CtIP protein dimerization is critical for its recruitment to chromosomal DNA double-stranded breaks. J Biol Chem *287*, 21471-21480.

Wang, H., Shi, L.Z., Wong, C.C., Han, X., Hwang, P.Y., Truong, L.N., Zhu, Q., Shao, Z., Chen, D.J., Berns, M.W.*, et al.* (2013a). The interaction of CtIP and Nbs1 connects CDK and ATM to regulate HR-mediated double-strand break repair. PLoS genetics *9*, e1003277.

Wang, H., Shi, L.Z., Wong, C.C., Han, X., Hwang, P.Y., Truong, L.N., Zhu, Q., Shao, Z., Chen, D.J., Berns, M.W.*, et al.* (2013b). The interaction of CtIP and Nbs1 connects CDK and ATM to regulate HR-mediated double-strand break repair. PLoS Genet *9*, e1003277.

Wang, J., Chen, R., and Julin, D.A. (2000). A single nuclease active site of the Escherichia coli RecBCD enzyme catalyzes single-stranded DNA degradation in both directions. J Biol Chem *275*, 507-513.

Wang, J.C. (2002). Cellular roles of DNA topoisomerases: a molecular perspective. Nat Rev Mol Cell Biol *3*, 430-440.

Wang, M., Wu, W., Rosidi, B., Zhang, L., Wang, H., and Iliakis, G. (2006). PARP-1 and Ku compete for repair of DNA double strand breaks by distinct NHEJ pathways. Nucleic Acids Res *34*, 6170-6182.

Wang, T.F., Kleckner, N., and Hunter, N. (1999). Functional specificity of MutL homologs in yeast: evidence for three Mlh1-based heterocomplexes with distinct roles during meiosis in recombination and mismatch correction. Proc Natl Acad Sci U S A *96*, 13914-13919.

Wang, X., and Haber, J.E. (2004). Role of Saccharomyces single-stranded DNA-binding protein RPA in the strand invasion step of double-strand break repair. PLoS biology *2*, E21.

Watt, P.M., Hickson, I.D., Borts, R.H., and Louis, E.J. (1996). SGS1, a homologue of the Bloom's and Werner's syndrome genes, is required for maintenance of genome stability in Saccharomyces cerevisiae. Genetics *144*, 935-945.

Weterings, E., and van Gent, D.C. (2004). The mechanism of non-homologous end-joining: a synopsis of synapsis. DNA Repair (Amst) *3*, 1425-1435.

White, C.I., and Haber, J.E. (1990). Intermediates of recombination during mating type switching in Saccharomyces cerevisiae. Embo J *9*, 663-673.

Wilkins, A.S., and Holliday, R. (2009). The evolution of meiosis from mitosis. Genetics *181*, 3-12.

Williams, R.S., Dodson, G.E., Limbo, O., Yamada, Y., Williams, J.S., Guenther, G., Classen, S., Glover, J.N., Iwasaki, H., Russell, P.*, et al.* (2009). Nbs1 flexibly tethers Ctp1 and Mre11-Rad50 to coordinate DNA double-strand break processing and repair. Cell *139*, 87-99.

Williams, R.S., Moncalian, G., Williams, J.S., Yamada, Y., Limbo, O., Shin, D.S., Groocock, L.M., Cahill, D., Hitomi, C., Guenther, G.*, et al.* (2008). Mre11 dimers coordinate DNA end bridging and nuclease processing in double-strand-break repair. Cell *135*, 97-109.

Wozniak, K., and Blasiak, J. (2002). Recognition and repair of DNA-cisplatin adducts. Acta biochimica Polonica *49*, 583-596.

Wu, L., Chan, K.L., Ralf, C., Bernstein, D.A., Garcia, P.L., Bohr, V.A., Vindigni, A., Janscak, P., Keck, J.L., and Hickson, I.D. (2005). The HRDC domain of BLM is required for the dissolution of double Holliday junctions. Embo J *24*, 2679-2687.

Wu, L., and Hickson, I.D. (2003). The Bloom's syndrome helicase suppresses crossing over during homologous recombination. Nature *426*, 870-874.

Wu, L., and Hickson, I.D. (2006). DNA helicases required for homologous recombination and repair of damaged replication forks. Annual review of genetics *40*, 279-306.

Wu, Q., Ochi, T., Matak-Vinkovic, D., Robinson, C.V., Chirgadze, D.Y., and Blundell, T.L. (2011). Non-homologous end-joining partners in a helical dance: structural studies of XLF-XRCC4 interactions. Biochem Soc Trans *39*, 1387-1392, suppl 1382 p following 1392.

Wu, S.Y., Culligan, K., Lamers, M., and Hays, J. (2003). Dissimilar mispair-recognition spectra of Arabidopsis DNA-mismatch-repair proteins MSH2*MSH6 (MutSalpha) and MSH2*MSH7 (MutSgamma). Nucleic Acids Res *31*, 6027-6034.

Wyatt, H.D., Sarbajna, S., Matos, J., and West, S.C. (2013). Coordinated actions of SLX1-SLX4 and MUS81-EME1 for Holliday junction resolution in human cells. Mol Cell *52*, 234-247.

Wyatt, H.D., and West, S.C. (2014). Holliday junction resolvases. Cold Spring Harb Perspect Biol *6*, a023192.

Xie, A., Kwok, A., and Scully, R. (2009). Role of mammalian Mre11 in classical and alternative nonhomologous end joining. Nature structural & molecular biology *16*, 814-818.

Xu, L., and Kleckner, N. (1995). Sequence non-specific double-strand breaks and interhomolog interactions prior to double-strand break formation at a meiotic recombination hot spot in yeast. Embo J *14*, 5115-5128.

Yamagata, K., Kato, J., Shimamoto, A., Goto, M., Furuichi, Y., and Ikeda, H. (1998). Bloom's and Werner's syndrome genes suppress hyperrecombination in yeast sgs1 mutant: implication for genomic instability in human diseases. Proc Natl Acad Sci U S A *95*, 8733-8738.

Yang, L., Handa, N., Liu, B., Dillingham, M.S., Wigley, D.B., and Kowalczykowski, S.C. (2012). Alteration of chi recognition by RecBCD reveals a regulated molecular latch and suggests a channel-bypass mechanism for biological control. Proc Natl Acad Sci U S A *109*, 8907-8912.

Yang, W. (2008). Structure and mechanism for DNA lesion recognition. Cell research *18*, 184-197.

Yano, K., Morotomi-Yano, K., Wang, S.Y., Uematsu, N., Lee, K.J., Asaithamby, A., Weterings, E., and Chen, D.J. (2008). Ku recruits XLF to DNA double-strand breaks. EMBO reports *9*, 91-96.

Yokoi, M., Masutani, C., Maekawa, T., Sugasawa, K., Ohkuma, Y., and Hanaoka, F. (2000). The xeroderma pigmentosum group C protein complex XPC-HR23B plays an important role in the recruitment of transcription factor IIH to damaged DNA. J Biol Chem *275*, 9870-9875.

You, J.S., Wang, M., and Lee, S.H. (2003). Biochemical analysis of the damage recognition process in nucleotide excision repair. J Biol Chem *278*, 7476-7485.

You, Z., and Bailis, J.M. (2010). DNA damage and decisions: CtIP coordinates DNA repair and cell cycle checkpoints. Trends in cell biology *20*, 402-409.

You, Z., Chahwan, C., Bailis, J., Hunter, T., and Russell, P. (2005). ATM activation and its recruitment to damaged DNA require binding to the C terminus of Nbs1. Molecular and cellular biology *25*, 5363-5379.

You, Z., Shi, L.Z., Zhu, Q., Wu, P., Zhang, Y.W., Basilio, A., Tonnu, N., Verma, I.M., Berns, M.W., and Hunter, T. (2009). CtIP links DNA double-strand break sensing to resection. Mol Cell *36*, 954-969.

Youds, J.L., and Boulton, S.J. (2011). The choice in meiosis - defining the factors that influence crossover or non-crossover formation. Journal of cell science *124*, 501-513.

Yu, X., and Chen, J. (2004). DNA damage-induced cell cycle checkpoint control requires CtIP, a phosphorylation-dependent binding partner of BRCA1 C-terminal domains. Mol Cell Biol *24*, 9478-9486.

Yu, X., Fu, S., Lai, M., Baer, R., and Chen, J. (2006). BRCA1 ubiquitinates its phosphorylation-dependent binding partner CtIP. Genes Dev *20*, 1721-1726.

Yuan, J., and Chen, J. (2009). N terminus of CtIP is critical for homologous recombination-mediated double-strand break repair. J Biol Chem *284*, 31746-31752.

Zakharyevich, K., Ma, Y., Tang, S., Hwang, P.Y., Boiteux, S., and Hunter, N. (2010a). Temporally and biochemically distinct activities of Exo1 during meiosis: double-strand break resection and resolution of double Holliday junctions. Mol Cell *40*, 1001-1015.

Zakharyevich, K., Ma, Y., Tang, S., Hwang, P.Y., Boiteux, S., and Hunter, N. (2010b). Temporally and biochemically distinct activities of Exo1 during meiosis: double-strand break resection and resolution of double Holliday junctions. Mol Cell *40*, 1001-1015.

Zakharyevich, K., Tang, S., Ma, Y., and Hunter, N. (2012). Delineation of joint molecule resolution pathways in meiosis identifies a crossover-specific resolvase. Cell *149*, 334-347.

Zalevsky, J., MacQueen, A.J., Duffy, J.B., Kemphues, K.J., and Villeneuve, A.M. (1999). Crossing over during Caenorhabditis elegans meiosis requires a conserved MutS-based pathway that is partially dispensable in budding yeast. Genetics *153*, 1271-1283.

Zha, S., Boboila, C., and Alt, F.W. (2009). Mre11: roles in DNA repair beyond homologous recombination. Nature structural & molecular biology *16*, 798-800.

Zhang, L., Kim, K.P., Kleckner, N.E., and Storlazzi, A. (2011). Meiotic double-strand breaks occur once per pair of (sister) chromatids and, via Mec1/ATR and Tel1/ATM, once per quartet of chromatids. Proc Natl Acad Sci U S A *108*, 20036-20041.

Zhang, X., and Paull, T.T. (2005). The Mre11/Rad50/Xrs2 complex and non-homologous end-joining of incompatible ends in S. cerevisiae. DNA repair *4*, 1281-1294.

Zhou, Y., Caron, P., Legube, G., and Paull, T.T. (2014). Quantitation of DNA double-strand break resection intermediates in human cells. Nucleic Acids Res *42*, e19.

Zhu, J., Petersen, S., Tessarollo, L., and Nussenzweig, A. (2001). Targeted disruption of the Nijmegen breakage syndrome gene NBS1 leads to early embryonic lethality in mice. Curr Biol *11*, 105-109.

Zhu, Z., Chung, W.H., Shim, E.Y., Lee, S.E., and Ira, G. (2008). Sgs1 helicase and two nucleases Dna2 and Exo1 resect DNA double-strand break ends. Cell *134*, 981-994.

Zierhut, C., and Diffley, J.F. (2008). Break dosage, cell cycle stage and DNA replication influence DNA double strand break response. The EMBO journal *27*, 1875-1885.

Zimmermann, M., and de Lange, T. (2014). 53BP1: pro choice in DNA repair. Trends Cell Biol *24*, 108-117.

Zimmermann, M., Lottersberger, F., Buonomo, S.B., Sfeir, A., and de Lange, T. (2013). 53BP1 regulates DSB repair using Rif1 to control 5' end resection. Science *339*, 700-704.

6. Acknowledgment

I would like to thank Prof. Petr Cejka for not only providing opportunity to pursue PhD in his lab but also for the constant encouragement even when things do not go right. I greatly admire his work ethics and try to emulate them in my life as well. His passion for science is contagious and has positively influenced my carrier choice. Apart from imparting scientific knowledge, he has taught me the value of being fair and transparent.

I also would like to thank my PhD thesis committee members Prof. Josef Jiricny and Prof. Primo Schär for their valuable advices and positive support whenever I needed it. In fact, both of them encouraged me to try test the available recombinant CtIP prep rather than waiting for the better preparation causing unnecessary delay, which later turned out to be the key in my PhD.

There were and are many people, who positively influenced my journey. I am really grateful for all of them. I would like to especially thank Elda Cannavo for guiding and helping me throughout my DNA end resection project and making my life much easier. My entire lab also deserves huge thanks for keeping the lab environment positive and healthily competitive. They all have inspired me to work better and harder. I would like to thank Mariela for helping me with the preparation of various DNA substrates. I would also like to thank the wonderful people of IMCR, who were always cheerfully helpful whenever I needed their help.

During this entire journey and before, my life was made easier as two persons were sharing it together. Therefore, It is impossible for me to overstate the importance of Lepakshi's presence in my life. She has supported me immensely both personally as well as professionally and has always taken me out of every stressful situation. My special thanks also goes to Shruti for being great and wonderful friend and making life fun when things go spirally downward.

I would like to thank my family, who have stood by me throughout my life. Despite of being relatively younger to me, my brother has been my best friend. I cannot thank enough my mother as she has quietly supported and guided me throughout my life and the journey of PhD was therefore no exception. At last, I would like to thank my father, who unconditionally loved and supported me. My success and all my achievements belong to him and my mother and I am forever indebted to both of them.

7. Curriculum Vitae

Name	**ROOPESH ANAND**
Date of Birth	15 August 1983
Nationality	Indian

Education

10/2012 - present - **PhD** studies, Cancer Biology PhD program, Group of Prof. Petr Cejka, Institute of Molecular Cancer Research, University of Zurich, Switzerland. Title of PhD thesis: From resection to resolution: Biochemical investigation of early and late steps of homoloous recombination.

2010 - 2011 **Master of Science in Transfusion and Transplantation Sciences**, University of Bristol, Bristol, UK. Master thesis in the laboratory of Prof. Geoff Daniel, NHSBT Filton Blood Centre, Filton, Bristol. Title: Molecular investigation of the KEL gene from ten unrelated samples with serologically weak Kell antigens

2007 - 2009 **Bachelor of Science in Medical Laboratory Technology**, Punjab Technical University, INDIA

2001 - 2003 **Diploma in Medical Laboratory Technology**, Indian Medical Association, New Delhi, INDIA.

1999 - 2001 **All India Senior Secondary Certificate Examination** (High-School), Central Board of Secondary Education, INDIA.

Professional Experience

09/2003-02/2005 **Junior Laboratory Technician**, Holy Family Hospital, Delhi, India

06/2005 - 03/2007 - **Blood Bank Technician,** Department of Transfusion Medicine, Max Devki Devi Heart and Vascular Institute, Delhi, India

04/2007-09/2010 - **Manager Applications**, Morepen Laboratories Limited, Delhi, India.

Teaching Experience

02/2015 - 02/2016 Supervision of master student, laboratory of Prof. Petr Cejka.

04/2013, 04/2014, 04/2016 Teaching assistant, practical block course "Genome instability and Molecular Cancer Research", University of Zurich.

Awards and Fellowships

- Academic award in Diploma in medical laboratory technology.

Scientific Conferences and Workshops

Nuclease Meeting "Structure-specific Endonucleases in Genome stability", Brno, Czech Republic, 04-06 Nov. 2015. Oral presentation: Biochemical characterization of human MLH1-MLH3 and its interplay with human MSH4-MSH5.

Publication

Ranjha Lepakshi, **Anand R** and Cejka P. The *Saccharomyces cerevisiae* Mlh1-Mlh3 heterodimer is an endonuclease that preferentially binds to Holliday Junctions. J Biol Chem. 2014 Feb 28;289(9):5674-86.

Lu H, Shamanna R A, Keijzers G, **Anand R**, Rasmussen LJ, Cejka P, Croteau DL, and Bohr VA.RECQL4 promotes DNA end resection in repair of DNA double-strand breaks. Cell Reports 2016 June 16, 161-173.